Table of contents

List of figures

List of tables

List of abbreviations, symbols and chemical formulae

A	Alpha
B	Beta
Γ	Gamma
E	Epsilon
e^-	Electron
%	Percentage
ºC	Degrees Celsius
±	Plus, or minus
µl	Microliter
µm	Micrometre
µg	Microgram
µg/kg	Microgram per kilogram
µg/L	Microgram per litre
µg/ml	Microgram per millilitre
µm	Micrometre
µM	Micro molar
µmol/L	Micromoles per litre

A

AAPH	2,2'-azobis(2-amidinopropane) dihydrochloride
ACE	Angiotensin converting-enzyme
ADAM	a disintegrin and metalloproteinase
ADAMTS13	a disintegrin and metalloproteinase with a thrombospondin type 1 motif, member 13
ADP	Adenosine diphosphate
AEC	Animal Ethics Committee
Alb	Albumin
Al	Aluminium
ALT	Alanine transaminase
ALT/AST	Alanine transaminase/Aspartate transaminase ratio
ANGII	Angiotensin II
ANOVA	Analysis of variance
AOx	Antioxidant
AP	Alkaline phosphatase

ApoE-KO	Hypercholesterolemic a lipoprotein E knockout
As	Arsenic
ASMC	Arterial smooth muscle cells
AST	Aspartate transaminase
ATP	Adenosine triphosphate
ATPase	Adenosine triphosphatase

B

Bcl	B-cell lymphoma
BH_4	(6R-)5,6,7,8-tetrahdrobiopterin
BVS	Blood vascular system

C

CAT	Catalase
5-CMFAD	5-chloromethylflorescein diacetate
$C_6H_3N_3O_7$	Picric acid
Ca^{2+}	Calcium (ion)s
CaMKII	Ca^{2+}/calmodulin-dependent protein kinase II
cAMP	Cyclic adenosine monophosphate
CBVD	Cerebrovascular disease
CD	Cluster of differentiation
Cd	Cadmium
$CdCl_2$	Cadmium chloride
CK	Creatine kinase
CK-MB	Creatine kinase-MB
Cl^-	Chloride ion
Co	Cobalt
COX-1	Cyclooxygenase-1
COX-2	Cyclooxigenase-2
Cr	Chromium
CRP	C-reactive protein
CTGF	Connective tissue growth factor
Cu	Copper
CVA	Cerebrovascular accident
CVD	Cardiovascular disease
CVS	Cardiovascular system

D

DAMPs	Damage associated molecular pattern molecules
DAPI	4′,6-diamidino-2-phenylindole
DCPIP	2,6-dichlorophenolindophenol
ddH$_2$O	Double distilled water
DMD	Dense matted deposits
DNA	Deoxyribonucleic acid

E

ECG	Electrocardiogram
ECM	Extracellular matrix
EGF	Epidermal growth factor
ELISA	Enzyme-linked immunosorbent assay
eNOS	Endothelial nitric oxide synthase
EPCR	Endothelial protein C receptor
ER	Endoplasmic reticulum
ET-1	Endothelin-1
et al.	et alia
ETC	Electron transport chain

F

F	Factor
FA	Formaldehyde
FADH$_2$	Flavin adenine dinucleotide
Fc	Fragment crystallisable
FcεRI	Fragment crystallisable epsilon receptor I
Fe	Iron
fII	Prothrombin
fIIa	Thrombin
fIX	Factor IX
fIXa	Activated factor IX
fV	Factor V
fVa	Activated factor V
fVII	Factor VII
fVIIa	Activated factor VII
fVIII	Factor VIII
fVIIIa	Activated factor VIII
fX	Factor X

fXa	Activated factor X
fXI	Factor XI
fXIa	Activated factor XI

G

G	Gram
g/µl	Grams per microliter
g/l	Gram per litre
GA	Glutaraldehyde
GGT	gamma-glutamyl transferase
GPx	Glutathione peroxidase
GSH	Glutathione
GSNO	S-nitrosglutathione

H

H&E	Haematoxylin and eosin
H_2O	Water
H_2O_2	Hydrogen peroxide
H_4B	Tetrahydrobiopterin
Hg	Mercury
HMDS	Hexamethyldisilazane

I

ICP-MS	Inductively coupled plasma mass spectrometry
IFN-γ	Interferon gamma
IgE	Immunoglobulin E
IL-10	Interleukin 10
IM	Intramuscular
ISH	Isolated systolic hypertension
isoPBS	Isotonic phosphate buffered saline
IV	Intravenous

J

JNK	C-Jun N-terminal kinase

K

K^+	Potassium ion

$KAl(SO_4)_2$	Potassium aluminium sulphate
KCl	Potassium chloride
Kg	Kilogram

L

L	Litres
LDL	Low density lipoprotein
LD_{50}	Lethal dosage that kills 50% of an animal population
LM	Light microscopy (e)
LOX	Lysyl oxidase
LOXL1	Lysly oxidase like 1

M

M	Molar
MAPK	Mitogen-activated protein kinase
Met	Methionine
METC	Mitochondrial electron transport chain
mg/L	Milligram per litre
Ml	Millilitres
MLKL	mixed lineage kinase domain like
mmol/L	Millimoles per litre
MMP	Matrix metalloproteinase
Mn	Manganese
MPTP	mitochondrial permeability transition pore
mRNA	Messenger ribonucleic acid

N

Na^+	Sodium ion
NaCl	Sodium chloride
NADH	Nicotinamide adenine dinucleotide
NADPH	Reduced nicotinamide adenine dinucleotide phosphate
NaH_2PO_4	Sodium dihydrogen phosphate
$NaIO_3$	Sodium iodate
NaP	Sodium potassium phosphate
NCCD	Non communicable diseases

Ni	Nickel
Nm	Nanometre
nm	Nanometre
NO	Nitric oxide
NOS	Nitric oxide synthase
NOX	Nitric oxidase
NS	Non-significant

O

-OH	Hydroxide
OECD	The Organisation for Economic Co-operation and Development
ONOO⁻	Peryoxynitrite
OsO4	Osmium tetroxide

P

PAI-1	Plasminogen activator inhibitor-1
PAD	Peripheral artery disease
PC	Prostacyclin
Pb	Lead
PBS	Phosphate buffered solution
PDGF	Platelet derived growth factor
PG	Prostaglandin
pH	Potential hydrogen
PO4 $^{3-}$	Phosphate ion
PR	Picrosirius red
Proα(I)	Type I Procollagen gene
Proα(III)	Type III Procollagen gene
PRP	Platelet-rich plasma
PRP+T	Platelet rich plasma with thrombin
PS	Phosphatidylserine

R

RBC(s)	Red blood cell(s)/ erythrocyte(s)
RER	Rough endoplasmic reticulum
rER	Rough endoplasmic reticulum
RIP	receptor-interacting protein
RNA	Ribonucleic acid

RNS	Reactive nitrogen species
ROS	Reactive oxygen species

S

S	Significant
SA	South Africa
SD	Standard deviation
SEM	Scanning electron microscopy
SFFF	Spontaneous fibrin fibre formation
SMA	Smooth muscle actin
SMC	Smooth muscle cells
SMAD	Mothers against decapentaplegic homolog
SOD	Superoxide dismutase

T

TAC	Total antioxidant capacity
TAFI	Thrombin activatable factor inhibitor
TB	Total bilirubin
TEG®	Thromboelastography®
TEM	Transmission electron microscopy
TF	Tissue factor
TFPI	tissue factor pathway inhibitor
TGF-β	Transforming growth factor β
TNF	Tumour necrosis factor
TP	Total protein
tPA	Tissue plasminogen activator
TSP	Total serum protein
TUNEL	Terminal deoxynucleotidyl transferase dUTP nick end labelling
TWI	Tolerable weekly intake
TXA	Thromboxane
Tyr	Tyrosine

U

U/l	Units per litre
U/ml	Unit per millilitre
UN	Urea nitrogen
UPBRC	University of Pretoria Biomedical Research Centre

Ur	Uranium

V

VEGF	Vascular endothelial growth factor
Vs.	*Versus*
VvG	Verhoeff van Gieson
vWF	von Willebrand factor
vWfCP	von Willebrand factor-cleaving protease

W

WB	Whole blood
WB+T	Whole blood with thrombin
WHO	World Health Organization

X

x	Times (multiplied by)
XO	Xanthine oxidase
XDH	Xanthine dehydrogenase

Z

Zn	Zinc

Chapter 1: Introduction

South Africa is a highly industrialised country with increasing anthropogenic activity, and so high levels of heavy metals in certain areas are a reason for concern (Coetzee *et al.,* 2004). A number of different heavy metals are of economic importance in South Africa due to their natural geological occurrence. These metals include cadmium (Cd), cobalt (Co), and chromium (Cr), copper (Cu), lead (Pb), zinc (Zn) and nickel (Ni) (Herselman, 2007). The main anthropogenic sources of heavy metals are agriculture, transport, mining and related operations (Al-Attar, 2011). The interest and research in heavy metal toxicity has increased over the past decades as the toxic effects of these metals on humans and the environment are becoming more apparent every day (Malan *et al.*, 2015) as more heavy metals are entering our water, food and air supply. Additional sources of heavy metal exposure in the population include exhaust fumes (Järup, 2003), smoking (Whitfield, *et al.*, 2010), medicinal plant contamination (Singh *et al.*, 2011; Ndhlala *et al.,* 2011) and informal industrial activities such as welding. Cd and Hg are used in electronic consumer products (Hussain and Mumtaz, 2014; Tansel, 2014) and the environmental levels of heavy metal contamination are increasing due to electronic waste processing (Wittsiepe *et al.*, 2016). These heavy metals might have a negative impact on human health, especially on those living in rural areas close to mines (Venter *et al.*, 2015) and informal settlements that are dependent on river water for drinking, washing and irrigation. Heavy metals are absorbed through the skin, by inhalation and/or orally (Awofolu *et al.*, 2005) and can have toxic, carcinogenic, mutagenic and/or teratogenic effects on humans (García-Niño and Pedraza-Chaverrí, 2014; Venter *et al.,* 2015).

The degree of heavy metal toxicity depends on dose, duration of exposure, route of administration and other physiological factors, especially overall nutritional status (Al-Attar, 2011). In South Africa heavy metal exposure is mostly through the ingestion of contaminated water; either by drinking the water, food preparation, or crop irrigation (Awofolu *et al.*, 2005). The water in the Tyume River in the Eastern Cape Province, as well as the Wonderfontein catchment in South Africa is used for domestic as well as irrigative purposes. A major concern is the effect this may have on the people living in these areas. The question that arises is what the effect of being continuously exposed to low levels of heavy metal mixtures is. According to a study done by Coetzee in 2004, the mean levels of heavy metals, including Co, Zn, arsenic (As), Cd and uranium (Ur), but especially Cd and Ur in the Wonderfonteinspruit catchment area is of concern, as these levels are higher than the natural background concentrations, as well as regulatory levels.

The effects of acute and chronic toxicity to high levels of heavy metals are well described (Pinto *et al.,* 2003; Duruibe *et al.*, 2007; Kampa and Castanas, 2008). Reviewed by Jomova and Valko, 2011, many studies have described the association between heavy metal exposure and the development of certain types of occupational diseases but little is known regarding the effect of long-term exposure and the development of late onset diseases such as CVD.

Mine waste has the potential to cause heavy metal pollution, if not discarded correctly (Lusilao-Makiese *et al.,* 2013). Heavy metals such as Cd and Hg are highly persistent in the environment, and are present in soil and water and Cd and Hg are especially applicable in the South African and overall global context. In this study, the possible adverse effects of two heavy metals, Cd and Hg on the CVS with specific focus on the myocardium and aorta as well as the coagulation system were investigated. These metals were chosen based on their relevance in a South African context (Herselman, 2007).

Due to varying and numerous heavy metal pollutants present in the environment, exposure is not limited to a single metal but to complex mixtures of different metals often at low concentrations. While previous studies have demonstrated the acute and chronic effects of heavy metals both in population and laboratory based studies (Pinto *et al.*, 2003; Duruibe *et al.*, 2007; Kampa and Castanas, 2008), the question that arises is what the consequences are of being exposed to different metals as part of mixtures. While the effects of heavy metals including Cd and Hg have been extensively investigated on kidney and liver tissue, information on the effect of both metals alone and in combination on the CVS is limited. Heavy metals are known to have an effect on the coagulation system and studies have included the effects of iron (Fe), Zn and Ni (Sangani *et al.,* 2010; Pretorius and Lipinski, 2013), however little is known regarding the effects of Cd and Hg alone and in combination on the coagulation system. Therefore, the aim of this study is to investigate the effects of the heavy metals Cd and Hg alone and in combination on the CVS as well as the effects on the coagulation system.

Chapter 2: Literature review

2.1.   Heavy metal toxicity

Heavy metals occur naturally in soil and groundwater; however human activity has led to an increase in these natural levels (Awofolu *et al.*, 2005). Contaminated water leads to increased human exposure through drinking, preparation of food and irrigation of food crops. Within the body these metals disrupt normal cellular processes. In general, heavy metals are usually poorly absorbed, but once absorbed many of these metals bio-accumulate in various organ systems. Symptoms of acute toxicity are well described (Jomova and Valko, 2011; Bernhoft, 2013; Akoto *et al.,* 2014), however the effects of long-term exposure of several years to sub-acute levels of several heavy metals as part of mixtures is unknown, and this type of low dosage exposure is characteristic of the risk posed by environmentally relevant concentrations.

2.2.   Heavy metals exposure in the South African context

In South Africa, mining is the single industry sector with the largest by volume water quality impact. Decrease in water pH, increase in salinity, increase in metal content and increase in sediment load is some of the effects of mining. The polluted groundwater discharging into streams in the area contributes to 20% of the stream flow in the mining areas around Johannesburg (South Africa) (Naicker *et al.*, 2003). Naicker and co-workers in 2003 found that the effects of the contaminated water from the mines could persist for more than 10 km beyond the source (Naicker *et al.*, 2003).

The quality of South Africa's fresh water resources is declining due to urbanization, acid mine drainage, inflows of treated and untreated sewage, deforestation, agricultural return flows and energy use (Oberholster *et al.*, 2010). Lowering of pH over time due to human-induced acidification, as a result of industrial effluents, mine drainage and acid rain results in the deterioration of water quality (Oberholster *et al.*, 2010), degradation of soil quality and aquatic habitats. Mine drainage and soil degradation also cause the mobilization of elements such as, aluminium (Al), Cd, Co, Cu, Hg, Fe, manganese (Mn), Ni, Pb and Zn, due to increased solubility of these trace metals in sediments (Oberholster *et al.*, 2010). Electronic waste recycling is also a source of Al, As, Cd, Co, Cr, Cu, Hg, Mn, Ni, Pb and Zn contamination which have been shown to cause chronic respiratory, cardiovascular, nervous, urinary and reproductive disease, as well as aggravation of pre-existing symptoms and disease (Zeng *et al.*, 2016).

In developing countries such as South Africa, the incidence of CVD is increasing with a high proportion of deaths occurring in the working age population (Gersh *et al.,* 2010). Little is known regarding the mortality of miners in South Africa due to cardiovascular and neurodegenerative diseases, although concern has been expressed regarding the increase in CVD in the working-class population of Brazil, India and South Africa (Lopez *et al.*, 2006; Gaziano *et al.*, 2010). Gómez

3

et al. reported an increase in Hg miner mortality due to hypertension, cerebrovascular as well as other cardiac diseases (Gómez *et al.*, 2007).

A limited availability of information on the effects of long-term heavy metal exposure may be due to lack of data and/or the late onset of associated symptoms. Additional contributing factors are gender, age, genetic polymorphisms, nutritional status and exposure to other heavy metals for example Cd through cigarette smoke (Satarug and Moore, 2004). An increase in illegal mining and consequent unregulated exposure to heavy metals during mining and metal processing is an additional source of exposure.

In a Chinese mining population, artisanal mining has been identified as a large source of Hg exposure (Li *et al.*, 2011). The total concentration of Hg in stream water ranged from 43 to 2100 ng of Hg per litre, and elevated values were reported in close vicinity to artisanal Hg mines. Surface soil contamination by Hg has been shown to be a result of both large scale and artisanal mining (Li *et al.*, 2011). Hg causes pollution in crops and soils surrounding coal fired power plants (Li *et al.*, 2017). Calculations of a recent study by Li and colleagues (2017) suggested that the weekly intake of Hg for residents in areas of Hg contamination such as the coal mine may exceed the safety limit when all the sources of exposure including crops, water and ambient air are considered. Combined effects of metals or an additional load of Hg from different sources may contribute to the overall body burden of Hg (Maramba *et al.*, 2006; Li *et al.*, 2017). This same principle, although not calculated, can be applied to all toxin exposures, including Cd. Therefore, it is safe to suggest that in populations living in heavy metal contaminated areas or having access to heavy metal contaminated water may have additional loads or sources of heavy metal exposure, all of which bioaccumulate within the body. For these reasons, even if soil or water levels are within the safety levels, these safety levels do not consider the additional sources of contamination.

In a recent systematic review and meta-analysis of epidemiological studies of metals including Cd and Hg, Hg has not been found to be associated with cardiovascular risk in areas such as Europe, North America and the Asia-Pacific (Chowdhury *et al.*, 2018). However, unacceptably high levels of Cd and Hg have been observed in the environment, especially in Sub Saharan Africa, although the levels of environmental pollution differ by site location. Heavy metals have been found in umbilical cord blood samples, indicating a risk to unborn foetuses as well as to adults exposed to the heavy metals, as shown in maternal blood by Röllin *et al.* (2009). In developing industrialised areas, an appearance of informal settlements and highly concentrated urban living is an emerging challenge. The planting of fruit and vegetables in informal settlements and urban areas is a common practice in Sub Saharan Africa and poses another additional challenge, as heavy metals present in the soil due to petrochemical, industrial and mining waste and water used to irrigate the produce bioaccumulate in the plants, which are then consumed. Low- and middle-income countries that traditionally focused on controlling undernutrition and infectious diseases now have a growing burden from non-communicable chronic diseases (NCCD). This transformation in disease status

has occurred in a very short period, making it difficult for countries and international health and aid organizations to respond (Popkin, 1998; Popkin and Gordon-Larsen, 2004; Sepulveda and Murray, 2014).

Geophagy (soil-pica) has been reported as a source of heavy metals amongst other contaminants (Kutalek *et al.*, 2010). A risk of increased Hg exposure has been reported in children exposed to Hg contaminated soil and household dust in Slovenia, who ingested topsoil particles as a consequence of geophagia (Bavec *et al.*, 2018). Extra caution has been recommended for outdoor activities in urban areas and this caution would apply to mining areas as well. Geophagy is a cultural practice in many African countries and has been reported in the Transkei region of South Africa (Meel, 2012). Geophagy has been observed in pregnant women seeking to supplement mineral requirements during pregnancy, particularly iron (Louw *et al., 2007;* Young, 2010*).* The optimisation of nutritional status is important in the prevention of and detoxification of Hg toxicity (Bjørklund *et al.*, 2017).

Hg poisoning via vapour on accidental or occupational exposure has been reported in case studies, however this type of exposure is acute and not a good indication of low dose effects (Sarikaya *et al.,* 2010). Diagnosis of Hg poisoning in case studies has been delayed until a high enough urine Hg content was apparent (Smiechowicz *et al.,* 2017). Furthermore, the signs and symptoms of Hg exposure have been primarily observed in the central and peripheral nervous system, kidneys, immune system, endocrine system, skeletal muscle and skin (Bernhoft*,* 2012). Severe symptoms of Hg exposure develop after several weeks and in humans included pneumomediastinum, pneumonia, and respiratory failure, atypical of Hg exposure (Smiechowicz *et al.,* 2017). Initial symptoms of Hg toxicity may mimic viral illnesses (Sharma *et al.*, 2014), thus leading to diagnostic mistakes (Berhnoft, 2012). A case documented effects of intravenous (IV) injection of Hg, and pulmonary effects were recorded, including the decreased diffusion of CO and PO_2 which were suggested to be indicative of inflammation in the lung interstitium (dell'Omo *et al.,* 1997). Signs of catecholamine degradation by Hg include autonomic dysfunction, tachycardia, sweating, diarrhoea and abdominal pain (Rice *et al.*, 2014; Sharma *et al.*, 2014). Chelation therapy and a long-term treatment of 6 months are required to remove Hg symptoms (Smiechowicz *et al.,* 2017). Therefore, an insidious onset and nonspecific clinical manifestations can lead to misdiagnosis and delayed treatment.

Although methyl mercury (MeHg) has been shown to be more toxic than inorganic Hg (Crowe *et al.*, 2017), inorganic Hg has shown a higher pro-inflammatory effect, leading to lupus like syndrome in animals susceptible to metal induced autoimmunity (Crowe *et al.*, 2017). Immunoglobulin E (IgE) is increased in inorganic Hg treated rats, which mediates immune reactions such as allergic reactions, including asthma, urticaria and rhinitis. Hg has been associated with the development of autoimmunity and levels of Hg in autoimmune disease are under researched (Crowe *et al.*, 2017). Inorganic forms of Hg have been shown to perpetuate the markers of autoimmunity (Crowe *et al.*,

2017) leading to immunological toxicity and dysfunction (Bjørklund *et al.*, 2017). Results show that Hg exacerbates autoimmune myocarditis in female mice and alter innate immune signalling on peritoneal macrophages. Hg exposure promotes inflammation in already inflammatory prone models (Penta *et al.,* 2015). Hg was shown to induce lymphocyte stimulation independent of antigen stimulation (Weigand *et al.,* 2015). Low doses of Hg and Cd toxicity may therefore be confused with inflammatory conditions and not treated correctly.

2.3.   Cadmium in the environment

The primary Cd exposure in humans is via inhalation of Cd fumes and ingestion of Cd-containing food. Vegetables are the main carrier of Cd compounds when compared to other foods as these plants are continuously being exposed to atmospheric, soil and water sources of heavy metals (Kowalczyk *et al.*, 2002). Acidification of soils results in the elevation of Cd levels in crops such as rice, wheat and vegetables (Nordberg *et al.,* 2007). In natural water, Cd is mostly found in bottom sediments and suspended particles, and the concentration in the water phase is low. Concentrations in non-polluted natural waters are usually lower than 0.001mg/L (Nordberg *et al.,* 2007). Awofolu *et al.* in 2005 reported that water from the Tyume River in the Eastern Cape province of South Africa, had mean Cd levels of 0.03±0.002 - 0.044±0.003 mg/L (Awofolu *et al.*, 2005) and these levels were higher than the South African Target Water Quality Range (TWQR) and the WHO limits guidelines (WHO, 2011) for river water used for domestic purposes as well as crop irrigation and livestock watering (Awofolu *et al.*, 2005).

Another source of Cd is cigarette smoke. The prevalence of deaths due to tobacco smoking in South Africa is between 12 and 25% (Sitas *et al.*, 2013) and is likely to increase based on the populations' smoking patterns (Jha and Peto, 2014). However, smoking among the South African population has been reported to have decreased in a ten-year period (1993 to 2003), from 34 to 21.4% (Ayo-Yusuf and Olutola, 2013), and continues to do so with the increase in cigarette prices (Van Walbeek, 2006; Jha and Peto, 2014). However, the use of "roll-your-own" cigarettes has increased as a cheaper alternative to factory made cigarettes (Ayo-Yusuf and Olutola 2013), and increased popularity in youth culture has resulted in an increase in non-regulated consumption of Cd.

2.3.1. Cadmium absorption, distribution, metabolism and elimination

Cd binds to metallothionein once absorbed into the body and irreversibly accumulates in the liver, kidneys and testes as there are no excretory mechanisms for Cd. A high deposition of Cd can be seen in the kidneys, even in subjects that have had low exposure to the metal (Nawrot *et al.*, 2010). Its high affinity for these tissues is based on their ability to synthesise metallothionein.

The rate of Cd absorption in the gastrointestinal tract (GIT) is dependent on the nutritional status of an individual. Women often accumulate more Cd than men primarily because the menstrual cycle causes a decrease in iron (Fe) (Nordberg *et al.,* 2007) and in individuals with an Fe deficiency, Cd

absorption can be as high as 20% (Nordberg *et al.,* 2007). Hamilton *et al.* (1978) found that in mice fed a low Fe diet, Cd caused impaired Zn uptake leading to Zn deficiency (Hamilton *et al.*, 1978). In later studies it was observed that low protein content in the diet also leads to higher absorption of Cd and more severe signs of toxicity (Nordberg *et al.,* 2007). Indications were found that a low intake of calcium and other minerals, vitamin D and protein were contributing factors for Itai-Itai disease, a disease caused by the chronic uptake of high levels of Cd. Cadmium interferes with the normal calcium metabolism in both the kidneys and bones which may increase the risk for Itai-Itai disease, which is also associated with osteoporosis (Nordberg *et al.,* 2007).

2.3.2. Biochemical and cellular effects of Cd

Cellular redox balance between the reactive oxygen species (ROS) and antioxidant enzymes (AOx) such as catalase (CAT), superoxide dismutase (SOD), glutathione peroxidase (GPx), and metabolites such as glutathione (GSH), is necessary to prevent cellular damage. Cd indirectly affects the generation of ROS and reactive nitrogen species (RNS) (Waisberg *et al.*, 2003), by decreasing the available AOx (CAT, SOD and GPx) through chelation, and consequent enzyme inactivation leads to increased ROS (Kowalczyk *et al.*, 2002). Cadmium also generates hydrogen peroxide (H_2O_2) which in turn can be a source of free radicals in the Fenton reaction (Benedet and Shibamoto, 2008) (Figure 2.1). A mechanism explaining the indirect role of Cd in ROS formation suggests that Cd can replace Fe and Cu in various cytoplasmic and membrane proteins (e.g. ferritin, apoferritin), thus increasing the amount of unbound free or poorly chelated Cu and Fe ions that can, for example, act as catalysts of the Fenton reaction (Novelli *et al.*, 2000). Cd also interferes with calcium regulation and through this induces cell death and injury in biological systems (Awofolu *et al.*, 2005). Lipid peroxidation has been reported in heart, liver and spleen tissue of rats after Cd exposure (Yiin *et al.*, 2000).

Increased H_2O_2 formation by Cd can causes cellular damage, including mitochondrial damage (Nair *et al.*, 2013). Cd-induced oxidative damage to cellular macromolecules includes increased lipid peroxidation, protein carbonylation, and DNA damage (Ghosh and Indra, 2018). Reduced levels of antioxidants; α-tocopherol, ascorbic acid and activity of CAT, GSH, SOD and GPx following Cd exposure is suggested to be due to divalent ion displacing activity of Cd in AOxs and resulting in reduced levels of antioxidant molecules such as GSH. This imbalance has been identified to induce inflammation and apoptosis (Madejczyk *et al.*, 2015). Metals and the subsequently formed ROS are known to activate NFκB, a redox-sensitive transcription factor transactivating various genes involved in inflammation (Chen and Shi, 2002; Morgan and Liu, 2011). It has been established that Cd exposure triggers an inflammatory response through the upregulation of pro-inflammatory proteins NFκB, inducible nitric oxide synthase (iNOS), COX-2 and c-myc and a downregulation of anti-inflammatory cytokine IL-10 and HO-1 (Yazıhan *et al.*, 2011; Olszowski *et al.*, 2012; Luevano and Damodaran, 2014; Riemschneider *et al.*, 2015).

Induction of oxidative stress, inflammation, apoptosis and an increase in iNOS as well as a decrease in endothelial nitric oxide synthase (eNOS) are implicated as some of the primary risk factors in the development of CVD (Cotton *et al.*, 2002; Kim and Kang, 2010; Csányi and Miller, 2014; Golia *et al.*, 2014).
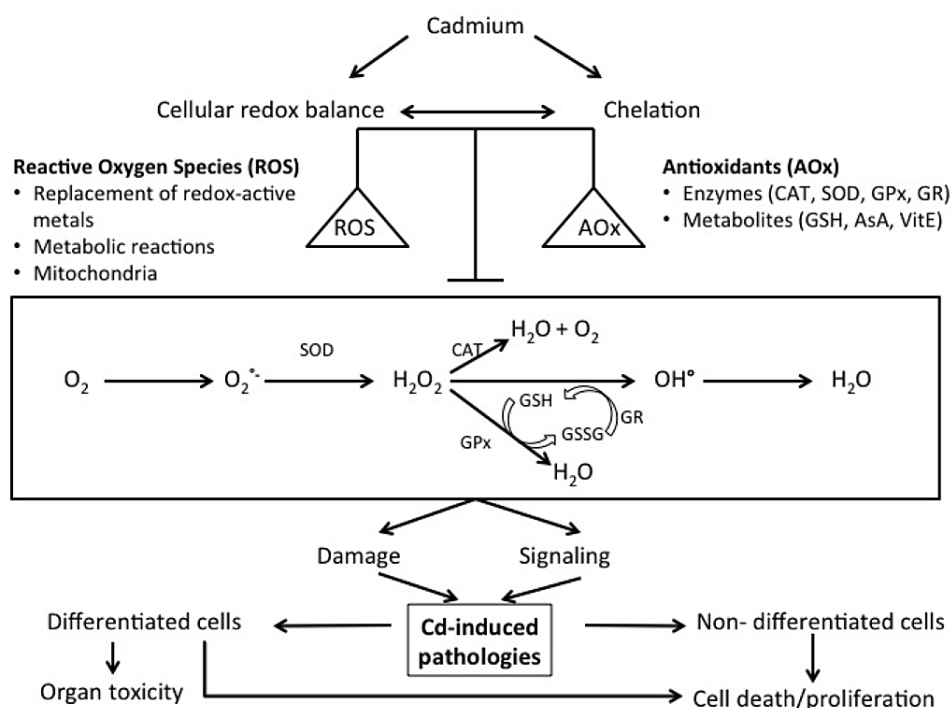
Figure 2.1: Cellular mechanisms by which Cd causes oxidative stress and associated cellular pathology (Nair *et al.*, 2013).

2.3.3. Clinical effects of Cd

Cd is a major constituent of tobacco smoke and according to Lee *et al.* (2011), is an underestimated risk factor in the development of CVD. Blood levels below the safety standard have been associated with peripheral arterial disease (PAD), and therefore Cd was found to be a partial mediator between smoking and PAD (Navas-Acien *et al.*, 2004). Argawal *et al*, (2011), found that cerebrovascular disease (CBVD) is associated with increased levels of exposure to Pb and Cd.

Potential mechanisms of action of Cd may also be a partial agonism for calcium channels and vasoconstrictive action (Varoni *et al.*, 2003). The primary mechanism of action of Cd on cells is its oxidative stress promoting action as well as the depletion of GSH and the alteration of SH homeostasis (Valko *et al.*, 2005). Cd deposition was found on vascular walls (Abu-Hayyeh *et al.*, 2001). Cd can be taken up by cells via channel transporters, endocytosis or by infiltration of the vessel walls (Kyselovic *et al.*, 2005; Steffensen *et al.*, 1994). Smooth muscles cells (SMCs) are able to retain high amounts of Cd (Abu-Hayyeh *et al.*, 2001) where the metal is able to affect ion homeostasis and has cytotoxic effects. Low Cd concentrations are able to stimulate SMC proliferation (Prozialeck *et al.*, 2008).

As mentioned above, CVS effects of Cd are suggested to occur as a result of the complex actions of these metals on the vascular endothelium and smooth muscle. These actions could be mediated by the generation of a pro-inflammatory state (Heo *et al.*, 1996), endothelium dysfunction (Kaji *et al.*, 1995), increased oxidative stress (Stohs *et al.*, 1995), or the down regulation of NO production (Demontis *et al.*, 1998; Vaziri *et al.*, 2001) in the presence of these metals. These processes lead to a disruption of angiogenesis, which in turn affects vascular remodelling (Prozialeck *et al.*, 2008). Studies on the effects of Pb and Cd on atherogenesis have been conducted as *in vivo* and *in vitro* studies on cell lines or non-human biological models, at concentrations higher than those in observational studies and reported by national agencies (Argawal *et al.*, 2011). Cd was found to exert effects on the CVS at low levels and therefore pathophysiological changes in vessel walls can be caused by Cd at levels well below toxic dosages (Bernhard *et al.*, 2006). Men living in areas with an increased Cd exposure, or the potential for an increase in exposure had increased CVS mortality, suggesting a causative or comorbidity factor (Menke *et al.*, 2009). Early epidemiological studies conducted on the relationship of Cd to the development of CVD had different methodologies and differences in findings. High levels of serum Cd have been reported in patients with myocardial infarction (Ponteva *et al.*, 1979; Adamska-Dyniewska *et al.*, 1983), while another study showed no association between blood Cd levels and CVD (Staessen *et al.*, 1996).

More recent studies have also shown inconsistencies and discrepancies, and this could be as a result of differences in study designs and population selection, data sampling and interpretation (Nawort *et al.*, 2003; Tellez-Plaza *et al.*, 2008). An association between blood and urinary Cd and peripheral artery disease suggests the involvement of Cd in arterial dysfunction (Navas-Acien *et al.*, 2005). Epidemiological studies have not established a link between Cd and CVD due to co-exposure to other heavy metals due to the lack of adjustments for smoking habits, as well as differences in data interpretations.

2.4.   <u>Mercury in the environment</u>

Hg emissions in South Africa from gold mining and coal combustion are more than 10% of all global emissions and South Africa was listed in the year 2000 as a major Hg polluter; only second to China (Pacyna *et al.,* 2006). Gold mining is also associated with increased water contamination with Hg. Gómez *et al.* in 2007 have reported an increased mortality amongst miners from the Almadén region of Spain exposed to Hg due to circulatory diseases specifically hypertension and CBVD (Gómez *et al.,* 2007). Sources of Hg contamination within these communities include water contamination due to gold mining and Hg leaching due to deforestation as well as the consumption of fish in which Hg has bio-accumulated. Data related to the risks in South Africa is limited, but in a study done by Fatoki and Awofolu in 2003, Cd, Hg and Zn levels were measured in the Umtata, Buffalo, Keiskamma and Tyume Rivers and in the Sandile and Umtata Dams in the Eastern Cape province of South Africa. It was found that the Cd levels were elevated, but the Hg and Zn levels

were overall normal and consequently Cd was the only metal that was a risk for the environment and human health (Fatoki and Awofolu, 2003).

Artisan mining such as the illegal gold mining involves the use of Hg for processing of gold alluvial deposits and during this process Hg can escape into the atmosphere and can be deposited into the surrounding soils and water (Rodrigues-Filho and Maddock, 1997; Cesar *et al.*, 2011; Castilhos *et al.*, 2015), from where it increases the risk of exposure to not only individuals who are in direct contact with the metal, but also people living in the nearby communities. Small scale mining operations are suggested to be important sources of Hg exposure. With artisanal gold mining in Brazil, exposure to Hg was high. In addition, the Hg levels are high in all communities due to atmospheric vapour inhalation as well as ingestion of Hg contaminated fish (Castilhos *et al.*, 2015). Exposure can be to different types of mercury where contaminated air and water contain Hg salts as ($HgCl_2$), while water and seafood contain methyl-Hg (MeHg), dental amalgam fillings contain metallic-Hg and some vaccines contain ethyl-Hg (Bjørklund *et al.*, 2017). Elemental Hg is converted to inorganic Hg in the soil, which is directly taken up by plants or converted by sulphate reducing bacteria in soil to MeHg and then is taken up by plants, which are eventually consumed by humans (Jia *et al.*, 2018).

2.4.1. Mercury absorption, distribution, metabolism and elimination

The extent to which an individual is exposed to Hg is reflected in the blood and urine levels (Berlin *et al.*, 2007). Hg has an especially high affinity for ectodermal and endodermal epithelial cells and glands. Organs with the longest retention times for Hg are the brain, kidneys, and testes but Hg is also accumulated in the epithelial lining of the intestinal tract; in the squamous epithelium of the skin and hair; in tissues like the salivary glands, thyroid, liver, pancreas, and the sweat glands; as well as the prostate gland (Reviewed by Bernhoft, 2011 Berlin *et al.*, 2007).

The absorption and toxicokinetic behaviour of Hg is dependent on the type and mode of biotransformation and is summarised in Figure 2.2. Hg vapour is readily absorbed by inhalation, but its absorption is extremely limited through the skin and GIT. Organic forms of Hg can be absorbed by inhalation and via the GIT. Once in the blood Hg is widely distributed to other tissues where it binds to sulfhydryl groups (SH-groups) such as the Cys residues of proteins and GSH. Inorganic mercury such as $HgCl_2$ has low lipophilicity that limits its ability to penetrate through the blood brain barrier (Goyer 2005, Holmes *et al.*, 2009). Once absorbed, Hg undergoes metallic interconversion within the body. Organic methyl-Hg is converted to inorganic Hg in the kidneys and the liver through the actions of microbial flora, production of ROS and reactions with sulphydryl groups (Holmes *et al.*, 2009). Hg also bio-accumulates in the same manner in several aquatic species, and often fish that contain bio-accumulated Hg is consumed.

Acute toxic effects of Hg are expected at levels of 50 µg Hg/L blood or 100 µg Hg/L urine, compared to normal (no effect) levels of up to 10 µg Hg/L blood or 10 µg Hg/L urine in humans

(Holmes *et al.*, 2009), with the fatal dose being approximately 100 mg organic mercury or 1 g mercury salts. Signs and symptoms of mercury intoxication include excessive salivation, sleep disturbances, tremors and ataxia (Bose O'Reilly *et al.*, 2016). Targets of acute toxicity include the nervous and immune systems and kidneys and, depending on exposure route, the GIT tract, lungs and skin (inorganic Hg), while chronic exposure has been shown to cause the most damage to the central nervous system (CNS). Other effects of Hg include anaemia, gastric disturbances, gum tenderness and metallic taste in the mouth (Holmes *et al.*, 2009), arrhythmia and cardiomyopathy (Tchounwou *et al.*, 2003).
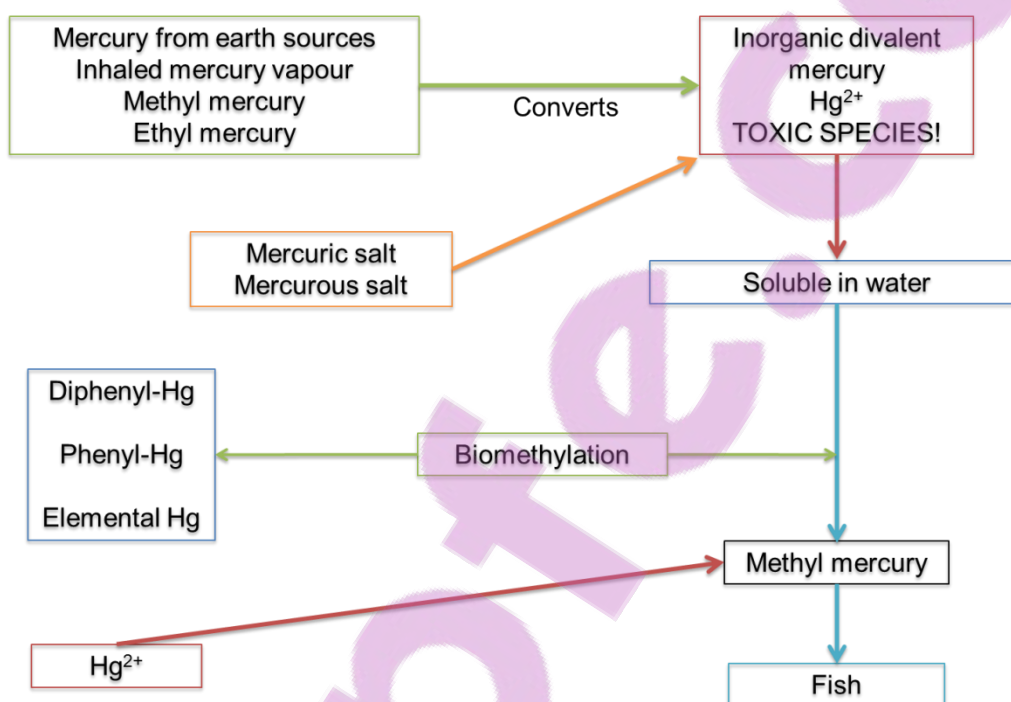
Figure 2.2: Types and forms of Hg as well as mechanisms of biological transformation (Adapted from Houston, 2014).

Most Hg is eliminated through urine, faeces and expired air. Inorganic Hg in particular is excreted via urine, bile and faeces, exhaled air, sweat, breast milk and saliva (Sweet and Zelikoff, 2001). The half-lives of Hg elimination are influenced by species, strain and dose. Age is an important factor in the body burden of Hg and children and neonates show greater rates of absorption and retention of the metal. For inorganic Hg the half-life in blood is 1 – 3 weeks and whole body is 1 - 2 months, 1 – 3 days in blood and 58 days in whole body for elemental, and 70 - 80 days for organic (Holmes *et al.*, 2009; Solenkova *et al.*, 2014). Human studies have shown the half-life of $HgCl_2$ to be 42 days (Bernhoft, 2012). The long half-life is the reason why Hg toxicity is difficult to manage as the body burden of Hg is slowly eliminated and lowered.

2.4.2. Biochemical and cellular effects of Hg

Hg is oxidized by erythrocytes to Hg^{2+} (Berlin *et al.*, 2007) which binds to SH-groups on proteins leading to a change in the normal tertiary and quaternary structure of these proteins as well as changing the binding properties of certain enzymes. This binding of Hg^{2+} also leads to modification and blocking of receptor binding, alteration in K^+ or Ca^{2+} flow through the pores of the cell membrane and ionic channels, which can affect the cell membrane potentials and intracellular and intercellular signals (Berlin *et al.*, 2007). The affinity of Hg for sulphur and SH-groups also leads to the interference with normal membrane structure and function and this includes lipid peroxidation (Berlin *et al.*, 2007). Due to its high affinity for SH-groups, ionic Hg binds to GSH, Cys, homocysteine, *N*-acetylcysteine, metallothionein, as well as albumin (Berlin *et al.*, 2007). This causes the inactivation of these AOx molecules and subsequent decrease in cellular AOx status (Berlin *et al.*, 2007). Furthermore, inhibition of SOD, CAT as well as GPx (Brandão *et al.*, 2008), important cellular AOx enzymes, also contributes to an altered AOx status. At a cellular level Hg is an apoptogen, as it causes the activation of caspase-3 via oxidative activation of the death signalling pathways (Rana, 2008). In the mitochondria Hg binds specific mitochondrial enzyme systems as shown in Figure 2.3 This leads to the depolarisation, autoxidation and peroxidation of the inner mitochondrial membrane. The consequential loss of the integrity of the inner mitochondrial membrane causes altered calcium homeostasis, an increase in H_2O_2 levels, depletion of GSH, increased lipid peroxidation and oxidation of cofactors nicotinamide adenine dinucleotide (NADH) and reduced nicotinamide adenine dinucleotide phosphate (NADPH). This increase in oxidative stress and depletion of mitochondrial oxidant defence would have an adverse effect in mitochondrial rich tissue types such as cardiac and smooth muscle. The effects Hg on the CVS are listed in Table 2.1.
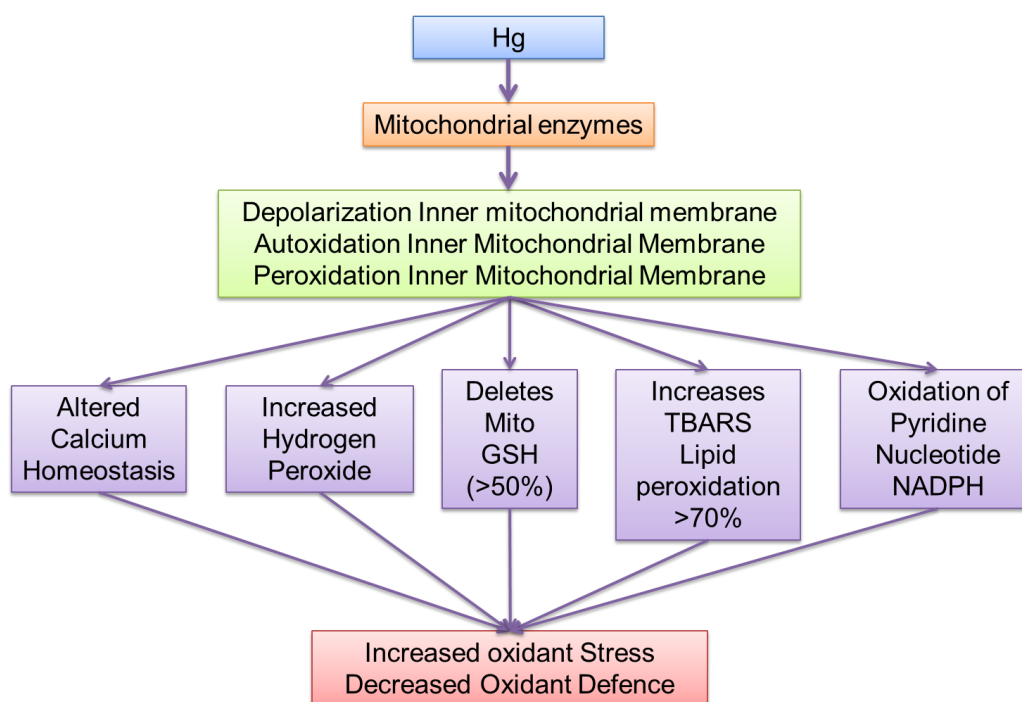
Figure 2.3: Oxidative effects of Hg in the mitochondria (Adapted from Houston, 2014).

Table 2.1: Summary of the effects of Hg on the CVS

Effect
Increase in free radical production
Inactivation of AOx defenses
Binds to thiol-containing mlecules
Binds to selenium (Se) forming Se-Hg complex, decreases Se availability for cofactor GPx
Inactivates GSH and the enzymes CAT and SOD
Increases lipid peroxidation in all organs
Increases oxLDL and oxLDL immune complexes
Increases platelet aggregation
Increase coagulation/thrombosis: increases Factor VII PF4 and thrombin and reduces protein C
Inhibits endothelial cell formation and migration
Increases apoptosis
Reduces monocyte function and phagocytosis, impairing immune function
Increases inflammation

Adapted from Houston, 2014.

2.4.3. Clinical effects of Hg

MeHg levels lower than those seen in neurotoxicity have CVS effects. High Hg content of hair, indicating high exposure to Hg was identified as cause for the increase in the progression of

13
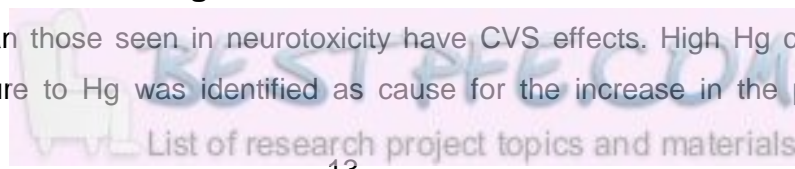
atherosclerosis and as risk factor for CVD (Salonen *et al.*, 2000). Hg induces oxidative stress and causes the reduction of oxidative defences in the body. Hg has various vascular effects, and these include increased oxidative stress and inflammation in vascular tissue, a reduction in the oxidative defence, thrombosis as well as vascular smooth muscle, endothelial and immune and mitochondrial dysfunction (Table 2.2) (Houston, 2011). These result in clinical consequences which include arrhythmias, reduced heart rate variability, increased carotid intima-media thickness and carotid artery obstruction. Increased blood pressure occurs due to the inactivation of catecholamine-Ө-methyl transferase by Hg with a resulting increase in serum and urinary epinephrine, norepinephrine and dopamine (Houston, 2011). Hg levels can be used to predict the levels of oxidised low-density lipoprotein (LDL), which is found in atherosclerosis (Salonen *et al.*, 1995; Yoshizawa *et al.*, 2002; Houston, 2007). Hg can also cause toxic effects through the inactivation of an enzyme paraxonase, which slows down the oxidation of LDL and thereby prevents atherosclerosis formation or progression (Hulthe and Fagerberg, 2002). $HgCl_2$ induces lung toxicity (Celikoglu *et al.,* 2015) in the form of edema as well as fibrosis, as a result of excessive formation of ROS.

Table 2.2: Clinical consequences of Hg exposure on the CVS

Effect
Oxidative stress
Inflammation
Thrombosis
Vascular smooth mucsle proliferation and migration
Endothelial dysfunction
Dyslipedimea (oxHDL and paraoxonase)
Immune dysfunction
Mitochondrial dysfunction

Adapted from Houston, 2014.

2.5.   Combinational studies: Hg or Cd and other heavy metals

Although studies have investigated the effects of heavy metals and their combinations both *in vitro* and *in vivo* (Dai *et al.*, 2013; Yuan *et al.*, 2014), no studies could be found on the effects of Hg and Cd alone and in combination on the CVS. Only effects that have been studied are the effects of these metals on several blood parameters (Hounkpatin *et al.*, 2012; Hounkpatin *et al.*, 2013). Alterations of AOx defence systems were observed in workers exposed chronically to Cd and Hg in coal fly-ash. The exposure affected the plasma levels of ascorbic acid and concentrations of SOD and GPx, increasing the risk for oxidative stress (Zeneli *et al.*, 2016).

2.6. Cellular formation of reactive oxygen species/ reactive nitrogen species

Oxidative stress is a result of an imbalance between cellular production of reactive oxygen species (ROS) and detoxification of ROS by the cellular AOx defence system. Several cardiovascular pathologies have been associated with oxidative stress and these include ischemia or reperfusion, hypercholesterolemia, and hypertension (Cooper *et al.*, 2002).

ROS are oxygen based molecular species which are highly reactive and include the free radicals superoxide and hydroxyl and non radical species such as H_2O_2. RNS include nitric oxide (NO) and peroxynitrite ($ONOO^-$) (D'Autreaux and Tolenado, 2007). RNS is formed via the reaction of NO with ROS. These reactions are summarised in Figure 2.4 and will be discussed in greater detail. The balance between the ROS/RNS and the removal of these molecules is known as the redox or nitroso-redox state of the cell. Oxidative states occurs when the reducing systems are insufficient to process ROS/RNS (Afanas'ev, 2011; Finkel and Holbrook, 2000; Rajasekaran *et al.*, 2007). During oxidative stress, cellular systems, including membrane lipids and DNA are damaged by oxidation. If the stress continues, cell death by apoptosis, necrosis and autophagy can occur (Essick and Sam, 2010; Hidalgo and Donoso, 2008). Benefits asociated with ROS activation include the activation of nuclear transcription factors, gene expression and a destructive effect on tumor cells and invading microorganisms (Simon *et al.*, 2000; El-Bahr, 2013). However, a redox balance must be maintained to ensure correct cellular functioning to prevent the harmful effects of ROS (El-Bahr, 2013).
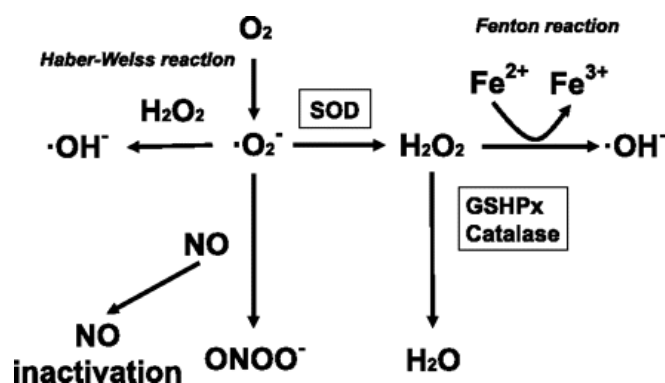
Figure 2.4: Reactions resulting in the generation and degradation of NOS and ROS (Tsutsui *et al.*, 2011).

2.6.1. Oxidant/antioxidant enzymes

A common mechanism in the toxicity of Cd and Hg is the formation of ROS, depletion of antioxidant molecules and AOx enzymes. ROS production is an important factor in cellular functions, where it initiates signalling of cellular processes and pathways such as proliferation and

survival, ROS homeostasis and AOx gene regulation, mitochondrial oxidative stress, apoptosis, and aging, iron homeostasis, and DNA damage response. The most important oxidant enzymes are NADPH oxidase, xanthine oxidase (XO), enzymes of the mitochondrial respiratory chain, and eNOS (Li et $al.$, 2013). To maintain redox status, enzymes that scavenge ROS include CAT, SOD and GPx (and associated GSH). These AOx enzymes and their reactions are illustrated in Figures 2.4 and 2.5.
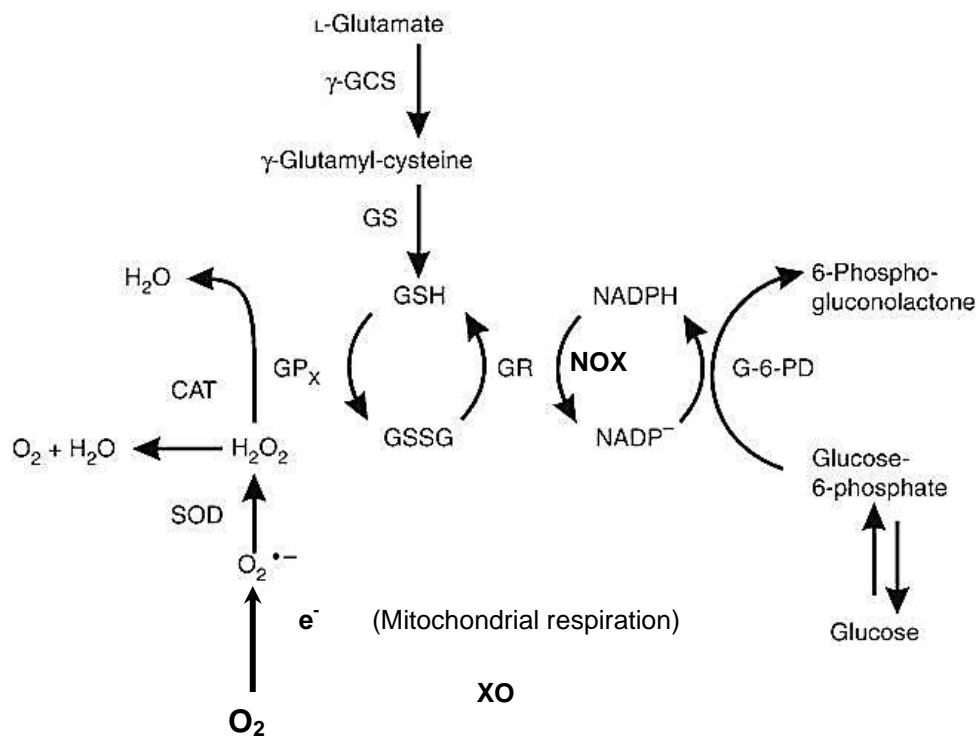
Figure 2.5: Reactions involved in the generation of ROS as well as the AOx enzymes involved in ROS scavenging. The figure illustrates the reactions involved in the generation of ROS from molecular oxygen and the AOx pathways responsible for ROS scavenging. The interrelation between the pathways shown is an important biochemical feature of AOx activity (Modified from Kehinde et $al.$, 2016).

2.6.1.1. *NADPH oxidases*

NADPH oxidases (NOX) (Figure 2.4 and 2.5) is a group of enzymes consisting of NADPH nitric oxide 1-5 (NOX 1-5), dual oxidase 1 and 2 (DUOX1 and 2) that are present in the endothelial cells, fibroblasts and SMCs of the vascular wall (Drummond et $al.$, 2011). The enzymes are localised at the plasma membrane and with co-factors NAD or NADPH catalyse the single-electron reduction of O_2 to generate O_2^- (Altenhofer et $al.$, 2012), producing superoxide. Multiple protein components of the NADPH oxidase must be assembled on the cell membrane for the enzymes to become active (Drummond et $al.$, 2011). Increased activity of these enzymes is associated with many disorders including the development of CVD.

2.6.1.2. Xanthine oxidase

XO is mostly found in the liver and is primarily synthesised as xanthine dehydrogenase (XDH) which is then converted to XO by proteolysis. Circulating XO adheres to endothelial cells by associating with endothelial glycosaminoglycans and produces O_2^- and H_2O_2 by donating electrons to molecular oxygen (Figure 2.5). Allopurinol and oxypurinol are inhibitors of XO. Oxypurinol reduces O_2^- production and improves endothelial function in blood vessels in hyperlipidemic animals (Ohara *et al.*, 1993), which suggests a contribution of XO to endothelial ROS production. Evidence also exists that epithelial cells also express XDH, which can be converted to XO, which is upregulated when the activity of NOX is increased (Forstermann, 2010).

In hypertension an increase in NOX is believed to be the primary source of ROS (Landmesser *et al.*, 2003; Matsuno *et al.*, 2003; Li *et al.*, 2006), with eNOS uncoupling being secondary to NOX activation, which is further attributed to (6R-)5,6,7,8-tetrahdrobiopterin (BH$_4$) oxidation (Landmesser *et al.*, 2003). In hypercholesterolemia patients with coronary artery disease, NOX and XO are the major sources of O_2^-, providing 62% and 25% of O_2^- respectively (Guzik *et al.*, 2002). Uncoupling of eNOS contributing to oxidative stress is again likely to be secondary to oxidative stress caused by NOX and XO. Native LDL and oxidised LDL have been shown to stimulate O_2^- and ONOO$^-$ production and to uncouple eNOS (Pritchard *et al.*, 1995; Stepp *et al.*, 2002). LDL treated endothelial cells have shown eNOS uncoupling and ROS production, both in hypercholesterolemic a lipoprotein E knockout (ApoE-KO) mice (Xia *et al.*, 2010) and in hypercholesterolemia patients (Stroes *et al.*, 1997).

Compounds in cigarette smoke such as Cd have been found to upregulate NOX (Jaimes *et al.*, 2004) and impair mitochondrial function, causing mitochondrial oxidative stress (Csiszar *et al.*, 2009). These compounds may potentiate the pro-oxidative activity of LDL by inducing oxidative modifications of LDL, as oxidised LDL is more potent in activating NOX than native LDL (Steffen *et al.*, 2012).

2.6.1.3. Catalase

CAT is a tetramer of four polypeptides, with four porphyrin heme iron groups that allows it to react with H_2O_2, accelerating its decomposition to oxygen and water. The overexpression of CAT has protective effects on the CVS, such as reduced atherosclerosis and inhibition of angiotensin II (ANGII) induced aortic wall hypertrophy (Zhang *et al.*, 2005).

No alterations were observed in CAT activity on Cd exposure (Novelli *et al.*, 2000), but another study showed that following exposure to Cd, CAT levels in rats were increased (Ognjanovic *et al.*, 2003). Hg causes an inhibition of CAT (Brandão *et al.*, 2008). Monteiro *et al.*, 2010 showed that following a 96-h exposure to inorganic Hg, significant alterations in the expression of the AOx enzymes SOD, CAT, GST, GPx, and GR were observed, leading to oxidation of lipids and

proteins. Induction of the SOD-CAT systems represents a rapid adaptive response to Hg exposure (Novelli *et al.*, 2000).

2.6.1.4. Superoxide dismutase

Three isoforms of SOD exist in humans, and all three catalyse the dismutation of O_2^- into oxygen and H_2O_2 (Figure 2.4) and therefore have an important AOx function. These isoforms of SOD are; SOD1 (Cu-Zn-SOD), which is a soluble enzyme located primarily in the cytoplasm but can also be found in the mitochondrial intermembrane space, SOD2 (Mn-SOD), which is found in the mitochondria and SOD3 (EC-SOD), which is a secreted extracellular enzyme (Förstermann and Sessa, 2012). Cd exposure lowers SOD activity (Kowalczyk *et al.,* 2002) and it was shown that Cd significantly lowered activity of AOx enzymes in rats including SOD (Novelli *et al.,* 2000). SOD activity is inhibited on exposure to Hg (Brandão *et al.*, 2008) and a decrease in SOD activity was observed in fish exposed to Hg (Monteiro *et al.*, 2010).

2.6.1.5. GPx and associated GSH

GPx has eight isoforms (GPx1-8) in humans, with GPx1 being the most abundant in the cytoplasm. It reduces H_2O_2 to water and lipid hydroperoxides to their alcohols. Mice with disrupted GPx1 gene function are susceptible to myocardial ischemia- reperfusion injury (Yoshida *et al.*, 1997). The activity of GPX1 in erythrocytes of patients with coronary artery disease is inversely associated with the risk of CVD (Blankenberg *et al.*, 2003). Cd and Hg exposure has also been found to significantly increased malondialdehyde (MDA) levels; a marker of lipid damage (Aflanie *et al.*, 2015).

GSH scavenges intracellular oxygen radicals either directly or via the GSH peroxidase/GSH system. Hg reacts with the thiol groups of GSH, which can induce GSH depletion and oxidative stress in tissue (Stohs and Bagchi, 1995). Several researchers have also observed increases in GSH levels following Hg exposure (Rana *et al.*, 1995; Elia *et al.*, 2000). Depletion of GSH was reported by Elia *et al.* (2003) and Mieiro *et al.* (2010). This could be the result of direct binding of the metal to GSH via the SH group and formation of a metal-SG complex, or of enhanced oxidation of this thiol (Elia *et al.*, 2003). In addition Hg can also inhibit the AOx enzymes (Figure 2.5).

2.6.2. Effect of ROS on lipid, protein and DNA

Lipid oxidation occurs in the phospholipid bilayers of cell membranes. A decrease of thermal denaturation of cells and lipid membrane mobility as well as an increased lipid surface charge are some of the effects of increased lipid peroxidation (El-Bahr, 2013). MDA is one of the most common products of lipid peroxidation and it is known to react with free amino acid groups of proteins and nucleic acids to induce immune system dysfunction. Increased lipid peroxidation products are found in atherosclerosis where oxidative alterations of LDL have been found to be associated with CVD (Girotti, 1998; Nedeljkovic, 2003; Vijaykumar and Lokesh, 2004).

Hydroxyl radicals cause protein modification which leads to oxidation of amino acid side chains, protein cross linkage and fragmentation. MDA from lipid peroxidation also reacts with amino groups, and NO and ONOO$^-$ are oxidising agents of protein (El-Bahr, 2013).

Mitochondrial DNA (mtDNA) is very susceptible to oxidative stress due to its close location to the ROS producing system, the mitochondrial electron transport chain (METC), the presence of DNA and lack of protective proteins. Hydroxyl radicals oxidise guaniosine or thymine, which can lead to carcinogenesis if the oxidative stress is too great and the glycosylase DNA repair system fails (El-Bahr, 2013).

2.7. <u>Oxidative damage and the cardiovascular system</u>

The CVS consists of the blood, the heart and blood vessels which are all interrelated and allow for the transport of all body fluids. The primary function of the CVS is the transport of oxygen and nutrients to tissues, and the transport of carbon dioxide and other metabolic waste from tissues. This system is also involved in hormonal transport, temperature regulation and transport of cells of the immune system. The blood vascular system and the lymph vascular system form the two functional components of the CVS (Tortora and Derrickson, 2006; Young and Heath, 2006), however for the purpose of this study, the focus will be on the blood vascular system.

Oxidative stress leads to both structural and functional changes which can result in pathological remodelling of the myocardium, fibrosis and contractile dysfunction of the heart and blood vessels and function of erythrocytes. The consquence of heavy metal induced oxidative damage on the major components of the blood vascular system will be discussed in greater detail.

2.7.1. Erythrocytes and platelets

Erythrocytes are the major cellular component of blood and transports oxygen and carbon dioxide. These cells are highly specialised and structurally adapted for this process. Erythrocytes consist of an outer plasma membrane enclosing haemaglobin and contain only a limited number of enzymes; those nescessary for the maintenance of the plasma membrane integrity and gaseous transfer. The cell nucleus is removed before their release from bone marrow into circulation and cell organelles degenerate. Erythrocytes have a biconcave disk shape, increasing the surface area for gaseous exchange (Young and Heath, 2006). The cells however do have have high levels of CAT, acting as an AOx enzyme due to the large amounts of cellular oxygen. In the experiments in which oxidative stress is evaluated, erythrocytes are used as cellular models due to their simple structure as well as the relatively large amounts of membrane associated polyunsaturated fatty acids (Akyol *et al.*, 2001). Erythrocyte membranes are very sensitive to oxidative stress *in vitro,* and this can be used to reflect the vulnerability of other cell membranes to oxidative damage *in vivo.*

Severe oxidative stress and inflammation activate redox-sensitive nuclear transcriptional factor kappa B (NFkB) (Manna *et al.*, 2005; Gloire *et al.*, 2006) which results in an inflammatory response

and tissue injury through the production of cyclooxygenases -1 and -2 (COX-1 and COX-2) (Liang *et al.*, 2007; Sagai and Bocci, 2011) prostaglandins (PG), thromboxanes (TXA) and prostacyclins (PC) whose production is elevated by COX are involved in alterations of vascular structure and function in CVD (Berk *et al.*, 2013; Ganesh, 2013; Hernanz *et al.*, 2014). COX-2, PG and TXA are also involved in the blood coagulation system. COX-1 and COX-2 are expressed in platelets and COX-1 dependant and independent mechanisms enhance the interactions between erythrocytes and platelets (Valles *et al.*, 2013), along with mediating the production of PGs and thromboxanes, which are also found in platelets (Goggs and Poole, 2012). Erythrocytes also contain PGs and express PC receptor (PG12) (Knebel *et al.*, 2013). Activated platelets produce TXAs (TXA$_2$) that have prothrombotic properties, stimulate the activation of platelets and increase their aggregation (Angiolillo *et al.*, 2013; Rao, 2013; Manolis *et al.*, 2013; de Sousa and Tricoci, 2013). In this process, erythrocytes become elongated and fibrin networks become matted and dense (Pretorius *et al.*, 2014).

Coagulation forms part of a normal wound healing process in a response to vascular injury and inflammation in order to prevent excessive blood loss (Monroe and Hoffman, 2012). The process of coagulation involves the formation of a stable blood clot, made up of aggregated platelets, trapped in a net or mesh of fibrin fibres (Versteeg *et al.*, 2013; Yau *et al.*, 2015). Coagulation occurs in two phases; the first is primary homeostasis where platelets aggregate to form a platelet plug and the secondary homeostasis involving activation. Recently the blood vessel wall has been included in the factors involved in the cell-based model of coagulation as it includes tissue factor expressing cells. The model is categorized into three phases: initiation, amplification and propagation (Pérez-Gómez and Bover, 2007; Smith, 2009; Van Rooy, 2015). These phases will be described in greater detail below.

The initiation phase occurs after vascular injury, resulting in an activation of the endothelial and sub-endothelial cells which includes the SMCs and fibroblasts. Sub-endothelial collagen is exposed to the blood and mediates the initial adhesion of circulating platelets to the exposed collagen surface via von Willebrand factor (vWf). The platelet aggregate that forms is responsible for stopping blood loss. Concurrently the injured endothelium releases tissue factor (TF) which is a powerful pro-coagulant molecule which binds with circulating coagulation factor (f) VII. TF acts as a cofactor for fVII promoting the proteolysis and activation of fVII to become active fVII (fVIIa). TF then also binds with fVIIa to form the TF/fVIIa complex. The TF/fVIIa complex then goes on to proteolytically cleave fIX and fX into fIXa and fXa, respectively. FIXa serves to generate more fXa and fXa serves to generate thrombin. In the amplification phase, circulating platelets that have migrated to and adhered to the site of injury become activated by thrombin and form a platelet aggregate. This provides a surface for the activation of other procoagulant factors. Thrombin also cleaves platelet derived fV and fVIII to fVa and fVIIIa. fVIIIa and fVa together form a prothrombinase complex and this complex further cleaves prothrombin III into thrombin IIa (Smith, 2009; Swanepoel, *et al.*, 2015). Additionally, thrombin converts fXI into fXIa and this then promotes

fIXa generation, and in the presence of calcium fV is cleaved into fVa on the surface of the platelet. This activation of platelets leads to morphological alterations to the platelets, which include shuffling of membrane phospholipids and a release of granular content. Thrombin also affects vWf of fVIII and activates it to fVIIIa. The free vWF can then mediate platelet adhesion and aggregation (Smith, 2009). This aggregation of platelets results in cell to cell interactions that cause an increase in the amount of granular content and a recruitment of more platelets into the thrombus.

In the last phase, the propagation phase, the thrombin generation and thrombin catalysed cleavage is further amplified on the surface of the platelets. The prothrombinase complex is formed through the binding of fVa and fXa, and the intrinsic tenase complex is formed through the binding of fVIIIa and fIXa. These two complexes serve to enhance the activities of fXa and fIXa previously generated in the amplification phase, thereby creating large quantities of thrombin from the binding of fXa to fVa, and cleavage of prothrombin (fII) into thrombin (fIIa) in order to produce sufficient quantities of fibrin through thrombin's cleavage of fibrinopeptide A from fibrinogen. Thrombin also cleaves fXIII into fXIIIa which serves to create cross links between fibrin chains to forms a network of fibrin fibres, creating a stable fibrin clot or thrombus that seals the site of injury, reinforcing the initial platelet plug and prevents blood loss (Smith 2009; Versteeg *et al.*, 2013, Yau *et al.*, 2015; Kell and Pretorius, 2017).

Tight regulation of the blood coagulation system is required to prevent unnecessary clot formation and the occurrence of thrombosis (Versteeg *et al.*, 2013; Yau *et al.*, 2015). The coagulation proteases and molecules can be inhibited by either direct inhibition of protease activity or through degradation of coagulation factors (Versteeg *et al.*, 2013; Yau *et al.*, 2015). Circulating protease inhibitors such as antithrombin, heparin cofactor II, tissue factor pathway inhibitor (TFPI) and C1 inhibitor are able to bind with the active site of proteases and inhibit protease activity, interrupting the coagulation cascade. The coagulation factors themselves can also be degraded by the activation of the protein C/protein S pathway. The protein C/protein S pathway inactivates fVa and fVIIIa and is catalysed by the presence of thrombomodulin and endothelial protein C receptor (EPCR) (Versteeg *et al.*, 2013; Yau *et al.*, 2015). The disruption of platelet adhesion and inhibition of further recruitment of platelets through the interruption of vWf by a disintegrin and metalloproteinase with a thrombospondin type 1 motif, member 13 (ADAMTS13) also known as von Willebrand factor-cleaving protease (vWfCP) is another coagulation control pathway (Versteeg *et al.*, 2013; Yau *et al.*, 2015). The final fibrinolysis, the dissolution of the thrombus matrix is triggered by activation of tissue-type plasminogen activator (tPA), which catalyses the conversion of plasminogen to plasmin (Versteeg *et al.*, 2013; Yau *et al.*, 2015). Plasmin breaks down the thrombus through proteolysis (Van Rooy, 2015). Premature clot dissolution is also under strict control via the plasminogen activator inhibitor – I (PAI-I) which serves to prevent the premature activation of plasminogen (Van Rooy, 2015). These individual events come together to ensure the strict regulation of the coagulation system.

Along with the platelets and erythrocytes which are classically associated with a clot, other cellular components of coagulation include the leukocytes (Gorbet and Sefton, 2004). The leukocytes release inflammatory mediators and oxidants such as H_2O_2 and SOD. The association of leukocytes and platelets may lead to platelets and leukocyte activation, the latter releasing inflammatory mediators, protecting against inhibitors of coagulation, in turn increasing the coagulation process (Gorbet and Sefton, 2004).

Due to its location, and close contact with the blood, the endothelium plays an essential role in thrombus development. Leukocytes and platelets adhere to the vascular endothelium and this is an important feature of the proinflammatory and prothrombogenic ability of the vascular endothelium, often observed in oxidative stress. The interactions of blood cells and endothelium have been linked to enhanced ROS production from XO, NADPH, and NOS. ROS promotes the proinflammatory and prothrombogenic potential of the vascular endothelium through several mechanisms. These mechanisms include NO formation, the activation of redox-sensitive transcription factors such as NFĸB that govern the expression of endothelial cell adhesion molecules, and enzymes that produce leukocyte-stimulating inflammatory mediators (Cooper *et al.*, 2002).

Alterations to the endothelium, erythrocyte, platelet, and fibrin fibres function and structure easily affects the closely regulated and step-dependant coagulation system. A haemostasis between antithrombotic and pro thrombotic activity is required to prevent thrombi formation or haemorrhage (Van Rooy, 2015). Heavy metals have been found to influence the coagulation system. An increase in the release of poorly ligated iron causes changes in fibrin and erythrocyte morphology (Bester *et al.*, 2012; Kell and Pretorius 2014; Pretorius and Kell 2014; Pretorius *et al.*, 2014b), such that added iron affect coagulation and erythrocyte structure (Lipinski *et al.*, 2012; Pretorius and Lipinski, 2013). Ferric ions can activate non-enzymatic blood coagulation which results in the formation of fibrin-like dense matted deposits (DMDs) (Pretorius and Lipinski, 2012; Pretorius *et al.*, 2013a; Pretorius *et al.*, 2013b). Iron is known to cause an oxidative modification of thrombin (Azizova *et al.*, 2009) and change the structural morphology of this protein (Lipinski *et al.*, 2012). Both Cd and Hg exposure is associated with increased oxidative stress and inflammation (Dallüge *et al.*, 2002; Sopjani *et al.*, 2008; Lupescu *et al.*, 2012; Fresquez *et al.*, 2013; Pretorius, *et al.*, 2014; Lang and Lang, 2015) and therefore can adversely affect blood haemostasis.

Changes in erythrocyte morphology may also affect the coagulation system. Eryptosis, the term given for apoptosis of erythrocytes, may be brought on by oxidative stress as well as energy depletion, hyperosmotic shock and hyperthermia. Eryptosis is characterised by morphological changes such as cell shrinkage, blebbing and membrane scrambling (Sopjani *et al.*, 2008; Lang and Qadri 2012; Pretorius *et al.*, 2014; Lang and Lang 2015). The process of eryptosis is triggered by the exposure of phosphatidylserine (PS) located on the outer leaflet of the cell membrane. The PS exposure leads to the formation of membrane vesicles, shedding of microparticles and

pathological alterations to erythrocyte morphology (Pretorius *et al.*, 2016). The presence of oxidative stress may increase cystolic Ca^{2+} in turn activating the Ca^{2+} sensitive K^+, causing cell shrinkage as a result of K^+ exit from cell (Pretorius *et al.*, 2016). An activation of scrambalase through the stimulation of ceramide formation from sphingomyelinase and subsequent Ca^{2+} and ceramide mediated scramblase activation also causes PS exposure (Pretorius *et al.*, 2016). Cell shrinkage and cell membrane scrambling are also mediated through Ca^{2+} activation of calpain which then degrades the R-complex of the cytoskeleton. Eryptotic erythrocytes are removed from the circulation by macrophages (Pretorius *et al.*, 2016). Eryptosis with regards to the heavy metals Cd and Hg and their combination is further discussed in chapters 5 and 6.

2.7.2. Endothelium

The endothelial layer is the internal layer of blood vessels and is in direct contact with blood and plays an important role in the physiological functioning of the circulatory system. The luminal surface of the endothelial cells contains heparin-sulphate which is a potent anticoagulant (Catieau *et al.*, 2018) while in contrast the type I and type III collagen of the blood vessels is thrombogenic (Sakariassen *et al.*, 1990; Cho and Mosher, 2006). The endothelium therefore acts as a smooth non-thrombogenic lining that separates the wall contents from the flowing blood. Along with the function in coagulation, endothelium allows selective transport of substances from the blood stream into other tissues of the body. Vasoactive substances such as NO, PC, endothelin (ET) 1 (ET-1) and ANGII, connective tissue (Type IV collagen and proteoglycans) are synthesised by the endothelium as well as growth regulatory molecules such as vascular endothelial growth factor (VEGF), platelet derived growth factor (PDGF), epidermal growth factor (EGF), and modifies plasma lipoproteins for transport into the arterial wall (Cahill and Redmond, 2016).

2.7.2.1. Nitric oxide formation and endothelial dysfunction

NO regulates cardiac function by vascular dependant and independent effects (Massion *et al.*, 2003). Vascular dependant functions include the regulation of vessel tone in coronary vessels, thrombogenicity and proliferative and anti-inflammatory properties. Cellular cross talk is also regulated by NO during angiogenesis. Vascular independent pathways include direct effects of NO on cardiomyocytes contractility and mitochondrial respiration (Massion *et al.*, 2003). The effects of excess NO on cardiac function include increased oxygen consumption and diastolic dysfunction (Sanders *et al.*, 2001).

Three nitric oxide synthase (NOS) isoforms exist in cardiac tissue; neuronal NOS (nNOS), endothelial NOS (eNOS) which are naturally expressed by the myocardium, and the inducible isoform NOS (iNOS). NOS enzymes catalyse the oxidation of L-arginine to L-citrulline with release of NO (Zhang *et al.*, 2002). Endothelial NO induces vasodilation and inhibits platelet aggregation and adhesion, as well as preventing atherogenesis. Endothelial dysfunction is associated with the inability of the endothelium to generate sufficient amounts of NO, and oxidative stress further

contributes to endothelial dysfunction by the rapid oxidative inactivation of NO by excess O_2^-, which reacts with NO reducing the availability of NO. This is the major mechanism of endothelial dysfunction observed in CVD (Forstermann, 2010). Secondary to this, is the resulting product of the reaction of O_2^- with NO reaction to form the peryoxynitrite ($ONOO^-$) which may disrupt eNOS functioning. Uncoupling of eNOS is evident in various animal models as well as in patients with endothelial dysfunction and it is thought to be mainly caused by a depletion of the essential cofactor for the eNOS enzyme, BH_4. BH_4 can be oxidised by $ONOO^-$, leading to a deficiency in BH_4 (Förstermann, 2008; Föstermann and Sessa, 2012).

A direct relationship exists between the levels of NO secretion and levels of iNOS expression (Sanders *et al.*, 2001). When stimulated by a proinflammatory stimulus, such as cytokine tumour necrosis factor (TNF-α), all cardiac cell types can express iNOS (Stein *et al.*, 1996). Elevated levels of iNOS are seen in age related CVD or dysfunction where the increased NO production from iNOS rather than eNOS may result in cellular toxicity (Rodriguez-Manas *et al.*, 2009; Wadley *et al.*, 2013). The reactions generating NOS and ROS are summarised in Figure 2.4 where $O_2^{\cdot-}$ is produced as a by-product of molecular oxygen metabolism during mitochondrial oxidative phosphorylation. NO or SOD inactivates $O_2^{\cdot-}$ SOD enzymes rapidly convert $O_2^{\cdot-}$ to H_2O_2, which is then degraded by GPx and CAT to water. A single-electron reduction of H_2O_2 may lead to the formation of highly reactive OH radicals, either via the Fenton reaction with iron as catalyst, or via Haber-Weiss reaction by reacting with $O_2^{\cdot-}$. The reaction of $O_2^{\cdot-}$ with NO results in the inactivation of cytoprotective NO and the formation of reactive $^{\cdot}ONOO^-$.

2.7.3. Cardiac and smooth muscle

Vascular smooth muscle cells (VSMC) are an important component of blood vessels walls. These cells are the predominant cell type in the tunica media of medium sized muscular arteries such as the coronary arteries. The tunica media of medium sized arteries contains well developed layers of muscle fibres and some fine elastic fibres. There may be 30 or more layers of SMCs while the internal elastic lamina is usually a distinct layer, while the external elastic lamina is less well defined. The tunica media of large arteries on the other hand is highly developed and contains 50+ layers of elastic fibres arranged in circumferential sheets between layers of SMCs and collagen. The tunica intima of large vessels contains endothelial cells with a thin underlying layer of fibro-collagenous tissue (Stevens and Lowe, 2010).

VSMCs are spindle shaped and are 100 μm long and 5 μm in diameter, except near the nucleus where they are slightly wider. SMC rest on a thin (40 – 80 nm) basement membrane, and communicate via gap junctions. Intracellular myofilaments are typically orientated along the axis of the cell, and cell to cell force transmission is accomplished through thin reticular collagen fibres which connect the membranous sheaths on each cell (Stevens and Lowe, 2010).

The myocardium is composed of cardiac muscle and the fibres are shorter in length and less circular in a transverse section when compared to skeletal muscle fibres. Cardiac muscle fibres also exhibit branching, and a typical fibre is 50 – 100 μm long, with a diameter of around 14 μm. The fibres usually have one central nucleus, with double nucleated cells occurring occasionally. Ends of cardiac muscle fibres connect to neighbouring fibres by intercalated disks which are irregular transverse thickenings of the sarcolemma and are held together by desmosomes. Gap junctions in the fibres allow muscle action potentials to conduct from one muscle fibre to the next. Mitochondria of cardiac muscle are larger in size and number, taking up 25% of the cytosolic space. Actin and myosin are arranged in the same way as in skeletal muscle, as well as the bands, zones and Z disks. Transverse tubules in cardiac muscle are wider than those in skeletal muscle but are less abundant, with one transverse tubule per sarcomere being located at the Z disk. Cardiac muscle fibres have a smaller sarcoplasmic reticulum and as a result smaller intracellular reserves of Ca^{2+} are present (Tortora and Derrickson, 2006).

2.7.3.1. Susceptibility of contractile tissue to oxidative damage

Muscle cells have high rates of energy utilization and therefore many mitochondria which are vulnerable to the effects of oxidative stress. Cellular functions naturally decline over time and this is accompanied by an increase in ROS or RNS production and autophagy causing ageing (Rubinsztein *et al.*, 2011; Morales *et al.*, 2014), as a consequence of oxidation and damage of mitochondria and cellular components. In cardiomyocytes, autophagy, ROS or RNS pathways communicate with each other through transcriptional and post-transcriptional events. This communication regulates events governing cardiac disease pathogenesis, such as the structural integrity of cardiomyocytes, promotion of proteostasis and reduction of inflammation (Morales *et al.*, 2014). ROS regulation and its association with autophagy and the maintenance of an optimal redox status is necessary for cellular homeostasis, as dysregulation can lead to pathogenesis (Nediani *et al.*, 2011; Chaiswing and Oberly, 2010; Hill and Olson, 2011; Kuster *et al.*, 2010; Shao *et al.*, 2010).

2.7.3.2. Mitochondrial electron transport chain

The METC is localized in the inner mitochondrial membrane. The METC is formed by a series of cytochrome-based enzymes (complex I: NADH dehydrogenase; complex III: cytochrome b-c1 oxidase; complex IV: cytochrome oxidase and the smaller molecules coenzyme Q) that transfers electrons to molecular oxygen (Tsutsui *et al.*, 2011). O^{2-} in significant amounts is formed by the electron transport chain (ETC) complexes I and III of the mitochondria as shown in Figure 2.6. Flavin adenine dinucleotide ($FADH_2$) in the ETC donates its e− directly to Q. During this process, the high free energy of the electrons is gradually extracted and converted into ATP. Physiologically, >98% of e⁻ are tightly coupled with the production of ATP, and only 1–2% "leak" to form superoxide and are scavenged by mitochondrial SOD. However, when the ETC is blocked at the level of complex I or III, e⁻ are inappropriately diverted by one electron reduction directly to O_2,

with the resulting formation of a large amount of O_2^-. Superoxide is released at complex I into the extracellular matrix (ECM) and this complex is considered the main producer of superoxide due to reverse electron flow in complex III under low adenosine diphosphate (ADP) conditions. The SOD-2 converts O_2^- to H_2O_2 which in turn is reduced to water by GPx or CAT. Superoxide dismutase -2 is therefore important in the detoxification of O_2^- to prevent the generation of $ONOO^-$ or oxidative damage of ETC proteins and mtDNA.

Superoxide is also released by complex III to the mitochondrial intermembrane space where it is dismutated by SOD1. Mitochondrial ROS production varies according to ETC efficiency, oxygen or electron donor availability, uncoupling proteins and cardiovascular risk factors. Mitochondria are also ROS sensitive and oxidative damage lowers activity and further increases ROS production (Davidson and Duchen, 2007). Mitochondrial ROS promote the activity of other ROS sources mentioned above (Schulz *et al.*, 2014), and stimulate the release of mitochondrial apoptotic factors, such as cytochrome c, AIFM1 or Diablo, with vascular cells showing differential sensitivity to stress conditions (Zeini *et al.*, 2007). An increase in cell death during the atherosclerotic process contributes to the formation of a necrotic core in plaques which can result in atherothrombosis (Madamanchi and Runge, 2007), indicating the role of oxidative stress in vascular disease, which is further highlighted by findings that cardiomyopathy occurs in SOD2$^{-/-}$ mice with elevated mitochondrial ROS levels (Kokoszka *et al.*, 2001).
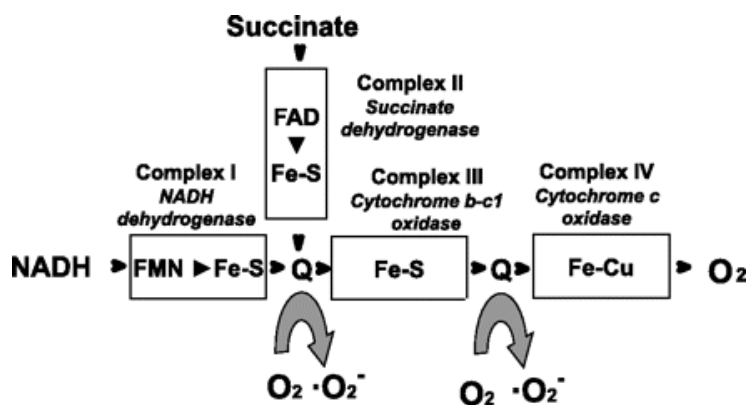
Figure 2.6: The METC. Transport starts with the transfer of e−from NADH+ to the iron-sulphur (Fe-S) centre of NADH dehydrogenase, which passes them to Q, complex III, cytochrome c, complex IV, and finally to molecular oxygen (Tsutsui *et al.*, 2011).

Lipid peroxidation occurs when free radicals react with membrane lipids, capturing the electrons to produce non radical species. Oxidised lipids and their products are then fragmented to produce MDA and 4-hydroxynonenal, together with a loss of membrane integrity. A controlled presence of ROS can induce cardioprotection, but an excess presence induces irreversible oxidation and amino acid nitration to trigger protein denaturation, aggregation and degradation. Protein oxidation can also be caused by a conjugation reaction with lipid peroxidation products. MDA and other

products of lipid peroxidation are able to form adducts with DNA bases, which can lead to gene expression alterations, and the induction of apoptosis (Tsutsui *et al.*, 2006; Morales *et al.*, 2014).

2.7.4. Fibroblasts and fibrosis

Cardiac fibroblasts contribute to cardiac development, structure and cell signalling. Histologically, these fibroblasts appear as elongated cells with condensed nuclei and are arranged parallel to the direction of collagen fibres. The cytoplasm is reduced in volume with long cytoplasmic processes that connect with other fibroblasts. Cardiac fibroblasts are large cells with a moderately condensed nucleus with a small quantity of cytoplasm, most of which is filled with rough endoplasmic reticulum (RER). Golgi apparatus and a few mitochondria are also present (Young and Heath, 2006). The fibroblasts produce collagen and elastic fibre.

The ECM in the vessel walls includes collagen and elastin (structural proteins) and laminin and fibronectin (adhesive proteins). Normal arteries consist of the collagens I and III (tunica intima, media and adventitia) and collagens I, III, IV and V are in endothelial and SMC membranes. Cardiac fibroblasts produce collagens I, III and VI (Camelliti *et al.*, 2005). Vascular fibrosis associated with hypertension involves an increase in the production and deposition of collagen, fibronectin and other ECM components in the arterial wall. A decrease of matrix metalloproteinase (MMPs) enzymes involved in the degradation of ECM proteins and an increase in MMP inhibitors may contribute to changes to the turnover of type I collagen, which may ultimately lead to increased collagen deposition. Together with this, there may be an increase in the cell-matrix attachment sites that may affect arterial structure (Intengan and Schiffrin, 2001). The thickening of arterial walls may increase the peripheral resistance and blood pressure, with collagen deposition increasing wall stiffness and reducing the diameter of the lumen. Oxidative stress has been found to trigger cardiac fibrosis in diabetic rats (Aragno *et al.*, 2008) indicating that low grade inflammation, vascular fibrosis and autophagy may determine the degree of remodelling that occurs (Intengan and Schiffrin, 2001).

Several studies have shown that oxidative damage causes fibrosis of the liver and lungs (Ghatak *et al.*, 2011; Ceresh *et al.*, 2013, Xiao *et al.*, 2014). No animal-based studies could be found that showed a direct link between oxidative damage and fibrosis of the CVS and heavy metal exposure. Studies in diabetic rats have shown increased levels of oxidative damage leads to fibrosis of the CVS (Aragno *et al.*, 2008).

2.7.5. Modes of cell death in the CVS as a result of oxidative stress

Cardiomyocytes are postmitotic cells incapable of replication and therefore rely greatly on the elimination of toxic proteins and dysfunctional organelles (Cao *et al.*, 2009; Pattison *et al.*, 2011; Tannous *et al.*, 2008). The contractile function of cardiomyocytes requires high levels of energy and consquently cardiomyocytes have a high mitochondral density. Impaired AOx mechanisms can lead to an increase in oxidative damage and mitochondrial dysfunction. Three classical forms

27

of cell death are apoptosis, autophagy, and necrosis. These three forms are classified according to the morphological features and distinct signalling pathways (Degterev *et al.*, 2005; Chen *et al.*, 2018; Zhe-Wei *et al.*, 2018). Autophagy is described as a form of degradation rather than cell death, with the ability to induce cell death. Autophagy is induced prior to apoptosis as a result of stimulation induced by stress, and apoptosis is induced when autophagic processes fail to prevent cellular dysfunction. Multiple signalling pathways therefore independently control different types of cell death. However, the pathways are interconnected, and the three types of cell death are able to be induced concurrently, successively or operate in parallel following exposure to harmful stimuli or stress (Chen *et al.*, 2018). In terms of cell survival potential after induction of each process, autophagy has the most potential for survival, followed by apoptosis and finally necrosis (Chen *et al.*, 2018). All three processes occur in cardiac myocytes and cell death; both gradual and acute are indicators of cardiac pathology including heart failure (HF) and myocardial infarction (MI) (Chiong *et al.*, 2011). The pharmacological inhibition of these processes has been used to improve cardiac function.

2.7.5.1. Autophagy

A fine balance between ROS formation and AOx elements such as (GSH, vitamin C and E) and enzymes (CAT, SOD and GPx) are required to ensure normal tissue functioning. An imbalance leads to activation of certain cellular pathways leading to fibrosis, defective Ca^{2+} metabolism, adnormal contraction and eventaully cell death. To retain normal cellular functioning, the process of autophagy removes defective and damaged organelles. In addition as described in Sections 2.6.1.1 and 2.6.1.2 NOX, XO as well as the different isoforms of NO play an important role in this process. The balance of ROS and RNS in cardic stress is shown in Figure 2.7. This balance between the oxidants and AOxs is important in normal cardiac function and a normal autophagic balance is required for homeostasis. ROS generation, accumulation and AOx systems decline in the CVS can be mediated by a variety of factors leading to a loss of redox balance. The loss of redox balance can then lead to a remodelling of organelles and ECM components. Thereby autophagy can be considered as an antioxidative response in maintaining the redox balance by removing damaged cellular components (Morales *et al.*, 2014).
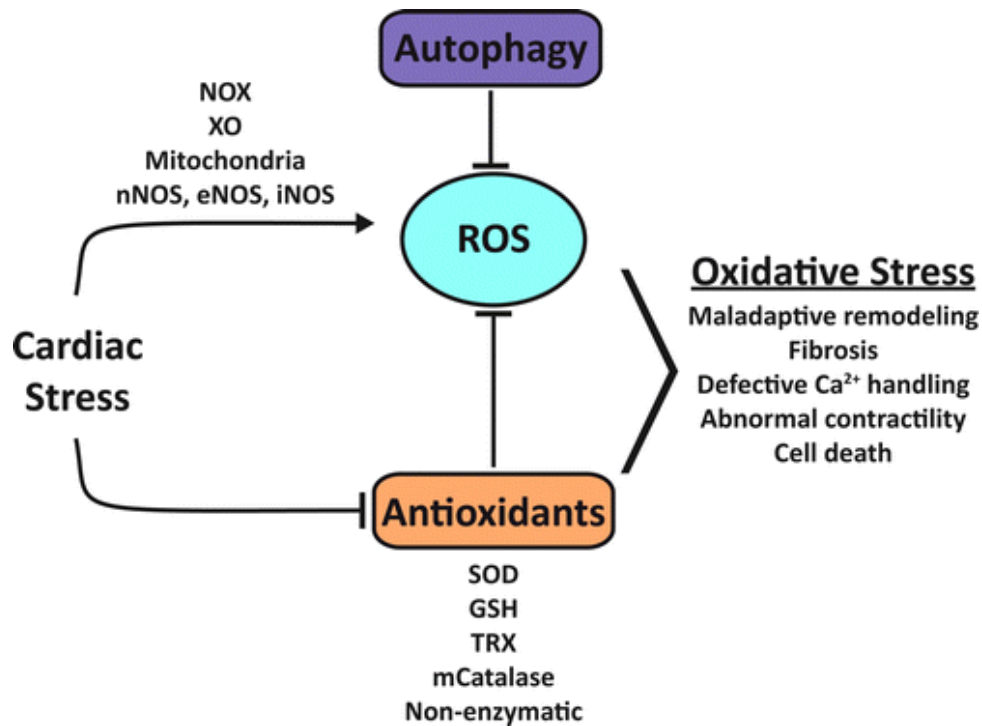
Figure 2.7: Summary of autophagy, AOx and ROS relationship in the maintenance of redox balance during cardiac stress (Morales *et al.*, 2014).

Autophagy is morphologically identified in tissue by the formation of the autophagosome, identified ultrastructurally by TEM. The autophagosome is a bilayered vesicle containing damaged organelles, proteins and other cytoplasmic components. Degradation of cellular components occurs when the autophagosome fuses with lysosomes. These are multiple cellular processes, which all lead to a degradation pathway mediated by lysosomes. Protein and organelle removal maintain homeostasis by elimination toxic or damaged cellular components (Cao *et al.*, 2009; Ravikumar *et al.*, 2010; Yang and Kilonsly, 2010). The degraded cellular components are then used as a source of energy and metabolites.

Autophagy is therefore a pro-survival mechanism utilised by cells (Chen *et al.*, 2018). Some of the trigger factors of autophagy include nutrient and oxygen deprivation, ROS, organelle and protein damage; the process taking place through the mammalian target of rapamycin (mTOR) dependant pathway (Chiong *et al.*, 2011). Mitophagy eliminates oxidative stress damaged mitochondria, removing a major potential source of ROS (Lee *et al.*, 2012; Morales *et al.*, 2014). Genetic models of defective autophagy highlight its role in oxidative stress, with various models (Listed by Morales *et al.*, 2014) showing increased ROS and the presence of enlarged and defective mitochondria (Mathew *et al.*, 2009; Pua *et al.*, 2009; Tal *et al.*, 2009; Takamura *et al.*, 2011). In the CVS autophagy has been observed in muscular dystrophy, CVA (Chen *et al.*, 2018) and mitochondrial damage in CVD (Bravo-San Pedro *et al.*, 2017). In animal models of CVD, there is increased autophagic activity (Nishino *et al.*, 2000; Chiong *et al.*, 2011; Nemchenko *et al.*, 2011; Xie *et al.*, 2011). Increased autophagy has been observed in human samples from diseased and failing

hearts (Kostin *et al.*, 2003). Recent evidence suggests that autophagy also removes atherosclerotic regions by hydrolizing cholesterol deposits in macrophages which prevents plaque formation and represses the inflammatory response (Liao *et al.*, 2012; Razani *et al.*, 2012).

An increase in the activity of Beclin1 has been suggested as a therapeutic target for autophagy related diseases (Chen *et al.*, 2018). Beclin1 is an essential element in the formation of an autophagosome, it dissociates from the B-cell lymphoma factor (Bcl-2) where it is localised to the phagophore to promote the recruitment of double membrane elongation factors (Ravikumar *et al.*, 2010; Yang and Kilonsly, 2010).

2.7.5.2. Apoptosis

Apoptosis is a caspase-mediated programmed process of cell death during which a cell undergoes self-destruction resulting in elimination of dying cells with minimal damage to the surrounding tissues (Averelli-Bates *et al.*, 2018; Chen *et al.*, 2018; Zhe-Wei *et al.*, 2018).

Apoptosis is characterised by cell shrinking, membrane blebbing, chromatin condensation and nuclear fragmentation, followed by the formation of apoptotic bodies that are digested by phagocytosis by neighbouring cells or macrophages (Averelli-Bates *et al.*, 2018; Chen *et al.*, 2018). Both intrinsic and extrinsic signals trigger apoptosis and these can include ROS, RNS, DNA damaging agents and environmental pollutants. Whether a cell dies by apoptosis or survives varies on the type of cell, its microenvironment and the toxicological agent (Redza-Dutordoir and Averill-Bates, 2016). Redza-Dutordoir and Averill-Bates provide a detailed explanation of the pathways of apoptosis as a result of ROS (Redza-Dutordoir and Averill-Bates, 2016). In the CVS apoptosis is also associated with ischemic CVA and heart disease. Targeting apoptotic pathways such as the broad-spectrum caspase inhibitor has been reported to treat apoptosis associated disease (Chen *et al.*, 2018).

Cadmium toxicity induces ER stress and apoptosis via impairing energy homoeostasis in cardiomyocytes (Chen *et al.*, 2015).

2.7.5.3. Necrosis and necroptosis

Loss of terminally differentiated cardiomyocytes is an important pathogenic factor in the development of heart failure. Myocardial apoptosis has been the main focus of cell death in the heart however necrosis has been recognised as a form of cell death in severe myocardial damage (Whelan *et al.*, 2010; Kung *et al.*, 2011; Zhang *et al.*, 2016).

For the longest time, necrosis has been considered an unregulated or passive and accidental cell death, with a non-physiological cause as it is predominantly caused, by physical or chemical trauma to the cell. Therefore, necrosis can be defined as a form of cell injury leading to cellular death of cells in tissues by autolysis (Zhe-Wei e*t al.*, 2018). Necrosis is characterised by the expansion or swelling of cellular organelles, loss of ATP, the rupture of plasma membranes,

release of cellular content and a subsequent secondary inflammatory response with potential pathological consequences (Chiong *et al.*, 2011; Chen *et al.*, 2018). Mitochondrial swelling and mitochondrial membrane rupture also produce necrosis (Chiong *et al.*, 2011). Recent research has shown that necrosis is in part regulated by signalling in a controlled manner. This type of necrosis has been termed necroptosis, programmed necrosis or caspase independent cell death (Chiong *et al.*, 2011). Necroptosis combines features of both necrosis and apoptosis (Zhang *et al.*, 2016). The signalling pathways of necroptosis involve the activation of ligands of death receptors by cytokines such as TNFα and activation of receptor-interacting protein (RIP) 1, which then mediates the activation of RIP3 and mixed lineage kinase domain like (MLKL), which are both necessary downstream mediators of necroptosis (Zhang *et al.*, 2016). RIP3-induced activation of Ca^{2+}/calmodulin-dependent protein kinase II (CaMKII), either by phosphorylation or oxidation or both, triggers the opening of the mitochondrial permeability transition pore (MPTP) and myocardial necroptosis. Elevated levels of ROS are therefore capable of causing necroptosis in this manner (Zhang *et al.*, 2016).

The regulation of factors and signalling pathways in necroptosis as well as its role in CVDs including vascular atherosclerosis, MI, myocarditis and cardiac remodelling are well discussed by Zhe-Wei *et al.* (2018). In the CVS, necroptosis has been proposed to be an important component in pathophysiology of CVD including vascular atherosclerosis, ischemia-reperfusion injury, myocardial infarction and cardiac remodelling as well as CVA (Zhe-Wei *et al.*, 2018; Chen *et al.*, 2018). An inhibition of necrosis was shown to reduce the CVD damage, and inhibitors of proteins involved in the necroptosis pathway have been created as treatments (Zhe-Wei *et al.*, 2018).

Heavy metals such as Cd and Hg are highly persistent in the environment, particularly in mine workers and in populations living near mining operations. South African operations, both industrial and artisan, have lead to the presence of these metals in the soil and water in the mining regions. Heavy metals are known to bioaccumulate and biomagnify in the food chain and become severely toxic to living organisms, causing toxicity in a variety of organ systems incuding reproductive (Yang *et al.*, 2003; Wirth and Mijal, 2010) central nervous system and urinary system (Bernhoft *et al.*, 2012). These toxic effects are considered to be an effect of the metals binding to and inactivating enzymes and functional proteins, as a result of oxidative damage which leads to the development of many pathological changes. The effects of heavy metals such as Cd and Hg alone and in combination on CVS was investigated in this study.

2.8.   Aim and objectives

2.8.1. Aim

The aim of this study was to investigate the effects of heavy metals Cd and Hg alone and in combination on the cardiovascular system.

2.8.2. Objectives

For Hg and Cd alone and in combination to objectives were to;

1. Investigate the effect of 28 day exposure to these metals on the cardiovascular system *in vivo* using the Sprague-Dawley rat model by;
    a. Firstly to establishing the Sprague-Dawley rat model.
    b. Determining the possible changes in the weights of the animals after exposure
    c. Determining the possible change in organ mass after exposure
    d. Determining the plasma levels of Cd and Hg after exposure
    e. Determining the effects on blood markers associated with toxicity.
    f. Evaluating the effects on tissue and cellular structure of the heart and aorta using light- and transmission electron microscopy.
    g. Determining whether the expression and distribution of connective tissue proteins in the heart and aorta was altered.

2. Investigate the effects of exposure to these metals on the blood vascular system *in vivo* using the Sprague-Dawley rat model to:
    a. Evaluate the effects on the ultrastructure of platelets using scanning electron microscopy.
    b. Evaluate the effects on the ultrastructure of fibrin networks using scanning electron microscopy.
    c. Evaluate the effects on the ultrastructure of erythrocytes using scanning electron microscopy.
    d. Evaluate the effects on the ultrastructure of the interaction between erythrocytes and fibrin networks in a blood clot by using scanning electron microscopy.

3. Investigate the effect of the heavy metals on an ex vivo human blood model to:
    a. Establish a human blood *ex vivo* model at Cd and Hg concentrations found in the rat model at termination after exposure.
    b. Evaluate the effects on the ultrastructure of platelets using scanning electron microscopy.
    c. Evaluate the effects on the ultrastructure of fibrin networks using scanning electron microscopy.

d. Evaluate the effects on the ultrastructure of erythrocytes using scanning electron microscopy.

e. Evaluate the effects on the ultrastructure of the interaction between erythrocytes and fibrin networks in a blood clot by using scanning electron microscopy

f. Compare the observed effects between the rat and human blood model

g. Determine whether the *ex vivo* human blood model can be used to study the effects of heavy metals.

Chapter 3: Implementation of the Sprague-Dawley rat model

3.1. Introduction

Animal models of CVD are widely used in the development of new pharmacological therapies (Leong *et al.*, 2015). In understanding CVD development, in animal models the environment and conditions can be controlled, and it is possible to investigate the effects on the heart and blood vessels which is not possible in human studies. Rodent physiology is similar to humans which allows research into disease as well as drug safety (Leong *et al.*, 2015). The Sprague-Dawley rat model is a successful model for studying human toxicity, pharmacology, reproduction and behavioural studies. This rat species is widely used in toxicity studies (Al-Attar, 2011; Radad *et al.*, 2014; Kazemi *et al.*, 2018) and as models of human conditions such as diabetes, obesity and CVD (Klocke *et al.*, 2007) including hypertension (Boluyt *et al.*, 1994; Leong *et al.*, 2008) and cardiotoxicity (Ansari *et al.*, 2013).

The adverse effects of heavy metals (Lindh *et al.*, 1996; Wirth *et al.*, 2010; Chuah and Teo, 2016; Kim *et al.*, 2018) have also been investigated using the rat model. The effects of Cd on the kidneys and liver (Brzóska *et al.*, 2003; Lee *et al.*, 2014; Alkushi *et al.*, 2018), blood morphology (Henríquez-Hernández *et al.*, 2017; Lopez – Rodriguez *et al.*, 2017), blood pressure (Puri and Shah, 2003) and the effect of Hg on the liver and kidneys have been investigated (Wang *et al.*, 2006; El-Shenawy and Hassan, 2008; Joshi *et al.*, 2014).

An investigation of combination of heavy metals on toxicity has a more practical significance as joint toxicity and interaction patterns within an organism need to be considered when conducting risk assessment of heavy metal exposure (Su *et al.,* 2017). The toxicity of mixtures Cd and MeHg in combination with Cr, Cu, Zn and Mn has recently been investigated (Su *et al.*, 2017), but the effect of Cd in combination with Hg has not been investigated. Studies have investigated the combined effects of heavy metals, including Cd and Hg on the endocrine system (Iavicoli *et al.*, 2009; Haouem *et al.*, 2013; Dardouri *et al.*, 2016) and on the cognitive function of rat offspring following metal administration at periconception (Camsari *et al.*, 2017). But, to our best knowledge, the combined effects of Cd and Hg on the CVS have not been investigated.

A major limitation of existing studies is that the concentration of the metals used is based on previous studies or the LD50 and not necessarily based on established limits of exposure. Although the concentrations are usually high, these studies do provide information on the type of tissue or cells that are susceptible to damage. In the present study, the WHO limits for each metal in drinking water is used. (WHO, 2011). As this is an established limit, it is expected that toxic effects would be minimal, and dosage accumulation over an extended period of time would result in tissue damage. For this reason a dosage of 1000 times this limit was selected. The duration of exposure and the mode of administration are important to reflect human consumption. Therefore

the metals were administered the metals orally by gavage and the experimental time was 28 days, representing a model of subacute toxicity according to the Organisation for the Economic Co-operation and Development (OECD) (OECD, 2001).

In evaluating the effects of toxins such as heavy metals two important confounding factors must be taken into consideration and these are age and sex. With ageing changes occur to the CVS and these include structural alterations such as an increase in collagenous and elastic tissue in heart and blood vessels (Strait and Lakatta, 2012), cardiomyocyte atrophy (Hees *et al.*, 2002) and thickening and dilation of large arteries (Lakatta *et al.,* 2009). Functional changes include a reduction in the cardiac wall strength and contractile efficiency (Strait and Lakatta, 2012), reduced ventricular filling as a result of slowed relaxation of the cardiac muscle and alterations in the relaxation pattern (Spina *et al.*, 1998; Hees *et al.*, 2002; Tan *et al.*, 2009; Strait and Lakatta, 2012). Alterations to the electrical conductivity of the cardiac muscle cause atrial and ventricular fibrillation and supraventricular tachycardia (Fleg and Lakatta, 2007). Age associated functional changes to blood vessels include reduced recoil as a result of connective tissue changes, decreases in vasodilators and increased in synthesis of vasoconstrictors as consequence of endothelial dysfunction, further increasing the inability to regulate vascular tone and contributing to diseases such as hypertension, hypercholesteremia and coronary and peripheral atherosclerosis (Csiszar *et al.*, 2008). Although Capitanio *et al.*, 2016 found that no changes in the CVS of Sprague-Dawley rats between young (6 weeks) compared with old (22 months) and senescent (30 month) rats when fed a restricted diet, it is still important to select young rats to eliminate any age-related effects on the CVS. Not only dietary and environmental factors can influence the outcome of an animal study, but normal physiological process can have a confounding effect. Female hormones have a cardioprotective effect, which may mask toxicity to the CVS while hormone cycling can influence the coagulation system (Gee *et al.*, 2008; Kellermann *et al.*, 2014; Swanepoel *et al.*, 2014). For these reasons male Sprague Dawley rat model were chosen.

The aim of this chapter is to implement of the Sprague Dawley rat model and to evaluate the effects of exposure on rat weight as well as the weight of the liver, kidneys and heart. In addition, plasma levels of each metal were determined as well as the effect of Cd and Hg alone and combination on blood blood markers associated with toxicity.

3.2.   Materials and Methods

3.2.1. Materials

This study used Male Sprague Dawley rats exposed to Cd and Hg alone in combination via oral gavage of aqueous solutions of $CdCl_2$ (Sigma-Aldrich, Randburg, South Africa) and $HgCl_2$ (Sigma-Aldrich, Randburg, South Africa) administered alone and in combination.

3.2.2. Methods

3.2.2.1. Implementation of the Sprague Dawley rat model

Six-week-old, male, Sprague-Dawley rats (average weights 250 - 300 g) were maintained at the University of Pretoria Biomedical Research Centre (UPBRC). Standard irradiated "Epol" rat pellets and municipal water were provided *ad libitum.* The rats were housed conventionally in cages complying with the sizes laid down in the SANS 10386:2008 recommendations. A room temperature of 22ºC (± 2), relative humidity of 50% (± 20) and a 12-hour night/dark cycle was maintained throughout the study. A total of 24 rats (n=6 per group) were used in the study. The rats were housed in pairs per cage and autoclaved pinewood shavings were used as bedding material, along with white facial tissue paper as enrichment as per the standard operating procedures at the UPBCRC. All experimental protocols complied with the requirements of the University of Pretoria Animal Ethics Committee (AEC) (Animal ethics number: H007-15). The rats were divided into the experimental groups at random and allowed to acclimatise for 7 days prior to dosage, after which the experimental period commenced, where the rats were administered the heavy metals alone or in combination for 28 days. The total housing period of the rats was therefore 35 days. The dosages are provided in the table below (Table 3.1). The rats were dosed at a 1000 times the safety limit of exposure levels established by the WHO (WHO, 2011). All live handling and dosing of rats was performed by trained personnel of the UPBRC.

The dosages were calculated using the human equivalent dose calculation of Nair and Jacob (2016). Dosage is based on a human with a weight of 60 kg, consuming 2 litres of water per day. Therefore, the daily intake is 0.006 and 0.012 mg/day for Cd and Hg respectively where a 1000x of this limit translates into a dosage of 6 and 12 mg/day for Cd and Hg respectively. For an adult human with a mass of 60 kg this is equivalent to 0.1mg/kg and 0.2 mg/kg respectively. Using the following equation:

Human equivalent dose (HED) (mg/kg) = rat equivalent dose (RED) (mg/kg) X (rat Km/human Km)

Km is the correction factor based on surface area and human Km = 37 for human and rat Km = 6 (Nair and Jacob, 2016).

The RED is therefore 0.62 and 1.23 mg/kg for Cd and Hg respectively.

Table 3.1: Experimental groups, dosage number of rats used for the study and time of exposure

Group	WHO limit (mg/l) (WHO, 2011)	Dosages (mg/kg rat weight)	mg/ml/day $MeCl_2$	Mg/ml/day Me^{2+}	mM Me
Control	-	0.5 ml saline			
Cd	0.003	0.62	0.186	0.114	1.17
Hg	0.006	1.23	0.369	0.273	1.34
Cd and Hg	-	0.62 and 1.23			

Me- Metal Cd or Hg

3.2.2.2. Observations during the experimental period

Throughout the study, the rats were checked by qualified veterinary technicians for changes in mass, condition and activity and loss of appetite. The rats were also weighed daily prior to administration of the metals and weekly average weights of rats were used to calculate dosages. The change in weight of each rat was calculated as follows:

Change in weight = Weight at day 28 (g) – Weight at day 1 (g)

3.2.2.3. Termination

Termination of animals was performed via isoflourane overdose according to standard methods employed by the UPBRC. The animals were weighed before termination.

3.2.2.4. Blood and tissue sample collection

Blood was collected via cardiac puncture into heparin and citrate tubes for subsequent biochemical and coagulation studies. Blood collected for scanning electron microscopy (SEM) was prepared as described in section 5.2.1. The organs were removed, placed in a beaker and weighed using semi-analytical scale (Lasec MP2000b). The organ mass was calculated as follows:

Mass of organ = Mass of organ and beaker – Mass of beaker

For each rat a heart/body weight ratio was then calculated. The heart and aorta of each rat processed for for light (LM)-and transmission (TEM) as described in sections 4.2.2 and 4.2.3.

3.2.2.5. Blood parameters

Half the volume of blood obtained through cardiac puncture on the day of termination was sent to the Department of Companion Animal clinical studies, Clinical Pathology section or IDEXX for toxicological analysis. The levels of Cd and Hg in the blood were quantified with inductively coupled plasma mass spectrometry (ICP-MS) (Table 3.2). The percentage absorbed was calculated relative to theoretical 100% metal gavaged converted to mg/ml rat blood volume.

% Metal absorbed = Blood levels (mg/ml rat blood)/Total gavage volume (mg/ml rat blood) X 100

Blood levels of total serum protein (TSP), sodium, potassium, gamma-glutamyl transferase (GGT), alanine aminotransferase (ALT), aspartate aminotransferase (AST), alkaline phosphatase (AP), urea, creatinine, bilirubin, globulin, albumin and glucose were determined as specific markers of liver and kidney damage. Blood levels of sodium and potassium were also determined.

3.2.2.6. Statistical analysis

Statistical analysis on the levels of heavy metals in the blood and blood chemistry analysis were performed on GraphPad Prism Version 6.01 using 1-way analysis of variance (ANOVA) and Tukey's multiple comparisons test, where a *p*-value of ≤0.05 was considered significant

3.3.   Results

No abnormal food intake or changes in behaviour were observed over the experimental period. During the experimental period of 28 days the weight of the rats increased steadily (Figure 3.1) and no differences were observed between the experimental groups compared to the control group.
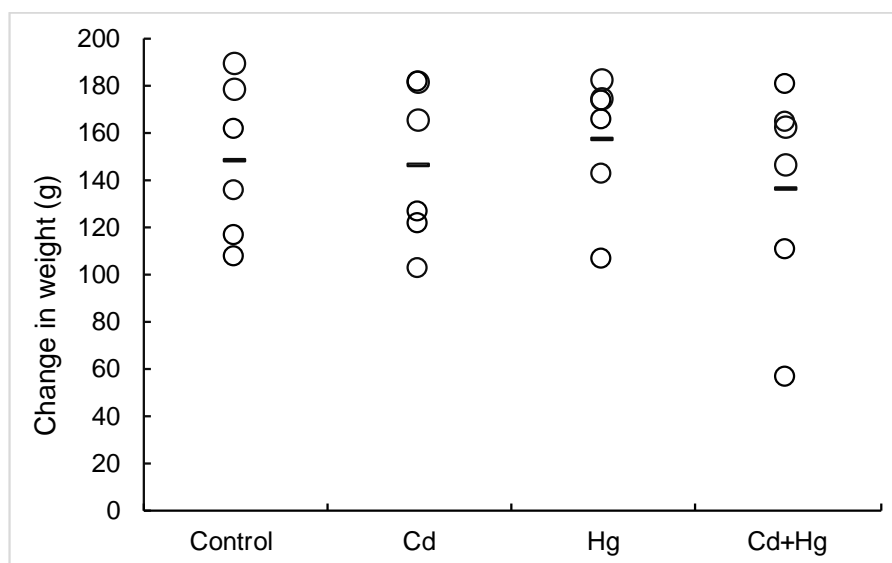
Figure 3.1: The mean change in weight of each group for the entire experimental period of 28 days. No statistical differences (p≤0.05) were observed between any of the groups.

Table 3.1: Metal blood levels at day 28 and calculated percentage absorbed

	Alone		Combination	
	Cd	**Hg**	**Cd**	**Hg**
	Mean ± SD	**Mean ± SD**	**Mean ± SD**	**Mean ± SD**
Blood concentration (nM)	16,69 ± 3.69	186,67 ± 22.12	121,06 ± 140.17	155,99 ± 41.12
% Absorbed	19.11 ± 4.22	43.24 ± 5.12	72.14 ± 83.52	51.75 ± 13.64

Differences between Cd and Cd levels in Cd+Hg and between Hg and Hg levels in Cd+Hg was not significant (p≤).05).

Metal levels in the plasma were increased with a narrow range for Cd alone, but Cd levels in the combination group had a large standard deviation as associated with rats with a lower change in weight (Figure 3.1). For Hg and Hg in combination, the range was similar. The % of each metal absorbed was calculated and was expressed relative to the dosage received based on the assumption of 100% absorption. Absorption of these metals (Table 3.1) was 19.11 ± 4.22% and 43.24 ± 5.12% respectively for Cd and Hg when administered alone, while in combination the absorption was increased to 72.14 ± 83.52 % and 51.75 ± 13.64% for Cd and Hg respectively in the Cd+Hg group. The percentage of Hg absorbed is also slightly higher in the combination group than when the metal is administered alone although differences are not significant.

Several parameters were evaluated as indicators of liver toxicity. An increase in mass is associated with liver enlargement. Both Alb and globulin are synthesised in the liver and changes in plasma levels may indicate altered liver function. In Table 3.2 the average mass of liver, TP, albumin and globulin levels for the control, Cd, Hg and Cd+Hg groups is presented. The mass, TP and globulin levels in all groups are similar. For rats exposed to Cd and Cd+Hg, Alb levels were increased and reduced respectively. Only differences between Cd and Cd+Hg were significant ($p \leq$ 0.05).

Table 3.2: Liver mass, total serum protein, albumin and globulin levels in rats exposed to Cd and Hg alone and in combination

	Mass (g) Mean ± SD	TP (g/L) Mean ± SD	Alb (g/L) Mean ± SD	Glob (g/L) Mean ± SD
Control	11.92 ± 0.98	58.30 ± 3.29	40.88 ± 3.03	17.30 ± 0.95
Cd	11.70 ± 0.95	60.18 ± 1.21	**42.07 ± 1.13***	18.12 ± 1.34
Hg	12. 32 ± 0.50	59.85 ± 1.86	40.38 ± 0.94	19.47 ± 1.55
Cd+Hg	11.40 ± 1.48	57.58 ± 2.56	**38.35 ± 1.52***	19.22 ± 2.19

*Statistical difference between Cd and Cd+Hg

Increased blood levels of liver enzymes are associated with liver damage. Levels of these enzymes, ALT, ASP, ALT/ASP ratio, GTT, bilirubin and AP levels are presented in Table 3.3. No significant differences were found between the control and the experimental groups. Compared to the control, AP levels were statistically lower in the Hg and Cd+Hg groups.

Table 3.3: Levels of liver enzymes in blood of rats exposed to Cd and Hg alone and in combination

	ALT (U/L) Mean ± SD	AST (U/L) Mean ± SD	GGT (U/L) Mean ± SD	BILI (µM/L) Mean ± SD	ALT/AST Mean ± SD	AP (U/L) Mean ± SD
Control	61.50 ± 5.58	94.67 ± 24.90	2.33 ± 1.37	0.70 ± 0.30	1.57 ± 0.54	201.67 ± 30.43
Cd	57.17 ± 6.37	81.50 ± 9.89	2.00 ± 1.55	0.93 ± 0.28	1.44 ± 0.24	183.33 ± 14.79
Hg	57.50 ± 5.82	94.67 ± 29.93	4.17 ± 2.48	1.43 ± 0.94	1.63 ± 0.40	**166.00 ± 10.53***
Cd+Hg	74.17 ± 30.75	106.83 ± 78.58	4.97 ± 4.30	2.67 ± 3.01	1.61 ± 1.16	**159.67 ± 20.46***

*Statistically different compared to control.

Indicators of kidney function were evaluated by measuring kidney mass as well as blood creatinine and urea nitrogen levels (Table 3.4). Kidney mass was unchanged while creatinine levels were statistically lower for the Cd+Hg group compared to the control. Levels in the Cd+Hg was highly variable, and this may be due to the variability in weight observed in the Cd+Hg group (Figure 3.1). Urea nitrogen levels of rats exposed to Cd+Hg were increased compared to the control and significant differences were only found between Cd and Cd+Hg.

Table 3.4: Kidney mass and blood levels of creatinine and urea nitrogen of rats exposed to Cd and Hg alone and in combination

	Mass (g) Mean ± SD	Creatinine (μM) Mean ± SD	Urea nitrogen (mM) Mean ± SD
Control	2.38 ± 0.20	27.17 ± 2.23	7.55 ± 0.41
Cd	2.38 ± 0.17	**24.17 ± 1.17****	**7.03 ± 0.78****
Hg	2.58 ± 0.11	21.83 ± 2.14	7.70 ± 0.74
Cd+Hg	2.53 ± 0.29	**12.97 ± 12.92*,****	**13.82 ± 7.96****

*Statistically different compared to control, ** Statistical difference between Cd and Cd+Hg

Glucose, sodium and potassium blood levels were measured as general indicators of toxicity (Table 3.5). Sodium levels in the Cd+Hg group were significantly decreased in comparison to control. The potassium levels all groups were similar to the control and differences were only found between Cd and Cd+Hg.

Table 3.5: Blood glucose, sodium and potassium levels of rats exposed to Cd and Hg alone and in combination

	Glucose (mM) Mean ± SD	Sodium (mM) Mean ± SD	Potassium (mM) Mean ± SD
Control	6.85 ± 1.06	141.33 ± 1.03	4.08 ± 0.35
Cd	6.43 ± 0.77	140.17 ± 0.41	**3.76 ± 0.28****
Hg	6.33 ± 1.10	140.33 ± 1.51	4.09 ± 0.71
Cd+Hg	7.57 ± 1.20	**139.17 ± 1.17***	**4.70 ± 0.56****

*Statistically different compared to control, **Statistical difference between Cd and Cd+Hg

As this study focused on the effects of Cd and Hg alone and in combination on the CVS, the mass of the hearts dissected from each rat was determined and the heart/body weight ratio was calculated (Table 3.6). Although the mass of the hearts of the Cd+Hg group was less than the control and exposed groups the differences were not significant. The heart/body weight ratio was the same for all groups.

Table 3.6: Heart weight and heart/body weight ratio of rats exposed to Cd and Hg alone and in combination

	Heart weight (g) Mean ± SD	Heart/body weight ratio Mean ± SD
Control	1.00 ± 0.10	0.01 ± 0.00
Cd	1.03 ± 0.09	0.01 ± 0.00
Hg	1.10 ± 0.05	0.01 ± 0.00
Cd+Hg	0.88 ± 0.2	0.01 ± 0.01

3.4. Discussion

In animal studies the effect of Cd either alone or in combination with other metals has previously been studied in relation to the changes in hematologic and biochemical parameters (Bersényi *et*

al., 2003) and on hepatic and renal toxicity (Yadaw and Khandelwal, 2006; Haouem *et al.*, 2007; Renugadevi and Prabu, 2010; Kumar *et al.*, 2010; Venter *et al.*, 2017). Hg, alone or in combination with other metals, has been studied in terms of its effect on the haematologic parameters and serum biomarkers of toxicity (Beresényi *et al.*, 2003). A limitation of many of these studies, is that the concentrations used are selected based on previous studies which makes it difficult to extrapolate findings to effects in exposed human populations. Several limits for the levels of metals in water have been established and this includes the WHO limit of 0.003 and 0.006 mg/l for Cd and Hg respectively. Using the human equivalent dose calculation of Nair and Jacobs 2013 an equivalent dosage for rats can be calculated. A limitation of using the WHO limit is that a chronic study design may provide some information on toxicity only after a long exposure time. To overcome this limitation a subacute study was undertaken where rats were exposed to 1000x the WHO limit for Cd and Hg for 28 days. If successful future studies can then evaluate the effects of lower levels of Cd and Hg alone and in combination.

3.4.1. Relevance of Cd and Hg blood levels.

In the present study both metals were absorbed, and the amount absorbed was 19.11 ± 4.22% and 43.24 ± 5.12% respectively for Cd and Hg. While in combination the absorption was increased to 72.14 $\pm$ 83.52 % and 51.75 ± 13.64% for Cd and Hg respectively in the Cd+Hg group which indicates that either this increase is due to a higher total metal intake or that one of the metals alters the permeability of the intestinal mucosa, resulting in an increase in absorption. Cadmium causes interstitial fibrosis (Yasuda *et al.*, 1995; Kowalczyk *et al.*, 2002) and this may increase intestinal permeability and consequently the uptake of other metals. A dose dependant sloughing of intestinal villi was reported with Hg exposure (Sheikh *et al.*, 2013). The effect can result in increased mucosa permeability which could account for the higher percentage of Cd found in the blood of the combination group.

The plasma levels of Cd in rats after oral exposure to 1000 times the WHO safety limits were 16.69 ± 3.69 nM which is equivalent to 1.872 ± 0.37 µg/L which were in the same order of that reported for several Cd exposed populations. Examples are 0.8 – 4.5 µg/L for an Egyptian population (Mortada *et al.*, 2002). 0.05 – 0.258 µg/L of Cd was reported for a South African female rural population, and mining population 0.06 – 0.39 µg/L (Röllin *et al.*, 2009), and for Swedish adult levels of 0.46 µg/L blood Cd were reported (Barregard *et al.*, 2016). For Canadian adults, men had a Cd level of 0.34 µg/L whereas women had levels of 0.43 µg/L (Garner and Levallois, 2016). In most European countries, populations are nearing the tolerable weekly intake (TWI) of Cd (2.5 µg/kg body weight). The detrimental effects due to environmental exposure of Cd can be accelerated by Cd exposure via tobacco smoking (Leduc *et al.*, 1993). People who smoke one pack of cigarettes per day take in an additional 1 - 3 µg of Cd (Matović, 2011). Likewise, in the present population smoking adds to the levels of exposure. Blood levels of Cd in smokers were

increased from 1.37 ± 0.45 µg/L to 2.67 ± 1.21 µg/L for an Egyptian population (Mortada *et al.*, 2002), whereas for Canadians these levels increased from an average of 0.21 µg/L to 1.64 µg/L for smokers compared to non-smokers (Garner and Levallois, 2016). An association between blood Cd levels in human population and blood pressure have been reported (An *et al.*, 2017). The mean level of Cd in blood of smokers was elevated as compared to the non-smoker group, 1.155 µg/L and 0.972 µg/L respectively. Although this does not represent oral exposure, it still provides information on blood levels and whether increased blood levels are associated with toxicity. Blood Cd levels have also been evaluated in normotensive and untreated hypertensive humans. In normotensive human blood Cd levels have been found to be 3.4 ± 0.5 ng/L, while living untreated hypertensive human blood Cd levels were reported at 11.1 ± 1.5 ng/L (Glauser *et al.*, 1976). This highlights that even low concentrations Cd can compromise the functioning of the CVS.

For Hg the plasma levels, after oral exposure to 1000x the WHO safety limits of Hg were 35.41 ± 2.60 µg/L which was higher than levels found in several populations. Plasma Hg levels were found to be an average of 3.08 ± 1.55 µg/L for a Korean male college population (n=43) (Jung *et al.*, 2016) and 4.6 ± 3.0 µg/L for a large population of Korean males (n=4283) (Lee, 2016). In an Egyptian population, Hg levels were 4.4 – 12.1 µg/L (Mortada *et al.*, 2002), and in a South African population 0.1 - 8.82 µg/L (Röllin *et al.*, 2009). In the study by Röllin *et al.* (2009) levels in South African rural women were 0.18 - 8.82 µg/L and for women living in mining areas were 0.28 - 1.25 µg/L (Röllin *et al.*, 2009). In contrast, in regions of the world where small scale gold mining occurs, serum levels of Hg were raised and were increased from 16.6 ± 10.7 µg/L to 102.0 ± 55.8 µg/L for different mining areas in Ghana. Bio-monitoring levels reported by Baeuml *et al.* (2011) found that the highest median Hg blood levels were found in Indonesia-Sulawesi and Zimbabwe and reported median levels were 11.1 µg/L and 10.2 µg/L respectively while the maximum Hg blood levels were 429 µg/L and 186 µg/L were reported for Indonesia-Kalimantan and Indonesia-Saluwesi respectively. An increase in cardiovascular events has been reported in people exposed to 0.05 µM Hg, equivalent to 10.29 µg/L Hg. In South Africa, informal small-scale gold mining occurs and no reported data could be found regarding Hg levels in this population. In the present study rat blood levels of 35.41 ± 2.60 µg/L represents the upper range of Hg exposure which is associated with cardiovascular risk. The levels of Hg were evaluated in a mining area in China by Jia *et al.*, 2018. Total Hg and MeHg concentration in soil ranged from 1.53 to 1054.97 mg/kg and 0.88 to 46.52 µg/kg respectively. Soil has been found to be an important source of Hg in vegetables. Total Hg concentration in vegetables ranged from 24.79 to 781.02 µg/kg total Hg and 0.01 to 0.18 µg/kg MeHg. Importantly Hg levels in edible plant parts were higher than in the rats (Jia *et al.*, 2018). Another study investigated the Hg levels in a former mining town in Slovenia, showing blood levels of 0.92 µg/L in school-aged children and 1.86 µg/L in females (Kobal *et al.,* 2017). Evaluation of Hg status in females of child bearing age has long been established as important, primarily in populations consuming fish-based products (Rebelo and Caldas, 2016). While Hg has neurotoxic effects which provide a risk to foetal development, a transfer of heavy metals to infants is possible

via breast milk, indicating that not only directly contaminated populations are at risk. The levels of Cd in breast milk were low, less than 2 µg/L, while Hg levels (MeHg) in breast milk were increased in fish eating populations of the Amazon, with a mean level of 59.4 µg/L (Dos Santos *et al.*, 2015; Rebelo and Caldas, 2016). Another study reported Hg detection in 100% of the samples, with a median concentration of 0.59 µg/L. This highlights the ability of breast milk to contribute to infant Hg exposure during the nursing time-frame (Park *et al.*, 2018). The mode of exposure in these populations is related to environmental pollution and includes respiratory and oral exposure. Therefore ,Hg levels found in rats is relevant and reflects some instances of human exposure.

3.4.2. Liver toxicity

Evaluation of liver function revealed no changes in TP or globulin levels for all exposed groups. In the present study GGT and bilirubin levels were higher in the Hg and Cd+Hg groups, although the differences were not significant. Raised GGT in serum is a marker of alcohol consumption and liver disease (Teschke *et al.*, 1977; Lee *et al.*, 2004). Serum GGT has been suggested as an early marker of oxidative stress (Lee *et al.*, 2004) and studies have shown an association between GGT and CVD risk factors (Nyström *et al.*, 1998; Lee *et al.*, 2003a; Lee *et al.*, 2003b). Bilirubin is a by-product of erythrocyte destruction and its elevation in serum can indicate liver dysfunction or an increased destruction of erythrocytes despite normal liver function (Giannini *et al.*, 2005). Elevated bilirubin levels are also indicative of oxidative stress (Dohi *et al*., 2003), and an inverse relationship has been reported for serum bilirubin levels and coronary artery atherosclerosis (Knag *et al.*, 2013). The liver is also responsible for energy metabolism (Rui, 2011) and low blood glucose levels may be due to altered liver function or may indicate an increase in glucose excretion in urine. Glucose excretion through increased filtration by the kidneys has been reported as a consequence of oxidative stress (Ozturk, 2012) or may be indicative of impairment in the resorption mechanism (Gerich, 2010; Mather and Pollock, 2011).

Liver damage results in several fold increase in the levels of ALT, AST and the ratio of ALT/AST. With heptic injury, ALT is released into the bloodstream and is a more specific marker for liver injury in small animals due to the large quantities of ALT released. AST is found in the liver, heart muscle, kidney and brain and following cellular damage is released into the blood stream. The ALT/AST ratio is also used as a biochemical marker of liver toxicity. In this study, although the AST and ALT levels were increased in the Hg and Cd+Hg groups differences compared to the control were not statisically significant. Hg intoxication induces a significant elevation in serum AST and ALT activities in rats (Jagadeesan and Sankarsami, 2007). Increases in ALT levels under Hg stress has been reported previously (Toshiko *et al.*, 1998; El-Maraghy *et al.*, 2001; Madhu *et al.*, 2005; Ejebe *et al.*, 2010; El-Dermadesh *et al.*, 2001; Sheikh *et al.*, 2013). Compared to previous studies the dose administered in the present study was low and this could account for the general lack of liver toxicity. However, low dosage of heavy metals, Cd and Cr has been shown to cause histopathological changes even when biochemical indicators of hepatic or renal damage are normal (Venter *et al.*, 2017).

43

In the present study Alb levels were not increased compared to the control group but there were significant differences between the Cd and Cd+Hg groups. Albumin is produced in the liver and low serum levels suggest liver disease, or kidney damage as reduced levels could be due to increased albumin passing through the glomeruli and being excreted in the urine. Urea albumin can be used as a risk factor for incident hypertension as it is dependent on the glomerular filtration rate (Munakata *et al.*, 2017). Cd is bound to albumin (Chaumont *et al.*, 2012; Akerstrom *et al.*, 2013) and an increase in albumin removal increases Cd excretion. An increased filtration of albumin and creatinine is indicative of increased glomerular filtration and renal damage (Low *et al.*, 2018). Low albumin levels were recorded for liver damage caused as a result of exposure to Hg and Cd administered simultaneously and had an additive effect on number of dead turkey chicks in an *in vitro* study (Hill and Matrone, 1970). A decrease in albumin levels has been reported for Sprague Dawley rats exposed for 90 day to Cd and Hg in combination with As, Pb and Cr (Zhu *et al.*, 2014) along with a decrease in erythrocyte levels and increased hepatotoxicity. Although some changes in Alb was measured, indications are that Cd, Hg and Cd+Hg does not alter Alb levels.

AP is closely associated with the lipid membranes in the canalicular zone of the liver and any disturbance with bile excretion, both intra and extrahepatic, leads to a decrease in serum AP (Merzoug *et al.*, 2009). In the present study AP levels were reduced in the Hg and Cd+Hg group in comparison to control. Reduced AP levels have been reported in rats administered $CdCl_2$ (Rana*, et al.*, 1996; El - Demerdash*, et al.*, 2001; Sharma *et al.*, 2005). Zn is essential for the correct synthesis and function of AP (Suzuki *et al.*, 2005) and prevents cell damage through apoptosis and necrosis (El-Damerdash *et al.*, 2004; Jacquillet *et al.*, 2006). Displacing Zn can therefore affect AP function and increase necrosis or apoptosis. Alterations in AP levels in rats indicate an early change to liver function as well as tissue and cellular morphology (Venter *et al.*, 2017). Reduced AP levels have also been reported for Wistar rats exposed to Hg (Sheikh *et al.*, 2013). Likewise, in the present study Hg and Cd+Hg caused a decrease in AP levels indicating early liver damage.

3.4.3. Kidney toxicity

In the present study blood creatinine levels were reduced in all the heavy metal groups compared to the control, although only significant for Cd+Hg. Blood creatinine level is used as a marker of kidney and liver function in many diseases such as diabetes (Low *et al.*, 2018) and low serum creatinine levels are a feature of severe hepatic disease (Takabatake *et al.*, 1988). Serum creatinine levels are also an indication of renal function and structural integrity and increased levels of creatinine in the urine are an indicator of kidney tubule damage. Hg accumulates in the renal epithelium (Zalups *et al.*, 1995), resulting in damage to tubular reabsorption and filtration mechanisms of the glomeruli. Significantly lowered Na^+ levels in the Cd+Hg group may be a result of poor tubular reabsorption (Table 3.5).

In a similar study by Venter *et al.*, 2017, in which rats were exposed to 1000x Cd and Cr for 28 days, TP, AP and creatinine levels were significantly lowered for Cd in combination with Cr. Low

blood creatinine levels have also been observed in patients with decreased muscle and bone mass, despite normal kidney function (Huh *et al.*, 2015). In the present study the mass of the exposed groups showed no significant difference when compared to the control, indicating no loss of bone or muscle mass.

Cd adversely affects renal glomerular and tubular function and is associated with lower serum creatinine levels. For metal combination of Cd and Cr, Venter *et al.*, 2017 found that creatinine levels were also lower. In rats, exposure to Cd and Cr alone and in combination was found to cause tissue necrosis as well as changes to the ultrastructure of the liver (Venter *et al.*, 2017). Changes to the kidney included dilation of the glomeruli. Bio-accumulation of Cd was also observed in both the liver and kidneys. The study also found significant changes in TP, AP and blood creatinine levels, with no changes in the levels of blood markers of liver and kidney function or damage in the single metal exposure groups but some changes were found for groups exposed to Cd+Cr.

According to Oluwafemi *et al.* 2014 an increase in urea and creatinine values is an indication of renal-tubular damage due to Cd induced nephrotoxicity. Once absorbed, Cd is taken up by the hepatocytes, and then from the liver enters the circulatory system bound to metallothionein. The Cd-metallothionein complex (Cd-Mt), because of its small molecular size, is easily filtered through the glomerular membrane and taken up by renal tubular cells (Jihen *et al.*, 2008) and in the process causes renal tubular damage. The results of the present study therefore suggested that the decreased serum levels of AP and creatinine in the combination group may be due to increased kidney damage due to increased filtration or poor resorption.

3.4.4. Cd and Hg effects on hepatic and renal injury markers

Cd causes liver and kidney toxicity and the reason is that the half-life of Cd is 1 month to 10 – 20 years (biphasic) while the biological half-life of Cd is 20-30 years in humans (Rani *et al.*, 2014). Organ specific half-life has been reported as 4 - 19 years for liver and 6 - 38 years in kidney (Solenkova *et al.*, 2014). Cd is known to induce tubular and nephrotoxic dysfunction in environmentally and occupationally exposed individuals. Cd selectively accumulates in the renal cortex, making up over 50% of the overall body burden (Faroon *et al.*, 2012). For this reason, blood or urine levels of Cd are poor indicators of the overall body burden (Buser *et al.*, 2016). Gross morphological changes include congestion, severe haemorrhage, necrosis and degenerative changes in the kidneys (Sheikh *et al.*, 2013). Dose and time dependant increase in liver and kidney damage were reported for Cd administration in albino rats (Alkushi *et al.*, 2018). Increase in inflammation in the liver tissue and vasculature was also observed with an increased dosage (2.5 and 5.0 mg/kg body weight). The authors also showed some regeneration of the degenerative changes following the administration of low doses, but not at higher doses (Alkushi *et al.*, 2018). In another study, an administration of 50 mg/l Cd reduced liver weight by 8% following Cd administration while the kidney weight remained unchanged (Brzóska *et al.*, 2003). The urine

creatinine and serum TP levels remained unchanged, but an increase in ALT and AST in the Cd treated animals compared to the control group was found and this correlated with the change in liver mass and histological investigation confirmed degenerative changes in the hepatocytes (Brzóska *et al.*, 2003). Epithelial damage to renal tubules was observed in the kidney, as well as glomerular dilatation. Thijsssen *et al.* (2007) showed no correlation between the Cd kidney content and Cd blood levels, indicating that measurement of kidney Cd content is an indication of chronic exposure while blood levels are good indicators of acute exposure. The urinary protein content which is a sign of proximal tubular damage was increased, but no glucose or enzymes were present in the urine (Thijssen *et al.*, 2007). Damage to the proximal tubule is time and concentration dependant and Cd accumulation results in functional and histological changes to the kidneys and due to bioaccumulation and kidney damage can occur when Cd levels in the environment are considered to be safe. Urine Cd levels are not a reliable indicator of total body burden when the body burden is low (Thijssen *et al.*, 2007). In the present study, rats were administered a dosage of 0,62mg/kg for 28 days (Table 3.1) and as reported by Venter *et al.* (2017), this dosage causes kidney damage.

In another study Wistar rats were exposed to 1 mg/L Cd for 9 months (Markiewicz-Górka *et al.*, 2015). These levels were higher than the maximum permissible limit of exposure and was used to take into account all the additional sources of exposure and include increased levels that have been reported in several population studies (Wang *et al.*, 2010; Mohod and Dhote, 2013). AST and bilirubin levels were increased and correlated with blood levels of Cd which indicated liver damage. Cd, at low environmental concentrations, has been shown to have an immediate oxidative effect in the liver, indicated by increased MDA levels measured immediately after exposure (Tandon *et al.*, 2001; Markiewicz- Gorka *et al.*, 2015).

The half-life of Hg in plasma is 3 days to 20 days (biphasic) (Keil *et al.*, 2011) A study modelling the short- and long-term exposure to Hg at doses of 2, 4 and 8 mg/kg body weight (Sheikh *et al.*, 2013) in Wistar rats showed a decrease in AP in a dose dependant manner at 14 and 28 days of exposure compared to the control, which were used to represent long term Hg exposure (Sheikh *et al.*, 2013). Hg exposure caused a dose dependant increase in serum ALT, GGT and creatinine compared with the control (Bandao *et al.*, 2005; Sheikh *et al.*, 2013). Increase in GGT concentration was observed at 28 days (Sheikh *et al.*, 2013) and blood urea and creatinine levels were also increased (Sheikh *et al.*, 2013 and Alam *et al.*, 2009). The kidney was identified as the most vulnerable organ, with presence of glomerular damage (Sheikh *et al.*, 2013). Likewise, in the present study, although minimal, Hg did cause some kidney damage.

A recent study on Wistar rats treated with intramuscular $HgCl_2$ for 30 days (first dose 4.6 µg/kg, then 0.07 µg/kg/day) suggested that the chronic low-level Hg exposure significantly altered the autonomic modulation of heart rate through a shift towards sympathetic control and blockage of

pacemaker activity of the sinoatrial node (Simões *et al.*, 2016). No studies, that specifically investigated the effects of Hg on cardiac tissue could be found.

3.4.5. Effects of co-administration of the two metals

Houem *et al.*, 2013 investigated the combined effect of Cd (20 mg/L CdCl$_2$) and Hg (80 mg/L HgCl$_2$) on the liver and identified a competitive interaction following co-administration. Levels of the blood enzymes were lower than Cd alone but higher than Hg alone. The authors reported increase in ALT and decrease in ALP and an indication of hepatic injury (Haouem *et al.*, 2013). A similar effect was observed for AP levels. Similar results have also been reported by Brzoka *et al.*, 2003 and Pari and Murugavel., 2005.

In general, an exposure to metal mixtures produces a more severe effect at both high and low dose exposure, with the effects being dependent on the dose and duration of exposure (Wang and Fowler, 2008). Interactions between metals were observed to be mostly synergistic in studies investigating heavy metal toxicity (Cobbina *et al.*, 2015; Su *et al.*, 2017). Su *et al.* 2017 investigated combined oral exposure to mixture of many metals and although toxicity is observed, the identification of specific heavy metals and combinations contributing to toxicity was difficult to determine. Increased NO production and a synergistic effect have been observed between LPS and Cd (Satarug *et al.*, 2000). Synergistic effects of Hg have been reported on co-administration with other toxic compounds; carbon tetrachloride co-administration increased lipid peroxidation (Rungby and Ernst, 1992). Co-administration of Cd and Hg has been reported to have a synergistic effect on nematode mortality (Chu and Chow, 2002). The effect of co-administration of environmentally relevant concentrations of Cd (100 mg/L) and Hg (25 mg/L) for 10 weeks was investigated by Dardouri and colleagues (2016) and the results showed a synergistic effect between the two metals on the liver, while an antagonistic effect was reported for markers of kidney function such as urea (Dardouri *et al.*, 2016). Mercury has been shown to have synergistic effects on secretion of IL-4 from mast cells (Walczak-Drzewiecka *et al.* 1999). Altered redox balance and macrophage dysfunctions were attributed to pulmonary emphysema as a result of Cd exposure (Ganguly *et al.*, 2018). Cd and Hg co-administration at periconception showed an increase in insulin resistance and altered glucose metabolism associated with metabolic tissue injury, which includes the liver of the offspring (Camsari *et al.*, 2017). This particular study is an example of the long-lasting effect of the metals, and the transplacental effects due to the long half-life of these metals.

Low Cd and Hg co-administration in Wistar rats caused destruction of erythrocytes while platelet levels increased following heavy metal administration, with Cd causing the largest increase in platelet levels. When co-administered, the effect of the heavy metal combination was lower than single metal exposure, indicating a competing effect of the two metals (Hounkpatin *et al.*, 2012).

According to FAO and WHO (2009), the chemical substances to which humans are exposed in the environment have almost infinite number of simple, binary, tertiary and quaternary combinations. Effects can be those of a dose addition where toxicity is produced through the same mode of action and this will result in a simple additive effect of toxicity. Alternatively, the interaction and/or effect of substances are different, and the observed effect is known as response addition. Synergism refers to a response greater than expected. This occurs when one substance changes the metabolism of the other potentially more toxic substance to enhance the internal dose or systemic exposure of the active form of the toxic component. Little is known on the effects of Cd and Hg in combination. As described in Sections (2.3.2 and 2.3.3 for Cd and 2.4.2 and 2.4.3 for Hg) Cd and Hg have different modes action and target different tissue types and therefore an addition effect or a synergistic effect can be expected. In the present study, where Cd and Hg were administerd in combination, synergism did not occur although some minor changes in some blood parameters may be due to an additive effect.

3.4.6. Cardiac specific markers – a review of relevance

Markers of liver and kidney toxicity are poor indicators of the type of interaction as well as cellular and tissue effects. Few blood markers are available to measure effects on the CVS and indirect measurement may be changes in blood pressure. Markers of damage to heart tissue include C reactive protein (CRP) an inflammatory marker (Ridker *et al.*, 1998), creatine kinase (CK), specifically CK-MB, as heart muscle expresses the B gene and therefore measurement of CK-MB has higher specificity. Levels of CK-MB are only raised when excessive damage has occurred for example with a heart attack, and individuals with a low muscle mass may not have elevated CK-MB levels. Furthermore, any skeletal muscle trauma for example in a motor vehicle accident, strenuous athletic exercise or post surgically will raise CK-MB levels, as would other myodegenerative diseases (Siegel *et al.*, 1981; Wu *et al.*, 1992; Vretou-Jockers and Vassilopoulos, 1989). The cardiac troponins I and T allow for the detection of MI even in situations where skeletal muscle injury is present (Ricchiuti *et al.*, 1998), and also allow the detection of future cardiac events (Newby *et al.*, 1998). Although the cardiac troponins are highly specific, the markers are primarily used to diagnose MI. Bodor, (2016) summarises that the markers can be used to diagnose myocardial injury not due to MI, but as a result of direct cardiac effects such as secondary heart injury. The direct and secondary effects that can be measured are listed below in table 3.7.

Table 3.7: Direct and secondary causes of myocardial injury giving positive cardiac injury marker results

Direct Cardiac Effects	Causes of Secondary Myocardial Injury
Tachy/Bradycardia	Respiratory failure
Aortic dissection	Pulmonary embolism
Hypertrophic cardiomyopathy	Rhabdomyolysis
Congestive heart failure	Sepsis, viral illness

Shock	Stroke
Cardiac contusion	Amyloidosis, sarcoidosis, hemochromatosis
Cardiac surgery ablation	Strenuous exercise
Cardiac ablation	Renal failure
Myocarditis, endocarditis, pericarditis	Burns of large body surface area

Adapted from Bodor, 2016.

A limitation of these markers is that between- and within- individual variation is great and the assessment of these markers needs to be population specific. The markers in an individual need to be adjusted for age and gender related ranges and an extremely detailed medical history. Additionally, these markers can also be present during minor illnesses. The use of the markers is therefore primarily to define a risk and not to establish diagnosis (Bodor, 2016). A variation in troponin T and CK-MB variation has been reported between animal and human studies (Olson *et al.*, 2000) making these two markers, although ideal within their own species, difficult to use in the identification of potential human targets of pathology. These effects may account for the lack of information of metals on the CVS as effects can only be observed following histological evaluation of tissue morphology.

3.4.7. Relationship with renal and vascular systems

Specific markers of vascular damage are limited, although changes in blood pressure are an indication of damage. Alterations in markers of kidney function have been associated with alterations in vascular permeability and function. Albuminuria and glomerular filtration rate are two factors linked to kidney and vascular function (Flack *et al.*, 2007). Increased glomerular filtration has been identified as a marker of early renal damage and pre-hypertension (Palatini, 2012; Fu *et al.*, 2014). Increased glomerular filtration may be caused by endothelial cell damage and proximal tubule damage (Vallon *et al.*, 2003; Barbieri *et al.*, 2011). Increased oxidative stress, due to metal accumulation in the kidney, results in deterioration of glomerular endothelial surface and increased vascular permeability (Kuwabara *et al.*, 2010), as is often described for smoking (Zoccali *et al.*, 2009; Sauriasari *et al.*, 2010). Hyperfiltration may also be caused secondary to systemic hypertension, and activation of the sympathetic nervous system (Luippold *et al.*, 2004; Zoccali, 2009). Hg is associated with sympathetic system activation in relation to regulation of pacemaker control. This shows that the effects of Hg on organ function can be direct as a result of oxidative damage on the particular system, but also secondary through influence of other systems. Renal hyperfiltration is also associated with alterations to arterial structure and function (Cherney *et al.*, 2010) as well as microvascular function (Cherney and Sochett, 2011). Fluctuation of kidney function may signify intra-glomerular microvascular hemodynamic instability and associated changes in glomerular filtration rate (Zhang *et al.*, 2018).

These studies show that Cd and Hg have well researched effects on the liver and kidney however little in known on the effects on the CVS and blood components and this is the focus of the research described in the following chapters.

3.5. <u>Conclusion</u>

In this study the *in vivo* rat model was used to investigate the effects of 1000x the WHO limit for Cd and Hg alone and in combination. Exposure to Cd and Hg alone and in combination for 28 days cause an increase in blood levels of Cd and Hg without a significant effect on the weight, organ/weight ratio of the liver, kidney and heart. Blood levels of ALT, AST, urea, glucose, TP and globulin remained unchanged. Albumin levels compared to the control were unchanged while AP levels were significantly decreased in the Hg and Cd+Hg groups. Creatinine levels were lower in all experimental groups but were only significantly lower in the Cd+Hg group when compared to the control and Cd groups. Na^+ levels were lower in the Cd+Hg group. These changes indicate some but minimal liver and kidney damage.

Chapter 4: Effects of Cd and Hg alone and in combination on the heart tissue and aorta of Sprague-Dawley rats

4.1. Introduction

CVD are a group of diseases that include atherosclerosis and hypertension, that affects the heart and blood vessels, which eventually lead to cardiac failure and CVA. CVD is associated with increased arterial stiffness as a result of decreased elastin and increased collagen content. Increased, irreversible, non-enzymatic cross linking of collagen, contributes to early vascular ageing (EVA) (Nilsson *et al.*, 2013, Nilsson *et al.*, 2009; Nilsson *et al.*, 2008, Strait and Lakatta, 2012). Increased oxidative stress and vascular inflammation are also implicated in CVD (Vendrov *et al.*, 2015). Atherosclerotic plaque formation is characterised by vascular inflammation resulting from endothelial cell dysfunction or injury and subsequent inflammatory cell movement into the vessel wall (Vendrov *et al.*, 2015). Mitochondrial dysfunction is well-documented as a cause of oxidative damage in VSMC (Vendrov *et al.*, 2015) as well as in cardiomyocytes (Jessup and Brazena, 2003) leading to CVD. Fibroblastic activity been linked to heart disease due to the ability of these cells to remodel the ECM causing increased collagen deposition within the connective tissue component of the myocardium, leading to fibrosis (Gourdie *et al.*, 2016; Leask, 2015; Moore – Morris *et al.*, 2015). CVD development is associated with dietary and lifestyle factors, advancing age, low socio-economic status and the development of conditions such as hypertension and hypercholerolemia (WHO, 2011). Early vascular ageing has recently been implicated as a factor for CVD along with atherosclerosis, plaque formation and rupture (Nilsson *et al.*, 2008).

Although smoking and exposure to Cd and Hg are associated with the development of hypertension and CVD (Puri and Shaha, 2003; Lopez *et al.*, 2006; Gomez *et al.*, 2007; Gaziano *et al.*, 2010; Hang *et al.*, 2013; Hecht *et al.*, 2016), little is known regarding the effects of environmental exposure to low levels of metals as part of complex mixtures. As mentioned in the previous chapter, exposure to these metals at 1000x the WHO water safety levels for 28 days did not cause significant changes in the levels of markers of liver and kidney damage (Chapter 3, Tables 3.3, 3.4 and 3.5). To further evaluate the effect of these metals on the CVS, the histological structure of the hearts and aortas of the rats were investigated in the current chapter. Histology is considered a valuable tool in assessing the toxicopathic impact of pollutants as it reflects the real health state of the animal better than other biochemical markers, especially for sub-lethal and chronic effects (Au, 2004; Annabi *et al.*, 2011; Kumar *et al.*, 2017).

4.2. Materials and Methods

4.2.1. Materials

The heart and aorta were dissected from each animal at the time of termination and processed for light microscopy (LM) and transmission electron microscopy (TEM). The left ventricle and the upper thoracic portion of the descending aorta of all animals in each of the experimental groups were evaluated and the most representative images of each group were used to document the changes in tissue and cell structure.

4.2.2. Methods

4.2.2.1. Evaluation of the tissue and cellular structure of the heart using light microscopy

Tissue prepared for paraffin wax embedding was fixed overnight in 4% formaldehyde (FA) in 0.1M phosphate buffer saline solution (PBS) (0.2 M Na_2HPO_4, 0.2 M $NaH_2PO_4 \cdot H_2O$, 0.15 M NaCl, pH = 7.4). The following day the samples were washed three times for 30 minutes with PBS buffer before being dehydrated in increasing concentrations of ethanol. These are 50% ethanol for 30 minutes, 70% ethanol for 1 hour, 90% ethanol for one hour, twice in 100% ethanol for one hour, and 100% ethanol overnight. The samples were then infiltrated with paraffin wax by first placing them in 50% xylene: ethanol for 30 minutes, then 100% xylene for 2 hours, followed by 30% wax in xylene for 1 hour, 70% wax in xylene for 1 hour and finally in 100% wax for two hours. All steps involving wax infiltration were undertaken at 60ºC. The samples were embedded in paraffin wax and cooled to 4°C prior to sectioning. The prepared blocks were sectioned at a thickness of 3 – 5 μm using a Leica RM2255 microtome. Staining was then performed according to the specific requirements for visualisation of tissue components. Prior to staining, all wax sections were de-waxed in xylene and rehydrated and then dehydrated with 90% and 100% ethanol to xylene according to standard protocols after completion of the staining.

For de-waxing, the slides were placed twice in 100% xylene for 5 minutes, and then twice in 100% ethanol for 2 minutes. The slides were then rehydrated in 90% and 70% ethanol for 1 minute each and finally in distilled water for 1 minute. Specific staining protocols were then followed. After the slides were stained they were rinsed in water and dehydrated in 70%, 90%, 100% ethanol, and finally in 100% xylene before mounting in Entellan with a coverslip.

4.2.2.2. General tissue morphology: Haematoxylin and Eosin

A 0.1% haematoxylin (He) stain solution was prepared by dissolving 1g of He in 1000 ml of distilled water. To this 0.2 g of sodium iodate and 50 g of potassium aluminium sulphate was then added and dissolved before adding 1 g citric acid and 50 g chloral hydrate. To prepare the eosin (E) stain, 2 g of yellowish eosin powder was dissolved in 200 ml of distilled water. Scott's buffer solution was

made by dissolving 2 g of potassium bicarbonate and 20 g of magnesium sulphate in 1000 ml distilled water.

To stain the tissue the slides were de-waxed and rehydrated as described above, before being stained with He stain for 10 minutes, treated with Scott's buffer for 10 minutes and finally dipped in E stain and washed with distilled water for one minute. The sections were then dehydrated and mounted with a coverslip.

4.2.2.3. Collagen distribution: Picrosirius Red staining

For PR staining, 0.5 g of Sirius red dye was dissolved in 500 ml of a saturated aqueous solution of picric acid. Acidified water was used for washing, made by adding 5 ml of glacial acetic acid to 1 L of distilled water. The tissue was stained in He for 8 minutes and rinsed in running tap water for 10 minutes. The PR solution was applied for 1 hour after which the slides were washed twice with acidified water. The tissue was then dehydrated three times in 100% ethanol and cleared with xylene before mounting (Velindala *et al.*, 2014).

4.2.2.4. Elastic distribution: Verhoeff van Gieson stain for elastin

Verhoeff's solution was made with 20 ml 5% alcoholic He, 8 ml 10% ferric chloride, 8 ml Weigert's iodine solution, and slides were stained for 1 hour. As tissue over stains during this method, differentiation was achieved by rinsing the slides in 2-3 changes of tap water and then with a 2% ferric chloride solution for 1-2 minutes.

Several changes of tap water were used to further stop differentiation, after which the slides were treated with a 5% sodium thiosulfate solution for 1 minute and washed again in running tap water for 5 minutes. The tissue was counterstained in Van Gieson's solution, made up of 5 ml of a 1% aqueous acid fuchsin in 100 ml of a saturated aqueous picric acid solution, for 3 - 5 minutes. The slides were dehydrated rapidly through 95% ethanol and two changes of 100% ethanol before being cleared in two changes of xylene for 3 minutes and mounted with a coverslip.

4.2.2.5. Transmission Electron Microscopy of the heart and aorta

Tissue samples were fixed in 2.5% glutaraldehyde (GA)/formaldehyde (FA) in 0.075 M phosphate buffer pH = 7.4 (NaP) for 1 hour and rinsed three times in NaP for 15 minutes before being placed in a secondary fixative, 1% osmium tetroxide solution, for 1 hour. Following secondary fixation, the samples were rinsed again as described above. The samples were then dehydrated in 30%, 50%, 70%, 90% and three changes of 100% ethanol and embedded in Quetol resin. Ultra-thin sections (70 - 100 nm), were cut with a diamond knife using an ultramicrotome, and contrasted with uranyl acetate for 15 minutes followed by 10 minutes of contrasting with lead citrate. Finally, the samples were allowed to dry for a few minutes before examination with the JEOL JEM 2100 TEM (JEOL Ltd., Tokyo, Japan).

4.3.   <u>Results</u>

4.3.1. Structural effects of Cd and Hg alone and in combination of the morphology of the heart

Haematoxylin and Eosin (H&E) staining was used to investigate the general tissue structure of the rat heart and aorta. In the heart, orientation and morphology of cardiac muscle fibres and nuclei were evaluated, as well as cellular changes such as the presence of cytoplasmic vacuoles and necrosis.

H&E staining cannot allow for the differentiation between the different types of connective tissue found in the heart. Fibrillar collagen types I and III are the predominant components of cardiac ECM (Fan *et al.*, 2012) and an excessive production and accumulation of ECM structural proteins such as collagen results in fibrosis. This causes an increase in the stiffness of the myocardium which affects ventricular contraction and relaxation. At the same time this fibrosis can lead to the overall distortion of the architecture and function of the heart. The heart tissue was therefore stained with PR to evaluate collagen distribution.

A major limitation of LM techniques is that associated staining methods only provide information on the structure and distribution of cells and connective tissue and limited information on membrane and organelle structure. In contrast, TEM provides information on the ultrastructure of tissue and intracellular structure. This includes the identification of membrane damage, changes to organelles such as the mitochondria and nucleus as well as changes in ribosome density and functioning of lysosomes i.e. autophagy.

In this section, the histology of normal rat cardiac tissue is described and changes in the structure of this tissue exposed to Cd and Hg alone and in combination are provided. The general morphological changes following H&E and PR staining are presented in Figures 4.1 – 4.4. Ultrastructural changes to the cardiac muscle myofibril and mitochondrial structure, myofibroblast distribution and collagen deposition patterns are presented in Figures 4.5 - 4.7.
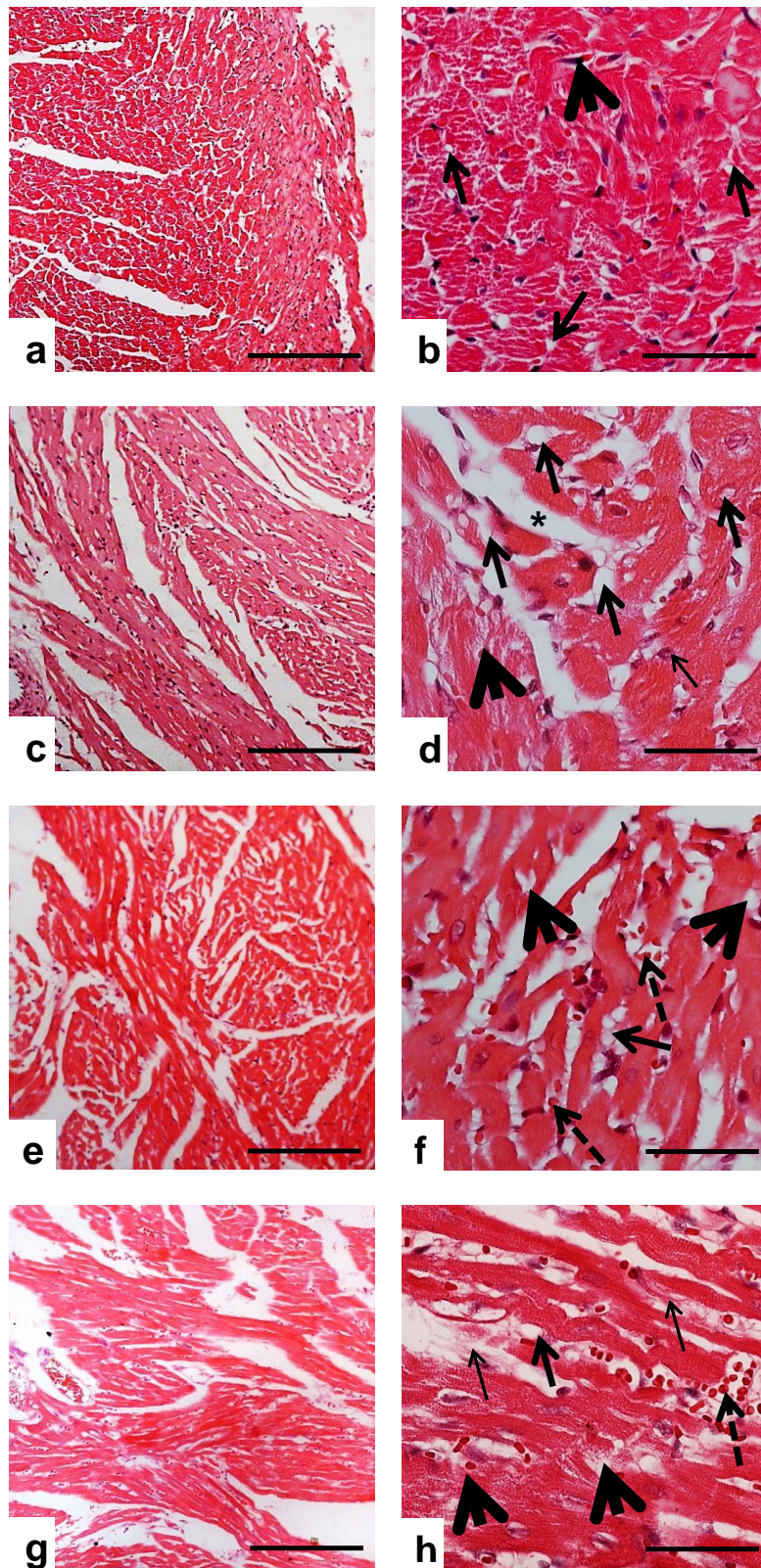
Figure 4.1: H&E stain of cardiac tissue in control sample (a) with neatly arranged myofibrils. In all heavy metal groups; Cd (c), Hg (e) and Cd+Hg (g), irregular and loose appearance of muscle tissue is visible at low magnification. At high magnification in control (b), single oval and centrally located nuclei (arrowhead) and small blood vessels and capillaries (arrows) are visible. Cd (d) shows presence of lipid vacuoles (arrow), irregular and flattened nuclei (thin arrow), destruction of myofibrils (arrowhead) and tissue dilatation (*). Further destruction of myofibrils is evident in the Hg exposed group (f) (arrowhead) with lipid droplet accumulation (arrow), and extravasation of erythrocytes (dashed arrow). In the Cd+Hg group (h), destruction of myofibrils (arrowhead) and erythrocytes extravasation (dashed arrow) are apparent and lipid deposition (arrow) as well as fine connective tissue fibrils are also present (thin arrow). Scale bars = 5 µm.
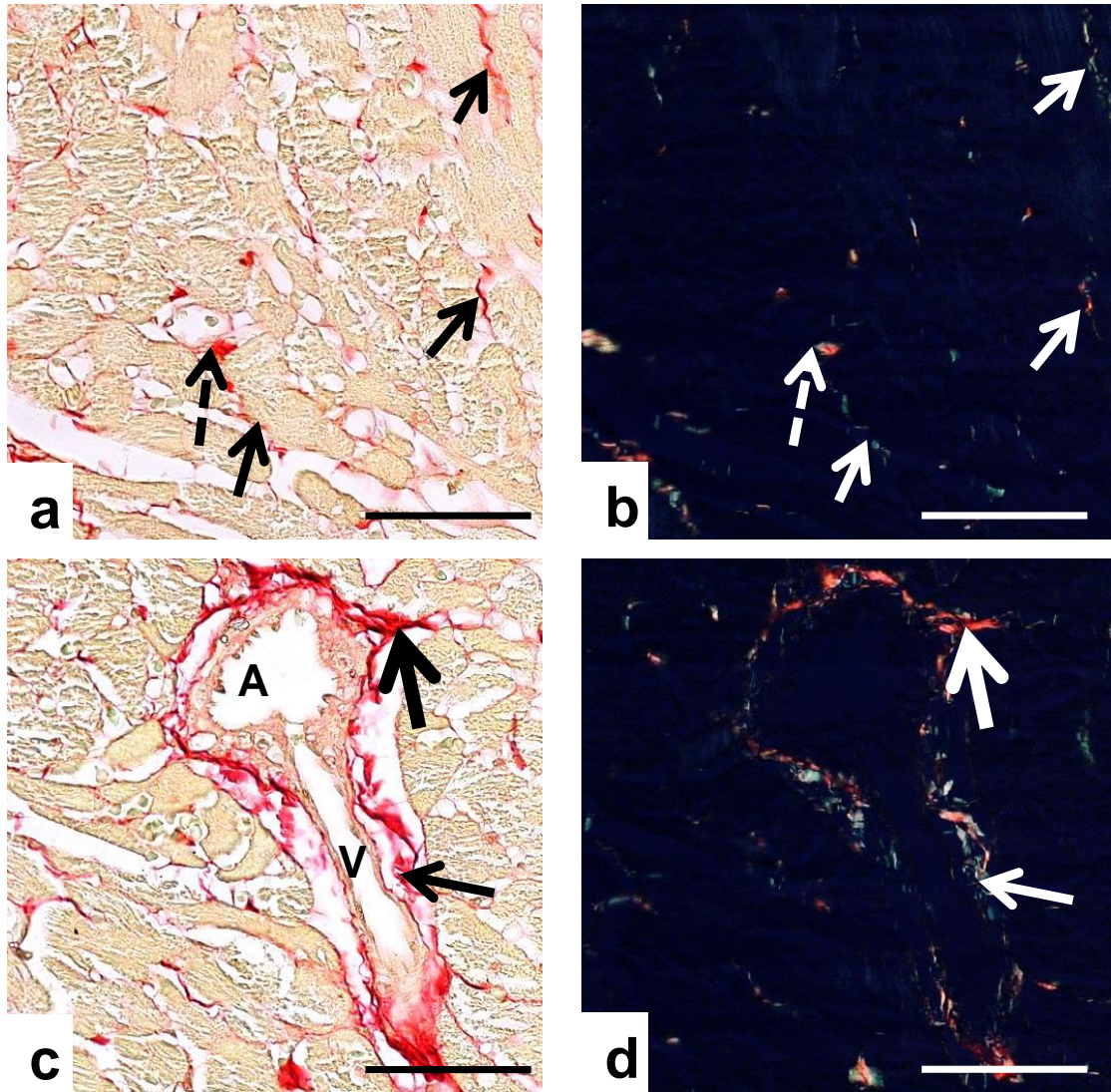
Figure 4.2: PR staining of control myocardium sections, showing differences in collagen distribution in normal heart tissue. Collagen found dispersed in the myocardium as endomysium surrounding muscle fibres (arrow) is shown in (a), viewed with brightfield microscopy. Image (b) shows the appearance of collagen with polarised light (arrow), with the collagen having a green to orange bifringance. Collagen is also found surrounding capillaries (a and b, dashed arrow) and is more apparent in brightfield (a) than in polarised light (b) due to it's fine structure. Images c and d represent the appearance of collagen surrounding larger blood vessels; arteriole (A) and venule (V) (c). In polarised light the collagen has a green to orange bifringenece and is confined to the perimeter of the blood vessel. Scale bars = 5 μm.
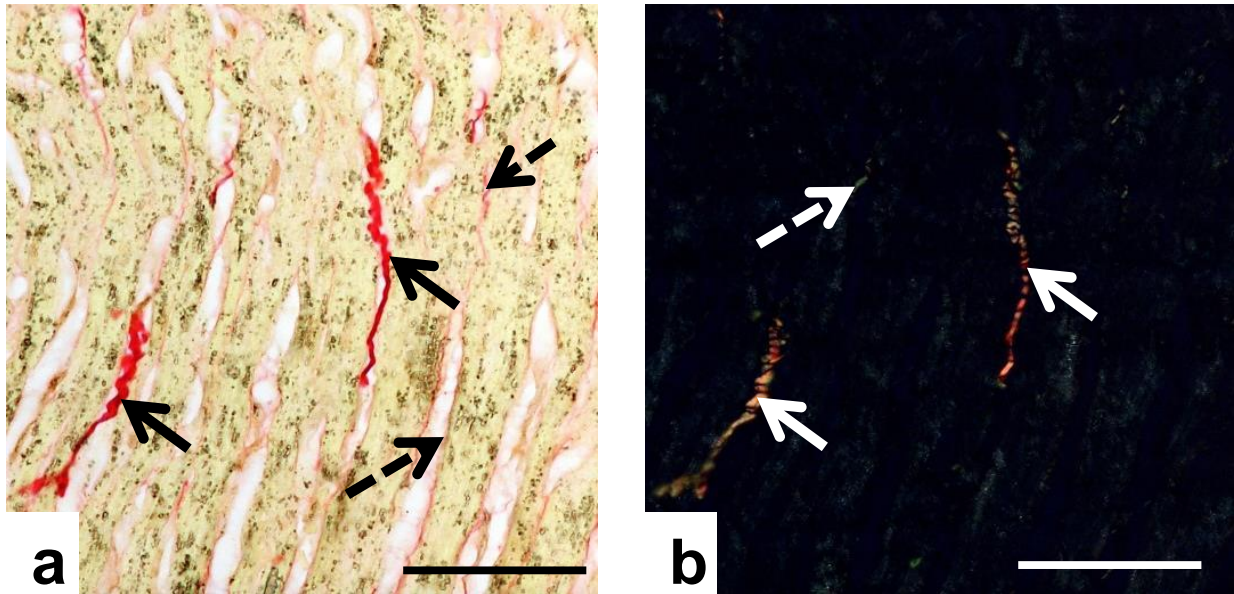
Figure 4.3: An example of a PR stained section indicating the differences between normal and fibrotic collagen in cardiac tissue of a rat exposed to Hg with brightfield (a) and polarised light (b). Normal endomysial collagen (dashed arrow) has a thin and fine fibre appearance (a) and low bifringence of a yellow to green colour (b). Fibrotic collagen is visible as thicker and wavy fibres (a) that have a strong orange to red birefringence with polarised light (b) than the normal green collagen of endomysium (dashed arrow). Scale bars = 40 µm.
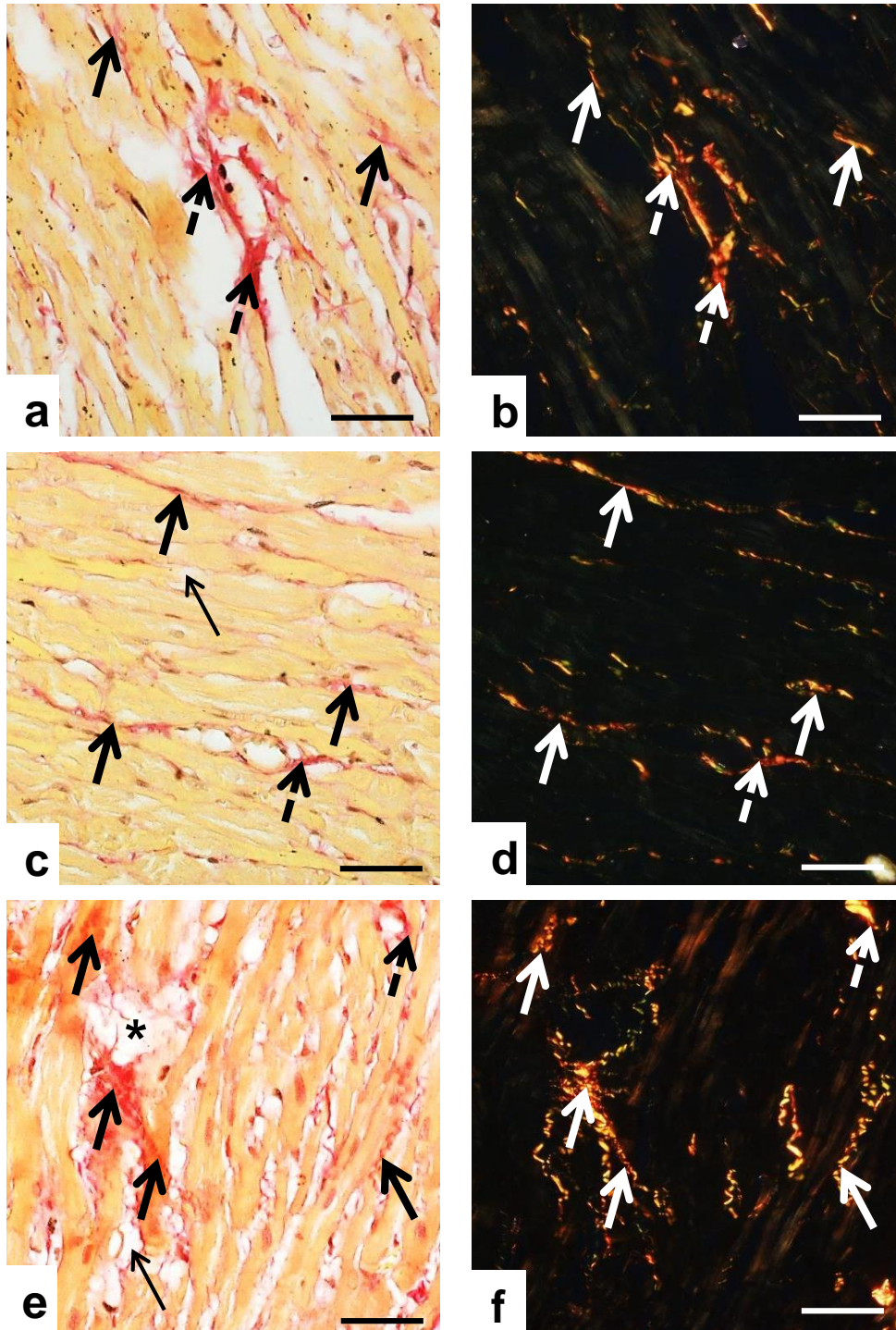
Figure 4.4: PR stained sections of experimental groups Cd (a and b) Hg (c and d) and Cd+Hg (e and f), showing collagen in the myocardium with brightfield (a,c,e) and polarised light (b,d,f). In the Cd group (a and b), a slight increase in collagen around blood vessels (dashed arrow) and in the endomysium (arrow) is present. Hg (c and d) had an increase primarily in the endomysium collagen (arrow) with a slight to unchanged appearance of collagen around the capillaries (dashed arrow). Slight destruction of the myocardium is evident by spaces in the tissue (thin arrow). The Cd and Hg group (e and f) showed the greatest pathology with increase in collagen around blood vessels (dashed arrow) and dense and wavy collagen in the connective tissue surrounding the muscle fibre and extending out into the interstitium (arrows). Lipid deposition (thin arrow) is evident with brightfield (e) and an accumulation of lipid droplets leading to the destruction of the myocardium is indicated (*). All groups showed fibrotic collagens with an orange to red birefringence. Scale bars = 40 μm.
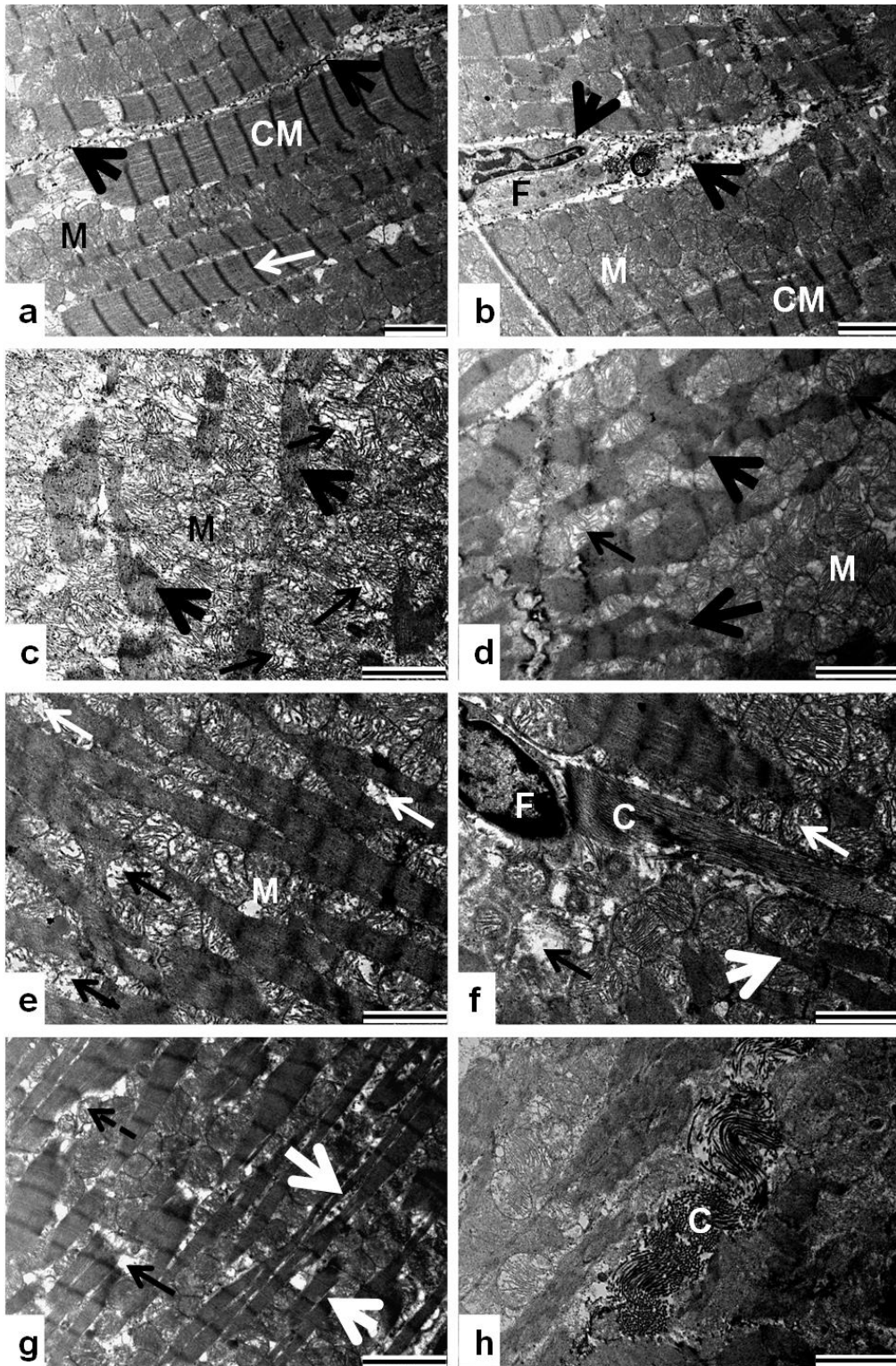
Figure 4.5: General ultrastructural features of cardiac muscle in control (a and b), Cd (c and d), Hg (e and f) and Cd+Hg group (g and h). Control (a) showed a normal ultrastructure with well organised parallel bands of mitochondria and cardiac muscle fibrils, with clear Z lines (arrow). Collagen fibrils are visible forming part of the endomysium (arrowheads). In (b) a myofibroblast is shown, with collagen fibrils surrounding it (arrowheads). Cd (c and d) shows a destruction of myofibrils (arrowheads) and areas of myofibre loss being replaced by mitochondria, which appear swollen (thin arrows). In (e and f), mitochondria appear larger in size with slight vacuolisation (arrows). In (f) thin, broken myofibrils are present (arrowheads) and very dense collagen accumulation (C) around a myofibroblast (F). Cd+Hg (g and h) group shows extensive thinning and destruction of myofibrils (arrowheads) as well as loss of myocardial tissue (arrow) and small, damaged mitochondria (dashed arrow) in (g). Interstitial collagen (C) deposition is shown in the combination group (h). Mitochondria (M), Cardiac myofibrils (CM), myofibroblast (F), Collagen (C). Scale bars = 2 μm.
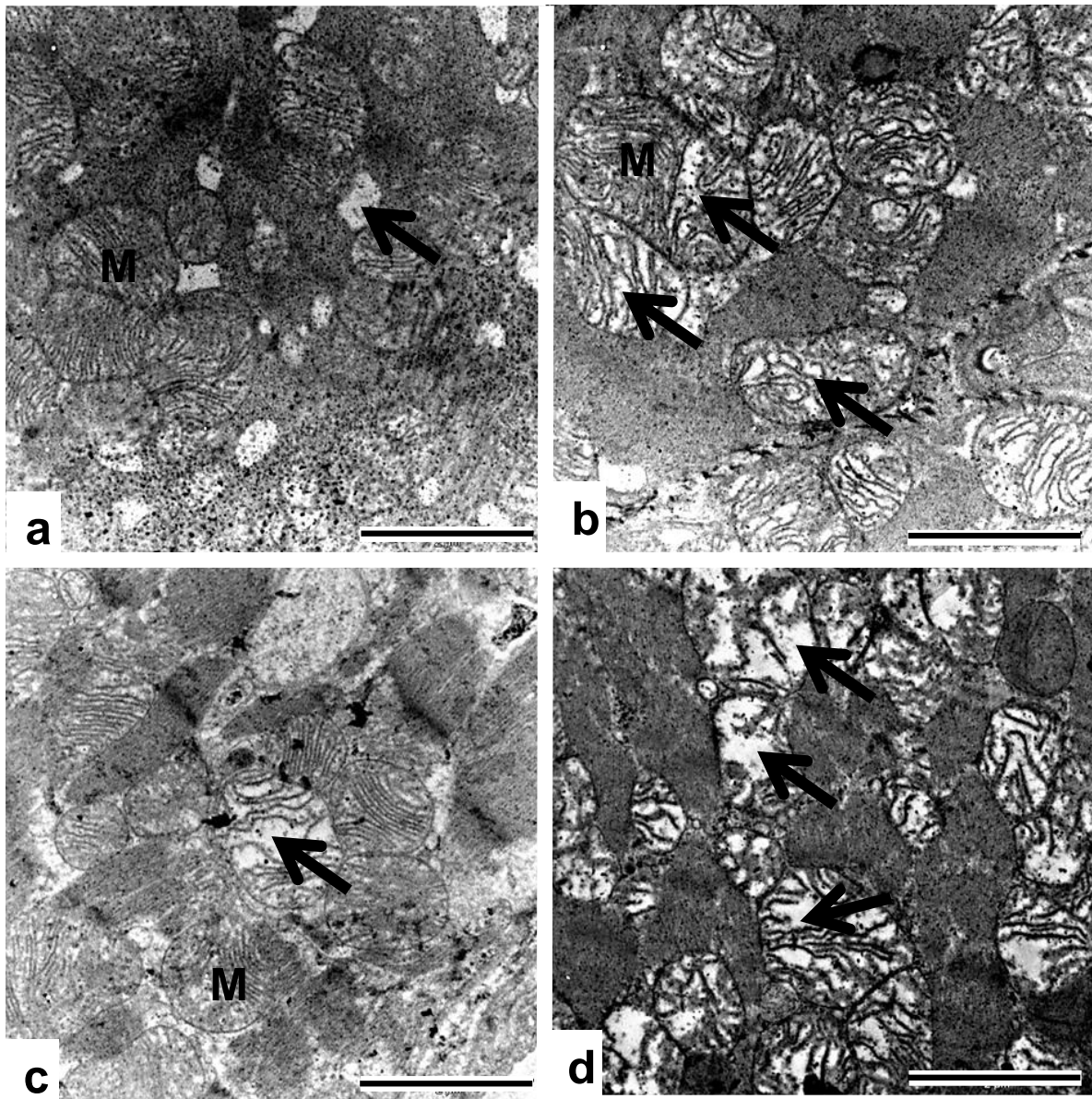
Figure 4.6: Detailed ultrastructure of mitochondria in transverse sections of the cardiac muscle. Abundant regular cristae are seen in control (a), with axial tubules, a normal feature of healthy cardiac muscle, indicated between the mitochondria (arrow). Damage due to swelling and loss of cristae is evident in experimental groups, found frequently as fragmented cristae (arrows) in Cd (b), less frequently in Hg (c) (arrow), and most frequently and to a higher degree of damage, with complete loss of cristae (arrows) in the Cd+Hg group (d). Normal appearing mitochondria (M). Scale bars = 2 µm.
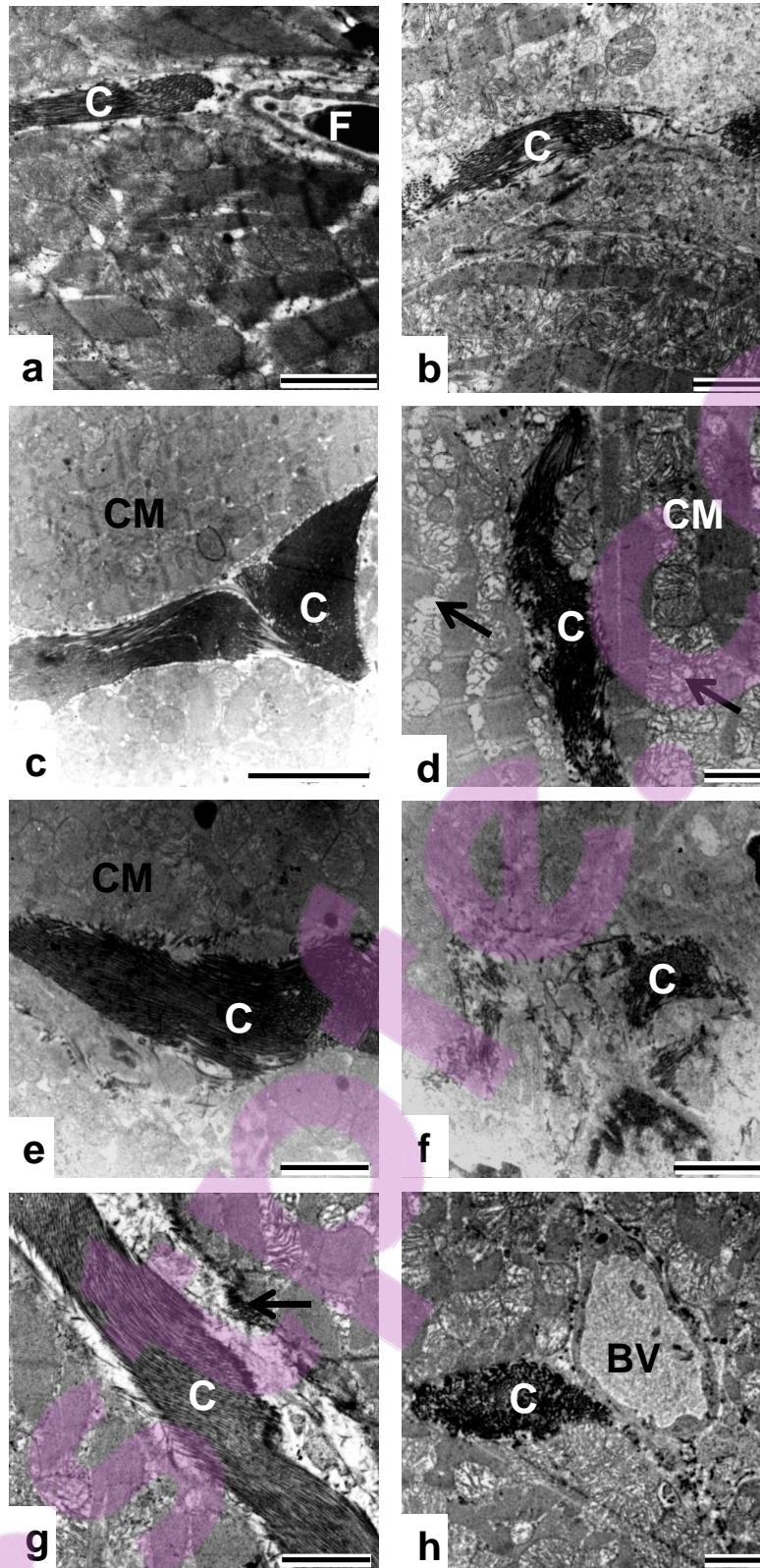
Figure 4.7: Ultrastructure of fibrotic collagen in cardiac muscle. Control tissue (a and b) shows normal collagen distribution near a fibroblast (F) in (a) and normal, finely dispersed collagen surrounding mitochondria (b). In the Cd group (c,d) dense accumulation of collagen fibrils is visible in (c) as well as intersitital collagen in (d). Damaged mitochondria in the vicinity are also shown (arrows). Intersitial collagen was also present in the Hg group (e and f), as collagen fibers made up of both densely packed collagen fibrils (e) and loosely dispersed collagen in between mitochondria and muscle fibrils (f). The Cd+Hg group (g and h) had extremely thick fibers made up of dense fibrils of collagen (g), which appears to have been directly attached to the muscle fibrils (arrow), and also collagen in the interstitium (h), in this case shown next to a blood vessel (BV),Collagen (C), cardiac muscle fibrils (CM). Scale bars = 2 µm.

61

4.3.1.1. Alterations to cellular structure of cardiac muscle

Figure 4.1a - f are representative of heart tissue samples obtained from the different experimental groups. Images show sections through the myocardium. Histological architecture of the heart showed clear variations from no damage in the control (Figure 4.1a), to mild lesions in Cd and Hg treated groups (Figure 4.1 c and e) to severe in the combination group (Figure 4.1g and h). Normal appearing oval and centred nuclei and a normal myofibrillar structure with striations, branched appearance and continuity with adjacent myofibrils are shown in the control (Figure 4.1 a). Small blood vessels and capillaries are often visible throughout the cardiac muscle. A distinct appearance of cardiotoxicity with various degrees of damage is visible in the experimental groups indicated by the irregular and loose appearance of muscle tissue visible at low magnifications (Figure 4.1c, e and f). Deformations in size and shape of nuclei and a disarrayed pattern of myofibres were common in all of the heavy metal exposed groups. Lipid droplets were present in the Cd treated group as well as flattened nuclei and a destruction of myofibrils and dilatation of the cardiac tissue, often associated with tissue oedema (Figure 4.1d). In the Hg group (Figure 4.1f) further destruction of myofibrils, lipid accumulation and the presence of erythrocytes outside of the blood vessels (extravasation) as a result of capillary and small blood vessel distortion, are apparent. The Cd+Hg group (Figure 4.1 g and h) showed the most pathology with the presence of an excessive erythrocyte extravasation as well as lipid deposition and accumulation. In addition, the presence of thin filaments of connective tissue were observed (Figure 4.1h thin arrow).

4.3.1.2. Alterations to collagen distribution in the cardiac muscle

In the PR stained sections, collagen was visualised in two areas, the endomysium which surrounds the individual muscle fibrils, and the connective tissue surrounding the blood vessels. Figure 4.2 provides an example of the appearance of collagen in the control group, representative of normal cardiac histology. With brightfield microscopy, collagen is found as thin strands of red staining fibres dispersed in the myocardium, present in the endomysium surrounding muscle fibres (Figure 4.2a, solid arrow). Upon polarization, the collagen has a green to orange birefringence (Figure 4.2b). The second area of collagen deposition investigated was the connective tissue surrounding the smaller blood vessels and capillaries as shown in Figure 4.2c. The collagen surrounding the capillaries in a control sample is better observed with brightfield microscopy (Figure 4.2a, dashed arrow) than with polarised light (Figure 4.2b, dashed arrow) as it has a faint birefringence due to its fine structure. In slightly larger blood vessels like arterioles and venules displayed in Figure 4.2c, the collagen is clearly visible and had a birefringence of alternating green – yellow and orange – red colour under polarised light (Figure 4.2d) which is representative of thinner type III and thicker type I collagen respectively. It is also important to note that in Figures 4.2 c and d, collagen can be observed surrounding the smaller blood vessels and it is apparent that the collagen fibres are localised to the periphery of the blood vessel and little to no collagen is found in the myocardial tissue surrounding the blood vessels.

An example of fibrotic collagen is shown in Figure 4.3 where it is compared to normal appearing collagen in the same sample. Cardiac tissue from the Hg exposed group was used to demonstrate the difference between normal endomysial and fibrotic collagen with brightfield and polarised light. Fibrotic collagen appears as a thick and slightly wavy or coiled band (Figure 4.3a, solid arrows) in comparison to the fine collagen (Figure 4.3a, dashed arrows). In the polarised light (Figure 4.3b) the collagen birefringence of the normal and fibrotic collagen is also different, with the normal endomysial collagen having a faint green birefringence (Figure 4.3b, dashed arrow) while the fibrotic collagen is a bright orange – red, which is indicative of deposition of thick type I collagen fibres in fibrosis (Figure 4.3b, solid arrow).

Excess collagen deposition is observed in all the experimental groups compared with the control, and is most apparent in the combination group (Figure 4.4 e and f). In the single exposure groups, Cd was found to increase the presence of collagen surrounding the blood vessels (Figure 4.4a and b, dashed arrow) as well as increases in the collagen within the enodomysium surrounding the myofibres (Figure 4.4 a and b, solid arrow), with both areas of collagen showing a strong orange – red birefringence (Figure 4.4b). The Hg group (Figure 4.4c and d) had an increased amount as well as a change in the structure of collagen fibrils; the pathogenic fibrils being thicker and coiled in appearance and located primarily in the endomysium (Figure 4.4c and d, solid arrows). Some collagen was also present surrounding the capillaries (Figure 4.4 c and d, dashed arrows) and tissue destruction was further evident in the Hg group, indicated by a thin arrow in Figure 4.4c. The combination group (Figure 4.4 e and f) once again showed the most tissue alterations, with excess collagen deposition being a prominent feature. Collagen also exhibited a strong birefringence and alterations in its structure, being wavy or coiled in the combination group (Figure 4.4e and f, solid arrow) and located in an area of tissue destruction (Figure 4.4e, asterix) which appears to be caused by lipid droplet accumulation. Other, smaller areas of tissue destruction are evident in the tissue and are indicated with the thin arrow in Figure 4.4 e.

4.3.1.3. Ultrastructural cellular changes and connective tissue distribution in cardiac muscle

Ultrastructural features of the cardiac muscle showed differences between the exposed groups and the control. Parallel bands of mitochondria and cardiac muscle fibrils, which are characteristic of normal cardiac muscle (Figure 4.5 a, arrow), were distorted following exposure to heavy metals. Interruptions of Z lines were evident in the Cd exposed group together with a clear destruction of the myofibrils making up the cardiac muscle (Figure 4.5b and c, arrowhead). As a result of myofibril destruction, fewer myofibrils are visible in the cardiac muscle, and are instead replaced by swollen mitochondria (Figure 4.5b and c, thin arrows). Similar myofibrillar damage was observed in the Hg group (Figure 4.5 f, arrowhead) and in the combination group (Figure 4.5g, arrowhead). In addition to the damage of myofibrils the mitochondria showed clear damage and destruction, visible as spaces and dilatations of the mitochondrial body in Hg (Figure 4.5e and f, thin arrows). These

changes to the myofibrils are indicative of cardiac myocyte necrosis and can be observed at low magnification in all the exposure groups in Figure 4.5. Along with the mitochondrial damage abnormal interstitial collagen deposition was observed in the low magnification images, and primarily in the Hg (Figure 4.5f, C) and Cd+Hg (Figure 4.5h, C) groups.

It was also apparent that areas where myofibrillar loss occurred were replaced by mitochondria. Therefore, the low magnification images showed a disturbance in the parallel arrangement of the myofibrils and mitochondria, as well as the areas of collagen deposition.

Changes to the mitochondrial size and the cristae making up the mitochondrial matrix are shown in more detail in Figure 4.6, and changes to these structures are apparent in the experimental groups when compared to the control. In the control the mitochondrial cristae are neatly and closely packed (Figure 4.6a) and the empty spaces visible in the tissue (indicated by the arrow), are axial tubules. Alterations to the mitochondrial cristae do occur in controls but these alterations are rare. In the exposed groups mitochondrial damage, as a result of toxicity, is evident by swelling and slight damage to the mitochondrial cristae in the Cd exposed group (Figure 4.6b, arrows). The Hg group (Figure 4.6c) showed mitochondrial toxicity, evident by the destruction of cristae (Figure 4.6c, arrow) however, damaged mitochondria were not observed as frequently in this group as in the Cd group. In the metal combination group (Figure 4.6d), increased mitochondrial toxicity was observed, with either an extensive swelling of the mitochondrial matrix, or a complete loss of cristae (Figure 4.6d, arrows). Interstitial collagen and fibre destruction with areas of empty or vacuolated matrix observed ultrastructurally at lower magnification (Figure 4.5g) were present in the combination group, as well as vacuolisation from the disintegrating mitochondria (Figure 4.6d) leading to larger vacuolated spaces between fibres, as observed in the LM images (Figure 4.1h and 4.4e).

Collagen deposition in the exposed groups compared to the control is shown in Figure 4.7. In typical healthy muscle tissue collagen is expected to be found around fibroblasts as these are the cells which synthesize collagen (Figure 4.7a) and also finely dispersed around the myofibrils and mitochondria, making up the endomysium (Figure 4.7b), as observed in the control muscle tissue. From the images it can be observed that ultrastructurally, in the heavy metal exposed groups, the collagen deposition is different when compared to the control. In the Cd group a dense deposition of collagen in the endomysium (Figure 4.7c) as well as in the interstitium (Figure 4.7d) surrounded by damaged mitochondria (Figure 4.7d, arrows) and myofibrils is present. Densely deposited collagen (Figure 4.7e) as well as extensive interstitial collagen deposition (Figure 4.7f) is also observed in the Hg group. The combination group (Figure 4.7g) shows extremely thick collagen fibres composed of dense fibrils, which appear to have been directly attached to the muscle fibres (Figure 4.7g, arrow). Collagen deposition around a blood vessel is also shown for the Cd+Hg group in Figure 4.7h.

4.3.1. Structural effects of Cd and Hg alone and in combination of the morphology of the aorta

In the aorta, the general morphology of the tunica intima, tunica media and tunica adventitia were evaluated with H&E. At a higher magnification the arrangement of the connective tissue, SMC and endothelial cells were also evaluated. The aorta is an example of an elastic artery and the distribution and arrangement of the elastic fibres was evaluated using the Verhoeff van Gieson (VvG) method (Cui *et al.*, 2014). The stain renders elastic fibres and nuclei blue to black in colour, collagen red and other tissue elements yellow. With the PR stain, elastin fibres may have a green birefringence which is easily confused with type III collagen. Therefore, for connective tissue in the aorta the VvG method was used to clearly distinguish the major connective tissue component of elastic arteries.

In this section the changes in the morphology of the aortas were evaluated at low magnification following H&E and VvG staining (Figure 4.8 and 4.9). The effects on connective tissue arrangement as well as cell and organelle morphology were also evaluated with TEM (Figures 4.10). The metal exposed groups were compared to the control.
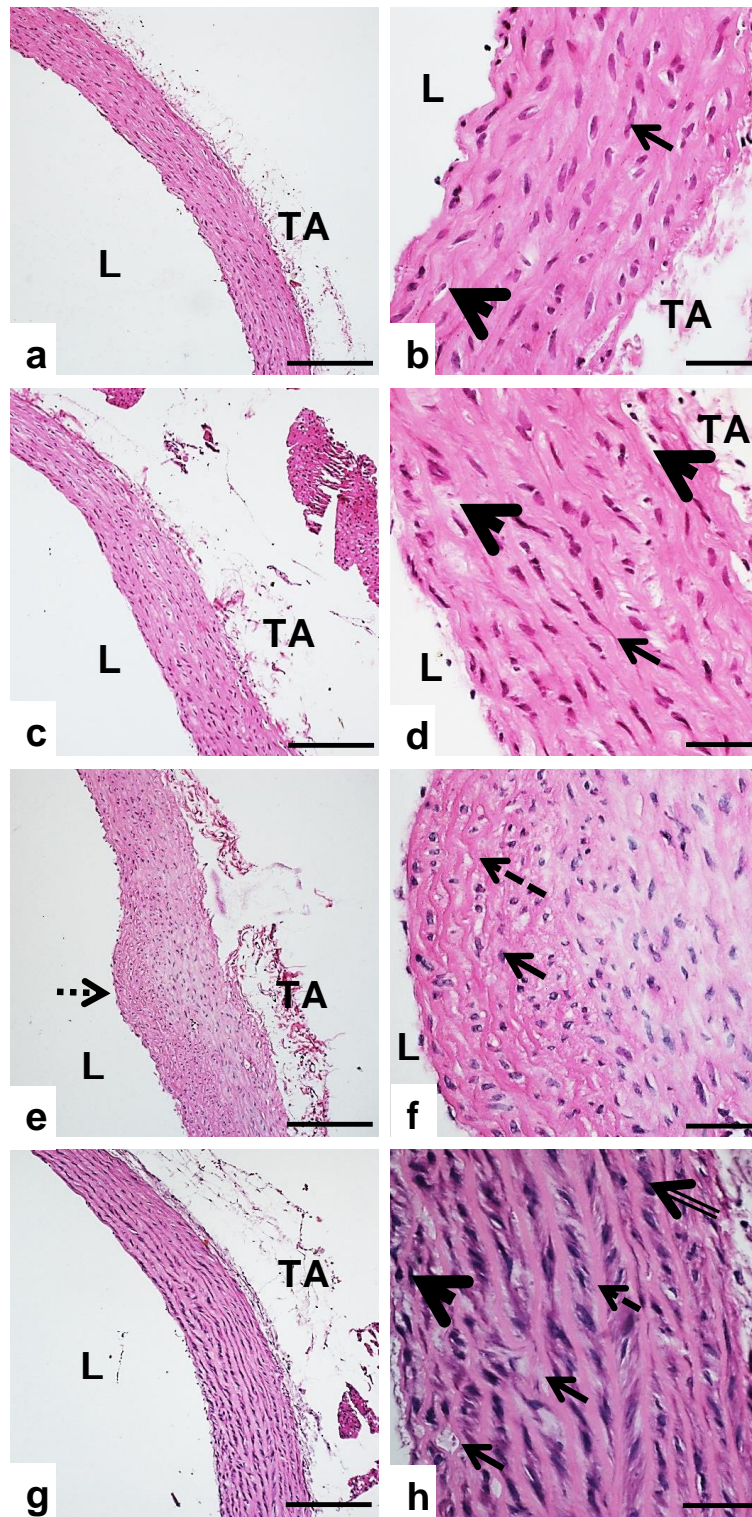
Figure 4.8: H&E stained sections of the aorta showing the general cell and tissue structure. In the control group at low magnification (a) showing even thickness throughout the aortic wall and oval nuclei (arrow) with little perinuclear space (arrow head) in (b). The Cd exposed group revealed slight changes in the appearance of the aortic wall (c) as well as flattened nuclei (arrow) and an increase in perinuclear space (arrowhead) in (d). In the Hg group, distortion of the aortic wall is shown in (e) (dashed arrow) and change in tissue structure of the area is visible at high magnification in (f), with rounded nuclei in the tunica intima (arrow), as well as connective tissue surrounding the cells (dashed arrow). The Cd+Hg group (g and h) revealed some distortion of the arterial wall at low magnification (g) with a loss of connective tissue banding in the tunica intima (arrow head), flattened nuclei (double arrow) and thick bands of connective tissue (dashed arrow) in the tunica media visible at higher magnification in (h). L = Lumen, TA = Tunica Adventitia, TI = Tunica Intima, TM = Tunica Media. Scale bars (a, c, e, g) = 200 μm, (b, d, f, h) = 40 μm.
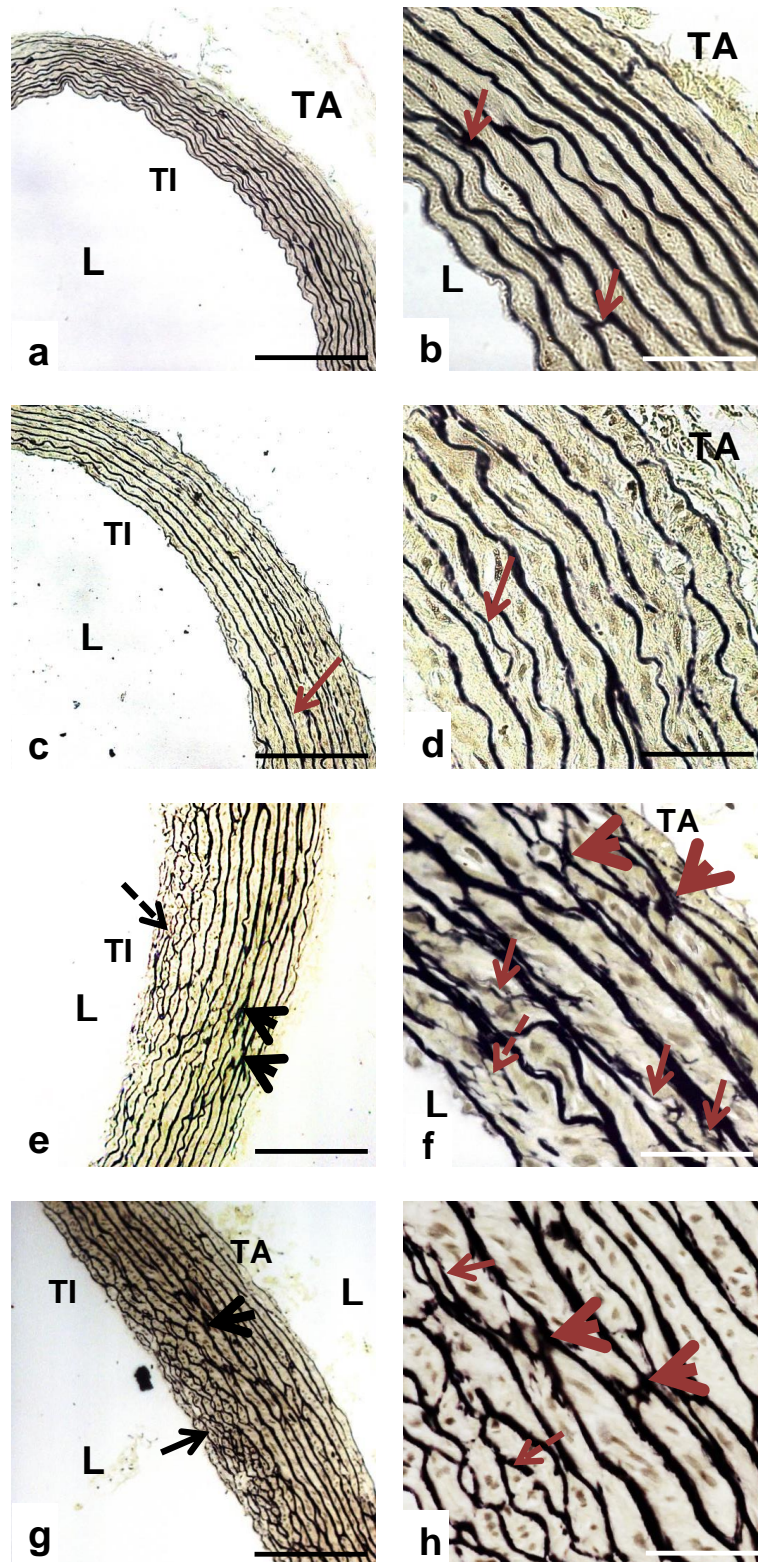
Figure 4.9: VvG stain showing elastic fibre arrangement in the aorta. Control (a and b) shows the aortic wall with evenly thick, regular arranged black staining bands of elastin at low magnification, and interlinkages between elastic laminae are visible at high magnification in (b) (arrow). The Cd group (c and d) showed changes in the elastin in areas of thickened aortic wall (c, arrow) at low magnification, with finer elastic fibres between the lamina (d, arrow) and spaces in the lamella visible at high magnification in (d). In the Hg group in (e and f) elastin deposition around cells of the tunica intima is present (e, dashed arrow) and increase in the linkages between the lamina (e, arrowhead). Fine fibre deposition in the Hg group is shown in (f) (arrows) and cross linkages between elastin laminae (f, arrowheads). The Cg + Hg group (g and h) showing elastin changes at low magnification in tunica intima (g, arrow) and large interlinkages between lamina (g and h) (arrow heads). Elastic fibre deposition is present surrounding the cells of the tunica intima (h, dashed arrow). L = Lumen, TA = Tunica Adventitia, TI = Tunica Intima. Scale bars (a, c, e, g) = 20 µm, (b, d, f, g) = 5 µm.
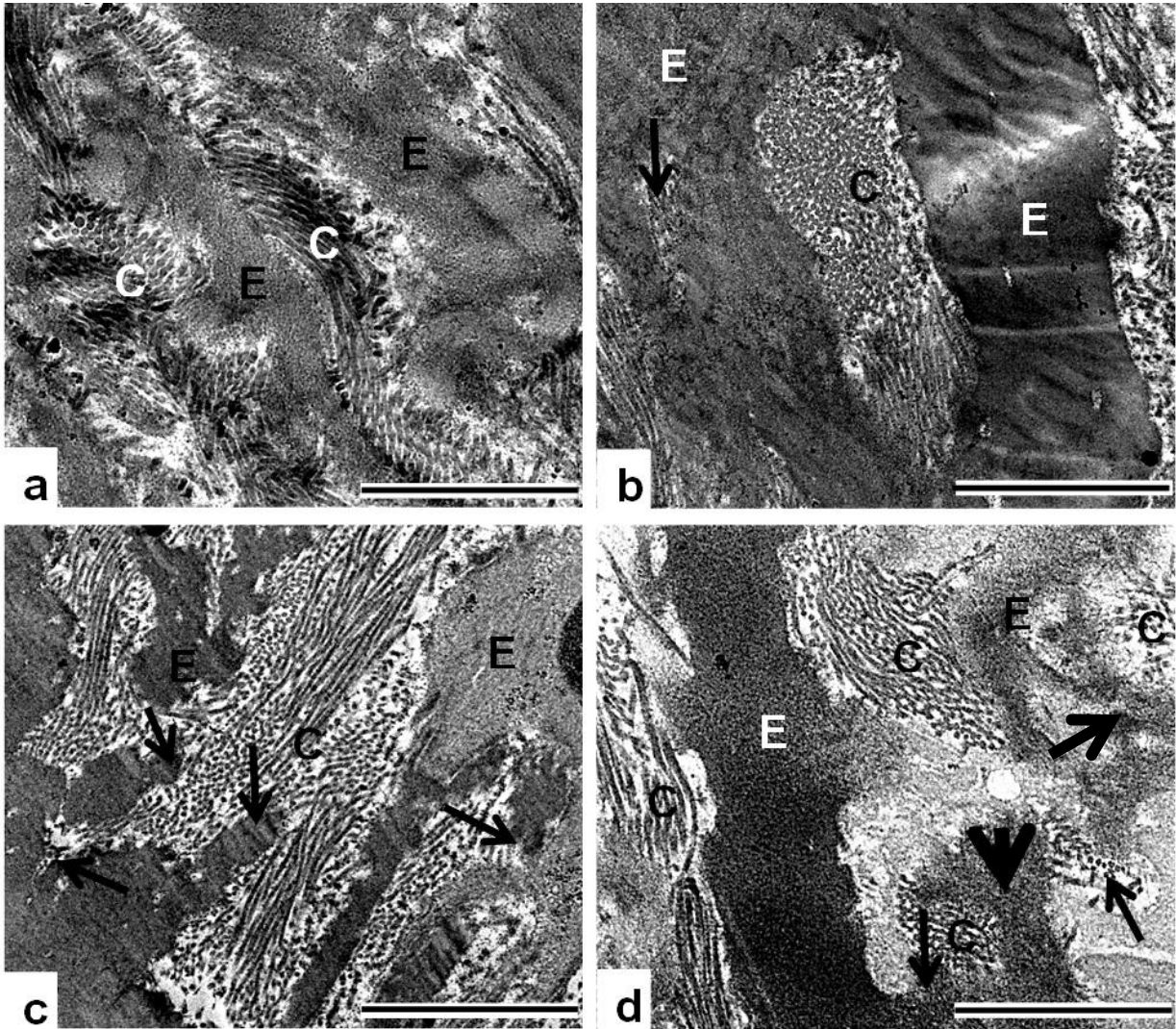
Figure 4.10: TEM images of the aorta showing differences in the elastin and collagen structure. In (a) control, alternating bands of collagen and elastin are visible. In (b) the Cd group showed collagen deposition in the elastin band (arrow) and elastin fibres with more electron density (E). In the Hg group (c), elastin bands are interrupted (arrows) and collagen fibres are deposited instead. The Cd+Hg group (d) showed elastin fragmentation (arrowhead) and collagen deposition in between the elastin (arrows). C = Collagen, E = Elastin. Scale bars = 2 μm.

4.3.1.1. Alterations in smooth muscle structure and elastin distribution in the aorta

In the control group, the blood vessel wall of the aortas had an even thickness throughout, with the VSMC having oval nuclei (Figure 4.8a). Some perinuclear spaces were observed in the controls, which is a normal feature of tissue shrinkage during processing. Elastin staining revealed structurally smooth, black staining bands of elastin with fibrillar projections forming interlinkages between neighbouring elastic laminae. These interlinkages are a normal feature and serve in communication and elastic recoil function between the laminae (Figure 4.9a and b). In the Cd exposed group, a slight change in the aortic wall was observed, primarily altered VSMC structure. The nuclei of the VSMC appeared flattened with an increase in the perinuclear space, causing vacuolisation of the aortic matrix. The thickness of the aortic wall in some areas also appeared increased (Figure 4.8c) and when viewed in more detail (Figure 4.8d) it is observed that this area contained more connective tissue and cells in the aortic wall layers. Changes to the elastin in the Cd group (Figure 4.8c) included a reduction in the wavy appearance of the elastin as well as the presence of finer elastic fibres between the elastic lamina in areas of the aorta where the aortic wall was thickened (Figure 4.9d, arrow). The most apparent alterations to the aortic morphology were observed in the Hg and in the combination group and these included changes to connective tissue structure and cellular arrangement of the aorta. In the Hg group, the structure of the aorta wall was altered as shown in Figure 4.8e with the presence of cell clusters associated with connective tissue that bulges outwards into the lumen (Figure 4.8e dashed arrow). The nuclei of these cells appeared smaller and rounded, often with bands of connective tissue surrounding the cells. Elastin deposition in the Hg group was observed around the cells of the tunica intima (Figure 4.9e dashed arrow) and was increased in the interlinkages between the lamina. The presence of elastin fibres (Figure 4.9f) was also observed. The combination group showed similar cellular and connective tissue changes, however the thickness in the wall was gradually increased (Figure 4.8g) as opposed to the bulge that extended into the lumen observed for the Hg group. At higher magnification (Figure 4.8h), the nuclei of the cells in the combination group also appeared flattened and closer together than found in the Hg group. The connective tissue of the combination group appeared to have lost definite banding and instead was surrounded by cells of flattened nuclei, in close proximity to one another. The elastin staining further showed the presence of excessive elastin present in the tunica intima (Figure 4.9g, arrow) as well as large interlinkages between the elastic laminae (Figure 4.9h, arrowheads).

Ultrastructural changes to the elastin and collagen are shown in the TEM images in Figure 4.10. The control tissue (Figure 4.10a) shows alternating bands of collagen and elastin as is expected in the connective tissue of elastic arteries. In the Cd exposed group collagen was observed to interrupt the elastic fibres (Figure 4.10b, label C) while an area of new collagen deposition and elastin destruction was observed adjacent in the elastin band (Figure 4.10b, arrow). In the Hg exposed group, interruptions in the horizontal elastic bands were observed. In the areas where

elastin was lost, collagen was present (Figure 4.10c). In the combination group, very electron dense elastin strands are present and with areas of lighter density along the main elastin fibre which appeared to be newly deposited elastin and similarly arranged elastin is located individually among the collagen bundles (Figure 4.10d, thick arrow, label E).

4.4.   Discussion

Although previous studies have identified changes in tissue structure in animal models exposed to metals (Aragwal *et al.*, 2010; Karaboduk *et al.*, 2015; Uzunhisarcikli *et al.*, 2016), the effects of Cd and Hg have been poorly investigated. In the animal models, the heart has been shown to be affected by heavy metal toxicity (Aureliano *et al.*, 2002; Soares *et al.*, 2006) leading to altered cardiac function (Tort and Madsen, 1991). A limitation of these studies is that the metal concentrations are often arbitrarily chosen or are selected based on other studies and this exposure cannot be extrapolated to relevant levels of environmental exposure. The present study was undertaken to address these limitations and rats were exposed to Cd and Hg based on the 1000x the WHO safety limits of exposure. Considering that every day in a rat is approximately 34.8 human days (Sengupta, 2013), the exposure period is therefore approximately equivalent to three-year chronic human exposure. Both the heart and the elastic arteries such as the aorta are the major components of the vascular system and any damage or functional changes can lead to the development of CVD.

Heart tissue contains many mitochondria and as sites of cellular energy production, any damage or alterations in structure, function and number will compromise cardiac tissue functioning. Due to the high density of mitochondria in cardiac tissue, associated oxidative stress has been identified as an important mechanism in cardiac disease (Dhalla *et al.*, 2000; Jawalekar *et al.*, 2010). Mitochondrial dysfunction includes a decrease in energy production, loss of myocyte contractibility and an increase in apoptosis and/or necrosis, which eventually leads to cardiac failure (Capentaki, 2002; Marín-García and Goldenthal, 2008).

LM with H&E staining revealed that in all metal groups the arrangement of the myocytes were irregular and had a loose appearance. The presence of lipid droplets, irregular and flattened nuclei, the destruction of myofibrils and tissue dilatation was observed in cardiac tissue exposed to Cd. For Hg, there was also lipid droplet accumulation as well as extravasation of erythrocytes. In the Cd+Hg group, destruction of myofibrils, lipid droplet accumulation and erythrocyte extravasation were also apparent and in addition, the presence of fine connective tissue fibrils was also observed. These findings indicate that both Cd and Hg alone and in combination cause damage to cardiac tissue.

Cd activates the necroptosis pathway (Cai *et al.*, 2017), resulting in myocardial damage. Mercury is a recognized cause of dilated cardiomyopathy (Frustaci *et al.*, 1999; Rice *et al.*, 2014). Exposure to low doses of Cd increases the levels of Cd in mammalian heart by 900-fold (Kopp *et al.*, 1978). Cd

has been suggested to be a source of dilated cardiac myopathy through action on vascular endothelial cells of the heart (Prozialeck *et al.*, 2006), via the disruption of vascular endothelium cadherin localisation (Prozialeck, 2000; Pearson *et al.*, 2003).

Oxidative stress is associated with lipid accumulation in organs, resulting in the development of liver and cardiac steatosis. Cardiac lipid accumulation as a result of mitochondrial dysfunction has been implicated in heart failure, chronic and binge ethanol consumption (Matyas *et al.*, 2016) as well as obesity (Sletten *et al.*, 2018). Lipid accumulation is also associated with failure of the contractile mechanism of the cardiac muscle, as mechanical unloading with a ventricular assist device has been shown to decrease lipotoxicity and normalise cardiac metabolism in failing hearts (Chokishi *et al.*, 2012). Occasional lipid droplets in Cd treated cells have been reported for CD434+ cells at 48 hr., 10 µM Cd exposure (di Gioacchino *et al.*, 2008). Some characteristics of autophagy were present and these were the presence of lipid vacuoles and mitochondrial swelling for the exposed groups. To conclude if autophagy has occurred further measurement of biological markers of autophagy will be necessary. The process of autophagy has been observed in cardiofibroblasts exposed to Pb for 12 hrs, with no loss of cell viability (Sui *et al.*, 2015). This protective mechanism occurs via the inhibition of the mammalian target of rapamycin complex 1 (mTORC1) pathway, thereby preventing stress to the ER. A study investigating Cd and As toxicity as autophagy inducing agents showed that exposure to $CdCl_2$ for up to 18 hr at doses lower than 10 µM causes autophagy, whereas exposure for 24 hrs to 1µM $CdCl_2$, caused apoptosis. This suggests that autophagy is a cell survival mechanism and is initiated at low concentrations for a limited exposure time, after which cytotoxicity and associated apoptosis occur (Chiarelli and Roccheli, 2012). Cd is shown to induce autophagy through ROS dependant pathways (Son *et al.*, 2011). Similar trends of autophagy at low concentrations, followed by necroptosis have been reported for exposure to etHg whereby autophagy served as a protective mechanism at low doses but was detrimental at high dose exposure (Choi *et al.*, 2016). The results of the present study showed that exposure to concentrations of 1000x the WHO safety limits and blood concentration levels of 16,69 nM (0.0167 µM) Cd and 186,67 nM (0.187 µM) Hg alone and 121,06 nM (0,121 µM) Cd and 155,99 nM (0,156 µM) Hg in combination (Table 3.2) did cause structural tissue alterations associated with autophagy but findings were not conclusive, but evidence of necroptosis is obvious.

Erythrocyte extravasation is associated with vascular leakage as a result of endothelial damage. Hg promotes vascular damage favouring vascular leakage into tissues and consequently interstitial edema (Sharma 1998). Increased presence of connective tissue fibres indicates that Cd+Hg induce fibrosis which often occurs due to oxidative damage as a result of mitochondrial dysfunction.

A comparison of heart tissue of control rats with the metal exposed groups by electron microscopy (Figure 4.5) revealed fragmentation and lysis of myofibrils. Similar results of myofibrillar

71

degeneration through fragmentation and lysis has been reported in a study investigating the effects of the anticancer drug doxorubicin (DOX) which causes severe cardiac damage through an oxidative mechanism (Al-Harthi *et al.*, 2014).

Cardiac myocytes contains 50 - 100 mitochondria and there are 1 - 10 molecules of mtDNA in each of the mitochondria (Attardi and Schatz, 1988). Enzymes, calcium, magnesium, DNA and RNA contained within the mitochondria all play a role in the energy production (Young and Heath, 2006). Early myocardial restructuring can occur as a response to injury or pathological stimuli. However, if a toxic insult is sustained the proliferation of mitochondria during the restructuring cannot match the increased energy demand of the damaged myocytes and eventually this leads to myocyte dysfunction and death (Huss and Kelly, 2005).

Damage to mitochondria is one of the most distinguishing features of oxidative stress, and it is seen in ageing, hypertrophy, heart failure, ischemia and reperfusion. Mitochondrial autophagy is nescessary for the control of oxidative states (Lemasters, 2005; Tsutsui *et al.*, 2008; Lee *et al.*, 2012; Morales *et al.*, 2014). As mtDNA lacks protective histones and has a limited ability to regenerate in comparison to nuclear DNA (nDNA) it is highly vulnerable to the effects of free radicals and ROS generated during cellular respiration (Tsutsui, 2001; Tsutsui *et al.*, 2009). Consequently, due to these factors, mtDNA is more susceptible to oxidative damage and acquires mutations faster than nDNA (Ames *et al.*, 1993; Lee and Wei, 2003). This can cause changes in mtDNA copy number and integrity and mitochondria number. Once mtDNA is damaged or mutated, a reduction of antioxidative capacity can further lead to an increase in ROS production and oxidative damage. Membranous organelles have high lipid content, are easy targets for oxidative damage through lipid peroxidation and alteration in membrane structure can lead to mitochondrial swelling due to increased fluid filtering into the mitochondrial matrix (Thophon*, et al.*, 2004).

Mitochondrial quality has been identified as an important indicator of whether muscle has undergone reversible or irreversible injury (Cheville, 2009). Intact mitochondria are indicators of reversible injury, while mitochondria with disintegrated cristae and matrix proteins and granular accumulation in the matrix are indicators of more severe injuries. If many mitochondria are affected, these changes eventually lead to cell death due to decreased ATP generation and a state of irreversible injury (Cheville, 2009). In addition, a reduction in mitochondrial energy generation also results in the releases of apoptosis triggers such as cytochrome C and/or a decreased mitochondrial SOD activity. Loss of mitochondrial function may also result in an accumulation of toxic compounds in the myocyte such as lactate build up or acidosis (Lesnefsky *et al.*, 2001).

The numbers of mitochondria in cells are regulated by the activation of specific transcription factors and signalling pathways (Berk *et al.*, 2007; Moyes and Hood, 2003; Attardi and Schatz, 1988). The mitochondria content of cardiac tissue is high and this is to compensate for minor damage and a decrease of mitochondrial function of 30 – 50 % is required before lower rates of energy production

occur (Lesnefsky *et al.*, 2001). An increase in the number of mitochondria is considered to be an adaptive response to mitochondrial damage and increased need for energy (Marín-García *al.*, 1995), as is the formation of large megamitochondria (Mashimo *et al.*, 2003), often associated with free radical generation (Wakabayashi *et al.*, 1997). Megamitochondria have been observed in chemical toxicity and can arise from fusion of adjacent mitochondria or suppression of division, leading to swelling (Cheville, 1994; Sudarikova *et al.*, 1997; Matsuhoshi *et al.*, 1998). In the present study, the mitochondria are swollen and megamitochondria formation is not induced as these mitochondria are 5-10 times larger than normal mitochondria.

Structural damage was most prominent in the combination group, indicating that Cd+Hg act additively or synergistically and the increased toxic burden causes increased damage. Vacuolization and complete loss of the cristae were previously observed by the oxidative effect of DOX (Al-Harthi *et al.*, 2014). Therefore, it can be concluded that especially Cd contributes to oxidative damage, leading to mitochondrial damage and dysfunction.

Cd has been shown to be deposited in the heart muscle (Petering *et al.*, 1979) and is cardiotoxic at concentrations as low as 0.1 µM (Limaye and Sheikh, 1999). A 60-day exposure to 15 mg/kg/day of Cd caused a 5x increase in the amount of Cd in the rat heart in comparison to an acute, single dosage, but only a 0.5x increase in blood levels compared to single dose (Ozturk *et al.*, 2009), indicating that Cd accumulates in cardiac tissue. Besides the effect on the mitochondria, thin and disintegrated muscle fibres, with disruption of normal myofibrillar organisation were observed in the cardiac tissue. In contrast, the morphological features of the endothelial and SMC are normal (Ozturk *et al.*, 2009).

Cd generates ROS and the resulting oxidative stress contributes to cardiac damage (Szuster-Ciesielska *et al.*, 2000; Lei *et al.*, 2011). Cd also binds intracellular thiols, like GSH and/or inhibits the activity of AOx enzymes such as CAT and SOD (Prozialeck and Edwards, 2012). The levels of ROS, H_2O_2, superoxide anion and the hydroxyl radical are then increased, causing lipid membrane peroxidation as well as protein and DNA damage (Bertin and Averbeck, 2006; Jomova and Valko, 2011). A decrease in eNOS levels and an increase in iNOS levels in the cardiac tissues of Cd treated animals have been reported (Ghosh and Indra, 2018). Increased expression of iNOS in cardiomyocytes is associated with inflammation and contractile dysfunction and is also expressed in high levels in the myocardium of heart failure patients (Cotton *et al.*, 2002). iNOS is found upregulated in response to inflammatory cytokines and the induction of iNOS expression is mediated by cytokine-inducible transcription factors like NFκB and IFN regulatory factor-1 (Mungrue *et al.*, 2002). Excessive production of NO derived from iNOS has deleterious effects (Seddon *et al.*, 2007). No indication of inflammation such as the presence of inflammatory cells in the tissue was observed.

Additive rather than synergistic effects have been observed between Cd and Pb on the metabolism and functioning of the heart as well as the kidneys and liver (Kopp *et al.*, 1980). Effects of Cd in

combination with Pb have been shown to have a synergistic oxidative damage effect on mitochondria of rat kidney and defective oxidative metabolism (Wang *et al.*, 2010). Distorted myofibrillar arrangement, vacuolization of the tissue and erythrocyte congestion in the cardiac tissue of Cd treated animals was observed by Ghosh and Indra (2018) and Ferramola *et al.* (2012). These studies correlate to the findings in the present study of Cd exposure. Cd exposure coupled with high cholesterol levels have been implicated as a risk factor for heart fibrosis (Türkcan *et al.*, 2015).

Cardiac effects of Hg are also observed even following low dose exposure due to the Hg bioaccumulation capacity of cells. Cardiac Hg accumulation contributes to cardiomyopathy, where Hg levels in the heart tissue of individuals who died from idiopathic dilated cardiomyopathy were found to be on average 22 000X higher than in individuals who died from other forms of heart disease (Haffner *et al.*, 1991; Frustaci *et al.*, 1999). Therefore, continuous exposure to low Hg levels, even considering the poor absorption of Hg, can have severe consequences on cardiac function. These effects include a reduction in isometric twitch force and lower activity of contractile proteins in the myofibrils, and consequently reduction in tectonic tension, as described by de Assis *et al.*, 2003. Acute cases of mercury chloride intoxication have been reported and renal failure has been the primary consequences of this type of poisoning (Verma *et al.*, 2010) with no mention of the cardiovascular effects. The cardiovascular physiological effects may not be the focus of clinical case reports as the primary target and the most dramatic effects of poisoning are the effect on the kidneys, and changes in heart function and tissue morphology have not been reported even in cases of death (Iino *et al.*, 2009). At the cellular level Hg exposure is associated with alterations in membrane permeability, changes in macromolecular structure due to its affinity for sulfhydryl and thiol groups, and DNA damage (Flora *et al.*, 2008; Rice *et al.*, 2014). Hg can increase ROS because of its ability to act as a catalyst of Fenton-type reactions (Peraza *et al.*, 1998). Hg has also been shown to induce oxidative stress and mitochondrial dysfunction (Lund *et al.*, 1993) which can result in alterations in calcium homeostasis and increased lipid peroxidation (Peraza *et al.*, 1998). Acute excess myocardial Ca^{2+} loading leads to dysregulation of Ca^{2+} homeostasis, impaired diastolic and systolic function, arrhythmias, and cell death (Lakatta, 1992). Cellular Ca^{2+} load is determined by membrane structure and permeability as well as by the intensity of stimuli that modulate Ca^{2+} influx or efflux through their influence on the membrane proteins. ROS affects both membrane structure and function and may increase Ca^{2+} levels during states of oxidative stress (Hano *et al.*, 1995; Lakatta *et al.*, 2001).

4.4.1. Collagen in heart tissue

Besides heart failure, hypertensive heart disease is another condition which has been shown to be associated with hypertrophy of cardiomyocytes and transition of fibroblasts to myofibroblasts, as well as increases in the perivascular, endomyseal and perimysial connective tissue (Berk *et al.*, 2007). These changes, which are observed in hypertensive heart disease, impair both systolic and diastolic function (Janicki and Brower, 2002). An increase in interstitial collagen (accumulated with

74

the perimysium) is associated with diastolic heart failure, whereas degradation of endomyseal and perimysial components of the collagen scaffolding is accompanied by ventricular dilatation and systolic heart failure (Iwanga *et al.*, 2002; Berk *et al.*, 2007). Increased cardiomyocyte size and collagen deposition are associated with reduced life expectancy and Helms *et al.* (2010) have shown that a reduction of cardiomyocyte cell size and reduced collagen content in the heart of Ames dwarf mice has a beneficial effect on longevity (Helms *et al.*, 2010).

Fibrillar collagens form a scaffolding network for the cardiomyocytes (Janicki and Brower, 2002) and consists of the epimysium, which is located on the endocardial and epicardial surfaces of the myocardium and provides support for endothelial and mesothelial cells. The perimysium surrounds a group of muscle fibres. The endomysium arises from the perimysium and surrounds individual muscle fibres. Endomysium holds muscle fibres together and function as connections to cytoskeletal proteins of the cardiomyocytes. Parts of the endomysium branch around blood vessels to form the scaffolding layer of the tunica adventitia (Berk *et al.*, 2007). Changes to the composition and the distribution of the connective tissue result in changes to the thickness and strength of the cardiac wall (Strait and Lakatta., 2012; Gerstenblith *et al.*, 1977) that in turn compromise the contractile efficacy and relaxation of the heart (Strait and Lakatta, 2012; Tan *et al.*, 2009; Spina *et al.*, 1998).

Following absorption, the vascular system is responsible for the distribution and consequently the endothelium of the vascular system is in direct contact with any absorbed toxins. Exposed cellular components include endothelial cells, SMC and fibroblasts producing the ECM. Studies suggest that even under non-pathologic conditions, the endothelium is capable of sensing hemodynamic changes, and signals the vascular cells to respond accordingly (Gimbrone *et al.*, 2000; Laughlin *et al.*, 2008). This can be a result of direct toxicity or the induction of indirect effects such as changes in cellular functioning. Direct toxicity includes apoptosis while indirect effects are an increase in cellular proliferation, changes in cellular cell migration and reorganisation, as well as changes to the composition and arrangement of the ECM in the blood vessel walls (Rudic and Sessa, 1999). The ECM of large blood vessels such as the aorta is composed of collagen and elastin. Elastin is the most prominent ECM protein and makes up elastic fibres which allow for arteries to perform the function of energy storage and release during systole and diastole. In addition, elastin is also able to control the contractile ability of VSMC, as well as serve as an autocrine factor through regulating the activation and availability of TGF-β (Lannoy *et al.*, 2014). Disruption of this process can lead to fibrosis that can compromise the contractibility of the smooth muscle components.

Collagen is a stable protein whose turnover in a healthy heart by cardiac fibroblasts is normally slow and is estimated to be 80 – 120 days (Shirwany and Weber, 2007). The balance of collagen turnover, its deposition and degradation, is controlled by fibroblasts under normal conditions and by myofibroblasts under pathological conditions. Myofibroblasts can secrete collagen and are able to migrate throughout tissue, unlike the fibroblasts which stay within one area. Both autocrine and

paracrine factors affect the collagen secretion by myofibroblasts. Endocrine hormones are also able to affect myofibroblast functions. Synthesis and degradation of collagen in fibrotic conditions are both altered, leading to an accumulation of collagen, as well as an increase in crosslinking of collagen, which together results in fibrosis (Berk *et al.*, 2007).

A fundamental characteristic of hypertensive cardiac remodelling is myocardial stiffness, which is associated with fibrosis, altered contractile and relaxation properties, and changes in cardiac cellularity (Berk *et al.*, 2007). The results of this study showed an increase in the content of collagen in the endomysium as well as the formation of interstitial fibrosis in the metal exposed groups. The most identifying morphological alterations in the remodelling process of heart failure are the accumulation of ECM proteins/fibrosis and myocyte death (Capassio *et al.*, 1990; Weber *et al.*, 2013). In the progression from compensated hypertrophy of cardiac muscle, to heart failure, the most important regulators of fibrosis are the members of the renin-ANG and aldosterone system (Hein *et al.*, 2003; Zhou *et al.*, 1996; Weber, 1990). TGF-β_1, growth factors and endocrine hormones are potent stimulators of fibrosis (Hein *et al.*, 2003; Hein and Schaper, 2001). ROS can lead to the activation of MMP's in the heart which results in increased collagen deposition (Vacek *et al.*, 2012).

TGF-β is a cytokine associated with inflammation, and inflammation in the myocardium is the preliminary step to several diseases such as atherosclerosis, cardiomyopathy and myocarditis (Magnani and Dec, 2006; Tuttolomondo *et al.*, 2012; Dominguez *et al.*, 2016). Myocardial stiffness is mostly attributed to changes in the composition and arrangement of ECM proteins, including type I and type III fibrillar collagens (Weber *et al.*, 1989; Weber, 1999). Myofibroblast collagen turnover is regulated by a number of growth factors such as ANGII, TGF - β_1, insulin-like growth factor 1 (IGF – 1), and TNF – α (Weber *et al.*, 1999). Growth factors are able to influence one another for example ANG II can be produced by both macrophages and fibroblasts and regulates the expression of TGF-β_1 by myofibroblasts while TGF-β_1 upregulates the expression of the genes which encode type I and III fibrillar collagen expression (Rosenkranz, 2004; Swaney *et al.*, 2005). In addition to the activation of over production of collagen, a decrease in the degradation of collagen also has a profibrotic effect. Degradation of collagens and other ECM proteins in the heart is performed by MMPs. These MMPs include the collagenases that initiate the ECM degradation process by cleaving the α-chains of type I and type II collagens and the gelatinases that further process collagen fragments (Ahmed *et al.*, 2006, Nagase *et al.*, 2006). MMP expression can be regulated by hormones, various growth factors and cytokines as well as mechanical strain on the tissue (Feldman *et al.*, 2001; Inokubo *et al.*, 2001). Although MMPs are involved in degradation of collagens, their activation can further promote the synthesis of additional collagen in tissues, and therefore creating a positive feedback mechanism for fibrosis (Galis and Khatri, 2002). The degradation pathways also often favour the degradation of healthy/already present collagen over newly formed collagen, which in fibrosis is oxidised and highly cross-linked and this results in the accumulation of stiffer collagen (Rucklidge *et al.*, 1992; Berk *et al.*, 2007). In disease levels of

myofibroblasts are increased and this causes an increase in the procollagen synthesis and secretion into the pericellular space, where it forms collagen fibrils that assemble into fibres. Functionally, any changes to the ECM components and MMP activity of the myocardium affects the contractile function of myocytes. The presence of collagen in smooth muscle has been shown to affect contractility as described in detrusor muscle and urinary retention (Belluci *et al.*, 2017). Myocytes mediate signal transduction between the cells, as well as growth factor release (Ginsberg *et al.*, 2005; Katsumi *et al.*, 2005; Berk *et al.*, 2007), the most important of which is TGF – β_1 (Sorescu, 2006; Wang *et al.*, 2006). Although increased collagen deposition was observed, the lack of inflammatory cells indicates an alternative mechanism of action. Measurement of markers of inflammation may provide conclusive evidence whether indirect inflammatory processes play a role.

Interstitial fibrosis associated with heart failure is regulated at the level of gene expression and is associated with elevated levels of fibronectin and type $pro\alpha(I)$ and $pro\alpha(III)$ collagen messenger ribonucleic acids (mRNAs). The consequent slowed cardiac contraction was also recorded together with a decrease in the levels of α-myosin. Levels of TGF-β mRNA was increased and was identified as one of the possible mechanisms by which fibrosis occurred (Boluyt *et al.*, 1994). The absence of TGF-β_1, prevents fibrosis indicating its role in pathogenesis (Pinto *et al.*, 2000; Schultz *et al.*, 2002). Activation of TGF-β_1 occurs following chronic exposure to ANG II. TGF-β_1 stimulates similar to mothers against/mothers against decapentaplegic-3 (SMAD3)-dependent gene expression in SMC and monocytes and increases the expression of ET-1 by endothelial cells and promotes a profibrotic environment. Inflammation and subsequent fibrosis occur by SMAD3 activation and increased ET–1 expression which activates fibroblasts by stimulating expression of the connective tissue growth factor (CTGF) and activation of a NFκB- dependent gene program that is also profibrotic (Wang *et al.*, 2006; Sorescu, 2006; Berk *et al.*, 2007). Increased pressure within the heart has shown to influence TNF-α (Zygner *et al.*, 2014) resulting in an altered homeostasis of collagen and ECM. Activation and cleavage of TGF-α is performed by a member of a disintegrin and metalloproteinases (ADAMs) ADAM17 (Kassiri *et al.*, 2001; Kassiri and Khokha, 2005). ADAMs have therefore been implicated in collagen remodelling through their ability to participate in growth factor release (Berk *et al.*, 2007).

Hypertension is also associated with collagen formation in humans as collagen degradation markers and hemodynamic load are reduced after antihypertensive treatment (Olsen *et al.*, 2005). This has also been confirmed in animal studies (Wei *et al.*, 1999). Increased collagen type I synthesis, as was observed in the present study (Section 4.3.1.2), has been described as a feature of spontaneously hypertensive rats but not in normotensive animals, indicating that increased collagen type I levels in the myocardium are associated with hypertension (Díez *et al.*, 1996). Increased collagen cross-linking has also been observed following cardiac hypertrophy in spontaneously hypertensive rats (Norton *et al.*, 1997). The suggested pathophysiology is that an increase in systemic blood pressure from arterial modifications affects protein synthesis by

cardiomyocytes and fibroblasts. Rapid increases in pressure in rat hearts increases collagen and total protein synthesis, with decreased protein breakdown (Morgan *et al.*, 1985; Gordon *et al.*, 1986). Studies also show that the synthesis and degradation of collagen returns to normal within in a few weeks, thereby reducing fibrosis (Moalic *et al.*, 1984). Even though the data suggests a reversible effect of the elevated collagen synthesis, it also suggests that even a slight increase in hypertension for short periods of time may lead to changes in ECM synthesis that can and result in fibrosis (Berk *et al.*, 2007).

Increased interstitial collagen has been identified in Wistar rats exposed to tobacco smoke (Rafacho *et al.*, 2011). These alterations were related to an increase in NOX activity, increased levels of lipid hydroperoxide and depletion of AOx (CAT, SOD GPx). This suggests that the oxidative pathway plays a role in ventricular remodelling with tobacco smoke exposure, with no indication of inflammation as the cardiac levels of IFN-γ, TNF-α and IL-10 were not different between the groups (Rafacho *et al.*, 2011).

The changes mentioned above to the to the cardiac wall and possible decreases in contractile efficacy are also age related changes (Strait and Lakatta, 2012). Even though this study did not measure the functional changes to the CVS, the structural alterations suggest a premature ageing mechanism caused by exposure to the metals Cd and Hg, which may potentially lead to more life-threatening conditions.

4.4.2. Vascular remodelling of the aorta

Vascular remodelling, developing after an injury or insult, is characterized by endothelial cell activation, inflammatory cell infiltration, and SMC proliferation and associated deposition of collagen in the vessel wall (Lee *et al.*, 2015). The endothelium is an important communication structure between flowing blood and the blood vessel wall (Haller, 1996). SMC within the arterial wall regulate elastic fibre assembly.

4.4.2.1. Elastin

Elastic fibres play a structural and mechanical role in arteries, providing elasticity and resilience to the tissue and serving as reinforcement to the high pressure of circulation (Faury, 2001; Lannoy *et al.*, 2014). Elastic fibres and SMC function together to allow dilatory and constrictive action of the arterial wall, recoil ability of elastic blood vessels, and ability to store the energy.

For elastin formation, the endothelial cells secrete soluble tropoelastin (Kozel *et al.*, 2006). Pericellular deposition of microfibrils composed of the protein fibrillin-1 then occurs. These microfibrils serve as site of aggregation for soluble tropoelastin (Kielty *et al.*, 2002). In the ECM elastin is then cross-linked by lysyl oxidase (LOX) and lysyl oxidase like 1 (LOXL1), forming elastin fibres of good integrity (Mäki *et al.*, 2005; Thomassin *et al.*, 2005). Studies have shown that elastic fibres first appear as small cell surface globules which over time arrange themselves into larger fibres (Czirok *et al.*, 2006; Kozel *et al.*, 2006). Mature elastic fibres have a smaller amount of

microfibrils as compared to elastic fibres in younger individuals, indicating that the ratio of microfibrils to elastin decreases with age. Elastin, fibrillin, fibronectin and proteoglycans are also altered in hypertensive heart disease (Berk *et al.*, 2007). In recent years *in vitro* and *in vivo* studies have demonstrated that TGF-β_1 plays an important role during vascular development as well as pathological progression including atherogenesis and neointimal proliferation. TGF-β_1 is known to regulate ECM synthesis, cell cycle progression, apoptosis, differentiation and migration of cells (Heinmark *et al.*, 1986; Shao *et al.*, 2003; Ghosh *et al.*, 2005) as well as myocardial remodelling and fibrosis (Bujak and Frangogiannis, 2007).

Oxidative stress mechanisms have been shown to affect elastin synthesis (Miller *et al.*, 2002; Maurice *et al.*, 2013) and in Sprague Dawley rats, as a result of oxidative insult, elastin and increased SMC were observed in the tunica intima creating neointimal tissue masses (Liaw *et al.*, 1997). Similarly, the present study showed areas of neointimal formation in the groups exposed to Hg (Figure 4.8e) and Cd+Hg (Figure 4.8g). Alterations to elastin structure have been reported to decrease arterial compliance. Studies have shown that mice and humans with insufficient amounts of fibulin-5 have reduced arterial compliance, which is correlated with hypertension, reduced cardiac function and an increased risk of death from CVD (Le *et al.*, 2014). Fibulin–5 deficient mice showed VvG staining of a lesser intensity than a compared with healthy arteries, with no cellular or collagen changes. The reduction in staining was due to fragmentation of the elastin fibres which was visible with electron microscopy (Le *et al.*, 2014; Nakamura *et al.*, 2002; Yanagisawa *et al.*, 2002). In the present study, the intensity of the staining was the same for all groups. Alterations in elastin arrangement were observed in the heavy metal exposed groups, being the most obvious in the Hg (Figure 4.9f) and Cd+Hg group (Figure 4.9g). The combination group had a greater degree of linking of elastin fibres between the lamellae compared to the Hg group. The Cd group presented with interruptions in the elastin lamellae viewed with LM (Figure 4.9d), while ultrastructurally the presence of collagen bundles caused the displacement of the elastic lamellae (Figure 4.10b).

ROS are able to induce apoptosis of vascular endothelial cells (Han *et al.*, 2012) and destroy their function as a barrier (Boueiz and Hassoun, 2009). Reduced production of eNOS causes VSMC to become more sensitive to the effects of vasodilators, resulting in increases in blood pressure (Tran *et al.*, 2009). Endothelial cells also participate in the structural and functional integrity of the vascular wall and damaged endothelial cells are associated with CVD (McCullagh *et al.*, 2016). The present study showed an altered appearance of the tunica intima, with a more prominent presence of SMC nuclei and surrounding elastin in the heavy metal exposed groups. This change to cell and elastin structure was most apparent in the combination group (Figures 4.8 and 4.9). Migration of SMC from the tunica media to the tunica intima occurs as a consequence of endothelial cell damage (McCullagh *et al.*, 2016). An increase in aortic thickness, is the result of SMC proliferation and elastin secretion within the tunica intima of the aortic wall as well as the disruption of elastin lamella in the tunica media were observed in rats exposed to Hg and Cd+Hg.

The resultant morphology resembles that of neointimal plaques formed after balloon catheter injury (Thyberg *et al.*, 1995). Medial SMC proliferation was previously observed in rats along with vascular rupture and thinning, and these changes were involved with the development of hypertension (Jin *et al.*, 2013). In the present study, straightening of the elastic fibres was observed in the metal exposed groups. Mahmoud and Elshazly, (2014) similarly showed that a loss of elasticity was observed in arteries where histological evaluation of sections showed relative straightening of the elastic fibres in the tunica media compared to the control.

Change in elastin structure through fraying of elastin bands in the medial layer of the aorta, as observed in the present study, is a feature of ageing (Lakatta and Levy, 2003). Although changes to the structure of elastin occur during ageing, the amount of elastin does not differ between young and old (Wheeler *et al.*, 2015). In humans, systolic blood pressure starts to rise after adolescence and continuously increases with age. Diastolic blood pressure also increases with age until around 50 years. After which around the age of 60, there is a natural loss of elasticity and a hardening of the arteries. Arterial stiffening reflects gradual fragmentation and loss of elastin fibres and accumulation of stiffer collagen fibres in the media of large arteries and occurs independently of atherosclerosis. The arterial compliance is determined by the ratio of elastin and collagen. Aging is associated with a decreased ratio of elastin/collagen which is due to, in part, an enhanced degradation of elastin and/or increased accumulation of stiffer collagen. Elastin degradation is associated with progressive aortic stiffening and all-cause mortality (Smith *et al.*, 2012). Arterial stiffening leads to an increase in pulse pressure and a continuous pattern of stiffening effects will have an additional influence on the risk for cardiovascular events (Wilkinson *et al.*, 2015). Premature aging associated with progeria is associated with accelerated vascular stiffening or vascular aging (Gerhard-Herman *et al.*, 2012). A disordered arrangement of elastin fibres was noted in the current study, presenting as large gaps and irregular connected layers in the metal exposed groups (Figure 4.9) indicating that metal exposure is a risk factor for premature arterial aging and the development of CVD.

4.4.2.2. Vascular smooth muscle cells

The histological alterations to VSMC are consistent with endothelial injury and abnormal functioning of the aorta. In the present study VSMC were more prominent in the tunica media of the Hg and Cd+Hg exposed groups, while the nuclear shape was altered in all metal exposed groups. Similar changes were reported by Jin and colleagues (2013) and these changes were associated with increased levels of serum endothelin while NO levels were reduced. A balance between endothelin and NO in the endothelium plays a role in maintaining the vascular baseline tension (Jin *et al.*, 2013). The VSMC proliferation is thought to occur as a result of NO deficiency where damaged endothelial cells are unable to produce enough NO, which is important in supressing the VSMC proliferation and growth (Davignon and Ganz, 2004; Jeremy *et al.*, 1999). Once VSMC reach the intima these cells begin to proliferate and cause a narrowing of the arterial lumen, which can further lead to restenosis (McCullagh *et al.*, 2016). Diseases such as restenosis

and atherosclerosis are associated with damage to the endothelium and a decline in endothelial NO levels (Kawashima *et al.*, 2004; Ahanchi *et al.*, 2007; Förstermann and Sessa, 2012; Madigan and Zukerbraun, 2013). NO also inhibits platelet aggregation, which if not controlled, contributes to atherosclerotic plaque formation (Kubes *et al.*, 1991). Cadmium has been reported to cause a decrease in eNOS levels (Ghosh and Indra, 2018).

eNOS is found in coronary and endocardial endothelial cells as well as in cardiomyocytes (Remya *et al.*, 2013). The eNOS-derived NO in contrast to iNOS derived NO has a beneficial effect on cardiomyocytes. NO derived from eNOS serves an important function in controlling the general physiological functioning of the heart. This is achieved by the modulation of excitation-contraction coupling, myocardial relaxation, myocardial oxygen consumption, diastolic function and the Frank-Starling response (the ability of the heart to change its force of contraction and therefore stroke volume in response to changes in venous return) (Shah and MacCarthy, 2000; Seddon *et al.*, 2007; Ghosh and Indra, 2018). Regulation of eNOS levels is important and a decrease of eNOS has been suggested to cause impairment of heart function and myocardial infarction (Giraldez *et al.*, 1997; Cotton *et al.*, 2002; Remya *et al.*, 2013). Tellez-Plaza *et al.* (2013) and Borné *et al.* (2015) have conducted epidemiological studies on this topic.

A large number of studies have suggested a link between Cd exposure and the development of atherosclerosis and hypertension (Tomera *et al.*, 1994; Nakagawa and Nishijo, 1996; Satarug and Moore, 2004; Navas-Acien *et al.*, 2005) and there is evidence suggesting that the vascular endothelium may be intimately involved in mediating these effects of Cd (Kaji, 2004). Cd can cause the release of a variety of proinflammatory mediators from endothelial cells that can facilitate the inflammatory component of the atherosclerotic process (Szuster-Ciesielska *et al.,* 2000; Kaji, 2004; Mlynek and Skoczynska, 2005). In addition, Cd stimulates the release of antithrombolytic agents and facilitates the adhesion of leukocytes and platelets to the endothelium (Yamamoto *et al.*, 1993; Kaji *et al.*, 1994; Hernandez and Macia, 1996). It also promotes the proliferation of VSMC and enhances production of ECM components that increase the stiffness of blood vessels (Fujiwara *et al.*, 1998; Abraham *et al.*, 2000; Jeong *et al.*, 2004; Kaji, 2004). Finally, Cd can inhibit the release and/or actions of endothelium-derived vasodilator substances such as prostanoids and NO (Kishimoto *et al.*, 1994; Grabowska-Maslanka *et al.*, 1998; Bilgen *et al.*, 2003; Skoczynska and Martynowicz, 2005), and can antagonize the actions of the vasoconstrictor endothelin (Wada *et al.*, 1991; Koschel *et al.*, 1995). However, other studies have shown primary cultures of coronary microvascular endothelial cells exposed to 2 µM CdCl$_2$ exhibit increased secretion of ET-I and ANGII (Kusaka *et al.*, 2000). In another study a dose of 100 mg/L CdCl$_2$ administered for 60 days resulted in increased blood pressure and blunted response to vasopressors (Donpunha *et al.*, 2011). Cd has been shown to cause hypertension through angiotensin converting enzyme (ACE) and calcium channel inhibition (Puri and Saha, 2003). Studies have also shown that Cd is able to supress acetylcholine induced vascular relaxation and the reduction of eNOS synthesis in endothelial cells (Yoopan *et al.*, 2008).

Endothelial dysfunction is a condition that has been mostly implicated with Hg toxicity (Omanwar and Fahim, 2015). Some of the mechanisms suggested for the toxic effects of Hg on the endothelium include a decrease in NO bioavailability, which alters the dilation properties of blood vessels (Lemos *et al.*, 2012; Rajaee *et al.*, 2015). Furthermore, a positive correlation between Hg levels in blood and blood pressure has been reported (Tinkov *et al.*, 2013).

The heavy metals Cd and Hg stimulated the proliferation of cultured rabbit aortic smooth muscle cells (ASMC) and contributing to the pathogenesis of atherosclerosis and hypertensive disease (Lu *et al.*, 1990). A more recent study showed that a long-term exposure of cultured VSMC to low doses of Hg induced vascular remodelling and proliferation through the activation of the MAPK signalling pathways that result in activation of the inflammatory proteins such as NOX and COX- 2 which in turn induce the proliferation of VSMC (Aguando *et al.*, 2013). The histological changes in this study were similar to those observed by Aguando *et al.* (2013), where $HgCl_2$ induced MAPK activation, oxidative stress and COX-2 expression and the inhibition of all three restored the altered cell proliferation and size (Aguado *et al.*, 2013).

Vascular remodelling as a result of hypertension is associated with structural and biochemical changes in the blood vessel wall, which include changes to the endothelial cells, VSMC and the ECM. Because hypertension itself is capable of promoting vascular remodelling, continuous exposure to metals such as Cd and Hg would continuously contribute to vascular remodelling and together with the remodelling effects of increased blood pressure, as described above, would amplify the damaging effects to the vascular system.

In humans, ageing and hypertension are two major factors contributing to arterial hardening (Nichols *et al.*, 2005; Nichols *et al.*, 2008). Formation of neointimal plaques is also associated with an increase in blood pressure (Ruiz-Feria *et al.*, 2004). Structurally neointimal plaques are similar to lesions caused by balloon catheter injury (Thyberg *et al.*, 1995), and are also similar to atheromatous plaques in human and animal models of atherosclerosis (Hanke *et al.*, 1990; Thyberg *et al.*, 1995). NO supression has been suggested as a mechanism for neointimal plaque formation (Ruiz-Feria *et al.*, 2004). Hypertension increases vascular ROS production via the activation of NOX (Cai and Harrison, 2000; Zalba *et al.*, 2001), which binds NO, reducing the levels of free NO and this causes endothelial dysfunction (Zalba *et al.*, 2001). Tetrahydrobiopterin (H_4B) is an important factor for endothelial NO synthesis as oxidation or reduction of H_4B by ROS in injured endothelium results in uncoupled eNOS (Gross and Wolin, 1995; Maxwell and Cooke, 1998; Cai and Harrison, 2000; Landmesser *et al.*, 2003). Uncoupled eNOS produces large amounts of ROS and $ONOO^-$ leading to a further enhancement of endothelial dysfunction and vascular lesions (Gross and Wolin, 1995; Landmesser *et al,* 2003; Simonet *et al.*, 2004). An increased ROS production also increases the production of H_2O_2 which appears to contribute to medial hypertrophy (Zalba *et al.*, 2001).

4.4.3. Clinical consequence of cardiac and aortal remodelling during premature ageing

In rodent and non-human primate models of arterial aging, central arterial intimal medial thickening is an age-associated process. The enzymatic, and molecular mechanisms behind the intimal/medial thickening including VSMCs activation and migration into the intima and the elevated levels or activity of molecules such as MMPs, ANGII and TGF-β, creates a metabolically active environment. These factors induce and/or contribute to endothelial dysfunction and altered permeability. These same age-associated alterations in metabolic, enzymatic, cellular, and endothelial function are increasingly recognized as factors playing a critical role in the genesis and promotion of atherosclerosis, vascular inflammation, vascular remodelling, and oxidative stress. Therefore, many of the factors involved in age-associated structural and functional intimal and medial alterations are also implicated in the pathogenesis of clinical CVD and the toxicity that accelerates these processes which can result in premature aging of the vascular system (Nilsson *et al.*, 2008). Histological evaluation of the heart tissue and elastic arteries of rats exposed to Cd and Hg alone and in combination revealed a phenotype associated with increased oxidative effects, myoblast degeneration and increased fibrosis which is characteristic of CVS premature aging. These effects can lead to hypertension and cardiovascular mortality as has been described for miners (García *et al.*, 2007; Gómez *et al.*, 2007; Rodriguez-Fernandez *et al.*, 2015) and premature heart failure (González *et al.*, 2018).

High blood pressure is a leading risk factor for CVD. A recent analysis identified that the incidence of high blood pressure, over the last three decades has been increasing (Forouzanfar *et al.*, 2017). A high salt intake and overweight/obesity are the classic risk factors for hypertension but environmental exposures to metals may also play an important role (Navas-Acien *et al.*, 2009; Eum *et al.*, 2008; Houston 2011; Abhyankar *et al.*, 2012). Increased levels of Cd in urine in an American Indian population were found to be associated with increased blood pressure in comparison to populations with a lower baseline Cd level (Oliver-Williams *et al.*, 2018). Blood pressure variability has been associated with increases in CVD risk, with maladaptive arterial remodelling and increased aortic stiffness being hypothesised as the underlying cause (Zhou *et al.*, 2018).

This year a meta-analysis of the association between Hg exposure and hypertension found a significant positive correlation (Hu *et al.*, 2018). A review of the mechanism underlying the toxicity of the heavy metals Cd, Hg and As suggests that in the case of hypertension and cardiovascular effects, a multiple mechanism for pathogenicity should be considered, due to complexity of the CVS (da Cunha Martins *et al.*, 2018).

In the present study, exposure to Hg, either alone or in combination with Cd, caused neointimal proliferation, which may not be associated with inflammation or atherosclerotic plaque formation.

4.5.   <u>Conclusion</u>

Exposure to Cd and Hg alone and in combination caused mitochondrial damage and myofibrillar necrosis, increased fibrosis and lipid deposition within the myocardium. In the aorta, Cd caused alteration in elastin, with interruptions of elastin lamella by collagen formation. Hg alone and in combination caused elastin fibrillation, collagen deposition as well as proliferation and migration of VSMC into the tunica intima, causing nonatherosclerotic neointimal plaque formation. The structural alterations were the most prominent in Cd+Hg exposed rats. The observed structural changes correlated with a phenotype of premature aging of the CVS that is known to lead to hypertension and premature cardiac failure.

Chapter 5: Effects of Cd and Hg alone and in combination on the blood coagulation system of Sprague-Dawley rats

5.1.   Introduction

Cardiac muscle tissue and blood vessels have been identified as targets of Cd and Hg toxicity. Likewise, following absorption, the blood cells are also exposed to these metals and exposure can also adversely affect blood haemostasis. Strong reciprocate interactions between the blood and the wall of blood vessels occur, and these physiological effects include changes in blood pressure and NO levels. The interaction between vessel walls and erythrocytes during coagulation facilitates the migration of platelets to the site of injury and the binding of inflammatory mediators to cell surface receptors (Pretorius and Kell, 2014).

The coagulation system plays an important part in the recovery of injured blood vessels and to prevent excessive blood loss through the formation of a blood clot or thrombus. The coagulation system therefore needs to be carefully controlled to ensure that unnecessary clot formation does not lead to a blockage of a blood vessels (Smith, 2009) or cause tissue damage in organs, as seen in complications such as CVA (Zhang *et al.,* 2015). The phases of the cell-based coagulation pathway contribute to the formation of the clot with platelets playing a crucial role in this process (Pérez-Gómeza and Bove, 2007; Smith, 2009; Van Rooy, 2015), that through the release of certain factors regulates the tautness of the fibrin fibres (Pérez-Gómeza and Bove, 2007; Van Rooy, 2015).

Several individual metals such as iron (Fe) and Zn have been shown to have a pro-coagulative effect (Sangani *et al.,* 2010) and Fe has been shown to alter the structure of fibrin networks (Pretorius and Lipinski, 2013) which implies that metal pollutants, as found in the environment, may also have an adverse effect on haemostasis and cardiovascular health. Studies on fibrin and thrombus formation provide physiologically relevant information about the possible risk for thrombosis associated diseases and a correlation has been found between *in vitro* and clinical studies (Undas and Ariens, 2011; Weisel and Litinov, 2013).

In the current chapter, the effects of Cd and Hg alone and in combination on the blood cells and coagulation system of Sprague-Dawley rats were investigated.

5.2. Materials and Methods

5.2.1. Materials

SEM was used to study erythrocyte, platelet and fibrin fibre morphology along with thickness of fibrin fibres. Blood from each animal in each of the experimental groups was prepared for whole blood (WB) and platelet-rich plasma (PRP) in order to examine the morphology of erythrocytes and fibrin networks respectively as described by Van Rooy *et al.*, 2015.

5.2.2. Methods

Blood was collected in citrate tubes as described in Section 3.2.2.4 and transported to the Unit for Microscopy and Microanalysis, University of Pretoria, where it was processed for SEM.

5.2.3. Scanning electron microscopy preparation of platelets, fibrin networks and erythrocytes

A volume of 10 µl of WB, with and without the addition of 5 µl human thrombin (20 U/ml; South African National Blood Service), was added to 10 mm round glass coverslips (Leica SA). This preparation was used to evaluate the erythrocyte morphology prior to thrombin addition and the interaction of fibrin fibres with erythrocytes on addition to thrombi, as a representation of a thrombus. Blood was then centrifuged for 10 minutes at 227xg to obtain PRP. A volume of 10 µl of the PRP, with and without the addition of 5 µl of human thrombin, was placed on a 10 mm round glass coverslip. This preparation was used to evaluate platelet and fibrin network morphology. The glass coverslips were allowed to dry for 10 minutes and placed in 24 well plates to which 0.075 M sodium potassium phosphate buffer, pH 7.4 (NaP) was added. The samples were washed for 20 minutes on a shaker to remove any blood proteins. This was followed by fixing with 2.5% GA/FA solution for 30 minutes and rinsing the samples three times in NaP for 3 minutes before secondary fixation in 1% osmium tetroxide (OsO_4) for 15 minutes. The samples were washed again three times as described above. The samples were then dehydrated in 30%, 50%, 70%, 90% and 3 times in 100% ethanol. The SEM sample preparation was completed by drying the samples in hexamethyldisilazane (HMDS), followed by mounting and coating with carbon and viewing using the Zeiss ULTRA Plus FEG-SEM and the ZEISS Crossbeam 540 FEG-SEM (Carl Zeiss Microscopy, Munich, Germany).

The thickness of the fibrin fibres was measured to determine any alterations to the normal major (thick) and minor (thin) fibre arrangement of the network (Van Rooy *et al.*, 2015). Fifty fibres were randomly chosen and measured on the SEM micrographs at X80000 using ImageJ (Version 1.49, Java).

5.2.4. Statistical analysis

Statistical analysis on fibrin fibre thickness were performed on GraphPad Prism Version 6.01 using 1-way analysis of variance (ANOVA), and Tukey's multiple comparisons test, where a p-value of ≤0.05 was considered significant.

5.3. <u>Results</u>

In this section the effects of exposure to Cd and Hg alone and in combination on the morphology of blood obtained from the *in vivo* rat model are provided and changes are discussed in comparison to the blood obtained from the controls of the rat model. Effects on platelets are presented in Figure 5.1 while effects on the fibrin morphology and thickness are presented in Figures 5.2 – 5.6. Changes to erythrocytes are presented in figures 5.7 – 5.10 and to the thrombus morphology in Figure 5.11.

5.3.1. Effects on Platelets and Fibrin Networks
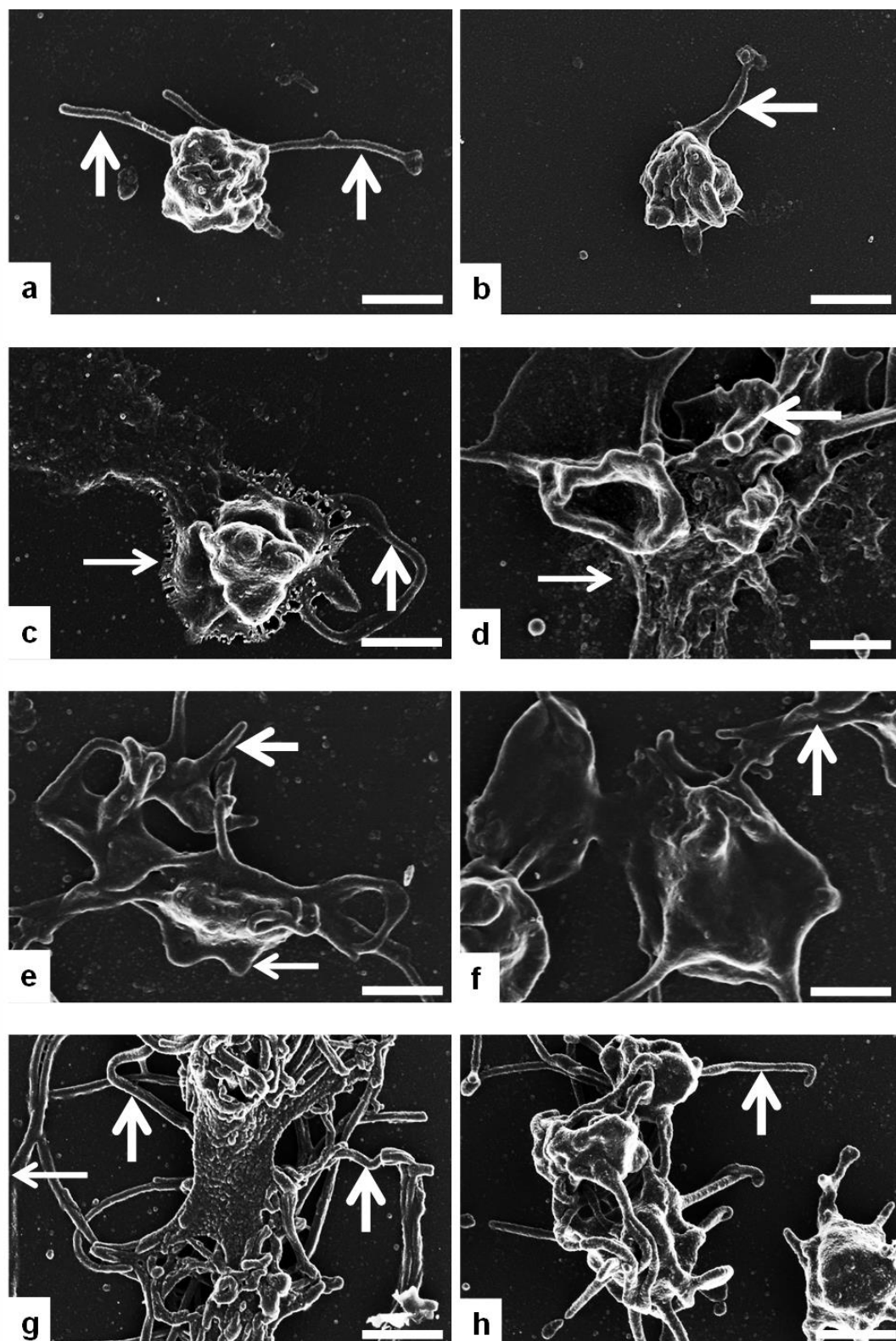
Figure 5.1: SEM micrographs of platelets prepared from PRP from the control (a and b), Cd (c and d), Hg (e and f) and combination (g and h) groups. (a and b) are representative of the control group with the arrows indicating pseudopodia. (c and d) are representative of the Cd group with pseudopodia and platelet spreading indicated by the thick and thin arrows respectively. Platelet spreading and pseudopodia forming a platelet mass are shown in (d). (e and f) are representative of platelets from the Hg exposed group where pseudopodia (thick arrow) and platelet spreading (thin arrow) are also present, as well as aggregation of platelets (f). (g and h) are representative of the combination group where the presence of many pseudopodia can be seen (thick arrows) with fibrin fibre formation (thin arrow) in (g), as well as platelet aggregations (h). Scale bars = 1 µm**.**

5.3.1.1. Platelet activation

Figures 5.1a - h are representative of platelets prepared from PRP in the control and exposed groups. In the control group (Figure 5.1a and b) round/oval platelets with some pseudopodia (arrows) were visible. Pseudopodia, change in platelet shape and spreading indicates platelet activation, which is not expected in the control group. The presence of pseudopodia in the control sample here is due to contact activation. (Van Rooy, *et al.*, 2015). Platelet activation can be seen in all the metal exposed groups (arrows in Figures 5.1c - h), with an increase in activation; relevant to the number of pseudopodia and amount platelet spreading, seen in the Cd (Figure 5.1c and d) and Hg (Figure 5.1e and f) and Cd and Hg groups (Figure 5.1g and h). Platelet-platelet interactions identified as aggregations of two or more platelets is observed in the Hg (Figure 5.1e and f) and in the combination groups (Figure 5.1g and h). Spontaneous fibrin fibre formation (Figure 5.1g) is also indicative of increased activation and consequently thrombotic potential of the exposed groups.
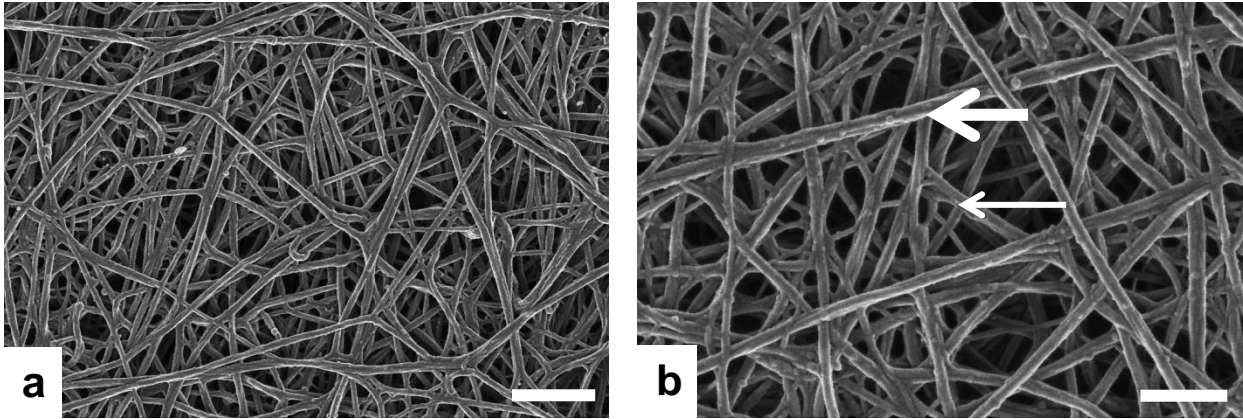
Figure 5.2: SEM micrographs of fibrin networks prepared from PRP with added thrombin from the control. (a) Regular network of fibrin fibres (b) Thick arrow indicating thick, major fibres and thin arrow indicating thin, minor fibres. Scale bars a = 1 µm b = 500 nm.
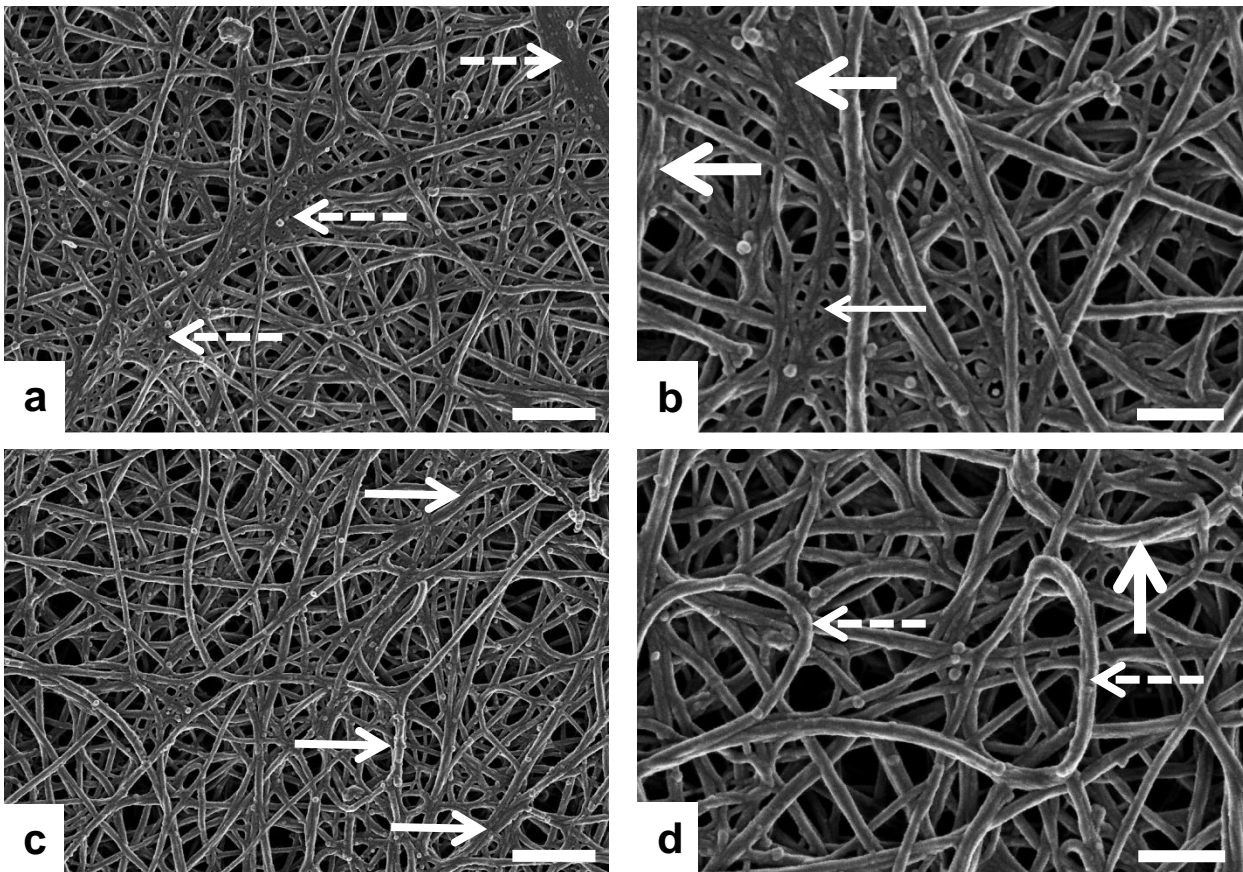
Figure 5.3: SEM micrographs of fibrin networks prepared from PRP with added thrombin from the Cd group. (a) Fibrin fibres formed dense fused areas visible at low magnification (dashed arrows). (b) Dense areas made up of fine fibres creating a net like structure (thin arrow) around thick fused fibres (thick arrows). (c) Areas of fibrin network with thickened fibres (arrow) seen at higher magnification in (d) (thick arrow). Coiling of thick fibres (dashed arrows). Scale bars a, c = 1 µm b, d = 500 nm.
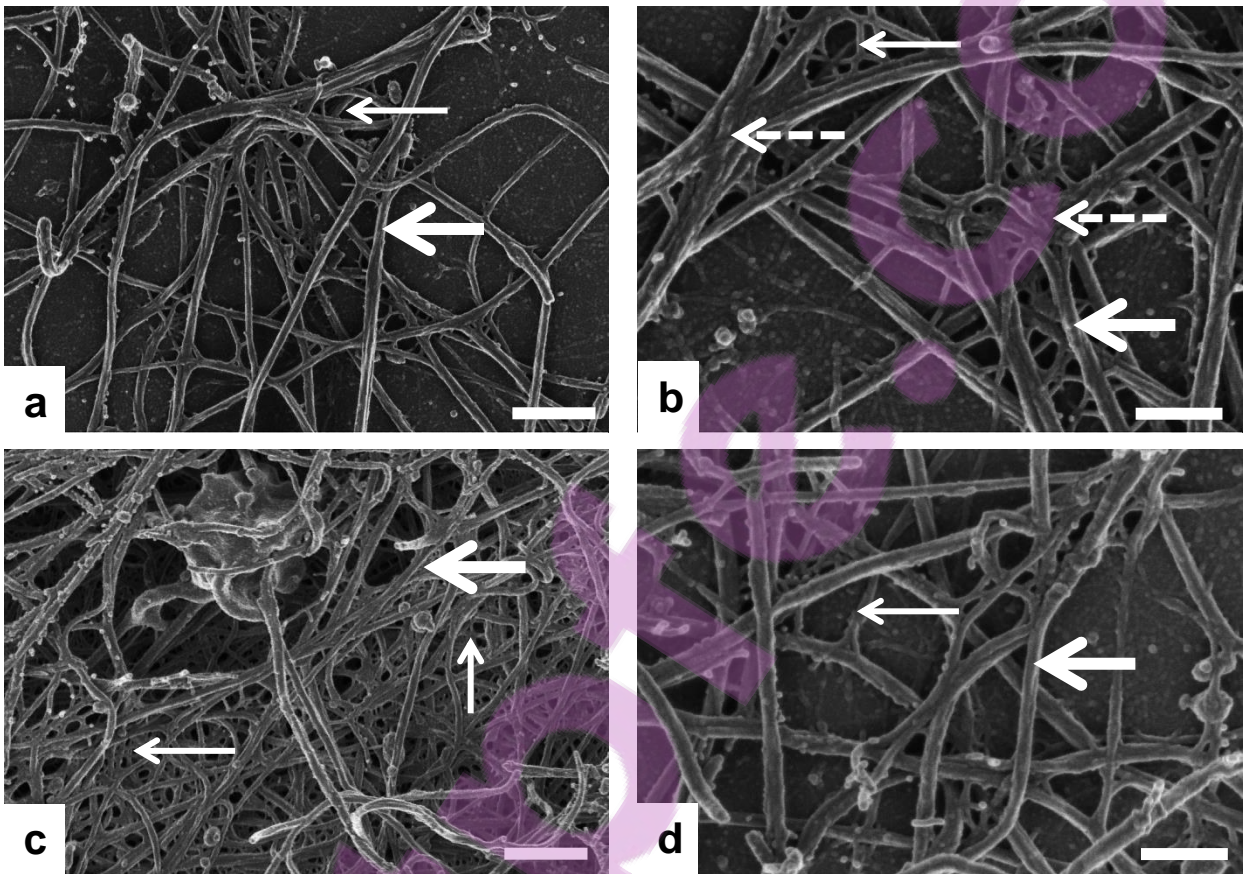
Figure 5.4: SEM micrographs of fibrin networks prepared from PRP with added thrombin from the Hg group. (a, b, d) Images show a sparse formation with both thick (thick arrow) and thin (thin arrow) fibres present. (b) Fused masses of thick fibres were present in some areas (dashed arrow). In (c), fewer fibrin fibres formed, with both thick (thick arrow) and thin (thin arrow) fibres present. (c) Net like structure created by thin fibres (thin arrow) around thick fused fibres (thick arrow). Scale bars a, c = 1 µm b, d = 500 nm.

91
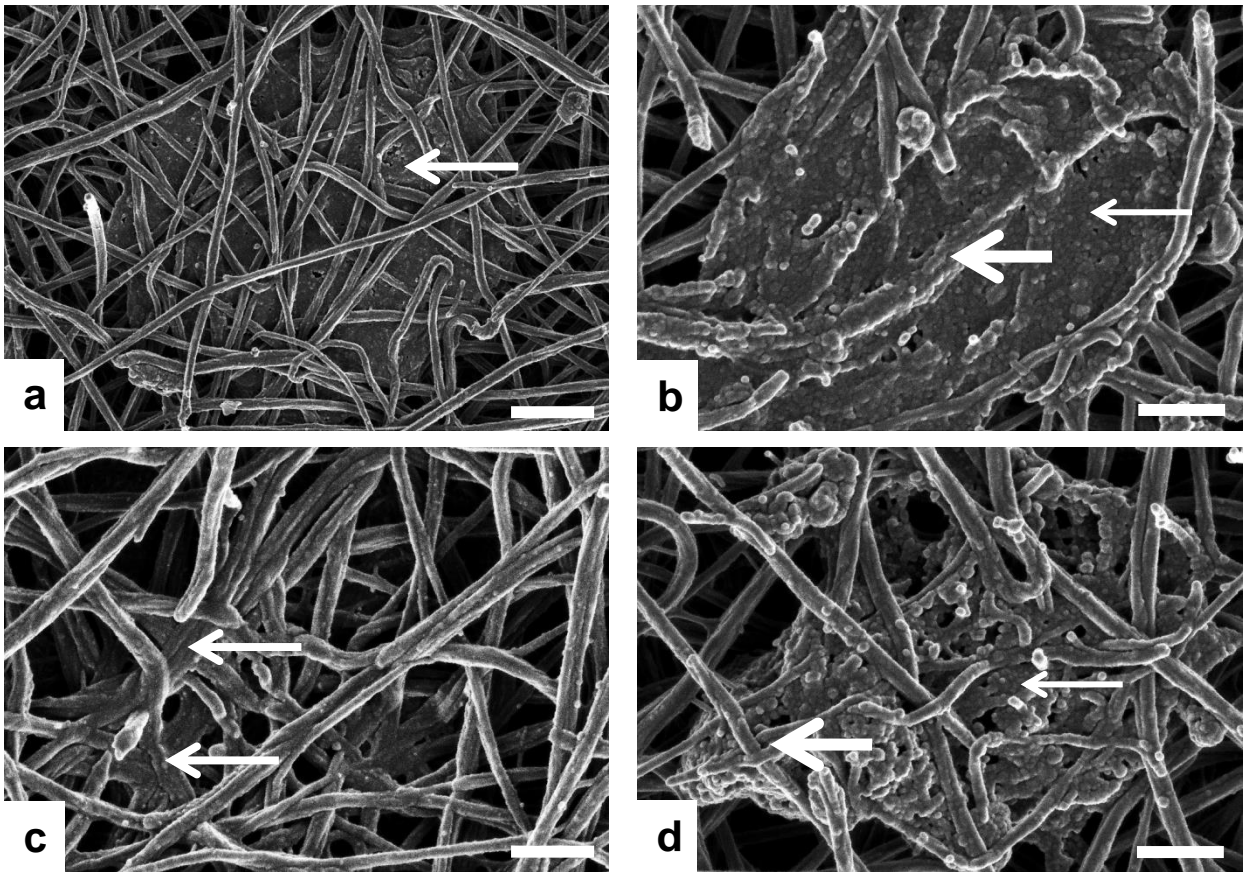
Figure 5.5: SEM micrographs of fibrin networks prepared from PRP with added thrombin from the Cd+Hg group. (a) Dense matted deposits (DMDs) observed within the fibrin network (arrow). (b) Higher magnification shows DMDs (thin arrow) in between thick fibres (thick arrow). (c) Aggregation of thick fibres into knot-like structures was also observed (arrow). (d) DMD deposition (thin arrow) around the aggregated fibres (thick arrow) (d). Scale bars a, = 1 µm b, c, d = 500 nm.
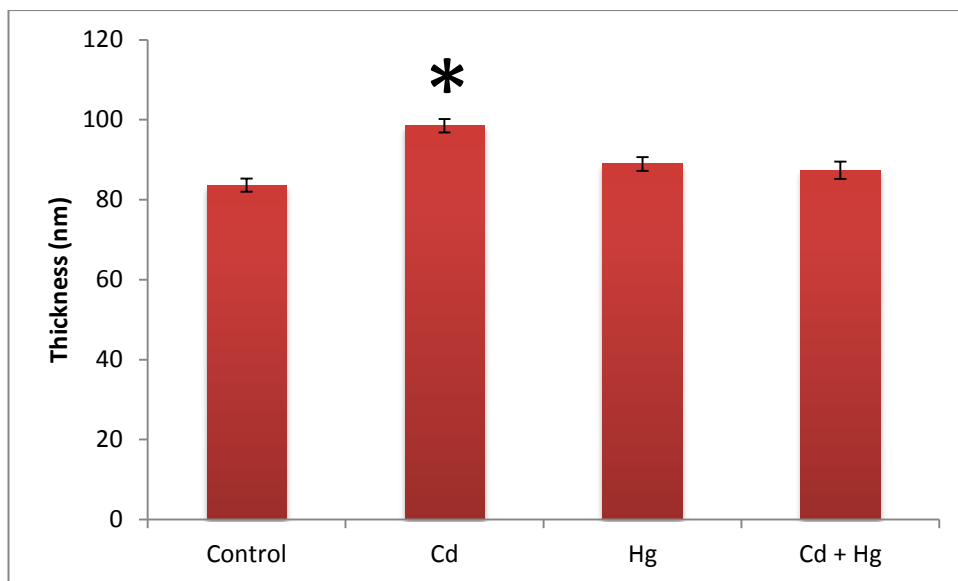
Figure 5.6: Average fibrin thickness (nm) of the control and metal exposed groups. Fibrin thickness was measured for at least 50 different fibres in each metal group and results are represented as an average ± SEM. *Represents significant differences compared to control, p-value ≤ 0.05.

5.3.1.2. *Fibrin network morphology*

Evaluation of the fibrin network in the control group (Figure 5.2a) revealed a typical fibrin network structure, with individual fibres of varying thickness in some cases overlapping to form a meshwork. As expected the fibrin fibres of the control group consisted of both thick, major fibres and thin, minor fibres (Pretorius *et al.*, 2011). Fibrin fibres in the Cd group (Figure 5.3 a-d) appeared denser as compared to the control and formed areas of fused fibres as indicated by the arrows. Fusion (Figure 5.3a and b) and coiling (Figure 5.3d) of fibres were also observed The Hg group revealed a sparse formation of fibres (Figure 5.4a - d), the sample from this group with the most fibrin network formation is shown in Figure 5.4c, where thick fibres (thick arrow) and thin fibres (thin arrow) are seen in a sparse network. The Cd+Hg combination group (Figure 5.5a - d) revealed denser and more aggregated fibres compared to the control and have areas where the fibres appear fused (Figure 5.5c, arrow) with the presence of DMDs. Knot like structures were present within the networks (Figure 5.5d). Evaluation of the fibrin fibre thickness revealed that Cd only had a statistically significant increase in fibre thickness as compared to the control and the other two experimental groups (*p*-value ≤ 0.05) (Figure 5.6).

5.3.2. Effects on erythrocytes and thrombus morphology
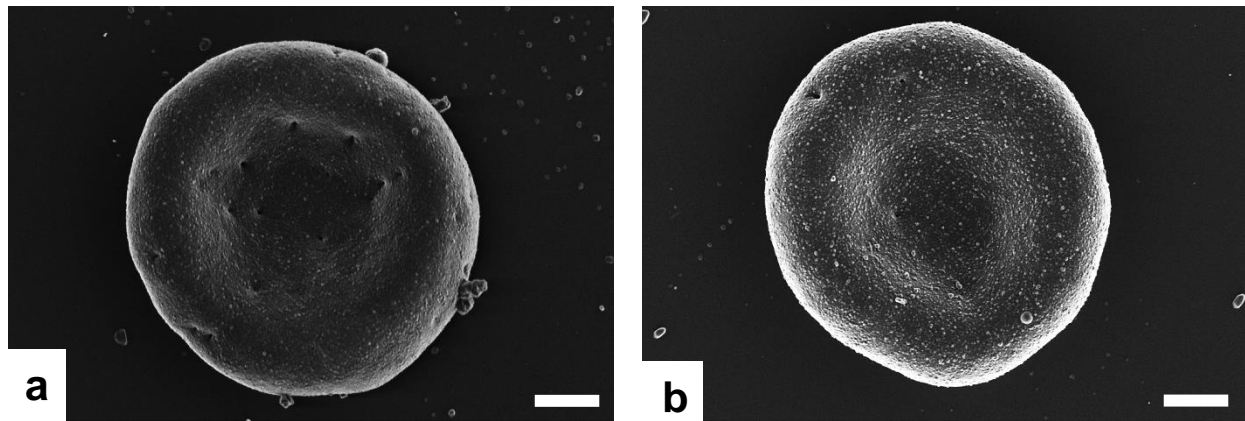
Figure 5.7: SEM micrographs of erythrocytes of control group, with a rounded appearance of the cell with central invagination forming a biconcave shape. The plasma membrane of the cell is smooth. Holes in membrane (a) and slightly rough appearance of membrane (b) are present. Scale bars = 1 µm.
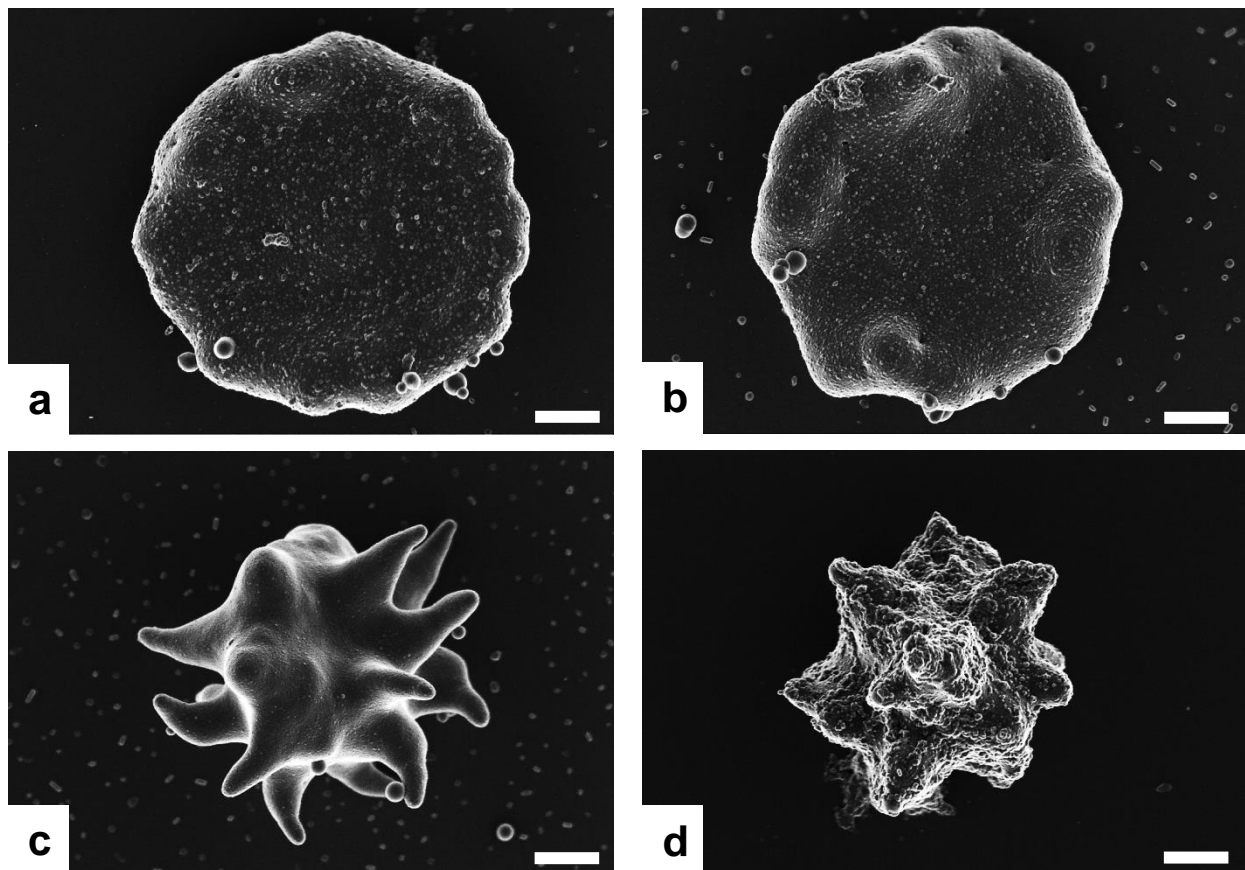
Figure 5.8: SEM micrographs of erythrocytes in Cd exposed group showing varying and most commonly observed cell morphologies. (a) Early elyptocyte formation (b) elyptocyte (c) echinocyte and (d) echinocyte with membrane damage. Scale bars = 1 µm.
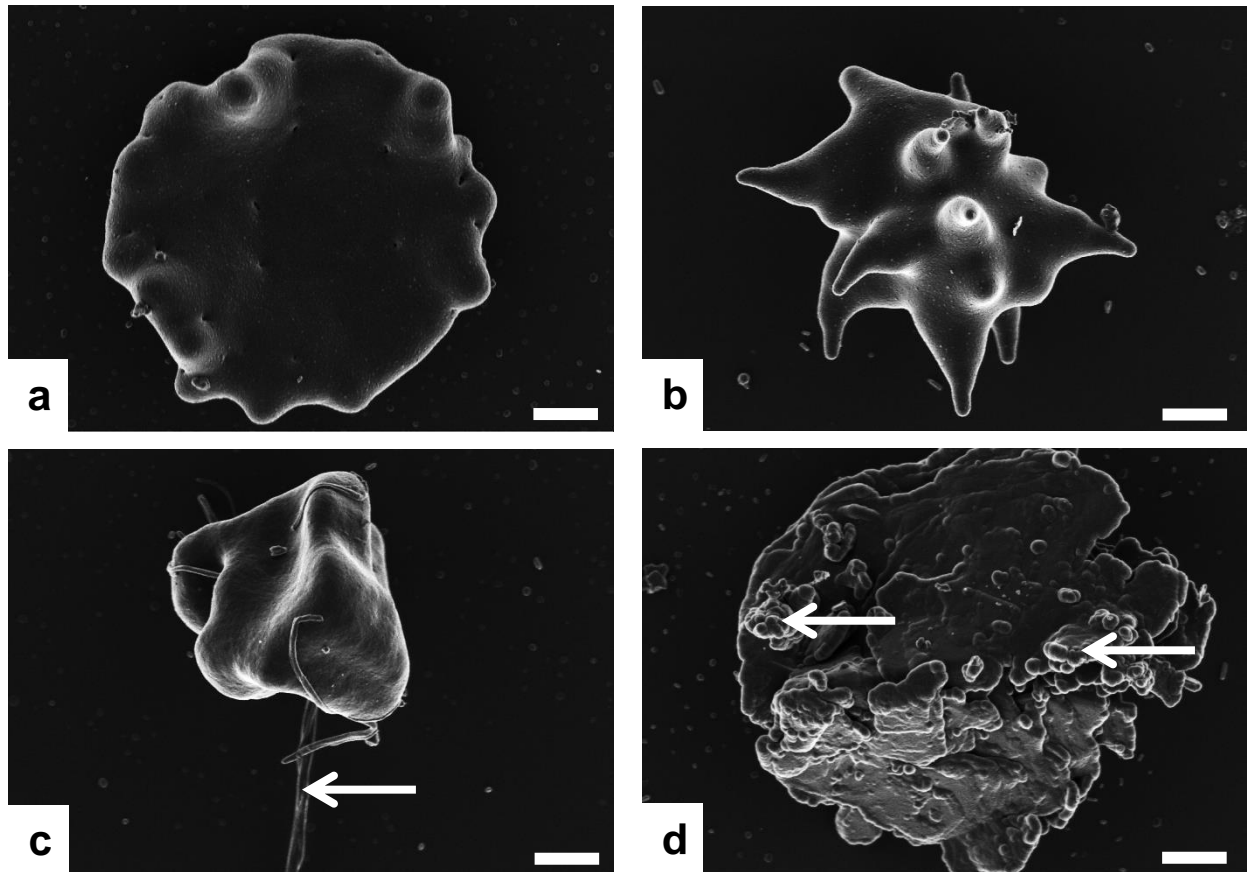
Figure 5.9: SEM micrographs of erythrocytes in Hg exposed group. Varying cell morphologies were observed in samples. (a) Progression of elyptoid cell into eryptosis (b) echinocyte formation (c) polyhedrocyte formation with spontaneous fibre formation (arrow) and (d) complete damage to plasma membranes and leakage of intracellular proteins (arrow). Scale bars = 1 µm.
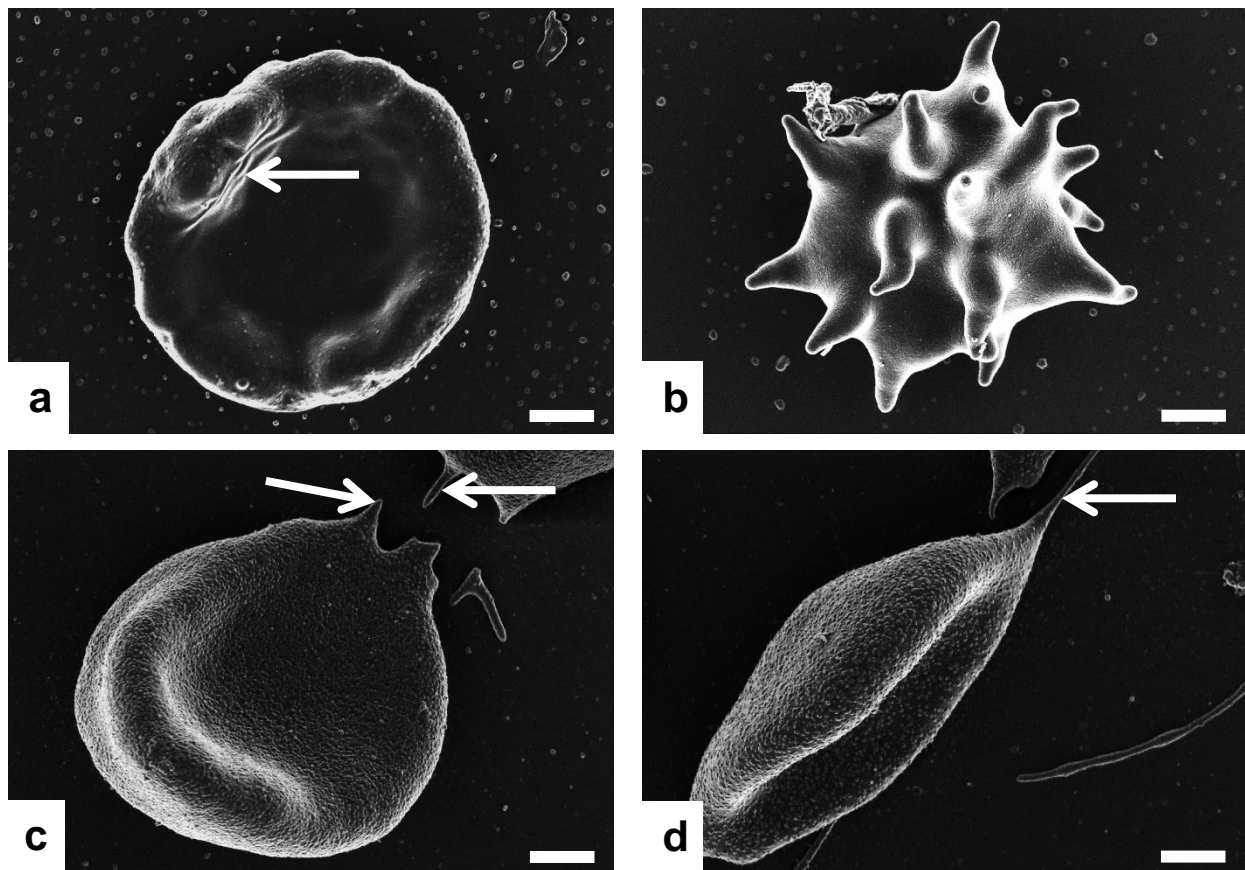
Figure 5.10: SEM micrographs of erythrocytes of the Cd+Hg exposed group showing most frequently observed cell shapes. (a) Early elyptocyte formation with crinkling of the plasma membrane (arrow). (b) Echinocyte morphology. (c and d) stomatocytes showing tear drop like morphology with plasma membrane extensions (arrows). Scale bars = 1 µm.

5.3.2.1. *Erythrocyte morphology*

Following platelet and fibre morphology, the morphology of erythrocytes was also evaluated. Erythrocytes from the control group (Figure 5.7a and b) have a rounded, biconcave appearance, typical of normal erythrocytes. The plasma membrane of the cell is smooth.

In the heavy metal exposed groups varying erythrocyte shapes were observed. Early elyptocyte shape, with elyptocyte formation was often observed in the Cd group (Figure 5.8) and membrane damage is visible in figure 5.8d. More extensive membrane damage was observed in the Hg group (Figure 5.9d). Spontaneous fibrin fibre formation was also observed around the erythrocytes in the Hg group (Figure 5.9c). Folding/crinkling of the plasma membrane were observed in the metal combination group on early elyptocytes (Figure 5.10a). Echinocytes and stomatocytes with tear drop morphology (Figure 5.10c and d) and membrane extensions were also observed (Figure 5.10d).
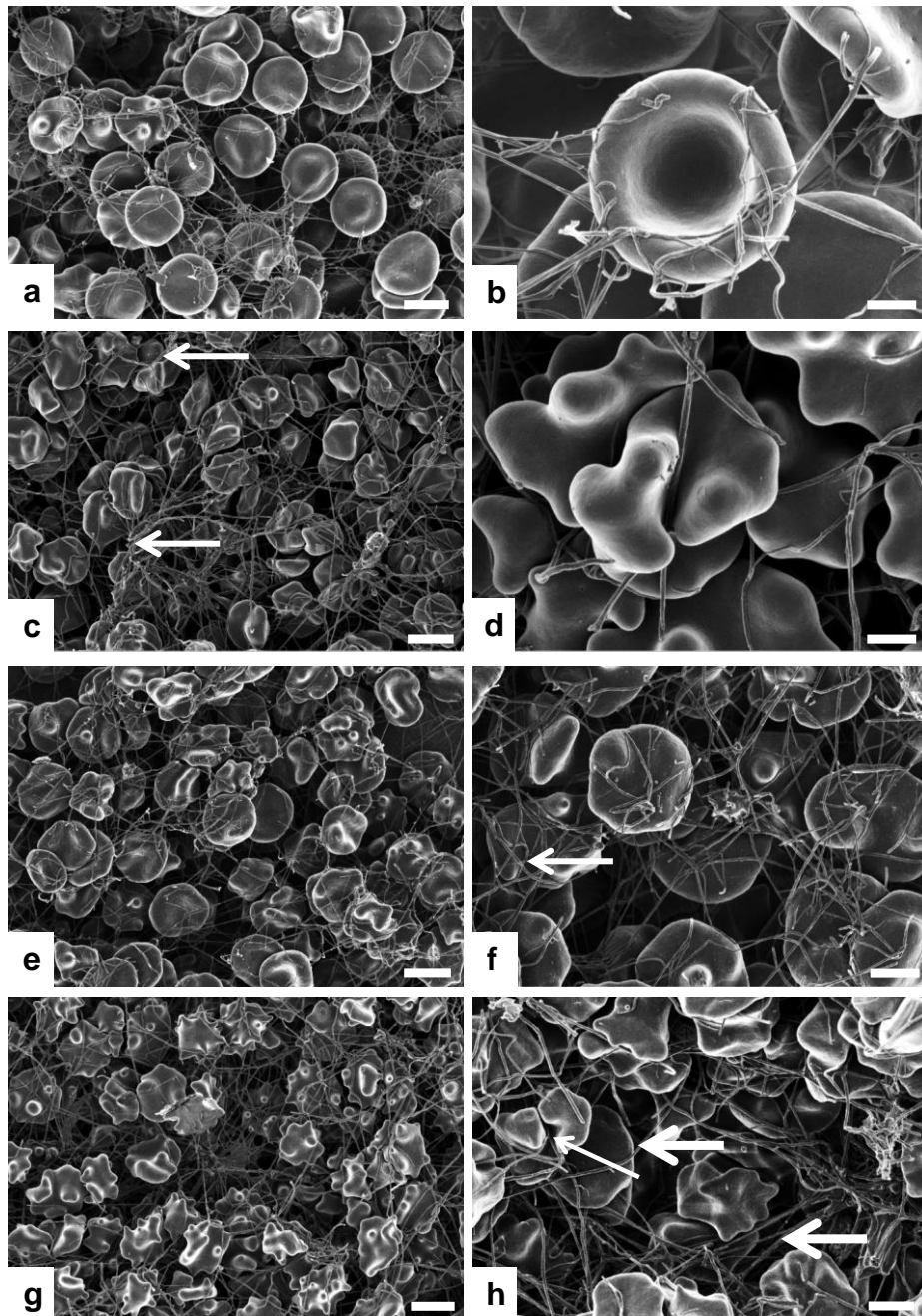
Figure 5.11: SEM micrographs of whole blood with added thrombin in order to demonstrate interactions between the fibrin networks and erythrocytes in a blood clot. (a) network composed of fine fibres and normal erythrocytes in the control group. (b) interaction between erythrocyte and fibrin fibres, erythrocyte membranes maintain shape on contact with fibrin fibre in control group. (c) network of thicker appearing fibres in some areas (arrows) and change in erythrocyte cell shape to elyptocytes and early eryptotic cells in Cd exposed group. (d) interaction between erythrocytes and fibrin fibres where eryptotic erythrocyte is folded over a fibrin fibre in Cd exposed group. (e) network of fine fibres and mostly elyptocytes in Hg exposed group. (f) interaction between erythrocytes and fibrin, where elyptoid cell bend around fibrin fibres (arrows). (g) Cd+Hg group showed a network of thicker appearing fibres and DMDs (arrows) with eryptotic cells. (h) eryptotic cells folding over fibrin fibre (thin arrow) and straight and taut appearance of fibrin fibre (thick arrow) in the Cd+Hg group. Scale bars a, c, e, g = 4 µm; b, d = 1 µm; f, h = 2 µm.

5.3.2.2. Thrombus morphology – Erythrocyte and fibrin interactions

The morphology of WB exposed to thrombin was evaluated in order to demonstrate interactions between the fibrin networks and erythrocytes in a blood clot. This also provides an indication of the tautness of the clot that forms. In WB samples with added thrombin, it was apparent that the metal exposed groups (Figure 5.11) showed the most erythrocytes damage when compared to the control (Figure 5.11a and b). Elyptocytes and early eryptotic cells were observed in the Cd (Figure 5.11c and d) and Hg groups (Figure 5.11e and f) while the combination group contained eryptotic cells (Figure 5.11g and h). Interactions between fibrin fibres and erythrocytes revealed that, unlike the control where fibrin fibres are smoothly wrapped around erythrocytes as shown in Figure 5.11b, in the metal exposed groups, the tension of fibres on the cell membranes was evident. As the erythrocyte membranes are damaged as indicated by the change in cell morphology, the folding of the cells around the fibres may be due to the membrane weakness as a result of the damaging effects of the heavy metals. In some areas the fibrin fibres of the Cd (Figure 5.11c, arrow) and combination group (Figure 5.11h) appeared straight and taut.

5.4.   <u>Discussion</u>

Disturbances in the coagulation system will increase the risk or exacerbate pre-existing CVD in population exposed to contaminated water and other sources of environmental heavy metal exposure. Interactions between platelets and fibrin networks are necessary in the coagulation cascade and therefore the alterations in the structure of platelets and fibres can be used as an indicator of changes in the coagulation system. Erythrocytes have already been established as a cellular model for indication of pathology in the circulatory system (Swanepoel and Pretorius, 2012; Pretorius *et al.*, 2016). Fibrin and thrombus formation *in vitro* and *in vivo* can be used to provide physiologically relevant information on diseases associated with thrombus complications as *in vitro* studies have previously been shown to correlate with clinical data (Undas and Ariens, 2011; Weisel and Litinov, 2013).

5.4.1. Platelet activation

Alterations to the platelet and fibrin structure can cause changes to the coagulation system (Lang and Qadri, 2012; Pretorius*, et al.*, 2016). Platelet changes consistent with activation, as described previously (Kuwahara *et al.*, 2002, Van Rooy *et al.*, 2015), were observed in this study, at varying degrees in the two metal groups alone and to a higher extent in the combination group. The degree of activation was evaluated based on the degree of pseudopodia formation as well as degree of platelet spreading, relative to the control. Low doses of heavy metals have been shown to disrupt normal structure and function of rat platelets (Kumar *et al.*, 2001). Platelets are known to increase clot elasticity (Carr and Alving, 1995), therefore these changes in platelet shape and membrane characteristics affect the formed thrombus, and have also been linked to inflammation (Van Rooy *et al.*, 2015).

5.4.2. Fibrin network morphology

Thickness of the fibrin fibres was increased in the Cd group, suggesting that Cd has pro-fibrotic effects on the coagulation system. An extensive literature search failed to show studies where the effects of Cd and Hg in combination on the fibrin networks and platelet activation have been investigated. Oxidation has previously been suggested to alter fibrin formation and degradation visible with ultrastructural studies (de Maat *et al.*, 2005; Undas and Zeglin, 2006; Undas *et al.*, 2008). Since heavy metals can catalyse the Fenton reaction and cause the formation of ROS (Waisberg *et al.*, 2003; Berlin *et al.*, 2007; Alissa and Ferns, 2011), the observed effects on fibrin networks and platelet activation may be a result of oxidative damage. A study showed that 10% oxidised fibrinogen is able to moderately activate the intrinsic pathway while inhibiting the extrinsic pathway of coagulation and a 20% oxidation would inhibit both, resulting in a decrease of thrombin formation and a decrease in the clotting rate (Roitman *et al.*, 2004). These findings could explain the difference between the two metal groups, Cd causing increased fibrin thickness while the Hg group revealed a decrease in fibre density in the networks. Oxidised fibrinogen is said to influence the rate of platelet aggregation (Aseichev *et al.*, 2002), however the mechanism remains unclear (Roitman *et al.*, 2004).

The structure and function of fibrin are important in the fibrinolytic process (Wolberg, 2007). During fibrinolysis fibrin plays a double role acting as a co-factor and a substrate to plasmin. As a result, altered fibrin structure has an altered susceptibility to fibrinolysis (Collet *et al.*, 2000; Marchi *et al.*, 2000; Wolberg, 2007) and these alterations can have significant physiological implications. Clots that are resistant to fibrinolysis are prone to thrombosis whereas fragile clots which are more susceptible to fibrinolysis are prone to lysis and consequent bleeding (Sugo *et al.*, 2000; Dunn *et al.*, 2005; Dunn *et al.*, 2006).

Thinner fibres have a slower rate of tissue plasminogen activator (t-PA) mediated plasmin generation than thicker fibres, resulting in a reduced fibrinolytic activity of the system and therefore a greater resistance to fibrinolysis. Even though when looking at single fibrin fibre strands, thicker fibres are lysed more slowly than thinner fibres (Collet *et al.*, 2000), clots produced by thicker fibres are loosely woven, providing fewer fibres as substrate for a given amount of fibrinogen when compared to clots composed of thinner, but more closely packed fibres (Collet *et al.*, 2000; Wolberg 2007; Wolberg *et al.*, 2012). During clot formation an initial fibrin scaffold may form followed by further branching and elongation of the fibrin fibres, as well as the addition of new fibres over time, resulting in different fibrin thickness throughout the sample (Wolberg *et al.*, 2005). Therefore, the overall structure of the clot, rather than the thickness of individual fibres determine the fibrinolytic activity on the clot system (Collet *et al.*, 2000; Bhattacharjee and Bhattacharyya, 2014).

Results of the present study showed the formation of DMDs within the fibrin fibres in the Cd and Hg combination group (Figure 5.5). Pretorius *et al.* (2010) showed that the fibrin fibre networks

prepared from the plasma of smokers had a net-like appearance in some areas, as well as areas where thick matted masses (DMDs) were present, and that these changes occurred immediately and not only over an extended period of time. The authors describe DMD formation to be most likely due to the generation of oxidative stress, specifically free radicals such as ROS. Platelets are involved in maintaining the tautness of fibrin fibres and the bending of the fibrin fibres observed in the Cd treated group may reflect functional changes to the platelets i.e. their inability to contract the thrombus, or a lack of thrombin production (Van Rooy *et al.*, 2015). The presence of less taut fibres due to the increased elasticity would result in coiling and disorganisation of the fibres, as shown for the Cd exposed group (Figure 5.3). Lateral aggregation was another feature observed in the results in the Cd exposed group, and this results in denser fibre networks which are often associated with a reduction of clot permeability and clot lysis (Undas *et al.*, 2009: Undas *et al.*, 2010; Stanford *et al.*, 2015).

Little is known about the effect of Hg on fibrin network formation. S-nitrosglutathione (GSNO) plays an important role in vascular homeostasis by inhibiting platelet activation and aggregation and fibrinogen binding to platelets. Akhter *et al.* (2002) and Geer *et al.* (2008) reported that GSNO reduced the initial rate of polymerisation. Bateman *et al.* (2012) observed that GSNO alters the secondary structure of fibrinogen where low dosages generates coarse networks with thicker fibres while higher dosages induce abnormal fibrin networks with the formation of fibrin aggregates. Hg can cleave the S-NO bond of GSNO resulting in increased NO levels. Vadseth *et al.* (2004) reported that exposure of fibrinogen to nitrating oxidants caused the rapid clot formation and crosslinking, while in contrast exposure to non-nitrating oxidants reduced the rate of clot formation and increased permeation. Shacter *et al.* (1995) showed that oxidative modification by Hg inhibits thrombin catalysed clot formation. Likewise in the present study Hg exposure causes a sparse fibrin network to form. *In vitro,* $HgCl_2$ oxidization of fibrinogen results in the formation of methionine sulfoxide residues with decreased fibrin polymerisation and reduced final turbidity. The clot that forms has decreased stiffness and viscosity although there is an increase in fibre density, decreased fibre diameter and pore size. Becatti *et al.* (2014) reported that carbonylation of purified human fibrinogen by 2,2'-azobis(2-amidinopropane) dihydrochloride (AAPH) that generates physiologically relevant hydroxyl radicals is responsible for a decrease in thrombin-induced clot formation due to an increase in protein carbonylation with the most susceptible amino acids being methionine and cysteine. An extensive review of the literature leads to the conclusion that Hg mediated depletion of GSNO did not lead to the formation of a denser fibrin network, but the observed effect is as a direct result of ROS accumulation, either due to direct binding to GSH and/or inhibition of the AOx pathways. Inflammatory sources of ROS can also contribute to this effect.

The metals in combination show an additive effect, with an increase in platelet activation. While there was no significant increase or decrease in fibrin fibre thickness in the combination group, there were morphological changes to the network structure, including the formation of a fibrin

network that was denser with more aggregated fibres and areas of fibre fusion with the presence of DMDs within the networks. It appears that Hg enhances the effect of Cd possibly via the oxidation of methionine residues Met[78], Met[367] and Met[476] the nitration of Tyr[292] and Tyr[422]. A possible mechanism is that Hg causes the oxidation of methionine residues, which alters the tertiary structure of fibrinogen, and consequently the tyrosine residues become more susceptible to Cd induced nitration (Ji *et al.*, 2012). In addition, increased NO levels due to Hg cleave of the S-NO bond of GSNO, results in the formation of a denser more thrombotic clot phenotype with increased risk for CVD.

The morphological features therefore suggest that for Cd alone and in combination, the thrombus although being denser and composed of thicker fibres may be structurally less stable, with the potential to dislodge and cause vascular occlusions. Single metal Hg exposure caused a sparse fibre network formation, suggesting impairment of the coagulation process, while in combination with Cd, Hg enhances its effect of a rigid yet less stable clot.

5.4.3. Erythrocyte morphology

Cell membranes are the first available targets for toxic damage, and circulating erythrocytes are the cells most likely to be affected by heavy metal toxicity. Alterations to the morphology of erythrocytes were also more prevalent in the heavy metal exposed groups, resulting in different forms including eliptocytes (loss of concave shape and appearance of wavy edges), echinocytes (erythrocytes with short projections stemming from the cell body), polyhedrocytes (loss of circular shape with a varying amount of sides on the erythrocyte), stomatocytes (swollen and spherical erythrocytes followed by a tear drop like appearance) (Swanepoel and Pretorius, 2012). Echinocytes and elyptocytes were primarily observed in this study. The shape changes are consistent with eryptosis, characterised by shrinking of cells, blebbing and membrane scrambling (Pretorius *et al.*, 2014). Cd and Hg caused oxidative stress in the erythrocytes via different pathways, but the results were the same, with erythrocyte damage - cell shape change and eventual rupturing. This erythrocyte damage has been suggested to be caused by oxidative damage as an increased generation of free radicals causes destruction of the cell membranes, inactivation of the Na^+/K^+ ATPase that allows Ca^{2+} entry in to the cells. The sustained increase in free calcium within the cell then leads to further free radical generation and inhibition of the Na^+/K^+ ATPase pump (Kumar *et al.*, 2002).

Recently the interaction of heavy metals with lipid bilayers has been under investigation (Kerek *et al.*, 2018). Correlating with the results of this study, a microscopic evaluation by Kerek *et al.* (2018) showed that Cd and Hg changed erythrocyte morphology while Hg caused erythrocyte rupture. Hg irreversibly cleaved the plasmalogens on the erythrocyte lipid bilayer resulting in an increase in membrane rigidity. Besides high levels being present in erythrocytes, these lipids are also enriched in cardiac muscle fibres and play a role in signalling and the protection against oxidative stress. In contrast to the effects of Hg effects, Cd induced rigidity by targeting negatively charged

phosphatidic acid, phosphatidylserine, phosphatidylinositol, phosphatidylglycerol and cardiolipin (Kerek *et al.*, 2018).

Echinocytosis of erythrocytes in rats exposed to Cd has been observed by Ghosh and Indra (2018) and in carp erythrocytes by Witeska *et al.* (2011). Cd was shown to have an echinocyte forming effect in human erythrocytes at 1 mM (Suwalsky *et al.*, 2004; Kerek *et al.*, 2018) as well as increased erythrocyte membrane rigidity (Payliss *et al.*, 2015; Kerek *et al.*, 2018). Similarly, the incubation of erythrocytes with 1 mM of Hg for one hour at 37°C caused a change in erythrocyte morphology from discoidal to echinocytes and stomatocytes (Suwalsky *et al.*, 2000). Changes to the membrane which result in the morphological alterations can be explained by the bilayer couple hypothesis proposed by Sheetz and Singer (1974), where a metal ion may affect only one membrane leaflet and not the other. The binding of a metal to the outermost layer increases surface area and causes irregular bulge formation on the membrane, resulting in echinocyte formation. If the metal was to bind to the innermost layer of the cell membrane, this would cause the membrane to invaginate and cause stomatocyte formation. Suwalsky *et al.* (2000) showed that based on this hypothesis, Hg interacts with both erythrocyte membrane layers, however echinocyte formation was the most prominent observed erythrocyte morphology following Hg exposure. Accumulation of Hg in erythrocytes and subsequent morphological changes (Pal and Ghosh, 2012) are associated with exposure or flipping of PS (Lim *et al.*, 2010). Erythrocyte shape changes include the creation of microvesicles (blebbing) on cell surface with prolonged low dose Hg ion exposure (0.25 – 5 μM for 1 – 48 hours) (Lim *et al.*, 2010). Hg inhibits flippase, and this inhibits the reversal of PS into the inner leaflet of the cell membrane. Scrambalase is then activated, causing lipid asymmetry in the cell membrane (Lim *et al.*, 2010). PS exposure may cause vassoclusion as erythrocytes with exposed PS and altered morphology stick more readily to endothelial cells and also provide a site for prothrombinase and tenase complex assembly and this in turn leads to the generation of thrombin and ultimately clotting.

The PS flip is influenced by Ca^{2+} alterations in the extracellular and intracellular environment, as both Cd and Hg are known to affect Ca^{2+} homeostasis (Suzuki *et al.*, 2004). Hg increases intracellular Ca^{2+} and depletes thiol content as well as ATP.

Consequently, an increase in thrombin generation and endothelial cell adhesion occurs, causing a prothrombotic effect. Rupture of erythrocytes was another observation with Hg exposure (Figure 5.9) and is consistent with previous reports (Kerek *et al.*, 2018). Eryptosis, a programmed cell death similar to apoptosis has been observed in erythrocytes (Lang and Lang, 2015) and nucleated and anucleated cells (Eisele *et al.*, 2006). The process of eryptosis is characterised by the features mentioned above; increase of Ca^{2+}, intracellular ATP depletion and ultimately morphological changes to the erythrocytes and their cell membrane structure, in which PS exposure is one of the main features (Lim *et al.*, 2010).

Besides the Ca^{2+} that activates the PS flip, it also affects the sensitive Ca^{2+}/K^+ channels which causes K^+ to exit the cells together with water and thus causing cell shrinkage (Sopjani, et al., 2008; Lupescu, et al., 2012; Pretorius, et al., 2016b). One of the earliest studies showed that both Cd and Hg promoted the release of K^+ from healthy human erythrocytes and when expressed as a ratio, that was 200 to 800 times more for Hg compared to Cd (Vincent and Blackburn, 1958). This K^+ release did not change in the presence of non-metallic thiol ion inhibitors, which suggests that even though Cd and Hg are able to bind sulfhydryl ions the K^+ release was independent of interactions between the metals and the sulfhydryl groups on the erythrocyte membrane proteins (Payliss et al., 2015). It has therefore been suggested that Hg is able to induce changes to the erythrocytes as a result of alterations to the lipid structure of the bilayer, and not necessarily to the proteins within the lipid bilayer. These changes could occur through disruption of the osmotic balance due to the rapid intake of $HgCl_2$ and aquaporin inhibition (Savage and Stroud, 2007) and the speed with which $HgCl_2$ crosses the erythrocyte membrane and reaches equilibrium concentrations. In earlier studies it was shown that $HgCl_2$ is able to cross intact human erythrocyte membranes in 4 minutes (Rabenstein and Isab, 1982). The K^+ release effect of the two metals can account for the elevated, although not significantly, K^+ in the blood obtained from the rat model in the Hg and Cd+Hg group (Table 3.6).

The PS flip, altered cell metabolism and altered functioning of osmotic pumps all affect membrane fluidity, making erythrocytes more fragile and less osmotic resistant, thereby increasing their susceptibility for mechanical and chemical stress (Stohs and Bagchi, 1995; Mahmood, 2017). Low erythrocyte and haemoglobin (Hb) in Cd treated animals were observed in previous studies (Karmakar et al., 2000; El-Demerdash et al., 2004; Ashour, 2014; Ghosh and Indra, 2018). The depletion of Hb in Cd treated animals indicates increased haemolysis, which can result in anaemia, as can abnormalities in iron metabolism caused by Cd (Horiguchi et al., 2011). The decrease in Hb content has likewise been observed with Hg exposure, as well as a decrease in the total erythrocyte count and packed cell volume (Hounkpatin et al., 2012; Sheikh et al., 2013). The loss of the biconcave shape of erythrocytes and fragility of cell membranes as a result of the exposure to the heavy metals would result in a shorter erythrocyte lifespan and a need for their removal from the circulation (Ichikawa et al., 1987). The altered morphologies of the erythrocytes indicate a possible shortened lifespan and a prothrombogenic potential through alterations in the cell membranes.

5.4.4. Heavy metals and coagulation

Analysis of whole blood provides an opportunity to investigate the interaction between blood cells and the type of clot that forms following the addition of thrombin. Cd compared to the control caused increased echinocyte formation with fibrin network formation similar to the control. Hg also caused increased echinocyte formation with the formation of a denser fibrin clot. In combination, most erythrocytes formed echinocytes and the metal combination, Cd+Hg caused a denser appearing clot formation compared to whole blood exposed to Cd and Hg alone. Abnormal clots

can either be loose or dense, both can cause cardiovascular problems where a loose clot may be easily dislodged causing a blockage in an artery or vein. In contrast, a denser clot can lead to less effective closure of site of injury and clots which are easily dislodged and may cause a vascular occlusion (Smith, 2009) causing tissue damage due to ischemia as in CVA (Zhang *et al.*, 2015).

During the coagulation cascade, Hg has been found to alter levels or functioning of fV and thereby increases the procoagulant activity of erythrocytes which represents another potential mechanism for the cytotoxic effects and thrombotic events associated with Hg (Lim *et al.*, 2010). Even low Hg levels enhance the procoagulant activity of erythrocytes, giving rise to Hg related thrombotic diseases (Lim *et al.*, 2010). Calcium allows for thrombin catalysed factor formation (fXIII) and a subsequent conversion of fibrinogen to fibrin, which stabilises fibrin fibres (Kell and Pretorius, 2017). Depletion of extracellular Ca^{2+} by Cd and Hg would inhibit this process resulting in a more fragile, unstable clot.

Cd and Cd+Hg exposure caused the formation of dense fibrin networks consisting of thicker and in some instances, coiled fibres. Coiled fibres are an indication of loss of tension within a clot and consequently increased fragility and decreased clot strength. This result is similar to what was observed for Cd and Cr exposure by Venter *et al.*, 2017 where less taut, coiled fibres were by SEM. Platelet activation observed in the serum of Cd and Hg exposure alone and in combination without the addition of thrombin in the present study could be an indication of fast initiation of the coagulation process, but a lower fibrin build up time, resulting in reduced cross linking and fragile and less stable clots as described for Cd and Cr by Venter *et al.*, (2017).

Hg on the other hand has an opposite effect with the formation of fine fibrin fibres and poor clot formation. In theory, thinner fibres have a slow rate of t-PA mediated plasmin generation than thicker fibres, and a greater resistance to fibrinolysis. Clots resistant to fibrinolysis are prone to cause vascular occlusions. The fine and fragile appearance of Hg clot morphology is contradictory, as fragile clots are more susceptible to lysis and consequent bleeding (Sugo *et al., 2000; Dunn et al., 2005; Dunn et al., 2006).* In contrast, Hg has been previously reported as having a prothrombotic effect (Wierzbicki *et al.*, 2002; Lim *et al.*, 2010). Further quantitative measure would have to be performed to deduce whether clots in the presence of Hg are pro- or antithrombotic.

The co-administrative effect of Cd and Hg was investigated in a study of the protective effect of vitamin C by Houkpatin *et al.* (2012) and showed that on both low and high doses of Cd (0.25 mg/kg and 2.5 mg/kg), Hg (0.12 mg/kg and 1.2 mg/kg) and co-administration` of the two at both low and high doses caused a decrease in erythrocyte numbers in comparison to the control, with numbers being lower in the Hg group compared to the Cd and the combination group, showing a synergistic effect between the two metals. In the higher concentration group Hg was more toxic and the combination again showed a more toxic effect. The results for platelet numbers were opposite and were increased on administration of the two metals alone and in combination; in this case Cd caused the greatest effect at both low and high doses, with higher platelet levels than

even the combination group (Hounkpatin *et al.*, 2012). These findings suggest a procoagulatory effect of both heavy metals, with Cd being the most procoagulative by increasing platelet numbers, a finding which correlates to the results of the present study of increased fibrin thickness in the Cd group as well as increased morphological alterations in the Hg group. The effect of the metal combination in the study by Hounkpatin and colleagues (2012) is further supported by the results of the present study.

Therefore, the exposure to these metals has profound effects on platelet function, fibrin fibre network formation and erythrocyte morphology. In conjunction with the findings in Chapter 5, Cd and Hg alone and in combination alter components of the cardiovascular system and blood haemostasis and environmental exposure, even at low concentrations of metals, might have serious health implications especially related to the development of CVD.

5.5. <u>Conclusion</u>

The heavy metals Hg and Cd alone and in combination were shown to affect platelet activation and fibrin fibre formation in an *in vivo* Sprague-Dawley rat model. Hg and Cd alone and in combination cause platelet activation. Cd increases the thickness of the fibrin fibres, causes aggregation and the formation of flat, fused areas of fibrin. Hg showed a decrease in fibre formation and the combination group revealed a dense fibrin fibre network with an extensive presence of matted deposits between the fibres, with no changes to the actual fibrin thickness. In WB the interaction of erythrocytes and fibrin fibres caused changes in erythrocyte morphology and fibrin network structure. Findings were that Hg enhances the effect of Cd on coagulation, forming a dense, yet possibly unstable thrombus. These findings together with the findings presented in Chapter 4 suggest a prothrombotic blood environment that, together with vascular remodelling induced by heavy metals, has the potential to aggravate atherosclerosis formation and stroke.

Chapter 6: Effects of Cd and Hg alone and in combination on haemostasis in an *ex vivo* human blood model

6.1.   Introduction

Animal models provide important preliminary information on the effects of toxins such as heavy metals. Evaluation of human exposure to heavy metals usually involves the measurement of markers of tissue damage such as liver and kidney function. However, as shown in Chapter 3 and published by Venter *et al.* (2017) these parameters are poor indicators of tissue damage. In chapter 4 and 5, both Cd and Hg alone and in combination caused vascular damage and altered blood coagulation parameters where Cd caused platelet spreading and pseudopodia formation in platelets, and dense and fused fibrin fibre formation on addition of thrombin. To confirm if the observed effects in the subacute *in vivo* rat model are a direct result of Cd and Hg toxicity, an *ex vivo* model of human blood was used and the effect of a single, acute dosage of each metal alone and in combination was evaluated. The concentrations selected was the same as that measured in rats after 28 days exposure to Cd and Hg alone and in combination.

An inherent problem with the evaluation of toxicity in human studies is that non-invasive methods are favoured such as the measurement of metal levels in hair, blood and urine (Aitito *et al.*, 1983; Berlin *et al.*, 1969; Berlin and Gibson 1963; Drach *et al.*, 1997; Bernhoft, 2012). Blood and hair Hg levels reflect recent exposure and do not correlate with the total body burden (Aitito *et al.*, 1983; Berlin *et al.*, 1969; Berlin and Gibbon 1996; Drach *et al.*, 1997; Bernhoft, 2012). In addition, the direct measurement of metals in blood does not provide any information on the effects of these metals. Following absorption, distribution within blood occurs and is often besides the GIT, the first tissue that is exposed. The easy accessibility to this tissue makes it an ideal tissue in human studies to investigate the effects of exposure on structure and function.

Clinically erythrocytes have been used as a biosensor in monitoring oxidative stress imbalances in management of COPD (Lucantoni *et al.*, 2016). In research, the evaluation of the effects of toxins on blood cell morphology *ex vivo* has been determined for exposure to cigarette smoke (Barua *et al.*, 2002; Barua *et al.*, 2010; du Ploy *et al.*, 2013), contraceptive hormones (Wang *et al.*, 2013; Swanepoel *et al.*, 2017), pharmaceuticals (Kerrigan *et al.*, 1989; Ajjan *et al.*, 2009), diabetes (*Buys et al.*, 2013), snake venom (Strydom *et al.*, 2016), bacterial toxins (Bhakdi *et al.*, 1988), oxidative damage products such as lysophosphatic acid produced by LDL oxidation (Seiss *et al.*, 1999) and nanomaterials (Asharani *et al.*, 2010; Feng *et al.*, 2014; Pajinc *et al.*, 2015; Wu *et al.*, 2017).

Likewise the effect of heavy metals on *ex vivo* blood cells has also been investigated. Ghosh and Indra, 2018 reported altered erythrocyte morphology on exposure to Cd. Altered erythrocyte morphology has also been reported for Hg exposure (Lim *et al.*, 2010; Pal and Ghosh, 2012; Kerek *et al.*, 2018) along with a procoagulatory effect of the metal (Lim *et al.*, 2010; Kerek *et al.*, 2018). A

combination of Cd and Hg was reported to have a procoagulatory effect at high and low dose through platelet activation (Hounkpatin *et al.*, 2012). Venter *et al.* 2017 similarly reported that Cd and Cr in combination caused eryptosis and an increased coagulation with resultant less stable clot formation.

The present study differs from previous studies on Cd and Hg exposure as it provides an indication of similarities and/or differences between the blood targets of *in vivo* rat and *ex vivo* human studies. The current chapter therefore provides the results obtained from the exposure of human blood to these metals alone and in combination at concentrations similar to what was found in the rat model component in this study.

6.2.   Materials and Methods

6.2.1. Materials

All materials used in this study were the same as used in section 5.2.

6.2.2. Methods

Human blood was drawn via venepuncture by trained phlebotomists into 3.2% trisodium citrate (9:1) tubes. Three consenting male adults (n=3) were used for the study to provide a triplicate experiment (Health Sciences Research Ethics Committee number: 489/2015). With the selection of blood donors, the inclusion criteria was that donors were healthy male non-smokers over the age of 18 years, without an inflammatory or hypersensitivity conditions such as asthma and that are not on any short term or chronic medication. Blood was collected as described in Section 3.2.4 into citrate tubes and transported to the Unit for Microscopy and Microanalysis, University of Pretoria, where it was processed for SEM. All samples were kept at room temperature, were exposed to heavy metals and then prepared for SEM within 4 hours after the blood was collected.

Stock solutions, 10 times the concentration found in blood were prepared in isotonic phosphate buffered saline (isoPBS: 0.137 M $NaCl_2$, 3 mM KCl, 1.9 Mm NaH_2PO_4, 8.1 mM $NaHPO_4$, pH 7.4) and 100 µl was added to 900 µl WB and the final concentrations of 16, 69 nM Cd and 186, 67 nM Hg alone and 121, 06 nM Cd and 155,99 nM Hg in combination were obtained (Table 3.2). To the controls 100 µl isoPBS was added.

6.2.3. Scanning electron microscopy

The WB was exposed for 10 min to Cd and Hg alone and in combination and all samples were further processed following standard laboratory protocols as described in Section 5.2.3.

6.2.4. Statistical analysis

Image generation and statistical analysis was the same as described in Section 5.2.4. The extent of differences between control and metal groups were scored using the method described by

Gibson-Corley *et al.*, 2013, adapted for the evaluation of erythrocytes, platelet activation and fibrin network formation between rat and human blood.

The effects on platelets were scored as follows: Normal (-), Spreading (+), spreading with pseudopodia (++), aggregation (+++), spontaneous fibrin network formation (++++). The effects on fibrin networks were scored as follows: Normal (-), dense with fibre fusion (+), sparse (++), sparse with fibre fusion (+++), dense with fibre fusion and DMDs (++++). The effects on erythrocytes were scored as follows: Biconcave (-), elyptocyte (+), echinocyte (++), polyhedrocyte (+++), stomatocyte (++++) and erythrocyte lysis (+++++). In whole blood the fibrin network and erythrocytes were scored as above.

6.3.   <u>Results</u>

In this section the effects of Cd and Hg alone and in combination on human blood at concentrations found in blood of the *in vivo* rat model are provided. Effects on platelets are presented in Figure 6.1 while effects on the fibrin morphology and thickness are presented in Figures 6.2 – 6.6. Changes to erythrocytes are presented in Figures 6.7 – 6.10 and to the thrombus morphology in Figure 5.11. A comparison between the effects of Cd and Hg and their combination on blood obtained from the rat model and human blood is provided in Table 6.1.

6.3.1. Effects on platelets and fibrin networks
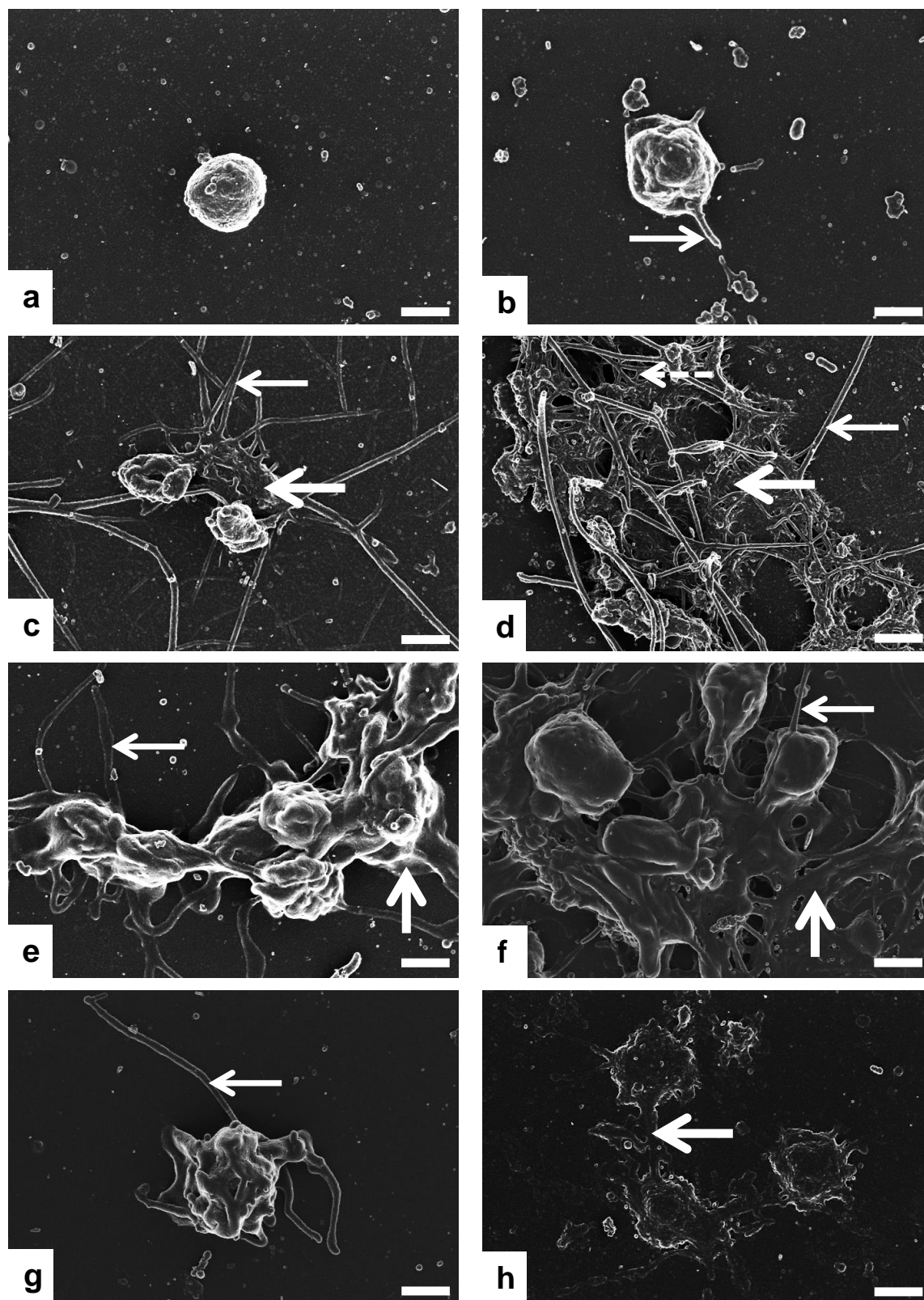
Figure 6.1: SEM micrographs of platelets prepared from PRP. (a and b) representative of the control group with no to little activation and pseudopodia formation (arrow). (c and d) representative of the Cd group with thick fibre mass in (c) (thick arrow) and fibre formation (thin arrow). (d) platelet aggregation and fibrin mass formation composed of thick fibres (thick arrow) and thin fibres (dashed arrow). (e and f) platelet aggregation with pseudopodia (arrow) and platelet spreading (thick arrow) forming a platelet mass in Hg. (g and h) platelets in the combination group with pseudopodia (arrow) in (g) and platelet spreading (thick arrow) in (h). Scale bars = 1 µm.

6.3.1.1. Platelet activation

Following exposure to Cd and Hg alone and in combination, human platelets showed varying degrees of activation (Figure 6.1). Cd induced the formation of spontaneous fibrin formation and thick fibrin masses (Figure 6.1c and d). Platelets exposed to Hg formed groups of aggregated platelets, joined together through platelet spreading, while pseudopodia as well as fibrin fibres extending from the platelet mass (Figure 6.1e and f). The combination group showed platelet activation, however it was not as extensive as was observed in the single heavy metal exposures (Figure 6.1g and h).
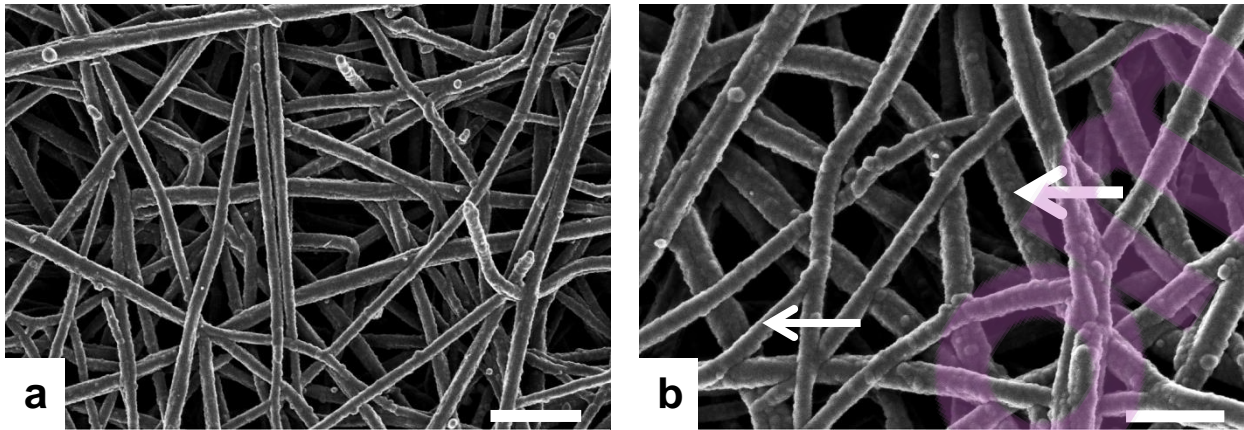
Figure 6.2: SEM micrographs of fibrin networks prepared from PRP with added thrombin from the control. (a) regular network of fibrin fibres representative of the control group. (b) large arrow indicating thick, major fibres and thin arrow indicating thin, minor fibres. Scale bars a = 1 µm b = 500 nm.
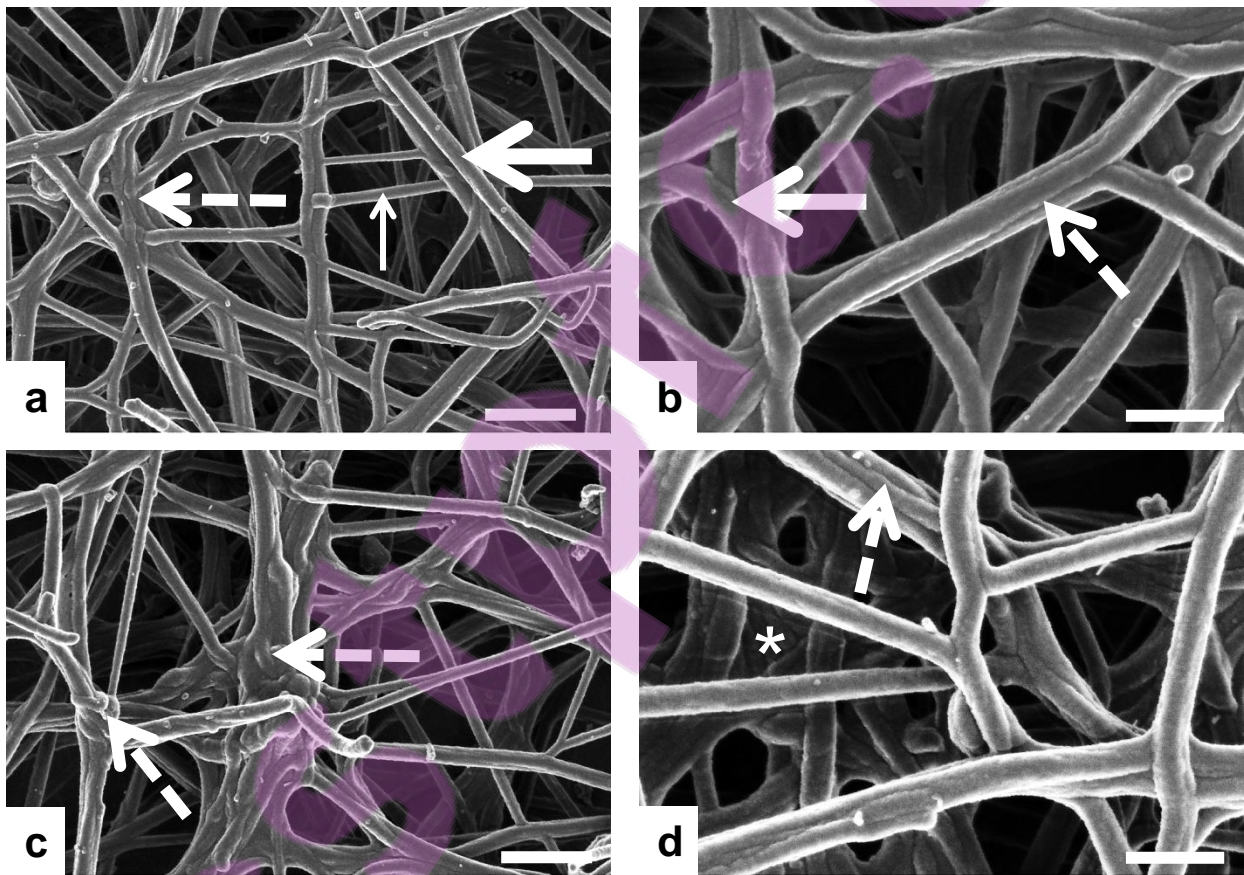
Figure 6.3: SEM micrographs of fibrin networks prepared from PRP with added thrombin from the Cd group. (a) thin (thin arrow) and thick (thick arrow) fibres present, with thick fibrin fibres aggregated to form dense fused areas visible at low magnification (dashed arrows). (b) thick fibre fusion (dashed arrow) and coiling of fibres (thick arrow). (c) thick fibres forming knot like structures where aggregated (dashed arrows). (d) thick fused fibres (dashed arrow) and densely fused areas appearing to be made of thick fibres (*). Scale bars a, c = 1 µm b, d = 500 nm.

111
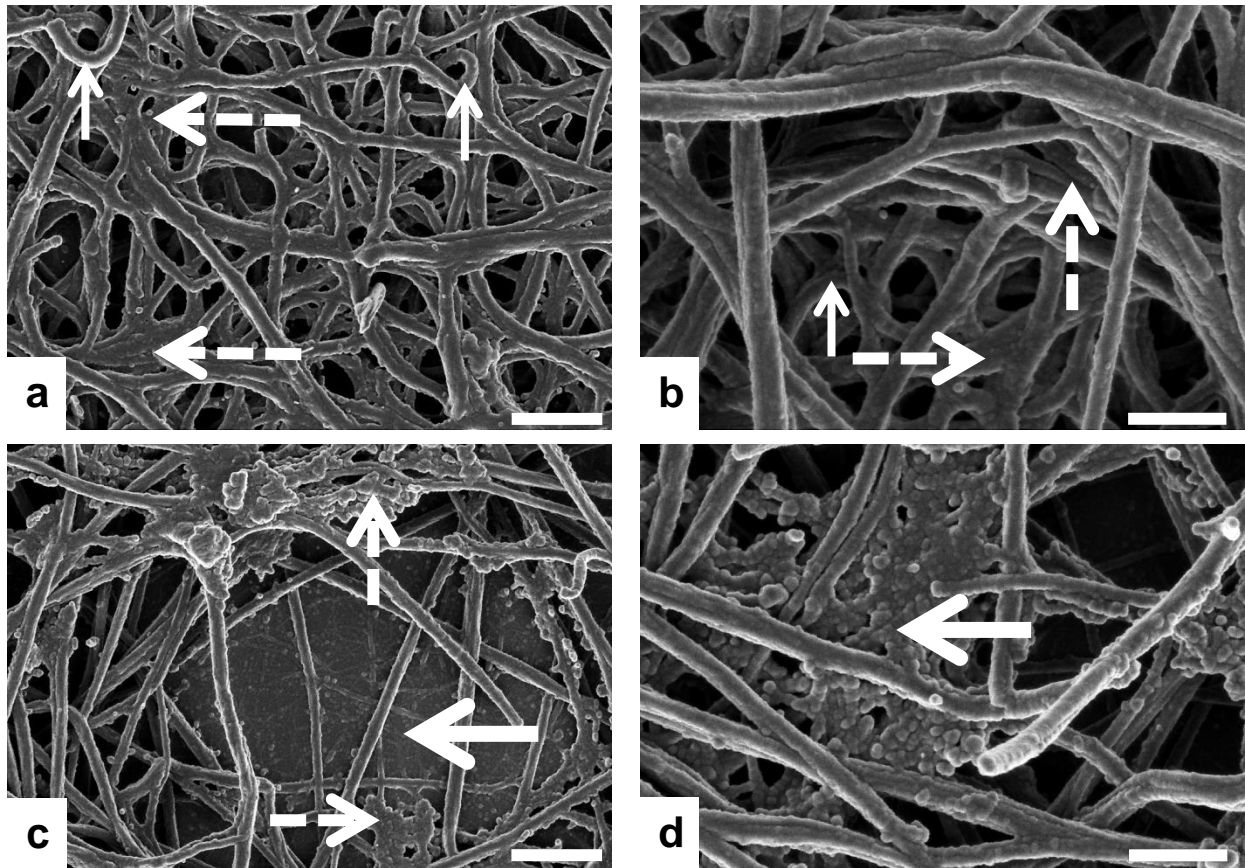
Figure 6.4: SEM micrographs of fibrin networks prepared from PRP with added thrombin from the Hg group. (a) thick fibre aggregation forming dense matted networks (dashed arrows) and coiling of fibres (arrows) and shown at higher magnification in (b), (c) slightly more sporadic fibre arrangement with smooth areas which appear to be made of thin fibres (thick arrow) and granular DMDs surrounding fibres (dashed arrow). (d) granular DMDs (thick arrow) located between fibrin fibres. Scale bars a, c = 1 μm b, d = 500 nm.
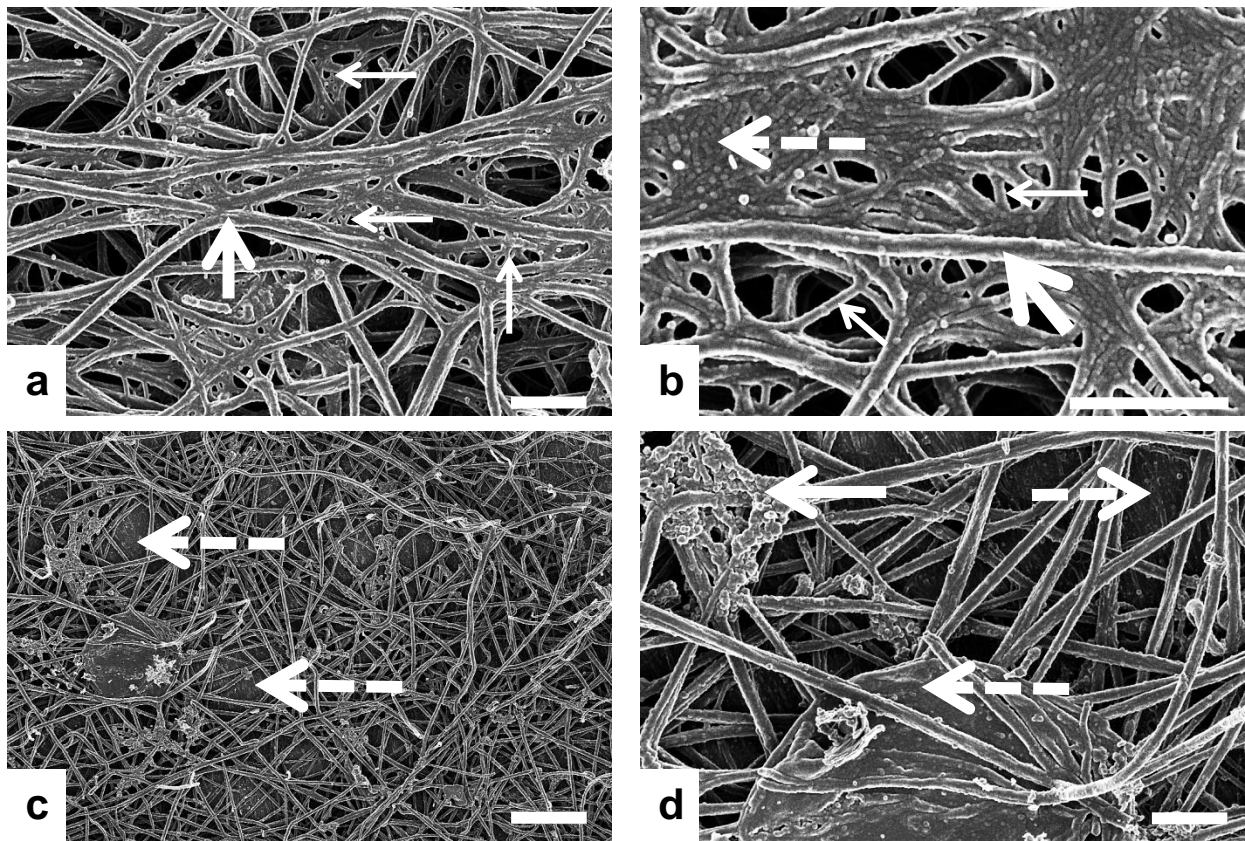
Figure 6.5: SEM micrographs of fibrin networks prepared from PRP with added thrombin from the Cd+Hg group. (a) fused masses of thick fibres (thick arrow) with net like structures connecting the thick fibres (thin arrow). (b) higher magnification shows DMDs (dashed arrow) which appear to be made of fusion of thin fibres (thin arrow) in between thick fibres (thick arrow). (c) DMDs below fibrin fibres (dashed arrows). (d) higher magnification shows DMDs fused to fibrin fibres as well as below the fibres (dashed arrows). Granulated deposits were also present around fibres (arrow). Scale bars a, b = 1 μm, c 4 μm, d 1 μm.
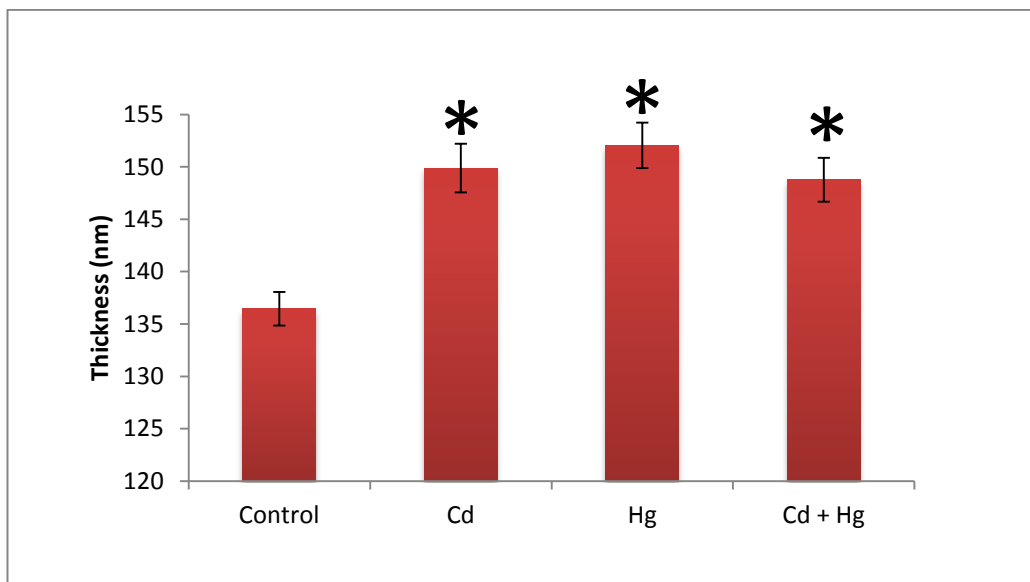
Figure 6.6: Average fibrin thickness (nm) of the control and metal exposed groups. Fibrin thickness was measured for at least 50 different fibres in each metal group and represented as an average ± SEM. *Represents significant differences compared to control, p-value ≤0.05.

6.3.1.2. Fibrin network morphology

Fibrin networks in the heavy metal exposed groups showed extreme morphological differences when compared to the control (Figure 6.2). In the Cd group dense, fused areas of fibrin were formed by thick fibres (Figure 6.3). Coiling of thick fibres as well as formation of knot like structures and densely fused and flattened masses of fibres with an overall appearance of an increase in fibre thickness were observed in the Cd exposed group. Hg induced dense matted networks when thrombin was added as well as coils in the fibre structure. The fibres in the Hg group also appeared to be fewer or sporadically formed in some areas while extremely dense in other areas. Smooth areas of fibrin deposits consisting of thin fibres were also present along with granular DMDs extending from the fibres (Figure 6.4). The combination group showed fused masses of thick fibres with a surrounding net like structure made up of thin fibrin fibres. DMDs were also observed in this group and occurred more frequently within the fibrin networks, located among the fibres, the surface as well as below the network. Granular deposits extending from the fibres were also present (Figure 6.5). Fibrin fibre thickness measurements revealed a significant difference in all three heavy metal exposure groups in comparison to the control (Figure 6.6).

6.3.2. Efffects on erythrocytes and thrombus morphology
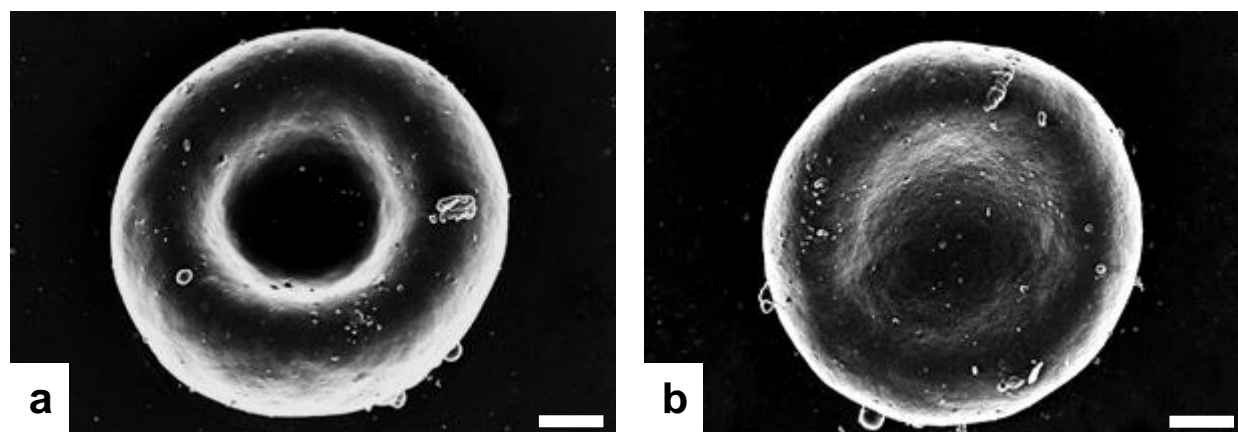
Figure 6.7: SEM micrographs of erythrocytes from the control group, (a and b) with a typical rounded appearance and a central invagination forming a biconcave shape. The plasma membranes of the cells are is smooth. Scale bars = 1 µm.
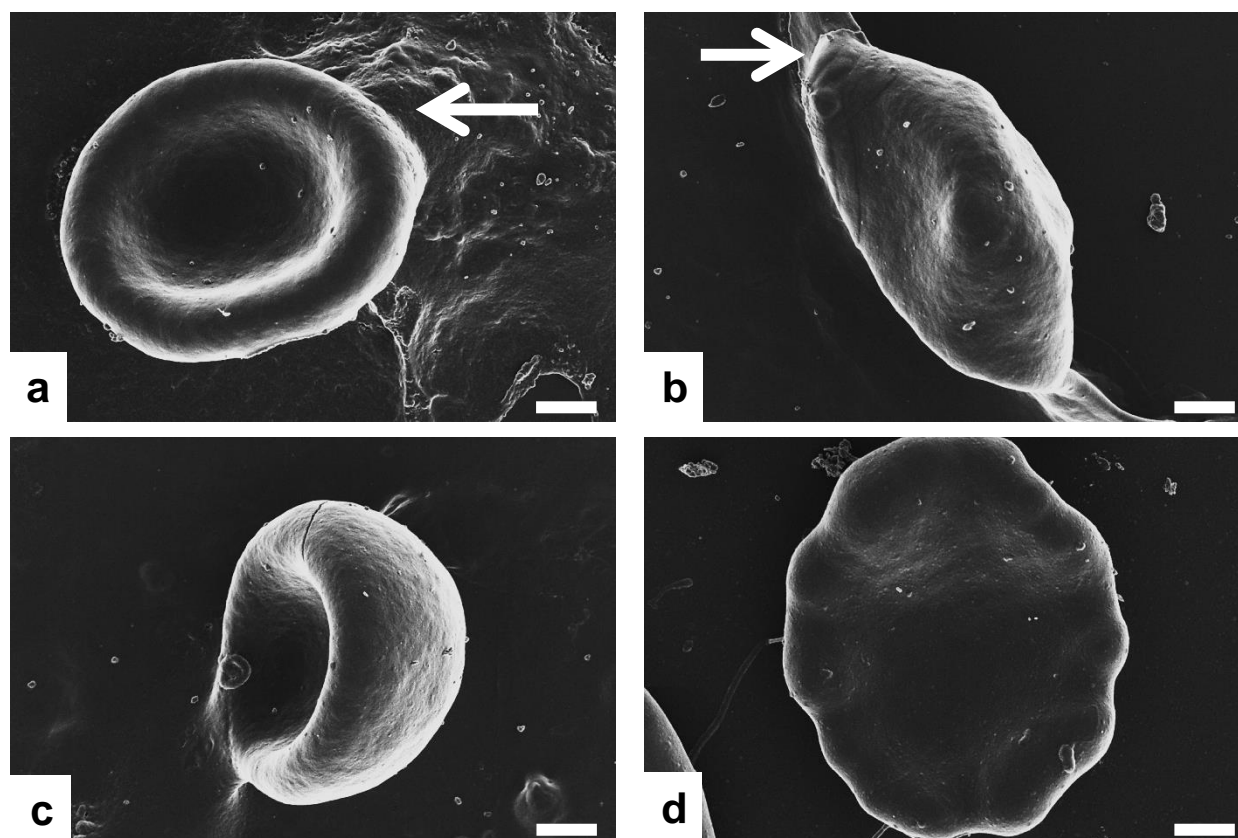
Figure 6.8: SEM micrographs of erythrocytes in the Cd exposed group showing varying and most commonly observed cell morphologies. (a) discocyte cell with irregular aggregated DMDs (arrow). (b) protein aggregates (arrow) in oval shaped cell. (c) stomatocyte and (d) elyptocyte. Scale bars = 1 µm.
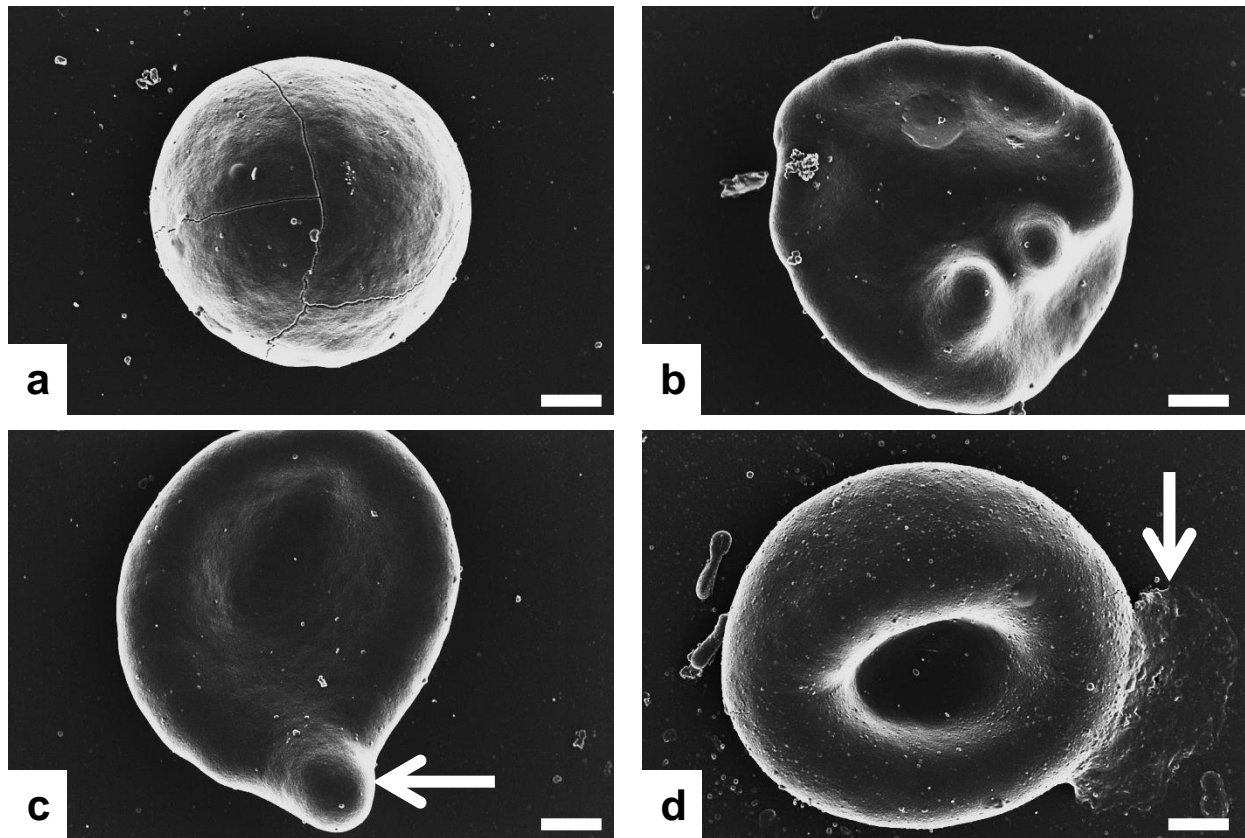
Figure 6.9: SEM micrographs of erythrocytes in Hg exposed group. Varying cell morphologies were observed. (a) spherocyte. (b) progression of elyptoid cell into eryptosis. (c) eryptotic membrane bulge (arrow) (d) protein aggregates (arrow). Scale bars = 1 μm.
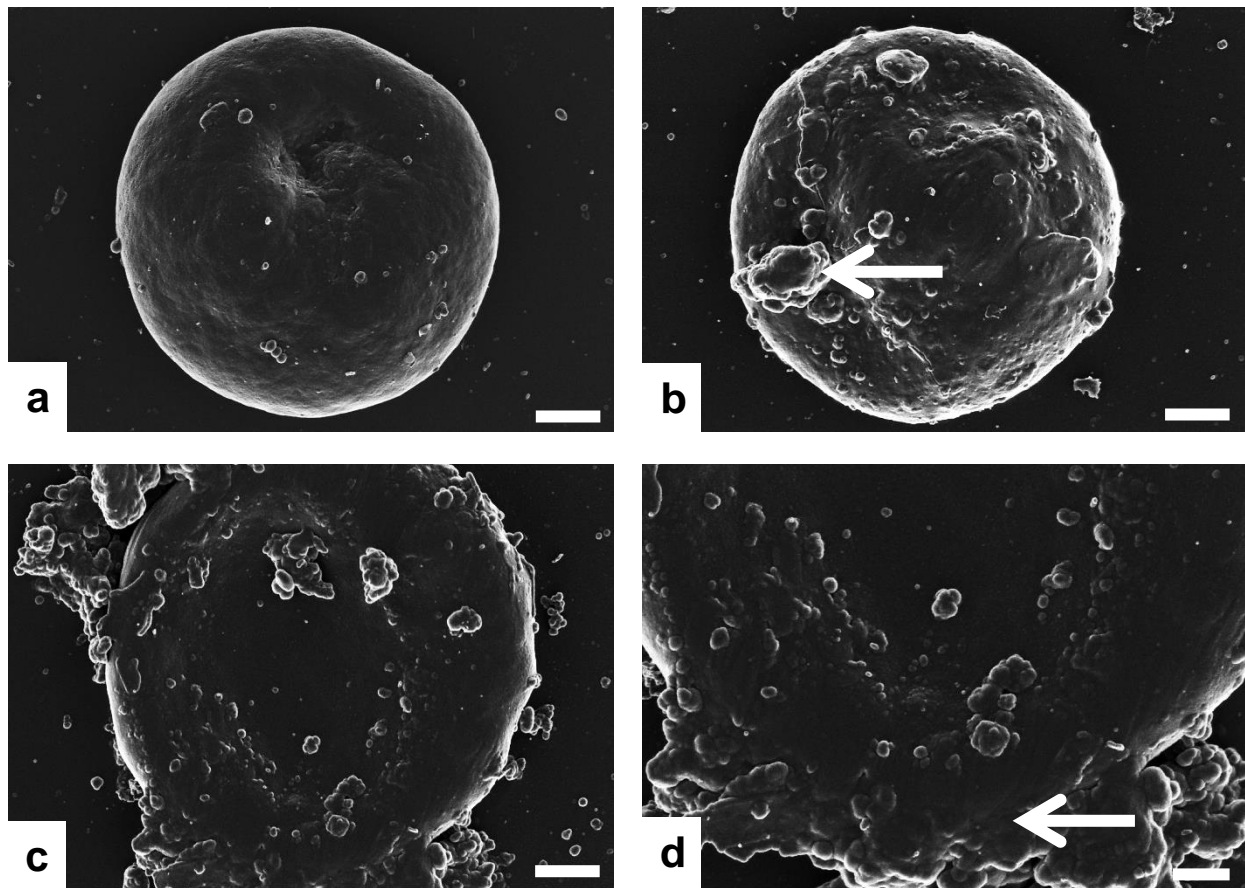
Figure 6.10: SEM micrographs of erythrocytes from the Cd+Hg exposed group showing cell membrane damage. (a) early spherocyte formation. (b) spherocyte with rough cell membrane and appearance of protein aggregates on surface (arrow). (c) erythrocyte with cell membrane rupture and intracellular protein leakage, shown in more detail in (d) (arrow). Scale bars a, b, c = 1 μm, d = 500 nm.

6.3.2.1. *Erythrocyte morphology*

Control erythrocytes had a biconcave appearance (Figure 6.7a) and a smooth cell membrane (Figure 6.7b). Erythrocyte changes in the heavy metal exposed groups consisted of a variety of shapes, including stomatocytes and elyptocytes observed in the Cd group (Figure 6.8c and d). Irregular DMD aggregates (Figure 6.8a) and protein aggregates next to the erythrocytes were also present in the Cd group (Figure 6.8b). Spherocytes and eryptotic cells were observed in the Hg group (Figure 6.9a - c). Protein aggregates on and around the cell were present (Figure 6.8d). Spherocytes were also observed in the metal combination group (Figure 6.10a), however the membrane damage in this group was most apparent, with protein aggregates forming on and around the erythrocytes as a result of intracellular protein leakage (Figure 6.10b - d).
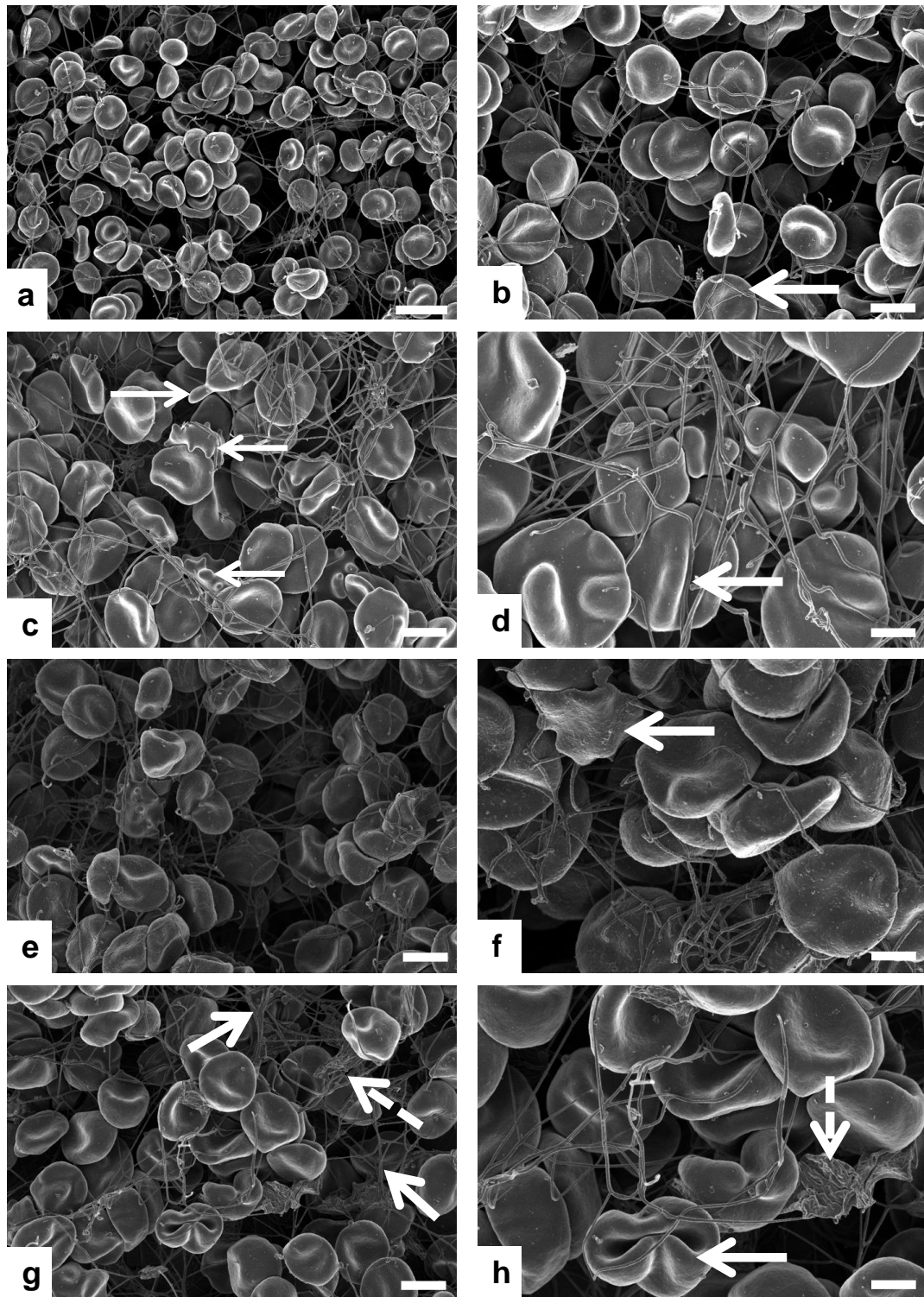
Figure 6.11: SEM micrographs of whole blood with added thrombin in order to demonstrate interactions between the fibrin networks and erythrocytes in a blood clot. (a) network composed of fine fibres and normal appearing erythrocytes in the control group. (b) interaction between erythrocytes and fibrin fibres; erythrocyte membranes maintain their shape upon contact with fibrin fibres in the control group. (c) strong fibrin fibre structure and change in erythrocyte cell shape to elyptocytes and eryptotic cells in the Cd exposed group. (d) interaction between erythrocytes and fibrin fibres where fibres distort the shape of eryptotic cells in the Cd exposed group (arrow). (e) network of fine and brittle appearing fibres in Hg exposed group. (f) presence of eryptotic erythrocytes (arrow). (g) Cd+Hg group revealed a network of thicker appearing fibres (arrows) and remnants of erythrocyte membranes (dashed arrow). (h) erythrocyte folded by the tension of the fibrin fibre (arrow) and erythrocyte plasma membrane after eryptosis (dashed arrow) in the Cd+Hg group. Scale bars a, b, c, e, g = 8 µm, d, f, g, h = 2 µm.

6.3.2.2. Thrombus morphology - Erythrocyte and fibrin interactions

Whole blood with added thrombin in the control group showed normal, biconcave erythrocytes embedded in a network of fine fibrin fibres (Figure 6.11a). The erythrocytes in the control group maintained the biconcave structure on contact with fibrin fibres (Figure 6.11b, arrow).

Whole blood with added thrombin revealed eryptotic cells in the heavy metal exposed groups as was also observed in the rat model. Strong appearing fibrin fibre structure with the presence of elyptocytes and eryptotic cells were observed in the Cd group with the thicker appearing fibrin fibres that caused distortion of the erythrocyte cell shape (Figure 6.11c and d, arrows) with the erythrocyte folding over the fibrin fibres. In the Hg exposed group (Figure 6.11e and f), the fibres appeared brittle and were broken, evident by the inability of fibres to maintain their structure in the clot (Figure 6.11e and f). Eryptotic erythrocytes were present in the Hg group (Figure 6.11f, arrow). The combination group (Figure 6.11g and h) showed a network of thicker appearing fibres (Figure 6.11g, arrows) as well as more remnants of erythrocyte cell membranes after eryptosis (Figure 6.11g and h, dashed arrows). Erythrocytes also folded against the tension of the fibrin fibres Cd+Hg group (Figure 6.11h, arrow).

6.3.3. Comparison of Cd and Hg effect on rat and human blood

The results showed an overall similar effect of the Cd and Hg alone and in combination on human blood to what was described in Section 5.3 for blood obtained from the rat model at the same concentration. Some differences in the severity of the effects exist and Table 6.1 compares the observed effects.

In the human blood model, the extent of platelet activation was greater than that observed in blood obtained from the animal model for groups exposed individually to Cd and Hg. Platelets in the Cd+Hg group appear less activated in human than in the blood obtained from the rat model. In the human blood model, exposure to Cd caused pseudopodia and spontaneous fibrin formation and in the Hg exposed human blood model, platelet aggregation was observed. In contrast, in blood obtained from the rat model only platelet spreading was observed. The combination group showed platelet activation, platelet aggregation and spontaneous formation of fibrin fibre networks in the rat blood model, while in the human blood model only the formation of pseudopodia and platelet spreading were observed.

The platelets of the Cd group (with added thrombin) presented with a network of thick, dense and knotted fibres. The greatest variation in the rat and human fibrin fibre network was observed in blood exposed to Hg. In blood obtained from the rat model the fibrin network was sparse and consisted of thin fibrin fibres, while in the human blood model the fibrin fibre morphology varied. There were areas with sparse fibres as well as areas of dense and thick fibres and DMDs. The alterations in the fibrin fibre networks on exposure to Cd+Hg were more severe in the human blood model. In blood obtained from the rat model, fibrin fibre networks were dense, with areas of fibre

fusion into knot-like structures and the presence of DMDs. In the human blood exposed to Cd+Hg the presence of DMDs and fibrin fibre fusion into dense masses appeared more extensive than in the rat blood.

Both rat and human blood exposed to Cd and Hg alone and in combination, presented with erythrocytes with a variety of different morphologies. In the Cd group, without the addition of thrombin, the effect on erythrocyte morphology was more apparent in the human blood model, with mainly elyptocyte formation and the additional presence of irregular, DMD like protein aggregates. Echinocyte were observed in the rat blood model, while stomatocytes with the presence of DMDs or protein aggregates were observed in the human blood model after Hg exposure. Cd+Hg exposure resulted in the formation of stomatocytes with some elyptocytes and echinocytes in the rat blood model, and erythrocyte lysis in the human blood model, indicating a more severe effect of both Hg and Cd+Hg presence in human blood.

Comparison of erythrocyte and fibrin fibre interactions in whole blood revealed that for Cd the fibrin structure of dense networks with fibre fusion and interactions with the erythrocytes were similar in the rat and human blood models. Rat erythrocytes showed a greater morphological alteration on Cd exposure than human erythrocytes, with the formation of echinocytes and elyptocytes respectively. Erythrocytes folded over thick and taut fibrin fibres indicating the membrane integrity of these cells are compromised. Sparse and brittle fibrin fibre networks with fibrin fusion were observed for both the rat and human blood models exposed to Hg with elyptocytes in rat and polyhedrocytes in human blood indicating a greater sensitivity of human blood to Hg. Furthermore, blood obtained from the animal model had erythrocytes folding over the fibrin fibres, indicative of a tense fibre. The same sensitivity trend was observed in Cd+Hg, where dense networks with fibre fusion and DMDs formed in both blood models with the presence of echinocytes in rat and polyhedrocytes in human blood. The fibrin fibre thickness in blood obtained from the rat model was only significantly increased in the Cd group, while in human blood, a significant increase in fibrin fibre thickness was observed for Cd and Hg alone and in combination when compared to the control.

Table 6.1: Comparison of effects of Cd and Hg alone and in combination on rat and human blood components

BLOOD LEVELS	RAT		HUMAN	
	Rat model, 28 days		*Ex vivo* human blood, 10 min exposure	
PLATELET ACTIVATION				
Control	-		-	
Cd	++		++++	
Hg	+++		++++	
Cd+Hg	++++		++	
FIBRIN NETWORK				
Control	-		-	
Cd	+*	Coiling	+*	
Hg	+++		++++*	
Cd+Hg	++++		++++*	
ERYTHROCYTES				
Control	-		-	
Cd	+		+	DMD
Hg	++		++++	DMD
Cd+Hg	++++	Some elyptocytes and echinocytes are present	+++++	
WHOLE BLOOD				
	Fibrin network	Erythrocytes	Fibrin network	Erythrocytes
Control	-	-	-	-
Cd	+	++	+	+
Hg	+++	+	+++	+++
Cd+Hg	++++	++	++++	+++

*Fibre thickness significantly different from control.

6.4.   <u>Discussion</u>

Animal models of toxicity such as the rat model implemented in this study provide important information on the uptake and blood levels of heavy metals. Following absorption, the first tissue that is exposed is the circulatory system. Cells, cell components and the proteins in blood are specific targets of toxicity (Pretorius *et al.*, 2010; Pretorius *et al.*, 2013; Pretorius *et al.*, 2017). Consequences of exposure are changes to cell morphology and blood coagulation. An *ex vivo* model can be used to further evaluate, in a human model, the effect of metal exposure on blood. This includes the effect on erythrocyte structure and blood coagulation.

Fibrin clot network alterations are associated with several diseases, including MI and diabetes, both of which are associated with the formation of atherothrombosis (Nair *et al.*, 1991; Jorreskog *et al.*, 1996). This study showed that exposure of human platelets and erythrocytes to heavy metals alters their morphological structure. Both heavy metals cause cell membrane damage to erythrocytes, to the extent of eryptosis, and also cause changes to the structure of fibrin clots as well as size of fibrin fibres. Both Cd and Hg and the combination of the two metals were found to induce a significant increase in the thickness of fibrin fibres when compared to the control.

6.4.1. Platelet activation

The effect of a single dosage of Cd and Hg alone and in combination at the same concentrations as found in the blood obtained from the rat model was evaluated. The effects of the heavy metals on blood coagulation in humans were similar to what was observed in the rat model exposed for 28 days. Some morphological differences between the human and rat model existed. In the control, as in the rat model, the platelets had a normal appearance; some instances of contact activation during processing were present. In the Cd group, where the rat model showed platelet spreading, the human model presented with pseudopodia formation as its activation feature, with spontaneous fibrin fibre formation and masses of fibrin. The effect in the Cd group in human platelets therefore appeared amplified. The effects of Cd on the human platelets were similar to a study by Venter *et al.* (2017), where the effects of the metals Cd and Cr alone and in combination on human blood at 1000x the WHO limits of water exposure were evaluated. Cd caused platelet activation and the extent of activation was similar to the rat model as well as to the effects of the *ex vivo* human blood model than that observed in the present study for blood exposed to Cd alone at 16,69 nM and in combination with Hg at 121,06 nM.

With relation to Hg, increases in cardiovascular events have been reported in Hg exposed populations with estimated blood levels of 0.05 μM. These are levels that correlate to the study done by Lim *et al.*, 2010, where procoagulant activation of erythrocytes was suggested to have a potential increase in CVD in methyl mercury or elemental mercury exposure. Levels of Hg used in the present study were 186,67 nM Hg alone and 155,99 nM in combination with Cd. Findings were that Hg induces platelet activation in human blood similarly to what was observed in platelets in

rats exposed to Hg for 28 days, with the additional feature of platelet aggregation present in the human blood as opposed to only platelet spreading. Lim *et al.* (2010) and Hounkpatin *et al.* (2012) reported Hg as having a procoagulatory effect through the increase in platelet numbers.

Cd and Hg alone caused the most platelet activation in comparison to the control group, with spontaneous fibrin formation and subsequent fibrin mass formation being the prominent feature of the Cd group, and platelet aggregation with activation being the most prominent feature of the Hg group. Both metals in combination, in human blood, caused a spontaneous formation of fibrin fibres, while the metals have a lesser effect on the activation of platelets and spontaneous fibrin formation (Figure 6.1). Platelet activation observed in serum without the addition of thrombin is an indication of fast initiation of the coagulation process, but a lower fibrin build up time, resulting in reduced cross linking and fragile and less stable blood clots (Venter *et al.*, 2017).

6.4.2. Fibrin network morphology

Extreme morphological alterations were observed in the fibrin fibres of metal exposed groups. Dense and fused fibrin was observed in the Cd exposed groups, along with fibre coiling (Figure 6.3). Compared to the study of Venter *et al.* 2015, the fibrin network that formed with Cd exposure had similar structural features. On exposure to Hg, coiling and DMDs were observed in the fibrin fibres. However, in some areas the fibres in the Hg group appeared to be fewer and sporadic. The combination group showed a large deposition of DMDs which was more prominent than in the other groups. The morphology for the Cd and Cd and Hg groups in human blood were similar to the blood obtained from the rat model exposed to the heavy metals for 28 days, with what appears to be a slight amplification of the effect in the human blood. The Hg group on the other hand had a great variation between the morphologies of the two blood models. The blood obtained from the rat model exposed to Hg for 28 days showed sparsely distributed and fine fibres of fibrin while in human blood, fibrin morphology varied in the samples, and both thin sparse areas of fibrin formation and thick and dense fibrin fibres were present along with DMDs.

Findings in the Cd exposed group were similar to that seen in a study that evaluated the effects of smoking on fibrin fibre formation (Pretorius *et al.*, 2010) and may be due to the presence of Cd in cigarette smoke. Studies have shown that cigarette smoke exposure affects platelet function (Rival *et al.*, 1987; Blache, 1995; Fusegawa *et al.*, 1999) and platelets isolated from smokers have been shown to have increased aggregation compared to non-smokers (Fusegawa *et al*, 1999).

Fibrinogen has been identified as the primary oxidized protein in the plasma of smokers. The most common alteration is the formation of two 3-nitrotyrosine, which increases fibrin polymerisation and turbidity while fibrin clot lysis is reduced. The identified viscoelastic properties that occur as a result of this oxidation are increased stiffness and viscosity with the formation of increased fibre clusters (Martinez *et al.* 2013). The findings of this study were therefore similar to previous literature, in that

123

compared to the control, the thickness of the Cd fibrin fibres was increased suggesting that Cd has a procoagulatory effect.

The significant increase in fibre thickness in Cd, Hg and Cd+Hg groups will further contribute to the alterations of the erythrocytes and clot formation, as it might cause a reduction in the lysis of the clots (Swanepoel *et al.*, 2016). Pathological thrombi can be caused by platelet activation as a result of oxidative stress and inflammation (Freedman, 2008; van Rooy and Pretorius, 2015; van Rooy *et al.*, 2015). Functional changes to the platelets or a decrease in thrombin production during the coagulation cascade may also occur due to ROS (van Rooy *et al.*, 2015). Fibrin networks act as a template for further clot development and the properties of the fibrin clot would therefore determine the clots' physical properties as discussed in Chapter 5. The alteration in fibre thickness can be due to the transition of the fibres α-helices into β-sheets and protein aggregation (Kell and Pretorius, 2017). Fibrin fibres consist of a combination of α-helices, β-sheets and turns, loops and random coils which contributes to the normal structure and function of the fibrin fibres (Kell and Pretorius, 2017).

Heavy metals such as Cd, Hg, Cr and Fe, deplete calcium ion levels in tissue (Swanepoel *et al.*, 2015). Calcium is an important factor in the coagulation cascade as it allows for thrombin and thrombin catalysed factor (fXIII) formation, in turn catalysing the formation of fibrin from fibrinogen and stabilise the fibrin fibres (Kell and Pretorius, 2017). Inhibition of this process will result in a in a fragile, less-stable clot. A study on the effects of Cd and Cr on the viscoelastic traces by TEG® which is used to evaluate whole blood coagulation in trauma care (Bolliger *et al.*, 2012), showed that minor, but not statistically significant, changes occurred to the measured parameters (Venter *et al.*, 2017). The results showed a delayed fibrin formation but with clot formation process being rapid once it starts. Venter *et al.* (2017) reported a decrease in clot strength in Cd and Cr exposed blood, as platelet-fibrinogen interactions are decreased and with less taut fibre appearance when viewed with SEM. The time for clot formation was also increased as assessed by TEG®, the slower clot formation causing structurally unstable/ weaker clots. The structurally weaker clots, with poor fibrinolytic susceptibility are concerning to CVS function, as their potential for detachment and subsequent thrombosis is increased.

Clinically, fibrin has been reported to be a component of atherosclerotic plaques, promoting their growth (Thompson and Smith, 1989; Mosesson *et al.*, 2001). Lower clot permeability has been reported in patients with venous thromboembolism as well as in their relatives, and fibrin properties have been suggested to be a major risk factor for thrombosis (Undas *et al.*, 2009). Altered fibrin clot structures have also been reported in relatives of patients with premature coronary artery disease (CAD) (Mills *et al.*, 2002).

Severe coronary artery disease patients have more rigid clot structures and elevated fibre mass-to-length ratios (Mills *et al.*, 2002). Abnormal structure of *ex vivo* fibrin clots is also observed in first degree relatives of patients with premature CAD. Clots display thicker, less porous fibrin fibres and

begin polymerisation at a faster rate than in non-CAD individuals (Mills *et al.*, 2002). Tight rigid and space filling fibrin network structures with small pores are associated with premature coronary artery syndrome (Fatah *et al.*, 1992; Collet *et al.*, 2006). In a study by Undas *et al.*, 2008, adverse clot properties were apparent in CAD patients despite aspirin administration. Aspirin is known to increase clot permeability and increase fibrinolysis (Scott *et al.*, 2004; Undas and Zeglin, 2006). Lower clot permeability has been reported in patients with venous thromboembolism as well as in their relatives, and fibrin properties have been suggested to be a major risk factor for thrombosis (Undas *et al.*, 2009). These effects are suggested to not occur in ACS due to processes triggered by vascular injury such as platelet activation, free radical formation and stimulation of inflammation. Patients with severe CAD have shown to have more rigid clot structures despite aspirin therapy (Grielich e*t al.*, 1994). These findings are consistent with those on MI (Fatah *et al.*, 1992; Fatah *et al.*, 1996). Thrombosis is often responsible for MI and sudden cardiac death and cigarette smoke exposure is known to increase the risk for these events as exposure to cigarette smoke is suggested to lead to a hypercoagulable state (Barua *et al.*, 2002; Barua *et al.*, 2003; Ambrose and Barua, 2004). Likewise exposure to metals such as Cd and Hg can also have an adverse effect on the CVS.

6.4.3. Erythrocytes and thrombus morphology

The study of blood morphology, more specifically clot microstructure, has been suggested in the risk stratification of patients with CAD and MI (Sabra *et al.*, 2014; Sabra *et al.*, 2018). Erythrocyte changes in the heavy metal exposed groups consisted of a variety of shapes, including stomatocytes and elyptocytes as observed in the Cd group. Protein leakage from the cells as a result of membrane rupture was also present in the Cd group (Figure 6.8). Spherocytes and eryptotic cells were observed in the Hg group together with intracellular protein leakage, indicative of membrane rupture. The Cd+Hg group showed the most membrane damage and rupture, as well as the presence of spherocytes. These results differed from the blood obtained from the rat model exposed for 28 days, as the erythrocyte shapes were more consistent with damage to the cell membranes and only the Hg group showed cell rupture. The human blood also did not have any spontaneous fibrin fibre formation prior to the addition of thrombin.

WB exposed to thrombin revealed elyptocytes and eryptotic cells in heavy metal exposed groups (Figure 6.10) similarly to the blood of rats exposed to the heavy metals for 28 days. Elyptocytes and eryptotic cells were observed in the Cd group, and thicker appearing fibrin fibres distorting the cell shapes, similarly to blood obtained from the rat model. Again, the major difference between blood obtained from the rat model and human blood was in the Hg group, where in the human blood the fibres appeared brittle and cells were eryptotic, with erythrocyte remnants, while in the blood obtained from the rat model the erythrocytes folded over the fibrin fibres (Figure 6.10h). Erythrocyte entrapment in fibrin networks and cell shape changes due to fibrin pressure on already stressed cells was shown previously by (Pretorius, 2013). The interaction between fibrin fibres and

erythrocytes in the Cd+Hg group in both human blood and blood obtained from the rat model was similar, with erythrocytes folding over tense fibres.

The human blood model showed changes in platelet activation, fibrin fibre and erythrocyte structure similar to what has been observed in Chapter 5 in the blood obtained from the rat model exposed to the heavy metals and their combination for 28 days. The thickness of fibrin fibres had a significant increase in the human blood in all of the metal exposure groups whereas the blood obtained from the rat model, although showing an increase in thickness, was only significant for the Cd group when compared to control. The pattern of Hg effects is similar although more pronounced in the human blood. The effects of the metals based on morphological/ observable and non-quantifiable parameters, appear to be more pronounced in the human blood. These differences may be attributed to differences between species, and also to the subacute *in vivo* model having the potential for some degree of systemic antioxidant function, and a resultant blunting of the toxicity of the two metals, which is not present in an *ex vivo* acute model. Oxidative effects of Cd have been suggested to be immediate (Tandon *et al.*, 2001) and therefore over time, in an *in vivo* model, antioxidant mechanisms may have reduced the damage, as observed in erythrocytes of rat vs. human at the same concentrations. As the coagulation process for both experiments was initiated *ex vivo* with direct addition of thrombin, it is difficult to evaluate the entire clotting factor cascade, although the results do give an indication of the end product.

It is important to note that conflicting opinions exist when it comes to animal modelling of human diseases. In this particular context, this study is used not to predict effects but to identify possible targets of the heavy metal effects on the CVS. The study has identified a need for more detailed analysis of human exposure to heavy metals, not only limited to physiological symptoms and biochemical markers, but structural alterations to identify pathological processes.

The oxidation mechanisms of Cd and Hg explained in Chapter 5 would apply to this model as well. Cd binds sulfhydryl groups of proteins and GSH and especially GSH depletion results in increased production of ROS such as H_2O_2, superoxide anion and hydroxyl radical (Stohs and Bagchi, 1995; Bertin and Averbeck, 2006; Hu *et al.*, 2016; Genchi *et al.*, 2017). Heavy metals induce ROS formation and impair the antioxidant capacity of erythrocytes (Husain and Mahmood, 2017). Hg strongly binds GSH and catalyses the Fenton reaction and a study showed it to be the most toxic in a series of metals tested (Uys, 2016). Catalysts of the Fenton reaction have been shown to increase ROS formation and alter erythrocyte membrane fluidity as a result. The altered membrane fluidity results in more fragile and less osmotic resistant erythrocytes (Stohs and Bagchi, 1995; Hussain and Mahmood, 2017).

The average life span of circulating erythrocytes usually exceeds one hundred days. Prior to that, however, erythrocytes may be exposed to oxidative stress in the circulation which could cause injury and trigger their suicidal death or eryptosis. Oxidative stress activates Ca^{2+}-permeable non-selective cation channels in the cell membrane, thus, stimulating Ca^{2+} entry and subsequent cell

membrane scrambling resulting in PS exposure and activation of Ca^{2+}-sensitive K^+ channels leading to K^+ exit, hyperpolarization, chloride -exit, and ultimately cell shrinkage due to loss of KCl and osmotically driven water. Recent evidence shows that oxidative stress is a feature of many diseases, such as diabetes and hepatic and renal disease and the effect of oxidative stress is accelerated by erythrocyte loss, an underlying mechanism for anaemia associated with these pathologies (Bissinger *et al.*, 2018).

6.4.4. Relevance of morphological findings in human population

In previous studies up to 80% correlation between rat and human studies has been described for cardiovascular modelling in toxicology studies investigated in a pharmacological context of drug effects/toxicity. Furthermore, a hematologic correlation of 91% between rodent and human studies has been shown (Olson *et al.*, 2000).

Hg has been shown to affect blood pressure in environmentally exposed populations in Brazil (Fillion *et al.*, 2006), as well as blood pressure and autonomic activity in indigenous populations of Canada (Valera *et al.*, 2008, 2009, 2011 - 2013). Hg has also been shown to affect blood pressure in children (Thurston *et al.*, 2007). Likewise, Cd has been shown to induce vascular dysfunction contributing to hypertension (Kukongviriyapan *et al.*, 2014).

A lowered risk of CVD is often reported with a higher quality lifestyle and diet (Reedy *et al.*, 2014), but a study on a Haitian population exposed to heavy metals showed no indication of lifestyle and diet influence in preventing the harmful effect and hypertension after heavy metal exposure. Instead, the age associated hypertension in Haiti was at least as high as those of developed countries leading less favourable lifestyles (Polsinelli *et al.*, 2017). A relationship between Cd body burden and increased blood pressure in American Indians, a population with increased CVD risk was recently established. The Cd exposure of this population was primarily environmental and occupational (Franceschini *et al.*, 2017). A study on mining populations living in mining areas in Papua New Guinea reported that hypertension was a key risk factor for noncommunicable disease development. A need for workplace health has been identified due to these risk factors (Rodriguez-Fernandez *et al.*, 2015).

Differences in blood pressure between African American and Caucasian populations have long been observed (Gillum, 1979). As early as 1932 data suggested elevated blood pressure in black populations (Adams, 1932). Highest prevalence of hypertension was reported in African adult populations (WHO, 2011), while the same population showed a two-fold risk of stroke in South Africans (Jones *et al.*, 2017). Hendry *et al.*, 2018 studied the genetics of blood pressure on South African individuals in order to accurately represent an African population, as opposed to African Americans. Hypertension has therefore been identified as one of the diseases with a genetic influence in African populations as compared to populations of European descent. This

predisposition includes a difference of exposure to environmental risk from 46-68% (Tishkoff and Williams, 2002).

The morphological changes in the heart and blood vessels after exposure to Cd and Hg reported in this study are consistent with premature CVS ageing and may have a possible effect on blood pressure and may have serious implications for the South African population.

6.4.5. Arterial structure and coagulation interaction

The key features observed in the present study were the degeneration of cardiac muscle, neointimal plaque formation and altered coagulation properties in the heavy metal exposed groups, along with alterations to blood vessels, which may affect regulation of blood pressure, causing premature vascular ageing and hypertension.

Isolated systolic hypertension (ISH) has been bi-directionally associated with central arterial stiffness. The aorta's main function is to dampen the pulsatile flow generated during left ventricular contraction. For this purpose, the aorta needs to be at an optimum mechanical conformation to maintain this structure through maintenance of a regular flow and also minimise cardiac work. Even small alterations to hemodynamic and arterial structure would affect the components necessary to maintain optimum blood flow and pressure. Changes to the mechanical properties of the aorta in ageing are complex and vary in early and advanced remodelling (Al Ghatrif and Lakatta, 2015), although the interactions in arterial structure and blood flow maintain their importance. More importantly ISH is not limited to older individuals, with hypertension risk being an emerging cardiovascular concern in adolescents and young adults (Sorof *et al.*, 2002; Mallion *et al.*, 2003; McEniery *et al.*, 2005; McEniery *et al.*, 2016). ISH has the potential to be aggravated by environmental exposure to heavy metals and a premature vascular ageing and in disease state has been associated with hypertension in children (Gerhard-Herman *et al.*, 2012).

Interactions between blood flow i.e. fluid dynamics and endothelium play a role in arterial remodelling as has been shown for the process of atherogenesis (Giddens *et al.*, 1993; Traub and Berk, 1998). Sheer stress on the endothelium caused by fluid flow is able to induce structural changes in endothelial cells and this has been observed in cell culture studies, and also has the ability to influence vascular function including the production of NO and intimal thickening (Rubanyi *et al.*, 1986; Traub and Berk, 1998). Areas with a low sheer stress and non-laminar flow – as is found around the aortic arch are prone to more endothelial damage and dysfunction. These factors have been implicated in the progression of atherosclerosis. The results of this study showed a change in the layers of blood vessels and similar changes have been reported for exposure to iron (Eckly *et al.*, 2011). The authors described this change as a contributor to arterial thrombosis as it disrupts the smoothness of the tunica intima in contact with the flowing blood, causing attachment to and activation of platelets. The neointimal formation observed in the present study, along with alterations in coagulation, are similar to the factors associated with atherosclerotic progression. It is

hypothesised that these features will further influence one another in the creation of excessive thrombosis and vascular occlusion. Neointimal formation may cause fibrin activation due to blood flow interruptions. In extensive stenosed conditions, the blood flow immediately distal to a severe atherosclerotic lesion may be significantly disturbed and possibly turbulent, promoting the formation of a fibrin-rich thrombus (Hutchison *et al.*, 1985; Sakariassen *et al.,* 2015). Similarly projections of the neointimal massed into the vascular lumen may cause the same effect. Thrombus formation involves platelet activation and the release of various growth factors, amongst which PDGFA is involved in plaque formation through the induction of VSMC proliferation (Wan *et al.*, 2018). These interactions may create a cycle of activation, abnormal proliferation and associated pathology.

6.5.   <u>Conclusion</u>

Cd and Hg alone and in combination caused eryptosis and alterations in coagulation and erythrocyte and fibrin fibre interactions in the *ex vivo* human blood model. Human platelet activation was present with a significant increase in the thickness of the fibrin fibres and aggregation as well as formation of dense matted deposits, increasing the thrombotic tendency. Exposure to Cd and Hg alone and in combination also caused erythrocyte cell membrane rupture consistent with eryptosis in all of the heavy metal exposed groups. The degree of platelet activation and changes to the morphology of erythrocytes were similar to that found in the rat animal model, which indicates that the *ex vivo* blood model will provide important, although indirect information on the effects of exposure on the blood vascular system in humans exposed to these metals. This can be used as a screening method for heavy metal toxicity prior to animal studies and can also be used to determine possible risk in exposed populations.

Chapter 7: Conclusion

7.1. Introduction

In the last several decades, an important rise in cardiovascular and other NCCDs burden has been documented particularly in developing low- and middle-income countries (Levenson *et al.,* 2002; WHO 2011a, Mendis and Alwan, 2011; Moran *et al.*, 2014; Barquera *et al.*, 2015). The prevalence of cardiovascular risk factors is high in South Africa specifically, with a report of 56% of patients diagnosed with hypertension and 54% with heart failure. CVD is also the second most common cause of death in South Africa (Peer *et al.*, 2008). Populations specifically in the Limpopo province had hypertension prevalence of 25.5% in women and 21.6% in men (Alberts *et al.*, 2005). Mine water contamination and consequent exposure to heavy metals as well as exposure through cigarette smoke may aggravate these cardiovascular conditions.

South Africans living in areas of mining and industrial activity are continuously being exposed to heavy metal pollutants and many of these metals are found in water which is used for drinking, cooking and washing as well as drinking water for livestock and the irrigation of crops. Water levels of heavy metals are often far beyond the acceptable levels for exposure established by the WHO. Exposure is never limited to a single metal but rather a mixture of metals that daily vary in concentrations and may be from multiple sources. In an attempt to understand these effects two metals, Cd and Hg were selected based on their high risk for exposure.

Many studies have been undertaken to determine the tissue and organ toxicity of a single dosage of Cd and Hg (Bernhoft 2013; Agrawal *et al.*, 2014; Celikoglu *et al.*, 2015; Schumacher and Abbot, 2017). These studies usually focus on the effect on the liver, kidney and reproductive system. These rat models represent acute exposure and provide very little information on longer exposure times to Cd and Hg alone or in combination. This study has attempted to address this lack of knowledge by exposing rats to Cd and Hg alone and in combination to levels 1000x the WHO safety guidelines for drinking water. Human exposure dosages were converted to equivalent dosages in rats and exposure via gavage was of 28 days that represents equivalent human exposure of three years.

7.2. Key findings

A Sprague-Dawley rat model was established for a 28 day exposure period to investigate the effects of Cd and Hg alone and in combination at a daily dose of 1000x the WHO safety limits for water consumption (WHO, 2011). Successful absorption of the heavy metals was confirmed by the presence of Cd and Hg in the blood without a significant change in weight, organ/weight ratio and markers of tissue damage. Furthermore, levels measured in the blood were similar to that found in the blood of populations exposed to Cd (Mortada *et al.*, 2002; Röllin *et al.*, 2009; Barregard *et al.*, 2016) and represented the upper limits of environmental Hg exposure.

Blood levels of ALT, AST, urea, glucose, TP and globulin remained unchanged. The albumin levels showed a significant increase in the Cd exposed group and were decreased in the Cd+Hg group, while AP levels were significantly lower for both groups. Creatinine levels were lower in all experimental groups but were only significantly lower in the Cd+Hg group when compared to the control and Cd groups. Na^+ levels were lower in the Cd+Hg group while K^+ levels were elevated in the Cd+Hg and decreased in Cd groups. These changes indicate some damage to the renal endothelium and filtration as well as to the erythrocytes. Although some significant changes in the blood parameters were observed, these could easily be overlooked in a clinical setting, but may still have a negative effect on the organ.

Cd and Hg alone and in combination caused mitochondrial damage and myofibrillar necrosis, increased fibrosis and presence of lipid within the myocardium. The Cd+Hg exposed myocardium showed the most prominent changes within the myocardium. In the aortas, Cd caused alterations in elastin, with interruptions of elastin lamella by collagen deposition. Hg alone and in combination with Cd caused elastin fibrillation and collagen deposition as well as VSMC proliferation and migration into the tunica intima, resulting in nonatherosclerotic neointimal plaque formation. The structural alterations to the aorta were the most prominent in Cd+Hg exposed rats. Observed structural changes correlated with a phenotype of premature aging of the CVS.

Evaluation of the blood vascular effects of Cd and Hg alone and in combination on blood morphology showed increased platelet activation. Cd increases the thickness of the fibrin fibres, causes fibrin aggregation and the formation of flat, fused areas. Hg caused a decrease in fibre formation and while in combination, the metals caused the formation of a dense fibrin fibre network with an extensive presence of matted deposits between the fibres, with no changes to the actual fibrin thickness. In WB the interaction of erythrocytes and fibrin fibres caused changes in erythrocyte morphology and fibrin network structure. Findings were that Hg enhances the effect of Cd on coagulation, forming a dense, yet structurally fragile or unstable thrombus. These findings suggest that these metals induce a prothrombotic blood environment that together with vascular remodelling might increase the risk for CVD and stroke.

7.3. Relevance of findings

This study provided preliminary data that confirms the toxicity of Cd and Hg alone and in combination. This study identified that the CVS is an important target of toxicity, where physiologically relevant levels of these metals induce structural changes to the CVS that presents with a phenotype of premature aging and consequently an increased risk for CVD and stroke. This study also identified the limitations of standard tests used for toxicity. The use of an *ex vivo*, human blood model to evaluate the toxicity of these metals was found to be relevant and reproduce several effects observed in the rat model. This study confirmed the relevance of such a model for the initial evaluation of heavy metal toxicity prior to animal studies.

7.4.   <u>Limitations and future recommendations</u>

Findings of this study were that the CVS is adversely affected when exposed to Cd and Hg alone and in combination. Changes in collagen and elastin distribution and structure, indicated that an increase in aortal stiffness can cause an increase in blood pressure. A limitation of the present study was that blood pressure was not determined. In future studies it would be of value to establish whether the reported morphological changes do affect blood pressure. The use of non-invasive blood pressure measurements with photoplethysmography, piezoplethmysmography and volume pressure recordings, as well as a recently suggested affordable instrumentation of pulse transducer with physiograph and a rat tail cuff (Allen, 2007; Gangwar *et al.*, 2014) will allow the evaluation of rat blood pressure throughout the study period and will provide important information on the consequence of vascular damage. Future studies should also evaluate the effects of lower concentrations so that a threshold value for toxicity can be calculated. This is the concentration of each metal in drinking water that does not cause CVD after an extended period of exposure.

Several studies have identified that oxidative stress is a common mode of action in heavy metal toxicity. A limitation of the present study was that these effects were not investigated. In future studies the effect of these metals on the antioxidant status of blood and the effect on AOx should be investigated. This can be achieved by measuring the total antioxidant capacity (TAC) of blood. Ciuti and Liguri, (2017) described a new photometric method which enables the measurement of TAC in WB based on a two electrons reduction of the chromogen 2,6-dichlorophenolindophenol (DCPIP), allowing a reaction with most blood antioxidants including GSH. This provides an overall indication of the redox equilibrium within a sample and is not influenced by the presence of Hb (Ciuti and Liguri, 2017). Levels of the enzymes of SOD, CAT, GSH and GPx can be individually determined in erythrocytes and in cardiac tissue. Likewise, eNOS and iNOS levels in the aorta, relative to the control, can be determined using Western blotting (Li *et al.*, 2007).

This study investigated the effect of Cd and Hg alone and in combination on the morphology of cardiac and aorta tissue as well as erythrocytes and platelet morphology. SEM only provides qualitative data and not quantitative data. The extent of myocyte degeneration can be quantified using confocal fluorescence microscopy by using α-actin–labelled antibody. Using DAPI staining the percentage labelled myocytes can be calculated. Likewise, the myocyte cross-sectional and longitudinal cell areas can be determined following vinculin-staining of the cardiac sections. Using fibronectin-stained sections the extent of the fibrosis can be quantified and can be expressed as percentage of total myocardium. Cellular death in tissue sections such as cardiac tissue can be quantified by determining the number of ubiquitin-, C9-, and TUNEL-positive cells using fluorescence confocal microscopy of each tissue section. The eryptosis can be evaluated in erythrocytes and platelets with flow cytometry. The PS externalisation or flip that occurs during eryptosis can be measured using a flourochrome conjugated to Annexin-V. Annexin-V binding to erythrocyte membrane can then be quantified with flow cytometry. The levels of intracellular Ca^{2+}

levels, an initiating factor for eryptosis and the PS flip may be quantified using fluo-3 acetoxymethyl hydrolysis as a marker. The levels of reduced GSH abundance using 5-chloromethylflorescein diacetate (5-CMFAD) as a marker (Pretorius *et al.* 2016).

Like cardiac muscle, skeletal muscle is rich in mitochondria and has a similar mode of contraction. It can therefore be speculated that skeletal muscle is also vulnerable to the effects of heavy metals, and therefore in future animal studies skeletal muscle should be collected and evaluated as was described for cardiac muscle.

A limitation is that this study involves an animal model exposed to Cd and Hg alone and in combination under controlled conditions and involved fixed concentrations of each metal and exposure time. This poorly reflects reality where exposure in humans involves mixtures of metals at different concentrations. In addition, other factors such as age, sex, genetics and nutritional status all impacts on the effects of heavy metals in humans. Future studies in exposed populations must first identify specific metals in the water sources before the levels of these metals can be measured in a consenting exposed population. The effects on blood pressure, the antioxidant capacity and coagulation parameters of blood can then be determined. Evaluation of femoral pulse wave velocity would give indications of arterial stiffness (Millasseau *et al.*, 2005), while ECG may give an indication on the effects of the heavy metals on the functionality of the CVS (Hayward *et al.*, 2011; Galrinho *et al.*, 2015).

Blood coagulation parameters can be quantified with TEG® (Venter *et al.*, 2017) and the levels of associated coagulation factors such as fXIII can be quantified with the enzyme-linked immunoabsorbent assay (ELISA) (Matsuura *et al.*, 2016). Creating clots in suspension and then fracturing, as opposed to coating on a coverslip would give a better indication of clot formation in fluid suspension (i.e. in blood) and give an indication of the interactions of clot components with each other and extent of clot contracture. Fractal dimension measurement of blood clots as in CAD may potentially be used as a biomarker for heavy metal induced oxidative stress or risk (Sabra *et al.*, 2018).

The liver and kidney, after exposure to low doses of Cd have been shown to recover (Alkushi *et al.*, 2018). In contrast the heart has a low regeneration capacity, while the ability of blood vessels to recover from the effects of heavy metals is unknown. The ability of the CVS to recover, from the insult of heavy metal will be an interesting area of future research.

Once the adverse effects of exposure to heavy metals have been identified in exposed populations, interventions can be developed which will reduce environmental exposure and nutritional intervention such as increasing polyphenol intake for both Cd and Hg (Passos *et al.*, 2007; Watkins *et al.*, 2007; Hamden *et al.*, 2008; Agarwala *et al.*, 2012; Yang *et al.*, 2012; Necib *et al.*, 2013; García-Niño and Pedraza-Chaverrí, 2014; Kukongviriyapan *et al.*, 2014; Zhai *et al.*, 2015; Ramakrishnan *et al.*, 2017; Wani *et al.*, 2017; Imafidon *et al.*, 2018; Tagliafierro *et al.*, 2015).

Chapter 8: References

Abhyankar LN, Jones MR, Guallar E, Navas-Acien A 2011. Arsenic exposure and hypertension: a systematic review. Environmental Health Perspectives 120(4): 494-500.

Abraham D, Hofbauer R, Schafer R, Blumer R, Paulus P, Miksovsky A, Traxler H, Kocher A, Aharinejad S, 2000. Selective downregulation of VEGF-A(165), VEGF-R(1), and decreased capillary density in patients with dilative but not ischemic cardiomyopathy. Circulation Research 87(8): 644-647.

Abu-Hayyeh S, Sian M, Jones KG, Manuel A, Powell JT 2001. Cadmium accumulation in aortas of smokers. Arteriosclerosis, Thrombosis, and Vascular Biology 21(5): 863-867.

Adams JM 1932. Some racial differences in blood pressures and morbidity in a group of white and colored workmen. American Journal of Medical Sciences 184: 342-50.

Adamska-Dyniewska H, Bała T, Florczak H, Trojanowska B 1982. Blood cadmium in healthy subjects and in patients with cardiovascular diseases. Cor et Vasa 24(6): 441-447.

Afanas'ev I 2011. ROS and RNS signaling in heart disorders: could antioxidant treatment be successful? Oxidative Medicine and Cellular Longevity 1: 1-13.

Agarwal R, Goel SK, Chandra R, Behari JR 2010. Role of vitamin E in preventing acute mercury toxicity in rat. Environmental Toxicology and Pharmacology 29(1): 70-78.

Agarwal S, Zaman T, Tuzcu EM, Kapadia SR 2011. Heavy metals and cardiovascular disease: results from the National Health and Nutrition Examination Survey (NHANES) 1999-2006. Angiology 62(5): 422- 429.

Agarwala S, Mudholkar K, Bhuwania R, Satish Rao BS 2012. Mangiferin, a dietary xanthone protects against mercury-induced toxicity in HepG2 cells. Environmental Toxicology 27(2): 117-127.

Agrawal S, Flora G, Bhatnagar P, Flora SJ 2014. Comparative oxidative stress, metallothionein induction and organ toxicity following chronic exposure to arsenic, lead and mercury in rats. Cell and Molecular Biology (Noisy-le-grand); 60(2): 13-21.

Aguado A, Galán M, Zhenyukh O, Wiggers GA. Roque FR, Redondo S, Peçanha F, Martín A, Fortuño A, Cachofeiro V, Tejerina T 2013. Mercury induces proliferation and reduces cell size in vascular smooth muscle cells through MAPK, oxidative stress and cyclooxygenase-2 pathways. Toxicology and Applied Pharmacology 268(2): 188-200.

Ahanchi SS, Tsihlis ND, Kibbe MR 2007. The role of nitric oxide in the pathophysiology of intimal hyperplasia. Journal of Vascular Surgery 45(6): A64-73.

Ahmed SH, Clark LL, Pennington WR, Webb CS, Bonnema DD, Leonardi AH, McClure CD, Spinale FG, Zile MR 2006. Matrix metalloproteinases/tissue inhibitors of metalloproteinases: relationship between changes in proteolytic determinants of matrix composition and structural, functional, and clinical manifestations of hypertensive heart disease. Circulation 113(17): 2089-2096.

Ajjan RA, Standeven KF, Khanbhai M, Phoenix F, Gersh KC, Weisel JW, Kearney MT, Ariëns RAS, Grant PJ 2009. Effects of aspirin on clot structure and fibrinolysis using a novel in vitro cellular system. Arteriosclerosis, Thrombosis, and Vascular Biology 29(5): 712-717.

Akerstrom M, Barregard L, Lundh T, Sallsten G 2013. The relationship between cadmium in kidney and cadmium in urine and blood in an environmentally exposed population. Toxicology and Applied Pharmacology 268(3): 286-293.

Akhter S, Vignini A, Wen Z, English A, Wang PG, Mutus B 2002. Evidence for S-nitrosothiol-dependent changes in fibrinogen that do not involve transnitrosation or thiolation. Proceedings of the National Academy of Sciences 99(14): 9172-9177.

Akoto O, Bismark Eshun F, Darko G, Adei E 2014. Concentrations and health risk assessments of heavy metals in fish from the fosu lagoon. International Journal of Environmental Research 8(2): 403-410.

Akyol Ö, İşçi N, Temel İ, Özgöçmen S, Uz E, Murat M, Büyükberber S 2001. The relationships between plasma and erythrocyte antioxidant enzymes and lipid peroxidation in patients with rheumatoid arthritis. Joint Bone Spine 68(4): 311-317.

Al Ghatrif M. and Lakatta EG 2015. The conundrum of arterial stiffness, elevated blood pressure, and aging. Current Hypertension Reports 17(2): 12-26.

Alam MS, Kaur G, Jabbar Z, Javed K, Athar M 2007. Eruca sativa seeds possess antioxidant activity and exert a protective effect on mercuric chloride induced renal toxicity. Food and Chemical Toxicology 45: 910-920.

Al-Attar AM 2011. Antioxidant effect of vitamin E treatment on some heavy metals-induced renal and testicular injuries in male mice. Saudi Journal of Biological Sciences 18(1): 63-72.

Alberts M, Urdal P, Steyn K, Stensvold I, Tverdal A, Nel JH, Steyn NP 2005. Prevalence of cardiovascular diseases and associated risk factors in a rural black population of South Africa. European Journal of Cardiovascular Prevention and Rehabilitation 12(4): 347-54.

Alessandria I, Pennisi M, Cataudella E, Frazzetto PM, Mala-guarnera M, Rampello L, Rampello L 2012. Neurotoxicity in cadmium-exposed workers. Acta Medica Mediterranea 28: 253-256.

Al-Harthi SE, Alarabi OM, Ramadan WS, Alaama MN, Al-Kreathy HM, Damanhouri ZA, Khan LM, Osman AM 2014. Amelioration of doxorubicin-induced cardiotoxicity by resveratrol. Molecular Medicine Reports 10(3): 1455-1460.

Alissa EM, Ferns GA 2011. Heavy metal poisoning and cardiovascular disease. Journal of Toxicology 1: 1-21.

Alkushi AG, Sinna MM, Mohammed EH, ElSawy NA 2018. Structural changes in adult rat liver following cadmium treatment. Pakistan Journal of Nutrition, 17(2): 89-101.

Allen J 2007. Photoplethysmography and its application in clinical physiological measurement. Physiological Measurement 28(3): R1-R39.

Altenhöfer S, Kleikers PW, Radermacher KA, Scheurer P, Hermans JR, Schiffers P, Ho H, Wingler K, Schmidt HH 2012. The NOX toolbox: validating the role of NADPH oxidases in physiology and disease. Cellular and Molecular Life Sciences 69(14): 2327-2343.

Ambrose JA, Barua RS 2004. The pathophysiology of cigarette smoking and cardiovascular disease: an update. Journal of the American College of Cardiology 43: 1731-1737.

Ames BN, Shigenaga MK, Hagen TM 1993. Oxidants, antioxidants, and the degenerative diseases of aging. Proceedings of the National Academy of Sciences 90(17): 7915-7922.

An HC, Sung JH, Lee J, Sim CS, Kim SH, Kim Y 2017. The association between cadmium and lead exposure and blood pressure among workers of a smelting industry: a cross-sectional study. Annals of Occupational And Environmental Medicine 29(1): 47-54.

Angiolillo DJ and Ferreiro JL 2013. Antiplatelet and anticoagulant therapy for atherothrombotic disease: the role of current and emerging agents. American Journal of Cardiovascular Drug; drugs, devices and other interventions 13: 233-250.

Annabi A, Messaoudi I, Kerkeni A, Said K 2011. Icadmium accumulation and histological lesion in mosquitofish (*Gambusia affinis*) tissues following acute and chronic exposure. International Journal of Environmental Research 5(3): 745-756.

Ansar S and Iqbal M 2016. Protective effect of diallylsulphide against mercuric chloride-induced hepatic injury in rats. Human and Experimental Toxicology 35(12): 1305-1311.

Ansari MA, Maayah ZH, Bakheet SA, El-Kadi AO, Korashy HM 2013. The role of aryl hydrocarbon receptor signaling pathway in cardiotoxicity of acute lead intoxication *in vivo* and *in vitro* rat model. Toxicology 306: 40-49.

Aragno, M, Mastrocola R, Alloatti G, Vercellinatto I, Bardini P, Geuna S, Catalano MG, Danni O, Boccuzzi G 2008. Oxidative stress triggers cardiac fibrosis in the heart of diabetic rats. Endocrinology 149(1): 380- 388.

Aseichev AV, Azizova OA and Zhambalova BA 2002. Effect of UV-modified fibrinogen on platelet aggregation in platelet-rich plasma. Bulletin of Experimental Biology and Medicine 133(1): 41-43.

Ashour TH 2014. Preventative effects of caffeic acid phenyl ester on cadmium intoxication induced hematological and blood coagulation disturbances and hepatorenal damage in rats. ISRN Hematology 1: 1-7.

Attardi G, Schatz G 1988. Biogenesis of mitochondria. Annual Review of Cell Biology 4(1): 289-331.

Au DW 2004. The application of histo-cytopathological biomarkers in marine pollution monitoring: a review. Marine Pollution bulletin 48(9-10): 817-834.

Aureliano M, Joaquim N, Sousa A, Martins H, Coucelo JM 2002. Oxidative stress in toadfish (Halobactrachus didactylus) cardiac muscle: acute exposure to vanadate oligomers. Journal of Inorganic Biochemistry 90(3-4): 159-165.

Awofolu OR, Mbolekwa Z, Mtshemla, Fatoki OS 2005. Levels of trace metals in water and sediment from Tyume River and its effects on an irrigated farmland. Water SA 31: 87-94.

Ayo-Yusuf OA, Olutola BG 2013. 'Roll-your-own' cigarette smoking in South Africa between 2007 and 2010. BMC Public Health 3(1): 597-602.

Azizova OA, Shvachko AG, Aseichev AV 2009. Effect of iron ions on functional activity of thrombin. Bulletin of Experimental Biology and Medicine 148: 776-779.

Baeuml J, Bose-O'Reilly S, Gothe RM, Lettmeier B, Roider G, Drasch G, Siebert U 2011. Human biomonitoring data from mercury exposed miners in six artisanal small-scale gold mining areas in Asia and Africa. Minerals 1(1): 122-143.

Bando I, Reus MIS, Andrés D, Cascales M 2005. Endogenous antioxidant defence system in rat liver following mercury chloride oral intoxication. Journal of Biochemical and Molecular Toxicology 19(3):154-161.

Barbieri SS, Zacchi E, Amadio P, Gianellini S, Mussoni L, Weksler BB, Tremoli E 2011. Cytokines present in smokers' serum interact with smoke components to enhance endothelial dysfunction. Cardiovascular Research 90(3): 475-83.

Barquera S, Pedroza-Tobías A, Medina C, Hernández-Barrera L, Bibbins-Domingo K, Lozano R, Moran AE 2015. Global overview of the epidemiology of atherosclerotic cardiovascular disease. Archives of Medical Research 46(5):328-38.

Barregard L, Sallsten G, Fagerberg B, Borné Y, Persson M, Hedblad B Engström G 2016. Blood cadmium levels and incident cardiovascular events during follow-up in a population-based cohort of Swedish adults: the Malmö Diet and Cancer Study. Environmental Health Perspectives 124(5): 594-600.

Barua RS, Ambrose JA, Saha DC, Eales-Reynolds LJ 2002. Smoking is associated with altered endothelial-derived fibrinolytic and antithrombotic factors: an *in vitro* demonstration. Circulation 106: 905-908.

Barua RS, Ambrose JA, Srivastava S, DeVoe MC, Eales-Reynolds LJ 2003. Reactive oxygen species are involved in smoking-induced dysfunction of nitric oxide biosynthesis and upregulation of endothelial nitric oxide synthase: an in vitro demonstration in human coronary artery endothelial cells. Circulation 107: 2342-2347.

Barua RS, Sy F, Srikanth S, Hunag G, üed U, Buhari C, Margoson D, Ambrose JA 2010. Effects of cigarette smoke exposure on clot dynamics and fibrin structure: An *ex vivo* investigation. Atherosclerosis, Thrombosis and Vascular Biology 30: 75-79.

Bashandy SA, El Awdan SA, Ebaid H, Alhazza IM 2016. Antioxidant potential of *Spirulina platensis* mitigates oxidative stress and reprotoxicity induced by sodium arsenite in male rats. Oxidative Medicine and Cellular Longevity 7174351: 1-8

Bateman RM, Ellis CG, Suematsu M, Walley KR 2012. S-Nitrosoglutathionine acts as a small molecule modulator of human fibrin clot architecture. PLoS One 7(8): 1-13.

Bavec Š, Biester H, Gosar M 2018. A risk assessment of human exposure to mercury-contaminated soil and household dust in the town of Idrija (Slovenia). Journal of Geochemical Exploration 187: 131-140

Becatti M, Maruci R, Bruschi G, Taddei N, Bani D, Gori AM, Giusti B, Gensini GF, Abbate R, Fiorillo 2014. Oxidative modification of fibrinogen is associated with altered function and structure in the subacute phase of myocardial infarction. Arteriosclerosis, Thrombosis, and Vascular Biology 34(7): 1355-1361.

Benedet JA and Shibamoto T 2008. Role of transition metals, Fe(II), Cr(II), Pb(II), and Cd(II) in lipid peroxidation. Food Chemistry 107: 165-168.

Berk BC, Fujiwara K, Lehoux S 2007. ECM remodeling in hypertensive heart disease. The Journal of Clinical Investigation 117(3): 568-575.

Berk M, Dean O, Drexhage H, McNeil JJ, Moylan S, Oneal A, Davey CG, Sanna L, Maes M 2013. Aspirin: a review of its neurobiological properties and therapeutic potential for mental illness. BMC medicine 11: 74-91.

Berlin M, Fazackerley J, Nordberg G, Kand M 1969. The uptake of mercury in the brains of mammals exposed to mercury vapor and to mercuric salts. Archives of Environmental Health: An International Journal 18(5): 719-729.

Berlin M, Gibson S 1963. Renal uptake, excretion, and retention of mercury: I. A study in the rabbit during infusion of mercuric chloride. Archives of Environmental Health: An International Journal 6(5): 617-625.

Berlin M, Zalups RK and Fowler BA 2007. Mercury. In: Handbook of Toxicology of Metals. Nordberg GF, Nogawa K, Nordberg M, and Friberg LT, editors. Academic Press Inc., Amsterdam and Boston 675-729.

Bernhard D, Rossmann A, Henderson B, Kind M, Seubert A, Wick G 2006. Increased serum cadmium and strontium levels in young smokers effects on arterial endothelial cell gene transcription. Arteriosclerosis, Thrombosis, and Vascular Biology 26(4): 833-838.

Bernhardt WM, Schmitt R, Rosenberger C, Münchenhagen PM, Gröne HJ, Frei U, Warnecke C, Bachmann S, Wiesener MS, Willam C, Eckardt KU 2006. Expression of hypoxia-inducible transcription factors in developing human and rat kidneys. Kidney International 69(1): 114-122.

Bernhoft RA 2011. Mercury toxicity and treatment: a review of the literature. Journal of Environmental and Public Health 1: 1-10.

Bernhoft RA 2012. Mercury toxicity and treatment: a review of the literature. Journal of Environmental and Public Health 2012: 1-10

Bernhoft RA 2013. Cadmium toxicity and treatment. Scientific World Journal 1: 1-7.

Bersényi A, Fekete SG, Szőcs Z, Berta E, 2003. Effect of ingested heavy metals (Cd, Pb and Hg) on haematology and serum biochemistry in rabbits. Acta Veterinaria Hungarica 51(3): 297-304.

Bertin G, Averbeck D 2006. Cadmium: cellular effects, modifications of biomolecules, modulation of DNA repair and genotoxic consequences (a review). Biochimie 88:1549-1559.

Bester J, Buys A, Lipinski B, Kell DB, Pretorius E 2013. High ferritin levels have major effects on the morphology of erythrocytes in Alzheimer's disease. Frontiers in Aging Neuroscience 6(5): 88-101.

Bhattacharjee P, Bhattacharyya D 2014. An insight into the abnormal fibrin clots: its pathophysiological roles. Fibrinolysis and Thrombolysis. Kolev K.(Ed.) InTech, Croatia University Press, Croatia. 3-29.

Bilgen I, Oner G, Edremitlioglu M, Alkan Z, Cirrik S, 2003. Involvement of cholinoceptors in cadmium-induced endothelial dysfunction. Journal of Basic and Clinical Physiology and Pharmacology 14(1): 55-76.

Bissinger R, Bhuyan AA, Qadri SM, Lang F 2018. Oxidative stress, eryptosis and anemia: a pivotal mechanistic nexus in systemic diseases. The FEBS Journal 1:1-29.

Bjørklund G, Dadar M, Mutter J and Aaseth J 2017. The toxicology of mercury: Current research and emerging trends. Environmental Research 159: 545-554.

Blache D 1995. Involvement of hydrogen and lipid peroxides in acute tobacco smoking-induced platelet hyperactivity. American Journal of Physiology 268: 679-685.

Blankenberg S, Rupprecht HJ, Bickel C, Torzewski M, Hafner G, Tiret L, Smieja M, Cambien F, Meyer J, Lackner KJ 2003. Glutathione peroxidase 1 activity and cardiovascular events in patients with coronary artery disease. New England Journal of Medicine 349(17): 1605-1613.

Bodor GS 2016. Biochemical markers of myocardial damage. EJIFCC 27(2): 95-111.

Bolliger D, Seeberger MD, Tanaka KA 2012. Principles and practice of thromboelastography in clinical coagulation management and transfusion practice. Transfusion Medicine Reviews 26(1):1-3.

Boluyt MO, O'neill L, Meredith AL, Bing OH, Brooks WW, Conrad CH, Crow MT, Lakatta EG 1994. Alterations in cardiac gene expression during the transition from stable hypertrophy to heart failure. Marked upregulation of genes encoding extracellular matrix components. Circulation Research 75(1): 23-32.

Borné Y, Barregard L, Persson M, Hedblad B, Fagerberg B, Engström G 2015. Cadmium exposure and incidence of heart failure and atrial fibrillation: a population based prospective cohort study. British Medical Journal Open 5(6): 007366-007366.

Bose-O'ReillyS, Schierl R, Nowak D, Siebert U, William JF, Owi FT, Ir, YI 2016. A preliminary study on health effects in villagers exposed to mercury in a small-scale artisanal gold mining area in Indonesia. Environmental Research 149: 274-281.

Boueiz A, Hassoun PM 2009. Regulation of endothelial barrier function by reactive oxygen and nitrogen species. Microvascular Research 77(1): 26-34.

Brandão R, Borges LP, Oliveira RD, Rocha JB, Nogueira CW 2008. Diphenyl diselenide protects against hematological and immunological alterations induced by mercury in mice. Journal of Biochemistry and Molecular Toxicology 22: 311-319.

Bravo-San Pedro JM, Kroemer G, Galluzzi L 2017. Autophagy and mitophagy in cardiovascular disease. Circulation Research 120(11): 1812-1824.

Brzóska MM, Kamiński M, Supernak-Bobko D, Zwierz K, Moniuszko-Jakoniuk J 2003. Changes in the structure and function of the kidney of rats chronically exposed to cadmium. I. Biochemical and histopathological studies. Archives of Toxicology 77(6): 344-352.

Brzóska MM, Rogalska J, Galazyn-Sidorczuk M, Jurczuk M, Roszczenko A, Tomczyk M 2015. Protective effect of *Aronia melanocarpa* polyphenols against cadmium-induced disorders in bone metabolism: a study in a rat model of lifetime human exposure to this heavy metal. Chemico-Biological Interactions 229: 132-146.

Bujak M and Frangogiannis NG 2007: The role of TGF-beta signaling in myocardial infarction and cardiac remodeling. Cardiovascular Research 74:184-195.

Cahill PA, Redmond EM 2016. Vascular endothelium-gatekeeper of vessel health. Atherosclerosis 248: 97-109.

Cai H, Harrison DG 2000. Endothelial dysfunction in cardiovascular diseases: the role of oxidant stress. Circulation Research 87(10): 840-844.

Cai J, Zhang Y, Yang J, Liu Q, Zhao R, Hamid S, Wang H, Xu S, Zhang Z 2017. Antagonistic effects of selenium against necroptosis injury via adiponectin-necrotic pathway induced by cadmium in heart of chicken. RSC Advances 7(70): 44438-44446.

Camelliti P, Borg TK, Kohl P 2005. Structural and functional characterisation of cardiac fibroblasts. Cardiovascular Research 65: 40-51.

Camsari C, Folger JK, McGee D, Bursian SJ, Wang H, Knott JG, Smith GW. 2017. Effects of periconception cadmium and mercury co-administration to mice on indices of chronic diseases in male offspring at maturity. Environmetal Health Perspective 125: 643-650.

Cao DJ, Gillette TG, Hill JA 2009. Cardiomyocyte autophagy: remodeling, repairing, and reconstructing the heart. Current Hypertension Reports 11: 406-411.

Capitanio D, Leone R, Fania C, Torretta E Gelfi C 2016. Sprague Dawley rats: A model of successful heart aging. EuPA Open Proteomics 12: 22-30.

Carr Jr ME, Alving BM 1995. Effect of fibrin structure on plasmin mediated dissolution of plasma clots. Blood Coagulation and Fibrinolysis 6: 567-573.

Castilhos Z, Rodrigues-Filho S, Cesar R, Rodrigues AP, Villas-Bôas R, de Jesus I, Lima M, Faial K, Miranda A, Brabo E, Beinhoff C 2015. Human exposure and risk assessment associated with mercury contamination in artisanal gold mining areas in the Brazilian Amazon. Environmental Science and Pollution Research 22(15): 11255-11264.

Catieau B, Devos V, Chtourou S, Borgel D, Plantier JL 2018. Endothelial cell surface limits coagulation without modulating the antithrombin potency. Thrombosis Research 167: 88-95.

Celikoglu E, Aslanturk A, Kalender Y 2015. Vitamin E and sodium selenite against mercuric chloride-induced lung toxicity in the rats. Brazilian Archives of Biology and Technology 58(4): 587-594.

Cesar R, Egler S, Polivanov H, Castilhos Z, Rodrigues AP 2011. Mercury, copper and zinc contamination in soils and fluvial sediments from an abandoned gold mining area in southern Minas Gerais State, Brazil. Environmental Earth Sciences 64(1): 211-222.

Chaiswing L, Oberley TD 2010. Extracellular/microenvironmental redox state. Antioxidants and Redox Signalling 13(4): 449-465.

Chang HR, Tsao DA, Yu HS, Ho CK 2005. The change of β-adrenergic system after cessation of lead exposure. Toxicology 207(1): 73-80.

Chaumont A, Nickmilder M, Dumont X, Lundh T, Skerfving S, Bernard A 2012. Associations between proteins and heavy metals in urine at low environmental exposures: evidence of reverse causality. Toxicology Letters 210(3): 345-352.

Chen CY, Zhang SL, Liu ZY, Tian Y, Sun Q 2015. Cadmium toxicity induces ER stress and apoptosis via impairing energy homoeostasis in cardiomyocytes. Bioscience Reports 35(3): e00214-e00222.

Chen F and Shi X 2002. Intracellular signal transduction of cells in response to carcinogenic metals. Critical Reviews in Oncology/ Hematology 42(1): 105-121.

Chen Q, Kang J, Fu C 2018. The independence of and associations among apoptosis, autophagy, and necrosis. Signal Transduction and Targeted Therapy 3(1): 8 -29.

Cherney DZ, Sochett EB 2011. Evolution of renal hyperfiltration and arterial stiffness from adolescence into early adulthood in type 1 diabetes. Diabetes Care 34(8): 1821-1826.

Cherney DZ, Sochett EB, Lai V, Dekker MG, Slorach C, Scholey JW, Bradley TJ 2010. Renal hyperfiltration and arterial stiffness in humans with uncomplicated type 1 diabetes. Diabetes Care 33(9): 2068-2070.

Cheville NF 1994. Blockade of metabolic pathways. In Ultrastructural Pathology. An Introduction to interpretation, pp. 129–139. Iowa State University Press, Ames, Iowa

Chiarelli R, Roccheri MC 2012. Heavy metals and metalloids as autophagy inducing agents: focus on cadmium and arsenic. Cells 1(3): 597-616.

Chiong M, Wang ZV, Pedrozo Z, Cao DJ, Troncoso R, Ibacache M, Criollo A, Nemchenko A, Hill JA, Lavandero S 2011. Cardiomyocyte death: mechanisms and translational implications. Cell Death Discovery 2: e244-e255.

Cho J, Mosher DF 2006. Impact of fibronectin assembly on platelet thrombus formation in response to type I collagen and von Willebrand factor. Blood 108(7): 2229-2236.

Choi JY, Won NH, Park JD, Jang S, Eom CY, Choi Y, Park YI, Dong MS 2016. From the cover: ethylmercury-induced oxidative and endoplasmic reticulum stress-mediated autophagic cell death: involvement of autophagosome–lysosome fusion arrest. Toxicological Sciences 154(1): 27-42.

Chokshi A, Drosatos K, Cheema FH, Ji R, Khawaja T, Yu S, Kato T, Khan R, Takayama H, Knöll R, Milting H 2014. Ventricular assist device implantation corrects myocardial lipotoxicity, reverses insulin resistance and normalizes cardiac metabolism in patients with advanced heart failure. Circulation 125(23): 2844-2853.

141

Chowdhury R, Ramond A, O'Keeffe LM, Shahzad S, Kunutsor SK, Muka T, Gregson J, Willeit P, Warnakula S, Khan H, Chowdhury S 2018. Environmental toxic metal contaminants and risk of cardiovascular disease: systematic review and meta-analysis. BMJ 362:k3310-k3343.

Chu KW and Chow KL 2002. Synergistic toxicity of multiple heavy metals is revealed by a biological assay using a nematode and its transgenic derivative. Aquatic Toxicology 61(1-2): 53-64.

Chuah XQ and Teo SS 2016. Evaluation of sub-chronic toxicity and heavy metal toxicity of *kappaphycus alvarezii in-vivo*. International Journal of Pharmaceutical Sciences and Research 7(2): 573-578.

Ciuti R, Liguri G 2017. A novel assay for measuring total antioxidant capacity in whole blood and other biological samples. Journal of Biomedical Science and Engineering 10(02): 60-76.

Cobbina SJ, Chen Y, Zhou Z, Wu X, Feng W, Wang W, Mao G, Xu H, Zhang Z, Wu X, Yang L 2015. Low concentration toxic metal mixture interactions: Effects on essential and non-essential metals in brain, liver, and kidneys of mice on sub-chronic exposure. Chemosphere 132:79-86.

Coetzee PP, Coetzee, LL, Puka R, Mubenga S 2004. Characterisation of selected South African clays for defluoridation of natural waters. Water South Africa 29(3): 331-338.

Collet JP, Allali Y, Lesty C, Tanguy ML, Silvain J, Ankri A, Blanchet B, Dumaine R, Gianetti J, Payot L, Weisel JW 2006. Altered fibrin architecture is associated with hypofibrinolysis and premature coronary atherothrombosis. Arteriosclerosis, Thrombosis, and Vascular Biology 26(11): 2567-2573.

Collet JP, Park D, Lesty C, Soria J, Soria C, Montalescot G, Weisel JW. 2000. Influence of fibrin network conformation and fibrin fiber diameter on fibrinolysis speed dynamic and structural approaches by confocal microscopy. Arteriosclerosis, Thrombosis, and Vascular Biology 20(5): 1354-1361.

Cooper D, Stokes KY, Tailor A, Granger DN 2002. Oxidative stress promotes blood cell-endothelial cell interactions in the microcirculation. Cardiovascular Toxicology 2(3):165-180.

Cotton JM, Kearney MT, Shah AM 2002. Nitric oxide and myocardial function in heart failure: friend or foe? Heart 88: 564-566.

Crowe W, Allsopp PJ, Watson GE, Magee PJ, Strain JJ, Armstrong DJ, Ball E, McSorley EM 2017. Mercury as an environmental stimulus in the development of autoimmunity–a systematic review. Autoimmunity Reviews 16(1): 72-80.

Csányi G, Miller FJ 2014. Oxidative stress in cardiovascular disease. International Journal of Molecular Science 15(1): 6002-6008.

Csiszar A, Labinskyy N, Jimenez R, Pinto JT, Ballabh P, Losonczy G, Pearson KJ, de Cabo R, and Ungvari Z 2009. Anti-oxidative and anti-inflammatory vasoprotective effects of caloric restriction in aging: role of circulating factors and SIRT1. Mechanisms of Ageing and Development 130(8): 518-527

Csiszar A, Wang M, Lakatta EG, Ungvari Z 2008. Inflammation and endothelial dysfunction during aging: role of NF-κB. Journal of Applied Physiology 105(4):1333-1341.

Cui JZ, Tehrani AY, Jett, KA, Bernatchez P, van Breemen C, Esfandiarei M 2014. Quantification of aortic and cutaneous elastin and collagen morphology in Marfan syndrome by multiphoton microscopy. Journal of Structural Biology 187(3): 242-253.

Czirok A, Zach J, Kozel BA, Mecham RP, Davis EC, Rongish BJ 2006. Elastic fiber macro-assembly is a hierarchical, cell motion-mediated process. Journal of Cellular Physiology 207(1): 97-106.

da Cunha Martins Jr A, Carneiro MF, Grotto D, Adeyemi JA, Barbosa Jr F 2018. Arsenic, cadmium, and mercury-induced hypertension: mechanisms and epidemiological findings. Journal of Toxicology and Environmental Health, Part B 21(2): 61-82.

Dai YJ, Jia YF, Chen N, Bian WP, Li QK, Ma YB, Chen YL, Pei DS 2014. Zebrafish as a model system to study toxicology. Environmental Toxicology and Chemistry. 33(1): 11-17.

Dallüge J, van Rijn M, Beens J, Vreuls RJ, Udo A 2002. Comprehensive two-dimensional gas chromatography with time-of-flight mass spectrometric detection applied to the determination of pesticides in food extracts. Journal of Chromatography A 965(1-2): 207-217.

Dardouri K, Haouem S, Gharbi I, Sriha B, Haouas Z, El Hani A, Hammami M 2016. Combined Effects of Cd and Hg on Liver and Kidney Histology and Function in Wistar. Journal of Agricultural Chemistry and Environment 5(4):159-169.

D'Autréaux B, Toledano MB 2007. ROS as signalling molecules: mechanisms that generate specificity in ROS homeostasis. Nature Reviews Molecular Cell Biology 8(10): 813-824.

Davidson SM and Duchen MR 2007. Endothelial mitochondria contributing to vascular function and disease. Circulation Research 100(8): 1128-1141.

Davignon J, Ganz P 2004. Role of endothelial dysfunction in atherosclerosis. Circulation 109(23 suppl 1):III-127.

De Assis GPS, Silva CEC, Stefanon I, Vassallo DV 2003. Effects of small concentrations of mercury on the contractile activity of the rat ventricular myocardium. Comparative Biochemistry and Physiology Part C: Toxicology & Pharmacology 134(3): 375-383.

De Maat M, Verschuur M 2005. Fibrinogen heterogeneity: inherited and noninherited. Current Opinions in Hematology 12: 377-383.

De Souza BF and Tricoci P 2013. Novel anti-platelet agents: focus on thrombin receptor antagonists. Journal of Cardiovascular Translational Research 6: 415-424.

Degterev A, Huang Z, Boyce M, Li Y, Jagtap P, Mizushima N, Cuny GD, Mitchison TJ, Moskowitz MA, Yuan J 2005. Chemical inhibitor of nonapoptotic cell death with therapeutic potential for ischemic brain injury. Nature Chemical Biology 1(2): 112-119.

dell'Omo M, Muzi G, Bernard A, Filiberto S, Lauwerys RR, Abbritti G 1997. Long-term pulmonary and systemic toxicity following intravenous mercury injection. Archives of Toxicology 72(1): 59-62.

Demontis MP, Varoni MV, Volpe AR, Emanueli C, Madeddu P 1998. Role of nitric oxide synthase inhibition in the acute hypertensive response to intracerebroventricular cadmium. British Journal of Pharmacology 123(1): 129-135.

Dhalla NS, Temsah RM, Netticadan T 2000. Role of oxidative stress in cardiovascular diseases. Journal of Hypertension 18(6): 655-673.

Di Gioacchino M, Petrarca C, Perrone A, Farina M, Sabbioni E, Hartung T, Martino S, Esposito DL, Lotti LV, Mariani-Costantini R 2008. Autophagy as an ultrastructural marker of heavy metal toxicity in human cord blood hematopoietic stem cells. Science of the Total Environment 392(1): 50-58.

Díez J, Panizo A, Gil MJ, Monreal I, Hernández M, Mindán JP 1996. Serum markers of collagen type I metabolism in spontaneously hypertensive rats: relation to myocardial fibrosis. Circulation 93(5): 1026-1032.

Dohi K, Mochizuki Y, Satoh K, Jimbo H, Hayashi M, Toyoda I, Ikeda Y, Abe T, Aruga T. Transient elevation of serum bilirubin (a heme oxygenase-1 metabolite) level in hemorrhagic stroke: bilirubin is a marker of oxidant stress. InBrain Edema XII 2003 (pp. 247-249). Springer, Vienna.

Dominguez F, Kühl U, Pieske B, Garcia-Pavia P, Tschöpe C 2016. Update on myocarditis and inflammatory cardiomyopathy: reemergence of endomyocardial biopsy. Revista Española De Cardiología (English Edition) 69(2): 178-187.

Donpunha W, Kukongviriyapan U, Sompamit K, Pakdeechote P, Kukongviriyapan V, Pannangpetch P 2011. Protective effect of ascorbic acid on cadmium-induced hypertension and vascular dysfunction in mice. Biometals 24(1):105-115.

Dos Santos FA, Cavecci B, Vieira JC, Franzini VP, Santos A, de Lima Leite A, Buzalaf MA, Zara LF, de Magalhães Padilha P 2015. A metalloproteomics study on the association of mercury with breast milk in samples from lactating women in the Amazon region of Brazil. Archives of Environmental Contamination and Toxicology 69(2): 223-239.

Drummond GR, Selemidis S, Griendling KK, Sobey CG 2011. Combating oxidative stress in vascular disease: NADPH oxidases as therapeutic targets. Nature Reviews Drug Discovery 10(6): 453-471.

Du Plooy JN, Buys A, Duim W, Pretorius E 2013. Comparison of platelet ultrastructure and elastic properties in thrombo-embolic ischemic stroke and smoking using atomic force and scanning electron microscopy. PloS one 8(7): 1-6.

Dunn EJ, Ariens RA, Grant PJ 2005. The influence of type 2 diabetes on fibrin structure and function. Diabetologia 48: 1198-206.

Dunn EJ, Philippou H, Ariens RA, Grant PJ 2006. Molecular mechanisms involved in the resistance of fibrin to clot lysis by plasmin in subjects with type 2 diabetes mellitus. Diabetologia 49: 1071-1080.

Duruibe JO, Ogwuegbu MOC and Egwurugwu JN 2007. Heavy metal pollution and human biotoxic effects. International Journal of Physical Sciences 2: 112-118.

Eckly A, Hechler B, Freund M, Zerr M, Cazenave JP, Lanza F, Mangin PH, Gachet C 2011. Mechanisms underlying FeCl$_3$-induced arterial thrombosis. Journal of Thrombosis and Haemostasis 9(4): 779-789.

Eisele K, Lang PA, Kempe DS, Klarl BA, Niemöller O, Wieder T, Huber SM, Duranton C, Lang F 2006. Stimulation of erythrocyte phosphatidylserine exposure by mercury ions. Toxicology and Applied Pharmacology 210(1-2): 116-122.

El-Bahr SM 2013. Biochemistry of free radicals and oxidative stress. Science International 1(5): 111-117.

El-Demerdash FM, Yousef MI, Kedwany FS, Baghdadi HH 2004. Cadmium-induced changes in lipid peroxidation, blood hematology, biochemical parameters and semen quality of male rats: protective role of vitamin E and beta-carotene. Food and Chemical Toxicology 42: 1563-1571.

Elia AC, Dorr AJM, Mantilacci L, Taticchi MI, Galarini R 2000. Effects of mercury on glutathione and glutathione-dependent enzymes in catfish (*Ictalurus melas R.*). In: Markert B, Friese K (eds.): Trace Elements-Their Distribution and Effects in the Environment: Trace Metals in the Environment. ElsevierScience, Amsterdam. 411-421.

Elia AC, Galarini R, Taticchi MI, Dorr AJM, Mantilacci L 2003. Antioxidant responses and bioaccumulation in *Ictalurus melas* under mercury exposure. Ecotoxicology and Environmental Safety 55: 162-167.

El-Maraghy SA, Gad MZ, Fahim AT, Hamdy MA 2001. Effect of cadmium and aluminum intake on the antioxidant status and lipid peroxidation in rat tissues. Journal of Biochemical And Molecular Toxicology 15(4): 207-214.

El-Shenawy SM, Hassan NS 2008. Comparative evaluation of the protective effect of selenium and garlic against liver and kidney damage induced by mercury chloride in the rats. Pharmacological Reports 60(2): 199-208.

Essick EE and Sam F 2010. Oxidative stress and autophagy in cardiac disease, neurological disorders, aging and cancer. Oxidative Medicine and Cellular Longevity 3(3): 168-177.

Fan D, Takawale A, Lee J, Kassiri Z 2012. Cardiac fibroblasts, fibrosis and extracellular matrix remodeling in heart disease. Fibrogenesis Tissue Repair 5(1): 15-29.

Faroon O, Ashizawa A, Wright S, Tucker P, Jenkins K, Ingerman L, Rudisill C 2012. Toxicological Profile for Cadmium, Agency for Toxic Substances and Disease Registry (ATSDR) Toxicological Profiles. Agency for Toxic Substances and Disease Registry (US), Atlanta (GA). 1-487.

Fatah K, Hamsten A, Blombäck B, Blombäck M 1992. Fibrin gel network characteristics and coronary heart disease: relations to plasma fibrinogen concentration, acute phase protein, serum lipoproteins and coronary atherosclerosis. Thrombosis and Haemostasis 68(2): 130-135.

Fatah K, Silveira A, Tornvall P, Karpe F, Blombäck M, Hamsten A 1996. Proneness to formation of tight and rigid fibrin gel structures in men with myocardial infarction at a young age. Thrombosis and Haemostasis 76(4): 535-540.

Fatoki OS and Awofolu R. 2003. Levels of Cd, Hg and Zn in some surface waters from the Eastern Cape Province, South Africa. Water SA 29: 375-380.

Faury G, Garnier S, Weiss AS, Wallach J, Fülöp T, Jacob MP, Mecham RP, Robert L Verdetti J 1998. Action of tropoelastin and synthetic elastin sequences on vascular tone and on free Ca^{2+} level in human vascular endothelial cells. Circulation Research 82(3): 328-336.

Feldman AM, Li YY, McTiernan CF 2001. Matrix metalloproteinases in pathophysiology and treatment of heart failure. Lancet 357: 654-655.

Feldman LJ, Mazighi M, Scheuble A, Deux JF, De Benedetti E, Badier-Commander C, Brambilla E, Henin D, Steg PG, Jacob MP 2001. Differential expression of matrix metalloproteinases after stent implantation and balloon angioplasty in the hypercholesterolemic rabbit. Circulation 103(25): 3117-3122.

Ferramola ML, Pérez Díaz MF, Honoré SM, Sánchez SS, Antón RI, Anzulovich AC, Giménez MS 2012. Cadmium-induced oxidative stress and histological damage in the myocardium. Effects of a soy-based diet. Toxicology and Applied Pharmacology 265: 380-389.

Fillion M, Mergler D, Passos CJ, Larribe F, Lemire M, Guimarães JR 2006. A preliminary study of mercury exposure and blood pressure in the Brazilian Amazon. Environmental Health 5(1): 29-37.

Finkel T and Holbrook NJ 2000. Oxidants, oxidative stress and the biology of ageing. Nature 408(6809): 239-247.

Flack JM, Duncan K, Ohmit SE, Quah R, Liu X, Ramappa P, Norris S, Hedquist L, Dudley A, Nasser SA 2007. Influence of albuminuria and glomerular filtration rate on blood pressure response to antihypertensive drug therapy. Vascular Health and Risk Management (6):1029-1037.

Fleg JL, Lakatta EG 2007. Normal aging of the cardiovascular system. Cardiovascular Disease in the Elderly 1: 1-46.

Flora SJ, Mittal M, Mehta A 2008. Heavy metal induced oxidative stress & its possible reversal by chelation therapy. Indian Journal of Medical Research 128(4): 501-523.

Forouzanfar MH, Liu P, Roth GA, Ng M, Biryukov S, Marczak L, Alexander L, Estep K, Abate KH, Akinyemiju TF, Ali R 2017. Global burden of hypertension and systolic blood pressure of at least 110 to 115 mm Hg, 1990-2015. JAMA 317(2): 165-82.

Förstermann U 2008. Oxidative stress in vascular disease: causes, defense mechanisms and potential therapies. Nature Clinical Practice Cardiovascular Medicine 5: 338-349

Förstermann U 2010. Nitric oxide and oxidative stress in vascular disease. Pflügers Archiv-European Journal of Physiology 459(6): 923-939.

Förstermann U and Sessa WC 2012. Nitric oxide synthases: regulation and function. European Heart Journal 33(7): 829-837.

Franceschini N, Fry RC, Balakrishnan P, Navas-Acien A, Oliver-Williams C, Howard AG, Cole SA, Haack K, Lange EM, Howard BV, Best LG 2017. Cadmium body burden and increased blood pressure in middle-aged American Indians: The Strong Heart Study. Journal of Human Hypertension (3): 225-230.

Freedman JE. 2008. Oxidative stress and platelets. Arteriosclerosis, Thrombosis, and Vascular Biology 28(3): s11-16.

Fresquez MR, Pappas RS, Watson CH 2013. Establishment of toxic metal reference range in tobacco from US cigarettes. Journal of Analytical Toxicology 37(5): 298-304.

Frustaci A, Magnavita N, Chimenti C, Caldarulo M, Sabbioni E, Pietra R, Cellini C, Possati GF, Maseri A 1999. Marked elevation of myocardial trace elements in idiopathic dilated cardiomyopathy compared with secondary cardiac dysfunction. Journal of the American College of Cardiology 33(6): 1578-1583.

Fu J, Lee K, Chuang PY, Liu Z, He JC 2014. Glomerular endothelial cell injury and cross talk in diabetic kidney disease. American Journal of Physiology-Renal Physiology 308(4): F287-297.

Fujiwara Y, Watanabe S, Kaji T 1998. Promotion of cultured vascular smooth muscle cell proliferation by low levels of cadmium. Toxicology Letters 94(3): 175-180.

Fusegawa Y, Goto S, Handa S, Kawada T, Ando Y 1999. Platelet spontaneous aggregation in platelet-rich plasma is increased in habitual smokers. Thrombosis Research 93: 271-278.

Galis ZS, Khatri JJ 2002. Matrix metalloproteinases in vascular remodeling and atherogenesis: the good, the bad, and the ugly. Circulation Research 90: 251-262.

Galrinho RD, Ciobanu AO, Rimbas RC, Manole CG, Leena BM, Vinereanu D 2015. New echocardiographic protocol for the assessment of experimental myocardial infarction in rats. Maedica 10(2): 85-90.

Ganesh T 2013. Prostanoid receptor EP2 as a therapeutic target. Journal of Medicinal Chemistry 57(11): 4454-4465.

Gangwar A, Kumar P, Rawat A, Tiwari S 2014. Noninvasive measurement of systolic blood pressure in rats: A novel technique. Indian Journal of Pharmacology 46(3): 351-352.

García GM, Boffetta P, Caballero KJ, Espanol S, Gómez Q J 2007. Cardiovascular mortality in mercury miners. Medicina Clínica 128(20): 766-771.

García-Niño WR and Pedraza-Chaverrí J 2014. Protective effect of curcumin against heavy metals-induced liver damage. Food and Chemical Toxicology 69: 182-201.

Garner and Levallois P 2016. Cadmium levels and sources of exposure among Canadian adults. Health Reports 27(2): 10-18.

Gaziano TA, Bitton A, Anand S, Abrahams-Gessel S, Murphy A 2010. Growing epidemic of coronary heart disease in low-and middle-income countries. Current Problems in Cardiology 35(2): 72-115.

Gee AC, Sawai RS, Differding J, Muller P, Underwood S, Schreiber MA 2008. The influence of sex hormones on coagulation and inflammation in the trauma patient. Shock (3): 334-341.

Geer CB, Stasko NA, Rus IA, Lord ST, Schoenfisch MH 2008. Influence of glutathione and its derivatives on fibrin polymerization. Biomacromolecules 9: 1876-1822.

Genchi G, Sinicropi M, Carocci A, Lauria G, Catalano A 2017. Mercury exposure and heart diseases. International Journal of Environmental Research And Public Health 14(1): 74-86.

Gerhard-Herman M, Smoot LB, Wake N, Kieran MW, Kleinman ME, Miller DT, Schwartzman A, Giobbie-Hurder A, Neuberg D, Gordon LB 2012. Mechanisms of premature vascular aging in children with Hutchinson-Gilford progeria syndrome. Hypertension 59(1): 92-97.

Gerich JE 2010. Role of the kidney in normal glucose homeostasis and in the hyperglycaemia of diabetes mellitus: therapeutic implications. Diabetic Medicine 27(2): 136-142.

Gersh BJ, Sliwa K, Mayosi BM, Yusuf S 2010. Novel therapeutic concepts. The epidemic of cardiovascular disease in the developing world: global implications. European Heart Journal 31(6): 642-648.

Gerstenblith G, Frederiksen JA, Yin FC, Fortuin NJ, Lakatta EG, Weisfeldt ML 1977. Echocardiographic assessment of a normal adult aging population. Circulation 56(2): 273-278.

Ghatak S, Biswas A, Dhali GK, Chowdhury A, Boyer JL, Santra A 2011. Oxidative stress and hepatic stellate cell activation are key events in arsenic induced liver fibrosis in mice. Toxicology and Applied Pharmacology 251(1): 59-69.

Ghosh J, Murphy MO, Turner N, Khwaja N, Halka A, Kielty CM, Walker MG 2005. The role of transforming growth factor β1 in the vascular system. Cardiovascular Pathology 14(1): 28-36.

Ghosh K, Indra N 2018. Cadmium treatment induces echinocytosis, DNA damage, inflammation, and apoptosis in cardiac tissue of albino Wistar rats. Environmental Toxicology and Pharmacology 59: 43-52.

Giannini EG, Testa R, Savarino V 2005. Liver enzyme alteration: a guide for clinicians. The Canadian Medical Association Journal 172(3): 367-379.

Giddens DP, Zarins CK, Glagov S 1993. The role of fluid mechanics in the localization and detection of atherosclerosis. Journal of Biomechanical Engineering 115(4B): 588-594.

Gillum RF 1976. Pathophysiology of hypertension in blacks and whites: a review of the basis of racial blood pressure differences. Hypertension 1(5): 468-475.

Gimbrone Jr MA, Topper JN, Nagel T, Anderson KR, Garcia-Cardeña GU 2000. Endothelial dysfunction, hemodynamic forces, and atherogenesis a. Annals of the New York Academy of Sciences 902(1): 230-240.

Ginsberg MH, Partridge A, Shattil SJ 2005. Integrin regulation. Current Opinion in Cell Biology 17: 509-516.

Giraldez RR, Panda A, Xia Y, Sanders SP, Zweier JL 1997. Decreased nitric-oxide synthase activity causes impaired endothelium-dependent relaxation in the postischemic heart. Journal of Biological Chemistry 272(34): 21420-21426.

Girotti AW 1998. Lipid hydroperoxides generation, turnover and effectors action in biological systems. Journal of Lipid Research 39: 221-230.

Glauser SC, Bello CT, Glauser EM 1976. Blood-cadmium levels in normotensive and untreated hypertensive humans. The Lancet 307(7962): 717-718.

Gloire G, Legrand-Poels S, Piette J 2006. NF-kappaB activation by reactive oxygen species: fifteen years later. Biochemical Pharmacology 72: 1493-1505.

Goggs R, Poole AW 2012. Platelet signaling–a primer. Journal of Veterinary Emergency And Critical Care 22(1): 5-29.

Golia E, Limongelli G, Natale F, Fimiani F, Maddaloni V, Pariggiano I, Bianchi R, Crisci M, D'Acierno L, Giordano R, Di Palma G 2014. Inflammation and cardiovascular disease: from pathogenesis to therapeutic target. Current Atherosclerosis Reports 16(9): 435-442.

Gomez JF, Zareba W, Moss AJ, McNitt S, Hall WJ 2007. Prognostic value of location and type of myocardial infarction in the setting of advanced left ventricular dysfunction. The American Journal of Cardiology 9(5): 642-646.

Gómez MG, Klink JDC, Boffetta P, Espanol S, Sallsten G, Quintana JG 2007. Exposure to mercury in the mine of Almaden. Occupational and Environmental Medicine 1: 389-395.

González A, Schelbert EB, Díez J, Butler J 2018. Myocardial interstitial fibrosis in heart failure: biological and translational perspectives. Journal of the American College of Cardiology 71(15): 1696-1706.

Gorbet MB, Sefton MV 2004. Biomaterial-associated thrombosis: roles of coagulation factors, complement, platelets and leukocytes. Biomaterials 25(26): 5681-5703.

Gordon EE, Kira YUJI, Demers LM, Morgan HE 1986. Aortic pressure as a determinant of cardiac protein degradation. American Journal of Physiology-Cell Physiology 250(6): C932-C938.

Gourdie RG, Dimmeler S, Kohl P 2016. Novel therapeutic strategies targeting fibroblasts and fibrosis in heart disease. Nature reviews Drug Discovery 15(9): 620-638.

Grabowska-Maślanka A, Janik A, Chłap Z, Szuperska-Ocetkiewicz A, Sławiński M, Grylewski RJ, Korbut R 1988. Influence of cadmium intoxication on thromboresistance of vascular endothelium in rabbits. Journal of Physiology and Pharmacology: an Official Journal of the Polish Physiological Society 49(1): 61-69.

Greilich PE, Carr ME, Zekert SL, Dent RM 1994. Quantitative assessment of platelet function and clot structure in patients with severe coronary artery disease. The American Journal of the Medical Sciences 307(1): 15-20

Gribble MO, Cheng A, Berger RD, Rosman L, Guallar E 2015. Mercury exposure and heart rate variability: a systematic review. Current Environmental Health Reports 2(3): 304-314.

Gross SS, Wolin MS 1995. Nitric oxide: pathophysiological mechanisms. Annual Review of Physiology 57(1): 737-769.

Guzik TJ, Mussa S, Gastaldi D, Sadowski J, Ratnatunga C, Pillai R, Channon KM 2002. Mechanisms of increased vascular superoxide production in human diabetes mellitus: role of NAD(P)H oxidase and endothelial nitric oxide synthase. Circulation 105: 1656-1662.

Haffner HT, Erdelkamp J, Göller E, Schweinsberg F, Schmidt V 1991. Morphological and toxicological findings after intravenous injection of metallic mercury. Deutsche medizinische Wochenschrift 116(36):1342-6.

Hamden K, Carrea USE, Ayadi Marki F, Masmoudi H, El Feki A 2008. Positive effects of green tea on hepatic dysfunction, lipid peroxidation and antioxidant defence depletion induced by cadmium. Biological Research 41(3): 331-339.

Hamilton DL, Bellamy JEC, Valberg JD and Valberg LS 1978. Zinc, cadmium, and iron interactions during intestinal absorption in iron-deficient mice. Canadian Journal of Physiology and Pharmacology 56: 384-389.

Han J, Shuvaev VV, Muzykantov VR 2012. Targeted interception of signaling reactive oxygen species in the vascular endothelium. Therapeutic Delivery 3(2): 263-276.

Hanke H, Strohschneider T, Oberhoff M, Betz E, Karsch KR 1990. Time course of smooth muscle cell proliferation in the intima and media of arteries following experimental angioplasty. Circulation Research 67(3): 651-659.

Hano OS, Bogdanov KY, Sakai MA, Danziger RG, Spurgeon HA, Lakatta EG 1995. Reduced threshold for myocardial cell calcium intolerance in the rat heart with aging. American Journal of Physiology-Heart and Circulatory Physiolog 269(5): H1607-H16012.

Haouem S, Hmad N, Najjar MF, El Hani A, Sakly R 2007. Accumulation of cadmium and its effects on liver and kidney functions in rats given diet containing cadmium-polluted radish bulb. Experimental and Toxicologic Pathology 59(1): 77-80.

Hasenfuss G, Mulieri LA, Leavitt BJ, Allen PD, Haeberle JR, Alpert NR 1992. Alteration of contractile function and excitation-contraction coupling in dilated cardiomyopathy. Circulation Research 70(6): 1225-1232.

Hayward R, Lien CY 2011. Echocardiographic evaluation of cardiac structure and function during exercise training in the developing Sprague-Dawley Rat. Journal of the American Association for Laboratory Animal Science 50(4): 454-461.

Hecht EM, Arheart KL, Lee DJ, Hennekens CH, HlainG WM 2016. Interrelation of cadmium, smoking, and cardiovascular disease (from the National Health and Nutrition Examination Survey). American Journal of Cardiology 118(2): 204-209.

Hees PS, Fleg JL, Lakatta EG, Shapiro EP 2002. Left ventricular remodeling with age in normal men versus women: novel insights using three-dimensional magnetic resonance imaging. The American Journal of Cardiology 90(11): 1231-1236.

Heimark RL, Twardzik DR, Schwartz SM 1986. Inhibition of endothelial regeneration by type-beta transforming growth factor from platelets. Science 233(4768): 1078-1080.

Hein S, Arnon E, Kostin S, Schönburg M, Elsässer A, Polyakova V, Bauer EP, Klövekorn WP, Schaper J 2003. Progression from compensated hypertrophy to failure in the pressure-overloaded human heart: structural deterioration and compensatory mechanisms. Circulation 25; 107(7): 984-991.

Hein S, Schaper J 2001. The extracellular matrix in normal and diseased myocardium. Journal of Nuclear Cardiology 8(2): 188-196.

Helms SA, Azhar G, Zuo C, Theus SA, Bartke A, Wei JY 2010. Smaller cardiac cell size and reduced extra-cellular collagen might be beneficial for hearts of Ames dwarf mice. International Journal of Biological Sciences 6(5): 475-490.

Hendry LM, Sahibdeen V, Choudhury A, Norris SA, Ramsay M, Lombard Z 2018. Insights into the genetics of blood pressure in black South African individuals: the Birth to Twenty cohort. BMC Medical Genomics 11(1): 2-10.

Henríquez-Hernández LA, Boada LD, Carranza C, Pérez-Arellano JL, González-Antuña A, Camacho M, Almeida-González M, Zumbado M, Luzardo OP 2017. Blood levels of toxic metals and rare earth elements commonly found in e-waste may exert subtle effects on hemoglobin concentration in sub-Saharan immigrants. Environment International 109: 20-28.

Heo Y, Parsons PJ, Lawrence DA 1996. Lead differentially modifies cytokine production *in vitro* and *in vivo*. Toxicology and Applied Pharmacology 1: 149-157.

Hernandez M, Macia M 1996. Free peripheral sulfhydryl groups, CD11/CD18 integrins, and calcium are required in the cadmium and nickel enhancement of human-polymorphonuclear leukocyte adherence. Archives of Environmental Contamination and Toxicology 30(4): 437-443.

Hernanz R, Briones AM, Salacies M, Alonso MJ 2014. New roles for old pathways? Acircuitous relationship between reactive oxygen species and cyclooxygenase in hypertension. Clinical Science (Londiin, England: 1979) 126: 111-121

Herselman JE 2007. The concentration of selected trace metals in South African soils. PhD, University of Stellenbosch, Stellenbosch, South Africa.

Hidalgo C and Donoso P 2008. Crosstalk between calcium and redox signaling: from molecular mechanisms to health implications. Antioxidants and Redox Signaling 10(7): 1275-1312.

Hill JA and Olson EN 2012. Muscle: Fundamental Biology and Mechanisms of Disease. Amsterdam: Elsevier/Academic Press, 1-17.

Holmes P, James KA, Levy LS 2009. Is low-level environmental mercury exposure of concern to human health?. Science of the total environment 408(2): 171-82.

Horiguchi H, Oguma E, Kayama F 2011. Cadmium induces anemia through interdependent progress of hemolysis, body iron accumulation, and insufficient erythropoietin production in rats. Toxicological Sciences 122(1): 198-210.

Hounkpatin ASY, Edorh PA, Guédénon P, Alimba CG, Ogunkanmi A, Dougnon TV, Boni G, Aissi KA, Montcho S, Loko F, Ouazzani N 2013. Haematological evaluation of Wistar rats exposed to chronic doses of cadmium, mercury and combined cadmium and mercury. African Journal of Biotechnology 12(23): 3731-3737.

Hounkpatin ASY, Johnson RC, Guedenon P, Domingo E, Alimba CG, Boko M, Edorh PA 2012. Protective effects of vitamin C on haematological parameters in intoxicated Wistar rats with cadmium, mercury and combined cadmium and mercury. International Research Journal of Biological Sciences 1(8): 76-81.

Houston MC 2007. The role of mercury and cadmium heavy metals in vascular disease, hypertension, coronary heart disease, and myocardial infarction. Alternative Therapies in Health and Medicine 13(2): S128-S133.

Houston MC 2012. Role of mercury toxicity in hypertention, cardiovascular disease and stroke. The Journal of Clinical Hypertention 13(8): 621-627

Houston MC 2014. The role of mercury in cardiovascular disease. Journal of Cardiovascular Disease and Diagnostics 2: 1-8.

Hu KH, Li WX, Sun MY, Zhang SB, Fan CX, Wu Q, Zhu W, Xu X 2015 Cadmium induced apoptosis in MG63 cells by increasing ROS, activation of p38 MAPK and inhibition of ERK 1/2 pathways. Cellular Physiology and Biochemistry 36(2): 642-654.

Hu XF, Singh K, Chan HM 2018. Mercury exposure, blood pressure, and hypertension: a systematic review and dose–response meta-analysis. Environmental Health Perspectives 126(7): 1-15

Huh JH, Choi SI, Lim JS, Chung CH, Shin JY, Lee MY 2015. Lower serum creatinine is associated with low bone mineral density in subjects without overt nephropathy. PloS one 10(7): 1-11.

Hulthe J and Fagerberg B 2002. Circulating oxidized LDL is associated with subclinical atherosclerosis development and inflammatory cytokines (AIR Study). Arteriosclerosis, Thrombosis, and Vascular Biology 22(7): 1162-1167.

Husain N, Mahmood R 2017. Hexavalent chromium induces reactive oxygen species and impairs the antioxidant power of human erythrocytes and lymphocytes: Decreased metal reducing and free radical quenching ability of the cells. Toxicology and Industrial Health 33(8): 623-635.

Huss JM, Kelly DP 2005. Mitochondrial energy metabolism in heart failure: a question of balance. The Journal of Clinical Investigation 115(3): 547-55.

Hussain M and Mumtaz S 2014. E-waste: impacts, issues and management strategies. Reviews on Environmental Health 29 (1-2): 53-58.

Hutchison KJ, Karpinski E 1985. *In vivo* demonstration of flow recirculation and turbulence downstream of graded stenoses in canine arteries. Journal of Biomechanics 18(4): 285-296.

Iavicoli I, Fontana L, Bergamaschi A 2009. The effects of metals as endocrine disruptors. Journal of Toxicology and Environmental Health, Part B 12(3): 206-223.

Ichikawa H, Ronowicz K, Hicks M, Gebicki JM 1987. Lipid peroxidation is not the cause of lysis of human erythrocytes exposed to inorganic or methylmercury. Archives of Biochemistry and Biophysics 259(1): 46-51.

Iino M, O'Donnell CJ Burke MP 2009. Post-mortem CT findings following intentional ingestion of mercuric chloride. Legal Medicine 11(3): 136-138.

Imafidon CE, Olukiran OS, Ogundipe, DJ, Eluwole AO, Adekunle IA, Oke GO 2018. Acetonic extract of *Vernonia amygdalina* (Del.) attenuates Cd-induced liver injury: Potential application in adjuvant heavy metal therapy. Toxicology Reports 5: 324-332.

Inokubo Y, Hanada H, Ishizaka H, Fukushi T, Kamada T, Okumura K 2001. Plasma levels of matrix metalloproteinase-9 and tissue inhibitor of metalloproteinase-1 are increased in the coronary circulation in patients with acute coronary syndrome. American Heart Journal 141(2): 211-217.

Intengan HD and Schiffrin EL 2001. Vascular remodeling in hypertension roles of apoptosis, inflammation, and fibrosis. Hypertension 38(3): 581-587

Iwanaga Y, Aoyama T, Kihara Y, Onozawa Y, Yoneda T, Sasayama S 2002. Excessive activation of matrix metalloproteinases coincides with left ventricular remodeling during transition from hypertrophy to heart failure in hypertensive rats. Journal of the American College of Cardiology 39(8): 1384-1391.

Jagadeesan G, Pillai SS 2007. Hepatoprotective effects of taurine against mercury induced toxicity in rat. Journal of Environmental Biology 28(4): 753-756.

Jaimes EA, DeMaster EG, Tian RX, Raij L 2004. Stable compounds of cigarette smoke induce endothelial superoxide anion production via NADPH oxidase activation. Arteriosclerosis, Thrombosis, and Vascular Biology 24(6): 1031-1036.

Janicki JS and Brower GL 2002. The role of myocardial fibrillar collagen in ventricular remodeling and function. Journal of Cardiac Failure 8(6): S319-S325.

Järup L 2003. Hazards of heavy metal contamination. British Medical Bulletin 68(1): 167-182.

Jawalekar SL, Kulkarni UJ, Surve VT, Deshmukh YA 2010. Status of lipid profile, MDA and protein carbonyl in patients with cardiovascular diseases. Archives of Appled Science Research 2(6): 8-14.

Jeong EM, Moon CH, Kim CS, Lee SH, Baik EJ, Moon CK, Jung YS 2004. Cadmium stimulates the expression of ICAM-1 via NF-κB activation in cerebrovascular endothelial cells. Biochemical And Biophysical Research Communications 320(3): 887-892.

Jeremy JY, Rowe D, Emsley AM, Newby AC 1999. Nitric oxide and the proliferation of vascular smooth muscle cells. Cardiovascular Research 43(3): 580-594.

Jessup M, Brozena SC 2003. Heart failure. New England Journal of Medicine 348: 2007-2018.

Jha P, Peto R 2014. Global effects of smoking, of quitting, and of taxing tobacco. New England Journal of Medicine 370(1): 60-68.

Ji YL, Wang H, Meng C, Zhao XF, Zhang C., Zhang Y, Zhao M, Chen YH, Meng XH, Xu DX 2012. Melatonin alleviates cadmium-induced cellular stress and germ cell apoptosis in testes. Journal of Pineal Research 52(1): 71-79.

Jia Q, Zhu X, Hao Y, Yang Z, Wang Q, Fu H, Yu H 2018. Mercury in soil, vegetable and human hair in a typical mining area in China: Implication for human exposure. Journal of Environmental Sciences 68: 73-82.

Jiang G, Duan W, Xu L, Song S, Zhu C, Wu L 2009. Biphasic effect of cadmium on cell proliferation in human embryo lung fibroblast cells and its molecular mechanism. Toxicology in Vitro 23(6): 973-978.

Jomova K, Valko M 2011. Advances in metal-induced oxidative stress and human disease. Toxicology 283(2-3): 65-87.

Jones ES, David Spence J, Mcintyre AD, Nondi J, Gogo K, Akintunde A, Hackam DG, Rayner BL 2017. High frequency of variants of candidate genes in black Africans with low renin-resistant hypertension. American Journal of Hypertension 30(5): 478-483.

Jorreskog G, Egberg N, Fagrell B, Fatah K, Hessel B, Jhonsson H, Brismar K, Blomback M 1996. Altered properties of the fibrin gel structure in patients with IDDM. Diabetologia 39: 1519-1523.

Joshi D, Mittal DK, Shukla S, Srivastav AK, Srivastav SK 2014. N-acetyl cysteine and selenium protects mercuric chloride-induced oxidative stress and antioxidant defense system in liver and kidney of rats: a histopathological approach. Journal of Trace Elements in Medicine and Biology 28(2): 218-226.

Jung E, Hyun W, Ro Y, Lee H, Song K 2016. A study on blood lipid profiles, aluminum and mercury levels in college students. Nutrition Research and Practice 10(4): 442-447.

Kaji T, Fujiwara Y, Yamamoto C, Sakamoto M, Kozuka H 1994. Stimulation by zinc of cultured vascular endothelial cell proliferation: possible involvement of endogenous basic fibroblast growth factor. Life Sciences 55(23): 1781-1787.

Kaji T, Suzuki M, Yamamoto C, Mishima A, Sakamoto M, Kozuka H 1995. Severe damage of cultured vascular endothelial cell monolayer after simultaneous exposure to cadmium and lead. Archives of Environmental Contamination and Toxicology 28(2): 168-172.

Kaji T. Cell biology of heavy metal toxicity in vascular tissue 2004. Yakugaku zasshi: Journal of the Pharmaceutical Society of Japan 124(3): 113-20.

Kampa M and Castanas E 2008. Human health effects of air pollution. Environmental Pollution 151: 362-367.

Kang SJ, Kim D, Park HE, Chung GE, Choi SH, Choi SY, Lee W, Kim JS, Cho SH 2013. Elevated serum bilirubin levels are inversely associated with coronary artery atherosclerosis. Atherosclerosis 230(2): 242-248.

Karaboduk H, Uzunhisarcikli M, Kalender Y 2015. Protective effects of sodium selenite and vitamin e on mercuric chloride-induced cardiotoxicity in male rats. Brazilian Archives of Biology and Technology 58(2): 229-238.

Karmakar R, Bhattacharya R, Chatterjee M 2000. Biochemical, haematological and histopathological study in relation to time-related cadmium-induced hepatotoxicity in mice. Biometals 13: 231-239.

Kassiri Z, Oudit GY, Sanchez O, Dawood F, Mohammed FF, Nuttall RK, Edwards DR, Liu PP, Backx PH, Khokha R 2005. Combination of tumor necrosis factor-α ablation and matrix metalloproteinase inhibition

prevents heart failure after pressure overload in tissue inhibitor of metalloproteinase-3 knock-out mice. Circulation Research 97(4): 380-390.

Katsumi A, Naoe T, Matsushita T, Kaibuchi K Schwartz MA 2005. Integrin activation and matrix binding mediate cellular responses to mechanical stretch. Journal of Biological Chemistry 280(17): 16546-16549.

Kawashima S, Yokoyama M 2004. Dysfunction of endothelial nitric oxide synthase and atherosclerosis. Arteriosclerosis, Thrombosis, and Vascular Biology 24(6): 998-1005.

Kazemi S, Khalili-Fomeshi M, Akbari A, Kani, SNM, Ahmadian SR, Ghasemi-Kasman M 2018. The correlation between nonylphenol concentration in brain regions and resulting behavioral impairments. Brain Research Bulletin 139: 190-196.

Kehinde BA, Abbasi N, Abolhassani F, Rastegar T, Daneshi E, Abbasi M 2016. The effects of an experimentally induced unilateral varicose ovarian vein on the activities of anti-oxidant enzymes in an adult rat ovary. International Journal of Morphology 34(4): 1436-1441.

Keil DE, Berger-Ritchie J, McMillin GA 2011. Testing for toxic elements: a focus on arsenic, cadmium, lead, and mercury. Laboratory Medicine 42(12): 735-742.

Kell DB, Pretorius E 2017. Proteins behaving badly. Substoichiometric molecular control and amplification of the initiation and nature of amyloid fibril formation: lessons from and for blood clotting. Progress in Biophysics and Molecular Biology 123: 16-41.

Kellermann K, Müller M, Blobner M, Kochs EF, Jungwirth B 2014. Influence of gender and sex hormones on blood coagulation and fibrinolysis after normothermic cardiopulmonary bypass in rats: 4AP1-8. European Journal of Anaesthesiology 31: 52-53.

Kerek E, Hassanin M Prenner EJ 2018. Inorganic mercury and cadmium induce rigidity in eukaryotic lipid extracts while mercury also ruptures red blood cells. Biochimica et Biophysica Acta (BBA)-Biomembranes 1860(3): 710-717.

Kielty CM, Stephan S, Sherratt MJ, Williamson M, Shuttleworth CA 2007. Applying elastic fibre biology in vascular tissue engineering. Philosophical Transactions of the Royal Society of London B: Biological Sciences 362(1484): 1293-1312.

Kim KS, Lim HJ, Lim JS, Son JY, Lee J, Lee BM, Chang SC, Kim HS 2018. Curcumin ameliorates cadmium-induced nephrotoxicity in Sprague-Dawley rats. Food and Chemical Toxicology 114: 34-40.

Kim NH and Kang PM 2010. Apoptosis in cardiovascular diseases: mechanism and clinical implications. Korean Circulation Journal 40(7): 299-305

Kishimoto T, Oguri T, Ohno M, Matsubara K, Yamamoto K, Tada M 1994. Effect of cadmium ($CdCl_2$) on cell proliferation and production of EDRF (endothelium-derived relaxing factor) by cultured human umbilical arterial endothelial cells. Archives of Toxicology 68(9): 555-9.

Klocke R, Tian W, Kuhlmann MT Nikol S 2007. Surgical animal models of heart failure related to coronary heart disease. Cardiovascular Research 74(1): 29-38.

Knebel SM, Elrick MM, Bowles EA, Zdanovec AK, Stephenson AH, Ellsworth ML, Sprague RS 2013. Synergistic effects of prostacyclin analogs and phosphodiesterase inhibitors on cyclic adenosine 3′,5′ monophosphate accumulation and adenosine 3′,5′ triphosphate release from human erythrocytes. Experimental Biology and Medicine 238(9): 1069-1074.

Kobal AB, Tratnik JS, Mazej D, Fajon V, Gibičar D, Miklavčič A, Kocman D, Kotnik J, Briški AS, Osredkar J, Krsnik M 2017. Exposure to mercury in susceptible population groups living in the former mercury mining town of Idrija, Slovenia. Environmental Research 152: 434-445.

Kokoszka JE, Coskun P, Esposito LA, Wallace DC 2001. Increased mitochondrial oxidative stress in the Sod2 (+/−) mouse results in the age-related decline of mitochondrial function culminating in increased apoptosis. Proceedings of the National Academy of Sciences 98(5): 2278-2283.

Kopp SJ, Glonek T, Erlanger M, Perry EF, Bárány M, Perry Jr HM 1980. Altered metabolism and function of rat heart following chronic low level cadmium/lead feeding. Journal of Molecular and Cellular Cardiology 12(12): 1407-1425.

Kopp SJ, Glonek T, Perry HM, Erlanger M, Perry EF 1982. Cardiovascular actions of cadmium at environmental exposure levels. Science 217(4562): 837-839.

Koschel K, Meissner NN, Tas PW 1995. Influence of cadmium ions on endothelin-1 binding and calcium signaling in rat glioma C6 cells. Toxicology Letters 81(2-3): 189-195.

Kostin S, Pool L, Elsässer A, Hein S, Drexler HC, Arnon E, Hayakawa Y, Zimmermann R, Bauer E, Klövekorn WP, Schaper J 2003. Myocytes die by multiple mechanisms in failing human hearts. Circulation Research 92(7): 715-724.

Kowalczyk E, Jankowski A, Niedworok J, Smigielski J, Tyslerowicz P 2002. Effect of long term cadmium intoxication on selected biochemical parameters in experimental animals. Polish Journal of Environmental Studies 11: 599-601.

Kozel BA, Ciliberto CH, Mecham RP 2004. Deposition of tropoelastin into the extracellular matrix requires a competent elastic fiber scaffold but not live cells. Matrix Biology 23(1): 23-34.

Kubes P, Suzuki M, Granger DN 1991. Nitric oxide: an endogenous modulator of leukocyte adhesion. Proceedings of the National Academy of Sciences 88(11): 4651-4655.

Kukongviriyapan U, Pannangpetch P, Kukongviriyapan V, Donpunha W, Sompamit K, Surawattanawan P 2014. Curcumin protects against cadmium-induced vascular dysfunction, hypertension and tissue cadmium accumulation in mice. Nutrients 6(3): 1194-1208.

Kumar N, Krishnani KK, Gupta SK, Singh NP 2017. Cellular stress and histopathological tools used as biomarkers in *Oreochromis mossambicus* for assessing metal contamination. Environmental Toxicology and Pharmacology 49: 137-147.

Kumar PV, Pricy AA, Kumar CS, Goud GK 2010. Hepatoprotective effect of green tea (*Camellia sinesis*) on cadmium chloride induced toxicity in rats. Journal of Chemical and Pharmaceutical Research 2(6): 125-128.

Kumar SV, Bose R, Bhattacharya S 2001. Low doses of heavy metals disrupt normal structure and function of rat platelets. Journal of Environmental Pathology, Toxicology and Oncology 20(1): 65-75.

Kumar SV, Maitra S, Bhattacharya S 2002. *In vitro* binding of inorganic mercury to the plasma membrane of rat platelet affects Na+-K+-ATPase activity and platelet aggregation. BioMetals 15(1): 51-57.

Kung G, Konstantinidis K, Kitsis RN 2011. Programmed necrosis, not apoptosis, in the heart. Circulation Research 108(8): 1017-1036.

Kusaka Y, Kelly RA, Williams GH, Kifor I 2000. Coronary microvascular endothelial cells cosecrete angiotensin II and endothelin-1 via a regulated pathway. American Journal of Physiology-Heart and Circulatory Physiology 279(3): H1087-H1096.

Kuster GM, Hauselmann SP, Rosc-Schluter BI, Lorenz V, Pfister O 2010. Reactive oxygen/nitrogen species and the myocardial cell homeostasis: an ambiguous relationship. Antioxidant and Redox Signalling 13: 1899-1910.

Kutalek R, Wewalka G, Gundacker C, Auer H, Wilson J, Haluza D, Huhulescu S, Hillier S, Sager M, Prinz A 2010. Geophagy and potential health implications: geohelminths, microbes and heavy metals. Transactions of the Royal Society of Tropical Medicine and Hygiene 104(12): 787-795.

Kuwabara A, Satoh M, Tomita N, Sasaki T, Kashihara N 2010. Deterioration of glomerular endothelial surface layer induced by oxidative stress is implicated in altered permeability of macromolecules in Zucker fatty rats. Diabetologia 53(9): 2056-2065.

Kuwahara M, Sugimoto M, Tsuji S, Matsui H, Mizuno T, Miyata S, Yoshioka A 2002. Platelet shape changes and adhesion under high shear flow. Arteriosclerosis, Thrombosis, and Vascular Biology 22(2): 329-334.

Kyselovic J, Martinka P, Batova Z, Gazova A, Godfraind T 2005. Calcium channel blocker inhibits Western-type diet-evoked atherosclerosis development in ApoE-deficient mice. Journal of Pharmacology and Experimental Therapeutics 315(1): 320-328.

Lakatta EG 1992. Functional implications of spontaneous sarcoplasmic reticulum Ca^{2+} release in the heart. Cardiovascular Research 26(3): 193-214.

Lakatta EG, Levy D 2003. Arterial and cardiac aging: major shareholders in cardiovascular disease enterprises: Part I: aging arteries: a "set up" for vascular disease. Circulation 107(1): 139-146.

Lakatta EG, Sollott SJ, Pepe S 2001. The old heart: operating on the edge. In Ageing Vulnerability: Causes and Interventions: Novartis Foundation Symposium 235 (Vol. 235, pp. 172-201). Chichester, UK: John Wiley & Sons, Ltd.

Lakatta EG, Wang M, Najjar SS 2009. Arterial aging and subclinical arterial disease are fundamentally intertwined at macroscopic and molecular levels. Medical Clinics of North America 93(3): 583-604.

Landmesser U, Dikalov S, Price SR, McCann L, Fukai T, Holland SM, Mitch WE, Harrison DG 2003. Oxidation of tetrahydrobiopterin leads to uncoupling of endothelial cell nitric oxide synthase in hypertension. Journal of Clinical Investigation 111: 1201–1209

Lang E, Lang F 2015. Mechanisms and pathophysiological significance of eryptosis, the suicidal erythrocyte death. In Seminars in Cell & Developmental Biology 39: 35-42. Academic Press.

Lang F, Qadri SM 2012. Mechanisms and significance of eryptosis, the suicidal death of erythrocytes. Blood Purification 33(1-3): 125-130.

Lannoy M, Slove S, Jacob MP 2014. The function of elastic fibers in the arteries: beyond elasticity. Pathologie Biologie 62(2): 79-83.

Laugesen M, Epton M, Frampton M, Glover M, Lea RA 2009. Hand-rolled cigarette smoking patterns compared with factory-made cigarette smoking in New Zealand men. BMC Public Health 9(1): 194-199.

Laughlin MH, Newcomer SC, Bender SB 2008. Importance of hemodynamic forces as signals for exercise-induced changes in endothelial cell phenotype. Journal of Applied Physiology 104(3): 588-600.

Le MT, Hassanin M, Mahadeo M, Gailer J, Prenner EJ 2013. Hg-and Cd-induced modulation of lipid packing and monolayer fluidity in biomimetic erythrocyte model systems. Chemistry and Physics of Lipids 170: 46-54.

Leask A 2015. Getting to the heart of the matter: new insights into cardiac fibrosis. Circulatory Research 116: 1269-1276.

Leduc D, De Francquen P, Jacobovitz D, Vandeweyer R, Lauwerys R, De Vuyst P 1993. Association of cadmium exposure with rapidly progressive emphysema in a smoker. Thorax 48(5): 570-571.

Lee DH, Blomhoff R, Jacobs DR 2004. Review is serum gamma glutamyltransferase a marker of oxidative stress? Free Radical Research 38(6): 535-539.

Lee DH, Ha MH, Kim JH, Christiani DC, Gross MD, Steffes M, Blomhoff R, Jacobs DR 2003a. Gamma-glutamyltransferase and diabetes—a 4 year follow-up study. Diabetologia 46(3): 359-364.

Lee DH, Jacobs DR, Gross M, Kiefe CI, Roseman J, Lewis CE, Steffes M 2003b. γ-glutamyltransferase is a predictor of incident diabetes and hypertension: The Coronary Artery Risk Development in Young Adults (CARDIA) Study. Clinical Chemistry 49(8): 1358-1366.

Lee J, Giordano S, Zhang J 2012. Autophagy, mitochondria and oxidative stress: cross-talk and redox signalling. Biochemical Journal 441(2): 523-40.

Lee MS, Park SK, Hu H, Lee S 2011. Cadmium exposure and cardiovascular disease in the 2005 Korea National Health and Nutrition Examination Survey. Environmental Research 111: 171-176.

Lee PK, Choi BY, Kang MJ 2015. Assessment of mobility and bio-availability of heavy metals in dry depositions of Asian dust and implications for environmental risk. Chemosphere 119: 1411-1421.

Lee S, Yoon JH, Won JU, Lee W, Lee JH, Seok H, Kim YK, Kim CN, Roh J 2016. The association between blood mercury levels and risk for overweight in a general adult population: results from the Korean National Health and Nutrition Examination Survey. Biological Trace Element Research 171(2): 251-261.

Lee YK, Park EY, Kim S, Son JY, Kim TH, Kang WG, Jeong TC, Kim KB, Kwack SJ, Lee J, Kim, S 2014. Evaluation of cadmium-induced nephrotoxicity using urinary metabolomic profiles in Sprague-Dawley male rats. Journal of Toxicology and Environmental Health Part A 77(22-24): 1384-1398.

Lei W, Wang L, Liu D, Xu T, Luo J 2011. Histopathological and biochemical alternations of the heart induced by acute cadmium exposure in the freshwater crab *Sinopotamon yangtsekiense*. Chemosphere 84(5): 689-694.

Lemasters JJ 2005. Selective mitochondrial autophagy, or mitophagy, as a targeted defense against oxidative stress, mitochondrial dysfunction, and aging. Rejuvenation Research 8: 3-5.

Lemos NB, Angeli JK, de Oliveira Faria T, Junior RFR, Vassallo DV, Padilha AS, Stefanon I 2012. Low mercury concentration produces vasoconstriction, decreases nitric oxide bioavailability and increases oxidative stress in rat conductance artery. PLoS One 7(11): 1-12

Leong XF, Aishah A, Aini UN, Das S, Jaarin K 2008. Heated palm oil causes rise in blood pressure and cardiac changes in heart muscle in experimental rats. Archives of Medical Research 39(6): 567-572.

Lesnefsky EJ, Moghaddas S, Tandler B, Kerner J, Hoppel CL 2001. Mitochondrial dysfunction in cardiac disease: ischemia–reperfusion, aging, and heart failure. Journal of Molecular and Cellular Cardiology 33(6): 1065-1089.

Levenson JW, Skerrett PJ, Gaziano JM 2002. Reducing the global burden of cardiovascular disease: the role of risk factors. Preventive Cardiology 5(4): 188-99.

Li H, Horke S, Förstermann U 2013. Oxidative stress in vascular disease and its pharmacological prevention. Trends in Pharmacological Sciences 34(6): 313-319.

Li H, Witte K, August M, Brausch I, Gödtel-Armbrust U, Habermeier A, Closs EI, Oelze M, Münzel T, Förstermann U 2006. Reversal of endothelial nitric oxide synthase uncoupling and up-regulation of endothelial nitric oxide synthase expression lowers blood pressure in hypertensive rats. Journal of the American College of Cardiology 47(12): 2536-2544.

Li P, Feng X, Qiu G, Shang L, Wang S 2012. Mercury pollution in Wuchuan mercury mining area, Guizhou, Southwestern China: The impacts from large scale and artisanal mercury mining. Environment International 42: 59-66.

Li R, Wu H, Ding J, Fu W, Gan L, Li Y 2017. Mercury pollution in vegetables, grains and soils from areas surrounding coal-fired power plants. Scientific reports 7: 1-9

Liang X, Wu L, Wang Q, Hand T, Bilak M, McCoughlan L, Andreasson K 2007. Function of COX-2 and prostaglandins in neurological disease. Journal of Molecular Neuroscience 33: 94-99.

Liao X, Sluimer JC, Wang Y, Subramanian M, Brown K, Pattison SJ, Robbins J, Martinez J,Tabas I 2012. Macrophage autophagy plays a protective role in advanced atherosclerosis. Cell Metabolism 15(4): 545-553.

Liaw L, Lombardi DM, Almeida MM, Schwartz SM, DeBlois D, Giachelli CM 1997. Neutralizing antibodies directed against osteopontin inhibit rat carotid neointimal thickening after endothelial denudation. Arteriosclerosis, Thrombosis, and Vascular Biology 17(1): 188-193.

Lim KM, Kim S, Noh JY, Kim K, Jang WH, Bae ON, Chung SM, Chung JH 2010. Low-level mercury can enhance procoagulant activity of erythrocytes: a new contributing factor for mercury-related thrombotic disease. Environmental Health Perspectives 118(7): 928-935.

Lindh U, Danersund A Lindvall A 1996. Selenium protection against toxicity from cadmium and mercury studied at the cellular level. Cellular and Molecular Biology 42(1): 39-48.

Lipinski B, Pretorius E, Oberholzer HM, Van Der Spuy WJ 2012. Iron enhances generation of fibrin fibres in human blood: implications for pathogenesis of stroke. Microscopic Research Techniques 75: 1185-1190.

Lopez AD, Mathers CD, Ezzati M, Jamison DT, Murray CJL 2006. Global and regional burden of disease and risk factors, 2001: systematic analysis of population health data. Lancet 367: 1747-1757.

López B, González A, Querejeta R, Larman M, Díez J 2006. Alterations in the pattern of collagen deposition may contribute to the deterioration of systolic function in hypertensive patients with heart failure. Journal of the American College of Cardiology 48(1): 89-96.

López-Rodríguez G, Galván M, González-Unzaga M, Ávila JH, Pérez-Labra M 2017. Blood toxic metals and hemoglobin levels in Mexican children. Environmental Monitoring and Assessment 189(4): 179-184.

Louw VJ, Du Preez P, Malan A, Van Deventer L, Van Wyk D, Joubert G 2007. Pica and food craving in adults with iron deficiency in Bloemfontein, South Africa. South African Medical Journal 97(11): 1069-1071.

Low S, Zhang X, Ang K, Yeo SJD, Lim GJ, Yeoh LY, Liu YL, Subramaniam T, Sum CF, Lim SC 2018. Discovery and validation of serum creatinine variability as novel biomarker for predicting onset of albuminuria in Type 2 diabetes mellitus. Diabetes Research and Clinical Practice 138: 8-15.

Lu KP, Zhao SH, Wang DS 1990. The stimulatory effect of heavy metal cations on proliferation of aortic smooth muscle cells. Science in China. Series B, Chemistry, Life Sciences and Earth Sciences 33(3): 303-310.

Luevano J and Damodaran C 2014. A review of molecular events of cadmium-induced carcinogenesis. Journal of Environmental Pathology, Toxicology and Oncology 33(3): 183-194.

Luippold G, Beilharz M, Mühlbauer B 2004. Chronic renal denervation prevents glomerular hyperfiltration in diabetic rats. Nephrology Dialysis Transplantation 19(2): 342-347.

Lund BO, Miller DM, Woods JS 1993. Studies on Hg (II)-induced H_2O_2 formation and oxidative stress in vivo and in vitro in rat kidney mitochondria. Biochemical Pharmacology 45(10): 2017-2024.

Lupescu A, Jilani K, Zelenak C, Zbidah M, Qadri SM, Lang F 2012. Hexavalent chromium-induced erythrocyte membrane phospholipid asymmetry. Biometals 25(2): 309-318.

Lusilao-Makiese JG, Cukrowska EM, Tessier E, Amouroux D and Weiersbye I 2013. The impact of post gold mining on mercury pollution in the West Rand region, Gauteng, South Africa. Journal of Geochemical Exploration 134: 111-119.

Madamanchi NR and Runge MS 2007. Mitochondrial dysfunction in atherosclerosis. Circulation Research 100(4): 460-473.

Madejczyk MS, Baer CE, Dennis WE, Minarchick VC, Leonard SS, Jackson DA, Stallings JD Lewis JA 2015. Temporal changes in rat liver gene expression after acute cadmium and chromium exposure. PloS One 10(5): 1-27.

Madigan M, Zuckerbraun B 2013. Therapeutic potential of the nitrite-generated NO pathway in vascular dysfunction. Frontiers in Immunology 4: 174-183.

Magnani JW, Dec GW 2006. Myocarditis: current trends in diagnosis and treatment. Circulation 113(6): 876-90.

Mahmoud AA, Elshazly SM 2014. Ursodeoxycholic acid ameliorates fructose-induced metabolic syndrome in rats. PLoS One 9(9): 1-8.

Mäki JM, Tikkanen H, Kivirikko KI 2001. Cloning and characterization of a fifth human lysyl oxidase isoenzyme: the third member of the lysyl oxidase-related subfamily with four scavenger receptor cysteine-rich domains. Matrix Biology 20(7): 493-496.

Malan M, Müller F, Cyster L, Raitt L and Aalbers J 2015. Heavy metals in the irrigation water, soils and vegetables in the Philippi horticultural area in the Western Cape Province of South Africa. Environmental Monitoring and Assessment 187: 1-8.

Mallion JM, Hamici L, Chatellier G, Lang T, Plouin PF, De Gaudemaris R 2003. Isolated systolic hypertension: data on a cohort of young subjects from a French working population (IHPAF). Journal of Human Hypertension 17(2): 93-100.

Manna SK, Sarkar S, Barr J, Wise K, Barrera EV, Jejelowo O, Rice-Ficht AC, Ramesh GT 2005. Single-walled carbon nanotube induces oxidative stress and activates nuclear transcription factor-κB in human keratinocytes. Nano Letters 5(9): 1676-1684.

Maramba NP, Reyes JP, Francisco-Rivera AT, Panganiban LC, Dioquino C, Dando N, Timbang R, Akagi H, Castillo MT, Quitoriano C, Afuang M 2006. Environmental and human exposure assessment monitoring of communities near an abandoned mercury mine in the Philippines: A toxic legacy. Journal of Environmental Management 81(2): 135-145.

Marchi R, Lundberg U, Grimbergen J, Koopman J, Torres A, de Bosch NB, Haverkate F, Piñango CLA 2000. Fibrinogen Caracas V, an abnormal fibrinogen with an Aα 532 Ser→Cys substitution associated with thrombosis. Thrombosis and Haemostasis 83(02): 263-270.

Marín-García J, Goldenthal MJ 2008. Mitochondrial centrality in heart failure. Heart Failure Reviews 13(2):137-150.

161

Marín-García J, Goldenthal MJ, Pierpont ME, Ananthakrishnan R 1995. Impaired mitochondrial function in idiopathic dilated cardiomyopathy: biochemical and molecular analysis. Journal of Cardiac Failure 1(4): 285-291.

Markiewicz-Górka I, Januszewska L, Michalak A, Prokopowicz A, Januszewska E, Pawlas N, Pawlas K 2015. Effects of chronic exposure to lead, cadmium, and manganese mixtures on oxidative stress in rat liver and heart. Archives of Industrial Hygiene and Toxicology 66(1): 51-62.

Martinez M, Weisel J, Ischiropoulos H 2013. Functional impact of oxidative posttranslational modifications on fibrinogen and fibrin clots. Free Radical Biology and Medicine 65: 411-418.

Mashimo K, Sato S, Ohno Y 2003. Chronic effects of ethanol on cultured myocardial cells: ultrastructural and morphometric studies. Virchows Archiv: European Journal of Pathology 442(4): 356-363.

Massion PB, Feron O, Dessy C, Alligand JL 2003. Nitric oxide and cardiac function ten years after and continuing. Circulation Research 93(5): 388-398.

Mather A, Pollock C 2011. Glucose handling by the kidney. Kidney International 79: S1-S6.

Mathew R, Karp CM, Beaudoin B, Vuong N, Chen G, Chen HY, Bray K, Reddy A, Bhanot G, Gelinas C, DiPaola RS 2009. Autophagy suppresses tumorigenesis through elimination of p62. Cell 137(6): 1062-1075.

Matović V, Buha A, Bulat Z, Đukić-Ćosić D 2011. Cadmium toxicity revisited: focus on oxidative stress induction and interactions with zinc and magnesium. Archives of Industrial Hygiene and Toxicology 62(1): 65-76.

Matsuhashi T, Karbowski M, Liu X, Usukura J, Wozniak M, Wakabayashi T 1998. Complete suppression of ethanol-induced formation of megamitochondria by 4-hydroxy-2, 2, 6, 6-tetramethyl-piperidine-1-oxyl (4-OH-TEMPO). Free Radical Biology and Medicine 24(1): 139-147.

Matsuno K, Yamada H, Iwata K, Jin D, Katsuyama M, Matsuki M, Takai S, Yamanishi K, Miyazaki M, Matsubara H, Yabe-Nishimura C 2005. Nox1 is involved in angiotensin II-mediated hypertension: a study in Nox1-deficient mice. Circulation 112: 2677-2685.

Matsuura I, Lourenco E, Grossman J, Skaggs B, McMahon M 2016. SAT0304 coagulation factor XIII might be a promising marker for predicting atherosclerosis in SLE. Annals of the Rheumatic Diseases 75: 778-778.

Matyas C, Varga ZV, Mukhopadhyay P, Paloczi J, Lajtos T, Erdelyi K, Nemeth BT, Nan M, Hasko G, Gao B, Pacher P 2016. Chronic plus binge ethanol feeding induces myocardial oxidative stress, mitochondrial and cardiovascular dysfunction, and steatosis. American Journal of Physiology-Heart and Circulatory Physiology 310(11): H1658-H1670.

Maurice P, Blaise S, Gayral S, Debelle L, Laffargue M, Hornebeck W, Duca L 2013. Elastin fragmentation and atherosclerosis progression: the elastokine concept. Trends in Cardiovascular Medicine 23(6): 211-221.

Maxwell AJ, Cooke JP 1998. Cardiovascular effects of L-arginine. Current Opinion in Nephrology And Hypertension 7(1): 63-70.

McCullagh KJ, Cooney R, O'Brien T 2016. Endothelial nitric oxide synthase induces heat shock protein HSPA6 (HSP70B′) in human arterial smooth muscle cells. Nitric Oxide 52: 41-48.

McEniery CM, Franklin SS, Cockcroft JR, Wilkinson IB 2016. Isolated systolic hypertension in young people is not spurious and should be treatedresponse to isolated systolic hypertension in young people is not spurious and should be treated: pro side of the argument: pro side of the argument. Hypertension 68(2): 269-275.

McEniery CM, Yasmin, Wallace S, Maki-Petaja K, McDonnell B, Sharman JE, Retallick C, Franklin SS, Brown MJ, Lloyd RC, Cockcroft JR 2005. Increased stroke volume and aortic stiffness contribute to isolated systolic hypertension in young adults. Hypertension 46(1): 221-226.

Meel BL 2012. Geophagia in Transkei region of South Africa. African Health Sciences 12(4): 566-568.

Mendis S, Alwan A, eds. 2011. Prioritized research agenda for prevention and control of noncommunicable diseases. Geneva, World Health Organization, 2011. 1-58

Menke A, Muntner P, Silbergeld EK, Platz EA, Guallar E 2009. Cadmium levels in urine and mortality among US adults. Environmental Health Perspectives 117(2): 190-196.

Mieiro CL, Ahmad I, Pereira ME, Duarte AC, Pacheco M 2010. Antioxidant system breakdown in brain of feral gulden grey mullet (*Liza aurata*) as an effect of mercury exposure. Ecotoxicology 19: 1034-1045.

Millasseau SC, Stewart AD, Patel SJ, Redwood SR, Chowienczyk PJ 2005. Evaluation of carotid-femoral pulse wave velocity: influence of timing algorithm and heart rate. Hypertension 45(2):222-226.

Miller Jr FJ, Sharp WJ, Fang X, Oberley LW, Oberley TD, Weintraub NL 2002. Oxidative stress in human abdominal aortic aneurysms: a potential mediator of aneurysmal remodeling. Arteriosclerosis, Thrombosis, and Vascular Biology 22(4): 560-565.

Mills JD, Ariëns RAS, Mansfield, Grant PJ 2002. Altered fibrin clot structure in the relatives of patients with premature coronary artery disease. Circulation 106: 1938-1942

Mlynek V, Skoczyńska A 2005. The proinflammatory activity of cadmium. Advances in Hygiene and Experimental Medicine 59: 1-8.

Moalic JM, Bercovici J, Swynghedauw B 1984. Myosin heavy chain and actin fractional rates of synthesis in normal and overload rat heart ventricles. Journal of Molecular and Cellular Cardiology 16(10): 875-884.

Monroe DM, Hoffman M 2012. The clotting system–a major player in wound healing. Haemophilia 18: 11-6.

Monteiro DA, Rantin FT, Kalinin AL 2010: Inorganic mercury exposure: toxicological effects, oxidative stress biomarkers and bioaccumulation in the tropical freshwater fish matrinxa, *Brycon amazonicus* (Spix and Agassiz, 1829). Ecotoxicology 19: 105-123

Moore-Morris T, Guimarães-Camboa N, Yutzey KE, Pucéat M, Evans SM 2015. Cardiac fibroblasts: from development to heart failure. Journal of Molecular Medicine 93(8): 823-830.

Morales CR, Pedrozo Z, Lavandero S, Hill JA 2014. Oxidative stress and autophagy in cardiovascular homeostasis. Oxidants and Redox Signalling 20(3): 507-518

Moran AE, Roth GA, Narula J, Mensah GA 2014. 1990-2010 Global Cardiovascular Disease Atlas. Glob Heart 1: 3-16

Morgan HE, Siehl D, Chua BH, Lautensack-Belser N 1985. Faster protein and ribosome synthesis in hypertrophying heart. Basic Research in Cardiology 80: 115-118.

Morgan MJ and Liu ZG 2011. Crosstalk of reactive oxygen species and NF-κB signaling. Cell Research 21(1): 103-115.

Mortada WI, Sobh MA, El-Defrawy MM Farahat S.E 2002. Reference intervals of cadmium, lead, and mercury in blood, urine, hair, and nails among residents in Mansoura city, Nile Delta, Egypt. Environmental Research 90(2): 104-110.

Mosesson MW, Siebenlist KR, Meh DA 2001. The structure and biological features of fibrinogen and fibrin. Annals of the New York Academy of Science 936: 11-30.

Moyes CD, Hood DA 2003. Origins and consequences of mitochondrial variation in vertebrate muscle. Annual Review of Physiology 65(1): 177-201.

Munakata M, Hattori T, Konno S 2017. Relationship between subtle urinary albumin excretion and risk of incident hypertension: modification by glomerular filtration rate. Hypertension Research 40(12): 994-998.

Mungrue IN, Gros R, You X, Pirani A, Azad A, CsontT, Schulz R, Butany J, Stewart DJ, Husain, M 2002. Cardiomyocyte overexpression of iNOS in mice results in peroxynitrite generation, heart block, and sudden death. The Journal of Clinical Investigation 109(6): 735-774.

Nagase H, Visse R, Murphy G 2006. Structure and function of matrix metalloproteinases and TIMPs. Cardiovascular Research 69(3): 562-573.

Naicker K, Cukrowska E and McCarthy TS 2003. Acid mine drainage arising from gold mining activity in Johannesburg, South Africa and environs. Environmental Pollution 122: 29-40.

Nair AB, Jacob S 2016. A simple practice guide for dose conversion between animals and human. Journal of Basic and Clinical Pharmacy 7(2): 27-37.

Nair AR, DeGheselle O, Smeets K, Van Kerkhove E, Cuypers A 2013. Cadmium-induced pathologies: where is the oxidative balance lost (or not)?. International Journal of Molecular Sciences 14(3): 6116-6143.

Nair CH, Azhar A, Wilson JD, Dhall D 1991. Studies on fibrin network structure in human plasma. Part II-Clinical application: diabetes and antidiabetic drugs. Thrombosis Research 64(4): 477-485.

Nakagawa H, Nishijo M 1996. Environmental cadmium exposure, hypertension and cardiovascular risk. Journal of Cardiovascular Risk 3(1): 11-17.

Nakamura T, Lozano PR, Ikeda Y, Iwanaga Y, Hinek A, Minamisawa S, Cheng CF, Kobuke K, Dalton N, Takada Y, Tashiro K 2002. Fibulin-5/DANCE is essential for elastogenesis *in vivo*. Nature 415(6868): 171-175.

Navas-Acien A, Guallar E, Silbergeld EK, Rothenberg SJ 2006. Lead exposure and cardiovascular disease-a systematic review. Environmental Health Perspectives 115(3): 472-482.

Navas-Acien A, Selvin E, Sharrett AR, Calderon-Aranda E, Silbergeld E, Guallar E 2004. Lead, cadmium, smoking, and increased risk of peripheral arterial disease. Circulation 109(25): 3196-3201.

Navas-Acien A, Silbergeld EK, Sharrett R, Calderon-Aranda E,Selvin E, Guallar E 2005. Metals in urine and peripheral arterial disease. Environmental Health Perspectives 113(2): 164-169.

Navas-Acien A, Tellez-Plaza M, Guallar E, Muntner P, Silbergeld E, Jaar B, Weaver V 2009. Blood cadmium and lead and chronic kidney disease in US adults: a joint analysis. American Journal of Epidemiology. 170(9): 1156-1164.

Nawrot TS, Staessen JA, Roels HA, Munters E, Cuypers A, Richart T, Ruttens A, Smeets K, Clijsters H, Vangronsveld J 2010. Cadmium exposure in the population: from health risks to strategies of prevention. Biometals 23(5): 769-782.

Ndhlala AR, Stafford GI, Finnie JF, Van Staden J 2011. Commercial herbal preparations in KwaZulu- Natal, South Africa: The urban face of traditional medicine. South African Journal of Botany 77(4): 830- 843.

Necib YO, Bahi AH, Zerizer S 2013. Amelioration of mercuric chloride toxicity on rat liver with Argan oil and sodium selenite supplements. International Journal of Pharma and Bio Sciences 4(2): 839-849.

Nedeljkovic ZS, Gokce N, Loscalzo J 2003. Mechanisms of oxidative stress and vascular dysfunction. Postgraduate Medical Journal 79(930):195-200.

Nediani C, Raimondi L, Borchi E Cerbai E 2011. Nitric oxide/reactive oxygen species generation and nitroso/redox imbalance in heart failure: from molecular mechanisms to therapeutic implications. Antioxidants and Redox Signaling 14: 289-331.

Nemchenko A, Chiong M, Turer A, Lavandero S, Hill JA 2011. Autophagy as a therapeutic target in cardiovascular disease. Journal of Molecular and Cellular Cardiology 51(4): 584-593.

Newby LK, Christenson RH, Ohman EM, Armstrong PW, Thompson TD, Lee KL, Hamm CW, Katus HA, Cianciolo C, Granger CB, Topol EJ 1998. Value of serial troponin T measures for early and late risk stratification in patients with acute coronary syndromes. Circulation 98(18): 1853-1859.

Nichols WW 2005. Clinical measurement of arterial stiffness obtained from noninvasive pressure waveforms. American Journal of Hypertension 18(S1): 3S-10S.

Nichols WW, Denardo SJ, Wilkinson IB, McEniery CM, Cockcroft J, O'rourke MF 2008. Effects of arterial stiffness, pulse wave velocity, and wave reflections on the central aortic pressure waveform. The Journal of Clinical Hypertension 10(4): 295-303.

Nilssen O, Førde OH, Brenn T 1990. The Tromsø Study: distribution and population determinants of gamma-glutamyltransferase. American Journal of Epidemiology 132(2): 318-326.

Nilsson PM, Boutouyrie P, Cunha P, Kotsis V, Narkiewicz K, Parati G, Rietzschel E, Scuteri A, Laurent S 2013. Early vascular ageing in translation: from laboratory investigations to clinical applications in cardiovascular prevention. Journal of Hypertension 31(8): 1517-1526.

Nilsson PM, Boutouyrie P, Laurent S 2009. Vascular aging: a tale of EVA and ADAM in cardiovascular risk assessment and prevention. Hypertension 54(1): 3-10.

Nilsson PM, Lurbe E, Laurent S 2008. The early life origins of vascular ageing and cardiovascular risk: the EVA syndrome. Journal of Hypertension 26(6): 1049-1057.

Nishino I, Fu J, Tanji K, Yamada T, Shimojo S, Koori T, Mora M, Riggs JE, Oh SJ, Koga Y, Sue CM, Yamamoto A, Murakami N, Shanske S, Byrne E, Bonilla E, Nonaka I, DiMauro S, and Hirano M 2000. Primary LAMP-2 deficiency causes X-linked vacuolar cardiomyopathy and myopathy (Danon disease). Nature 406: 906-910.

Nordberg GF, Nogawa K, Nordberg M, Friberg LT 2007. Cadmium. In: Handbook of Toxicology of Metals. Nordberg GF, Nogawa K, Nordberg M, and Friberg LT, editors. Academic Press Inc., Amsterdam and Boston, pp 445-486.

Norton GR, Tsotetsi J, Trifunovic B, Hartford C, Candy GP, Woodiwiss AJ 1997. Myocardial stiffness is attributed to alterations in cross-linked collagen rather than total collagen or phenotypes in spontaneously hypertensive rats.Circulation 96(6): 1991-1998.

Novelli ELB, Marques SFG, Almeida JA, Diniz YS, Faine LA, Ribas BO 2000. Mechanism of cadmium exposure on cardiac tissue Toxic Substances Mechanisms 19: 207–217.

Nwokocha C, Ejebe D, Nwangwa E, Ekene N, Akonoghrere R, Ukwu J 2010. The effects of bitter kola supplemented diet on hepatotoxicity of mercury in Wistar rats. Journal of Applied Sciences and Environmental Management 14(1): 89-95.

Nyström E, Bengtsson C, Lindstedt G, Lapidus L, Lindquist O, Waldenström J 1988. Serum gamma-glutamyltransferase in a Swedish female population: age-related reference intervals; morbidity and prognosis in cases with raised catalytic concentration. Acta Medica Scandinavica 224(1): 79-84.

Oberholster PJ, Myburgh JG, Ashton PJ, Botha AM 2010. Responses of phytoplankton upon exposure to a mixture of acid mine drainage and high levels of nutrient pollution in Lake Loskop, South Africa. Ecotoxicology and Environmental Safety 73(3): 326-335.

Ognjanovic BI, Pavlovic SZ, Maletic SD, Zikic RV, Stajn AS, Radojicic RM, Saicic ZS, Petrovic VM 2003. Protective influence of vitamin E on antioxidant defense system in the blood of rats treated with cadmium. Physiological Research 52: 563-570.

Ohara Y, Peterson TE, Zheng B, Kuo JF, Harrison DG 1994. Lysophosphatidylcholine increases vascular superoxide anion production via protein kinase C activation. Arteriosclerosis, Thrombosis, and Vascular Biology 14(6): 1007-1013.

Oliver-Williams C, Howard AG, Navas-Acien A, Howard BV, Tellez-Plaza M, Franceschini N 2018. Cadmium body burden, hypertension, and changes in blood pressure over time: results from a prospective cohort study in American Indians. Journal of the American Society of Hypertension 12(6): 426-437.

Olsen MH, Christensen MK, Wachtell K, Tuxen C, Fossum E, Bang LE, Wiinberg N, Devereux RB, Kjeldsen SE, Hildebrandt P, Dige-Petersen H 2005. Markers of collagen synthesis is related to blood pressure and vascular hypertrophy: a LIFE substudy. Journal of Human Hypertension 19(4): 301-307.

Olson H, Betton G, Robinson D, Thomas K, Monro A, Kolaja G, Lilly P, Sanders J, Sipes G, Bracken W, Dorato M 2000. Concordance of the toxicity of pharmaceuticals in humans and in animals. Regulatory Toxicology and Pharmacology 32(1): 56-67.

Olszowski T, Baranowska-Bosiacka I, Gutowska I, Chlubek D 2012. Pro-inflammatory properties of cadmium. Acta Biochimica Polonica 59(4): 475-482.

Omanwar S and Fahim M 2015. Mercury exposure and endothelial dysfunction: an interplay between nitric oxide and oxidative stress.International Journal of Toxicology 34(4): 300-307.

Organisation for Economic Co-operation and Development (OECD) 2001. Guidance Document on Acute Oral Toxicity Testing 24: 1-24.

Ozbek E 2012. Induction of oxidative stress in kidney. International Journal of Nephrology 1: 1-10

Ozturk IM, Buyukakilli B, Balli E, Cimen B, Gunes S, Erdogan S 2009. Determination of acute and chronic effects of cadmium on the cardiovascular system of rats. Toxicology Mechanisms and Methods 19(4): 308-317.

Pacyna EG, Pacyna JM, Steenhuisen F and Wilson S 2006. Global anthropogenic mercury emission inventory for 2000. Atmospheric Environment 40(22): 4048-4063.

Pal M, Ghosh M 2012. Prophylactic effect of α-linolenic acid and α- eleostearic acid against MeHg induced oxidative stress, DNA damage and structural changes in RBC membrane. Food and Chemical Toxicology 50: 2811-2818.

Palatini P 2012. Glomerular hyperfiltration: a marker of early renal damage in pre-diabetes and pre-hypertension. Nephrology Dialysis Transplantation 27(5): 1708-1714

Pari L, Murugavel P 2007. Diallyl tetrasulfide improves cadmium induced alterations of acetylcholinesterase, ATPases and oxidative stress in brain of rats. Toxicology 234(1-2): 44-50.

Park JD and Zheng W 2012. Human exposure and health effects of inorganic and elemental mercury. Journal of Preventive Medicine and Public Health 45(6): 344-352.

Park Y, Lee A, Choi K, Kim HJ, Lee JJ, Choi G, Kim S, Kim SY, Cho GJ, Suh E, Kim SK 2018. Exposure to lead and mercury through breastfeeding during the first month of life: A CHECK cohort study. Science of the Total Environment 612: 876-883.

Passos CJ, Mergler D, Fillion M, Lemire M, Mertens F, Guimarães JR, Philibert A 2007. Epidemiologic confirmation that fruit consumption influences mercury exposure in riparian communities in the Brazilian Amazon. Environmental Research 105(2): 183-193.

Pattison JS, Osinska H, and Robbins J 2011. Atg7 induces basal autophagy and rescues autophagic deficiency in CryABR120G cardiomyocytes. Circulatory Research 109: 151-160.

Payliss BJ, Hassanin M, Prenner EJ 2015. The structural and functional effects of Hg (II) and Cd (II) on lipid model systems and human erythrocytes: A review. Chemistry and Physics of Lipids 193: 36-51.

Pearson CA, Lamar PC, Prozialeck WC 2003. Effects of cadmium on E-cadherin and VE-cadherin in mouse lung. Life Sciences 72(11): 1303-1320.

Peer N, Steyn K, Dennison CR, Levitt NS, Nyo MT, Nel JH, Commerford PJ, Fourie JM, Hill MN. 2008. Determinants of target organ damage in black hypertensive patients attending primary health care services in Cape Town: the Hi-Hi study. American Journal of Hypertension 21(8): 896-902.

Penta KL, Fairweather D, Shirley DL, Rose NR, Silbergeld EK, Nyland JF 2015. Low-dose mercury heightens early innate response to coxsackievirus infection in female mice. Inflammation Research 64(1): 31-40.

Peraza MA, Ayala-Fierro F, Barber DS, Casarez E, Rael LT 1998. Effects of micronutrients on metal toxicity. Environmental Health Perspectives 106(suppl 1): 203-216.

Pérez-Gómez F, Bover R 2007. The new coagulation cascade and its possible influence on the delicate balance between thrombosis and hemorrhage. Revista Espanola De Cardiologia 60(12): 1217-1219.

Petering HG, Murthy L, Sorenson JR, Levin L, Stemmer KL 1979. Effect of sex on oral cadmium dose responses in rats: blood pressure and pharmacodynamics. Environmental Research 20(2): 289-299.

Pinto E, Sigaud-kutner TCS, Leitão MAS, Okamoto OK, Morse D, Colepicolo P 2003. Heavy metal induced oxidative stress in algae. Phycology 39: 1008-1018.

Polsinelli VB, Satchidanand N, Singh R, Holmes D, Izzo Jr JL 2017. Hypertension and aging in rural Haiti: results from a preliminary survey. Journal of Human Hypertension 31(2): 138-144.

Ponteva M, Elomaa I, Ba¨ckman H, Hansson L, Kilpio J 1979. Blood cadmium and plasma zinc measurements in acute myocardial infarction. European Journal of Cardiology 9(5): 379-391.

Popkin BM 1998. The nutrition transition and its health implications in lower-income countries. Public Health Nutrition 1(1): 5-21.

Popkin BM, Gordon-Larsen P 2004. The nutrition transition: worldwide obesity dynamics and their determinants. International Journal of Obesity and Related Metabolic Disorders 28(Suppl 3):S2eS9.

Pretorius E 2013. The adaptability of red blood cells. Cardiovascular diabetology 12(1): 63-70.

Pretorius E and Kell DB 2014. Diagnostic morphology: biophysical indicators for iron-driven inflammatory diseases. Integrative Biology 6(5): 486-510.

Pretorius E, Bester J, Vermeulen N, Alummoottil S, Soma P, Buys AV, Kell DB 2015. Poorly controlled type 2 diabetes is accompanied by significant morphological and ultrastructural changes in both erythrocytes and in thrombin-generated fibrin: implications for diagnostics. Cardiovascular Diabetology 14(1): 30-50.

Pretorius E, du Plooy JN, Bester J 2016. A comprehensive review on eryptosis. Cellular Physiology and Biochemistry 39(5): 1977-2000.

Pretorius E, du Plooy JN, Soma P, Keyser I, Buys AV 2013. Smoking and fluidity of erythrocyte membranes: A high resolution scanning electron and atomic force microscopy investigation. Nitric Oxide 35: 42-46.

Pretorius E, Lipinski B 2013. Differences in morphology of fibrin clots induced with thrombin and ferric ions and its pathophysiological consequences. Heart, Lung and Circulation 22(6): 447-449.

Pretorius E, Oberholzer HM, van der Spuy WJ, Meiring JH 2010. Smoking and coagulation: the sticky fibrin phenomenon. Ultrastructural Pathology 34(4): 236-239.

Pretorius E, Oore-ofe O, Mbotwe S Bester J 2016. Erythrocytes and their role as health indicator: Using structure in a patient-orientated precision medicine approach. Blood Reviews 30(4): 263-274

Pretorius E, Steyn H, Engelbrecht M, Swanepoel AC, Oberholzer HM 2011. Differences in fibrin fiber diameters in healthy individuals and thromboembolic ischemic stroke patients. Blood Coagulation and Fibrinolysis 22(8): 696-700.

Pretorius E, Swanepoel AC, Buys AV, Vermeulen N, Duim W, Kell DB 2014. Eryptosis as a marker of Parkinson's disease. Aging 6:788-819.

Pretorius E, Vermeulen N, Bester J, Lipinski B 2013a. Novel use of scanning electron microscopy for detection of iron induced morphological changes in human blood. Microscopy Research Techniques 76: 268-271.

Pretorius E, Vermeulen N, Bester J, Lipinski B 2013b. Oxidation inhibits iron induced blood coagulation. Current Drug Targets 14: 13-19.

Pritchard KA Jr, Groszek L, Smalley DM, Sessa WC, Wu M, Villalon P, Wolin MS, Stemerman MB 1995. Native low-density lipoprotein increases endothelial cell nitric oxide synthase generation of superoxide anion. Circulation Research 77: 510–518

Prozialeck WC 2000. Evidence that E-cadherin may be a target for cadmium toxicity in epithelial cells 2000. Toxicology and Applied Pharmacology 164(3): 231-249.

Prozialeck WC, Edwards JR 2012. Mechanisms of cadmium-induced proximal tubule injury: new insights with implications for biomonitoring and therapeutic interventions. Journal of Pharmacology and Experimental Therapeutics 343(1): 2-12.

Prozialeck WC, Edwards JR, Nebert DW, Woods JM, Barchowsky A, Atchison WD 2008. The vascular system as a target of metal toxicity. Toxicological Sciences 102(2): 207-218

Pua HH, Guo J, Komatsu M, He YW 2009. Autophagy is essential for mitochondrial clearance in mature T lymphocytes. The Journal of Immunology 182(7): 4046-4055.

Puri V, Saha S 2003. Comparison of acute cardiovascular effects of cadmium and captopril in relation to oxidant and angiotensin converting enzyme activity in rats. Drug and Chemical Toxicology 26(3): 213-218.

Rabenstein DL, Isab AA 1982. A proton nuclear magnetic resonance study of the interaction of mercury with intact human erythrocytes. Biochimica et Biophysica Acta (BBA)-Molecular Cell Research 721(4): 374-384.

Radad K, Hassanein K, Al-Shraim M, Moldzio R, Rausch WD 2014. Thymoquinone ameliorates lead-induced brain damage in Sprague Dawley rats. Experimental and Toxicologic Pathology 66(1): 13-17.

Rafacho BP, Azevedo PS, Polegato BF, Fernandes AA, Bertoline MA, Fernandes DC, Chiuso-Minicucci F, Roscani MG, dos Santos PP, Matsubara LS, Matsubara BB 2011. Tobacco smoke induces ventricular remodeling associated with an increase in NADPH oxidase activity. Cellular Physiology and Biochemistry 27(3-4): 305-312.

Rajaee M, Sánchez BN, Renne EP, Basu N 2015. An investigation of organic and inorganic mercury exposure and blood pressure in a small-scale gold mining community in Ghana. International Journal of Environmental Research and Public Health 12(8): 10020-10038.

Rajasekaran NS, Connell P, Christians ES, Yan LJ, Taylor RP, Orosz A, Zhang XQ, Stevenson TJ, Peshock, RM, Leopold JA, Barry WH 2007. Human αB-crystallin mutation causes oxido-reductive stress and protein aggregation cardiomyopathy in mice. Cell 130(3): 427-439.

Ramakrishnan R, Elangovan P, Pari L 2017. Protective role of tetrahydrocurcumin: an active polyphenolic curcuminoid on cadmium-induceddoxidative damage in rats. Applied Biochemistry and Biotechnology 183(1): 51-69.

Rana MN, Tangpong J, Rahman MM 2018. Toxicodynamics of lead, cadmium, mercury and arsenic-induced kidney toxicity and treatment strategy: A mini review. Toxicology Reports 5: 704-713.

Rana SVS 2008. Metals and apoptosis: recent developments. Journal of Trace Elements in Medicine and Biology 22(4): 262-284.

Rana SVS, Singh R, Verma S 1995. Mercury-induced lipid peroxidation in the liver, kidney, brain and gills of a fresh water fish *Channa punctatus*. Japanese Journal of Ichthyology 42: 255-259.

Rani A, Kumar A, Lal A, Pant M 2014. Cellular mechanisms of cadmium-induced toxicity: a review. International Journal of Environmental Health Research 24(4): 378-399.

Rao AK 2013. Inherited platelet function disorders; overview and disorders of granules, secretion and signal transduction. Haematology/Oncology Clinics of North America 24: 585-611.

Ravikumar B, Sarkar S, Davies JE, Futter M, Garcia-Arencibia M, Green-Thompson ZW, Jimenez-Sanchez M, Korolchuk VI, Lichtenberg M, Luo S, Massey DC 2010. Regulation of mammalian autophagy in physiology and pathophysiology. Physiological Reviews 90(4): 1383-1435.

Razani B, Chu Feng C, Coleman T, Emanuel R, Wen H, Hwang S, Ting JP, Virgin HW, Michael BK, Semenkovich CF 2012. Autophagy links inflammasomes to atherosclerotic progression. Cell Metabolism 15(4): 534-544.

Rebelo FM, Caldas ED 2016. Arsenic, lead, mercury and cadmium: Toxicity, levels in breast milk and the risks for breastfed infants. Environmental Research 151: 671-688.

Redza-Dutordoir M, Averill-Bates DA 2016. Activation of apoptosis signalling pathways by reactive oxygen species. Biochimica et Biophysica Acta (BBA)-Molecular Cell Research 1863(12): 2977-2992.

Reedy J, Krebs-Smith SM, Miller PE, Liese AD, Kahle LL, Park Y, Subar AF 2014. Higher diet quality is associated with decreased risk of all-cause, cardiovascular disease, and cancer mortality among older adults The Journal of Nutrition 144(6): 881-889.

Remya S, Chikku AM, Renjith RS, Arunima S, Rajamohan T 2013. Coconut kernel protein in diet protects the heart by beneficially modulating endothelial nitric oxide synthase, tumor necrosis factor-alpha, and nuclear factor-kappaB expressions in experimental myocardial infarction. Journal of Food and Drug Analysis. 21(3): 325-31.

Renugadevi J, Prabu SM 2010. Cadmium-induced hepatotoxicity in rats and the protective effect of naringenin. Experimental and Toxicologic Pathology 62(2): 1711-81.

Ricchiuti V, Voss EM, Ney A, Odland M, Anderson PA, Apple FS 1998. Cardiac troponin T isoforms expressed in renal diseased skeletal muscle will not cause false-positive results by the second generation cardiac troponin T assay by Boehringer Mannheim. Clinical Chemistry 1998 44(9): 1919-1924.

Rice KM, Walker Jr EM, Wu M, Gillette C, Blough ER 2014. Environmental mercury and its toxic effects. Journal of Preventive Medicine and Public Health 47(2): 74-83.

Ridker PM, Buring JE, Shih J, Matias M, Hennekens CH 1998. Prospective study of C-reactive protein and the risk of future cardiovascular events among apparently healthy women. Circulation 98(8): 731-733.

Riemschneider S, Herzberg M, Lehmann J 2015. Subtoxic doses of cadmium modulate inflammatory properties of murine RAW 264.7 macrophages. Biomed Research International 1: 1-8

Rival J, Riddle JM, Stein PD 1987. Effects of chronic smoking on platelet function. Thrombosis Research 45(1): 75-85.

Rodrigues Filho S and Maddock JEL 1997. Mercury pollution in two gold mining areas of the Brazilian Amazon. Journal of Geochemical Exploration 58(2): 231-240.

Rodriguez-Fernandez R, Rahajeng E, Viliani F, Kushadiwijaya H, Amiya RM, Bangs MJ 2015. Non-communicable disease risk factor patterns among mining industry workers in Papua, Indonesia: longitudinal findings from the Cardiovascular Outcomes in a Papuan Population and Estimation of Risk (COPPER) Study. Occupational and Environmental Medicine 72(10): 728-735.

Rodriguez-Manas L, El-Assar M, Vallejo S, Lopez-Doriga P, Solis J, Petidier R, Montes M, Nevado J, Castro M, Gomez-Guerrero C, Peiro C, Sanchez-Ferrer CF 2009. Endothelial dysfunction in aged humans is related with oxidative stress and vascular inflammation. Aging Cell 8(3): 226-238.

Roitman EV, Azizova OA, Morozov YA, Aseichev AV 2004. Effect of oxidized fibrinogens on blood coagulation. Bulletin of Experimental Biology and Medicine, 138(9): 245-247.

Röllin HB, Rudge CV, Thomassen Y, Mathee A, Odland JØ. 2009. Levels of toxic and essential metals in maternal and umbilical cord blood from selected areas of South Africa—results of a pilot study. Journal Environmental Monitering 11(3): 618-627.

Rosenkranz S 2004. TGF-β1 and angiotensin networking in cardiac remodeling. Cardiovascular Research. 63(3): 423-432.

Rubanyi GM, Romero JC, Vanhoutte PM 1986. Flow-induced release of endothelium-derived relaxing factor. American Journal of Physiology-Heart and Circulatory Physiology 250(6): H1145-H1149.

Rubinsztein DC, Mariño G, Kroemer G 2011. Autophagy and aging. Cell 146(5): 682-695.

Rucklidge GJ, Milne G, McGaw BA, Milne E, Robins SP 1992. Turnover rates of different collagen types measured by isotope ratio mass spectrometry. Biochimica et Biophysica Acta (BBA)-General Subjects 1156(1): 57-61.

Rudic RD, Sessa WC 1999. Nitric oxide in endothelial dysfunction and vascular remodeling: clinical correlates and experimental links. American Journal of Human Genetics 64(3): 673-677.

Rui L 2011. Energy metabolism in the liver. Comprehensive Physiology 4(1): 177-197.

Ruiz-Feria CA, Zhang D, Nishimura H 2004. Age-and sex-dependent changes in pulse pressure in fowl aorta. Comparative Biochemistry and Physiology Part A: Molecular and Integrative Physiology 137(2) 311-320.

Sabolić I, Breljak D, Herak-Kramberger CM, Ljubojević M 2013. Cadmium and metallothionein. In Encyclopedia of Metalloproteins pp. 342-352. Springer New York.

Sabra A, Lawrence MJ, Obaid D, Chase A, Smith D, Thomas P, Hawkins K, Williams PR, Morris K, Evans PA 2018. Validation of fractal dimension of the incipient blood clot in semi and stable coronary artery disease. The Lancet 383: S91-S91.

Sagai M and Bocci V 2011. Mechanism of action involved in Ozone therapy: is healing induced via a mild oxidative stress? Medical Gas Research 1: 29-46.

Sakariassen KS, Joss R, Muggli R, Kuhn H, Tschopp TB, Sage H, Baumgartner HR 1990. Collagen type III induced *ex vivo* thrombogenesis in humans. Role of platelets and leukocytes in deposition of fibrin. Arteriosclerosis, Thrombosis, and Vascular Biology 10(2): 276-284.

Sakariassen KS, Orning L, Turitto VT 2015. The impact of blood shear rate on arterial thrombus formation. Future science OA 1(4): 1-9.

Salonen JT, Nyyssönen K, Salonen R, Lakka HM, Kaikkonen J, Porkkala-Sarataho E, Voutilainen S, T. A. Lakka TA, Rissanen T, Leskinen L, Tuomainen TP, Valkonen VP, Ristonmaa U, Poulsen HE 2000. Antioxidant Supplementation in Atherosclerosis Prevention (ASAP) study: a randomized trial of the effect of vitamins E and C on 3-year progression of carotid atherosclerosis. Journal of Internal Medicine 248(5): 377-386.

Salonen, JT, Seppänen K, Nyyssönen K, Korpela H, Kauhanen J, Kantola M, Tuomilehto J, Esterbauer H, Tatzber F, Salonen R 1995. Intake of mercury from fish, lipid peroxidation, and the risk of myocardial infarction and coronary, cardiovascular, and any death in eastern Finnish men. Circulation 91(3): 645-655.

Sanders D, Dudley M, Groban L 2009. Diastolic dysfunction, cardiovascular aging, and the anaesthesiologist. Anaesthesiology Clinics 27(3): 497-517.

Sangani RG, Soukup JM, Ghio AJ 2010. Metals in air pollution particles decrease whole-blood coagulation time. Inhalation Toxicology 22(8): 621-626.

Sarikaya S, Karcioglu O, Ay D, Cetin A, Aktas C, Serinken M 2010. Acute mercury poisoning: a case report. BMC Emergency Medicine 10(1): 7-10.

Satarug S, Baker JR, Reilly PE, Esumi H, Moore MR 2000. Evidence for a synergistic interaction between cadmium and endotoxin toxicity and for nitric oxide and cadmium displacement of metals in the kidney. Nitric Oxide 4(4):431-40.

Satarug S, Moore MR 2004. Adverse health effects of chronic exposure to low-level cadmium in foodstuffs and cigarette smoke. Environmental Health Perspectives 112(10):1099-1103.

Sauriasari R, Sakano N, Wang DH, Takaki J, Takemoto K, Wang B, Sugiyama H, Sato Y, Takigawa T, Takahashi N, Kanbara S 2010. C-reactive protein is associated with cigarette smoking-induced hyperfiltration and proteinuria in an apparently healthy population. Hypertension Research 33(11): 1129-1136.

Schultz JE, Witt SA, Glascock BJ, Nieman ML, Reiser PJ, Nix SL, Kimball TR, Doetschman T 2002. TGF-β1 mediates the hypertrophic cardiomyocyte growth induced by angiotensin II. The Journal of Clinical Investigation 109(6): 787-796.

Schulz E, Wenzel P, Münzel T, Daiber A 2014. Mitochondrial redox signalling: interaction of mitochondrial reactive oxygen species with other sources of oxidative stress. Antioxidants and Redox Signalling 20(2): 308-324.

Schumacher L, Abbott LC 2017. Effects of methyl mercury exposure on pancreatic beta cell development and function. Journal of Applied Toxicology 37(1): 4-12.

Scott EM, Ariens RAS, Grant PJ 2004. Genetic and environmental determinants of fibrin structure and function: relevance to clinical disease. Atherosclerosis, Thrombosis and Vascular Biology 24: 1558-1566.

Seddon M, Shah AM, Casadei B 2007. Cardiomyocytes as effectors of nitric oxide signalling. Cardiovascular Research 75(2): 315-326.

Sengupta P 213. The laboratory rat: relating its age with human's. International Journal of Preventive Medicine 4(6): 624-630.

Sepulveda J, Murray C 2014. The state of global health in 2014. Science 345: e1275-e1278.

Shacter E, Williams JA, Levine RL 19955. Oxidative modification of fibrinogen inhibits thrombin-catalyzed clot formation. Free Radical Biology and Medicine 18(4): 815-821.

Shah AM, MacCarthy PA 2000. Paracrine and autocrine effects of nitric oxide on myocardial function. Pharmacology and Therapeutics 86(1): 49-86.

Shaikh ZA, Vu TT and Zaman K 1999. Oxidative stress as a mechanism of chronic cadmium-Induced hepatotoxicity and renal toxicity and protection by antioxidants. Toxicological and Applied Pharmacology 154: 256-263.

Shao D, Oka S, Brady CD, Haendeler J, Eaton P, Sadoshima J 2012. Redox modification of cell signalling in the cardiovascular system. Journal of Molecular and Cellular Cardiology 52: 550-558.

Shao ZH, Becker LB, Hoek TL, Schumacker PT, Li CQ, Zhao D, Wojcik K, Anderson T, Qin Y, Dey L, Yuan CS 2003. Grape seed proanthocyanidin extract attenuates oxidant injury in cardiomyocytes. Pharmacological Research 47(6): 463-469.

Sharma B, Singh S, Siddiqi NJ 2014. Biomedical implications of heavy metals induced imbalances in redox systems. Biomed Research International 1: 1-26

Sharma DC, Sharma PK, Sharma KK, Mathur JS, Singh PP 1998. Histochemical study of the metabolism and toxicity of mercury. Current Science 57(9): 483-485.

Sharma RK, Agrawal M 2005. Biological effects of heavy metals: an overview. Journal of Environmental Biology 26(2): 301-313.

Sheetz MP, Singer SJ 1974. Biological membranes as bilayer couples. A molecular mechanism of drug-erythrocyte interactions. Proceedings of the National Academy of Sciences 71(11): 4457-4461.

Sheikh TJ, Patel BJ, Joshi DV, Patel RB, Jegoda MD 2013. Repeated dose oral toxicity of inorganic mercury in Wistar rats: biochemical and morphological alterations. Veterinary World 6(8): 563-567.

Shirwany A and Weber KT 2006. Extracellular matrix remodeling in hypertensive heart disease. Journal of the American Coledge of Cardiology 48: 97-98.

Siegel AJ, Silverman LM, Holman BL 1981. Elevated creatine kinase MB isoenzyme levels in marathon runners: normal myocardial scintigrams suggest noncardiac source. JAMA 246(18): 2049-2051.

Simões MR, Azevedo BF, Fiorim J, Jr Freire DD, Covre EP, Vassallo DV, Dos Santos L 2016. Chronic mercury exposure impairs the sympathovagal control of the rat heart. Clinical and Experimental Pharmacology and Physiology 43(11): 1038-1045.

Simon HU, Haj-Yehia A, Levi-Schaffer F 2000. Role of reactive oxygen species (ROS) in the apoptosis induction. Apoptosis 5: 415-418.

Simonet S, Rupin A, Badier-Commander C, Coumailleau S, Behr-Roussel D, Verbeuren TJ 2004. Evidence for superoxide anion generation in aortas of cholesterol-fed rabbits treated with L-arginine. European Journal of Pharmacology 492(2-3): 211-216.

Singh R, Gautam N, Mishra A, Gupta R 2011 Heavy metals and living systems: An overview. Indian Journal of Pharmacology 43(3): 246-253.

Sitas F, Egger S, Bradshaw D, Groenewald P, Laubscher R, Kielkowski D, Peto R 2013. Differences among the coloured, white, black, and other South African populations in smoking-attributed mortality at ages 35–74 years: a case-control study of 481 640 deaths. The Lancet 382(9893): 685-693.

Skoczynska A, Martynowicz H 2005. The impact of subchronic cadmium poisoning on the vascular effect of nitric oxide in rats. Human & Experimental Toxicology 24(7): 353-361.

Sletten AC, Peterson LR, Schaffer JE 2018. Manifestations and mechanisms of myocardial lipotoxicity in obesity. Journal of Internal Medicine 284(5): 478-491.

Smiechowicz J, Skoczynska A, Nieckula-Szwarc A, Kulpa K, Kübler A 2017. Occupational mercury vapour poisoning with a respiratory failure, pneumomediastinum and severe quadriparesis. SAGE Open Medical Case Reports 5: 1-4

Smith ER, Tomlinson LA, Ford ML, McMahon LP, Rajkumar C, Holt SG 2012. Elastin degradation is associated with progressive aortic stiffening and all-cause mortality in predialysis chronic kidney disease. Hypertension 59: 973-978

Smith SA 2009. The cell-based model of coagulation. Journal of Veterinary Emergency and Critical Care 19: 3-10.

Soares SS, Martins H, Gutiérrez-Merino C, Aureliano M 2008. Vanadium and cadmium in vivo effects in teleost cardiac muscle: metal accumulation and oxidative stress markers. Comparative Biochemistry and Physiology Part C: Toxicology and Pharmacology 147(2): 168-178.

Solenkova NV, Newman JD, Berger JS, Thurston G, Hochman JS, Lamas GA 2014. Metal pollutants and cardiovascular disease: mechanisms and consequences of exposure. American Heart Journal 168(6): 812-822.

Son YO, Wang X, Hitron JA, Zhang Z, Cheng S, Budhraja A, Ding S, Lee JC, Shi X 2011. Cadmium induces autophagy through ROS-dependent activation of the LKB1–AMPK signaling in skin epidermal cells. Toxicology and Applied Pharmacology 255(3): 287-296.

Sopjani M, Föller M, Lang F 2008. Gold stimulates Ca^{2+} entry into and subsequent suicidal death of erythrocytes. Toxicology 244(2-3): 271-279.

Sorescu D 2006. Smad3 mediates angiotensin II- and TGF-beta1-induced vascular fibrosis: Smad3 thickens the plot. Circulatory Research 98: 988-989.

Sorof JM, Poffenbarger T, Franco K, Bernard L, Portman RJ 2002. Isolated systolic hypertension, obesity, and hyperkinetic hemodynamic states in children. The Journal of Pediatrics 140(6): 660-666.

Spina RJ, Turner MJ, Ehsani AA 1998. β-Adrenergic-mediated improvement in left ventricular function by exercise training in older men. American Journal of Physiology-Heart and Circulatory Physiology 274(2): H397-H404.

Staessen JA, Buchet JP, Ginucchio G, Lauwerys RR, Lijnen P, Roels H, Fagard R 1996. Public health implications of environmental exposure to cadmium and lead: an overview of epidemiological studies in Belgium. Journal of Cardiovascular Risk 3(1): 26-41.

Stanford SN, Sabra A, D'Silva L, Lawrence M, Morris RH, Storton S, Brown MR, Evans V, Hawkins K, Williams PR, Davidson SJ 2015. The changes in clot microstructure in patients with ischaemic stroke and the effects of therapeutic intervention: a prospective observational study. BMC Neurology 15(1): 15-22.

Steffen Y, Vuillaume G, Stolle K, Roewer K, Lietz M, Schueller J, Wallerath T 2012. Cigarette smoke and LDL cooperate in reducing nitric oxide bioavailability in endothelial cells via effects on both eNOS and NADPH oxidase. Nitric Oxide 27(3): 176-184.

Stein B, Frank P, Schmitz W, Scholz H, Thoenes M 1996. Endotoxin and cytokines induce direct cardiodepressive effects in mammalian cardiomyocytes via induction of nitric oxide synthase. Journal of Molecular and Cellular Cardiology 28(8): 1631-1639.

Stepp DW, Ou J, Ackerman AW, Welak S, Klick D, Pritchard KA 2002. Native LDL and minimally oxidized LDL differentially regulate superoxide anion in vascular endothelium *in situ*. American Journal of Physiology-Heart and Circulatory Physiology 283(2): H750-H759.

Stevens A and Lowe J 2010. Human Histology. 3rd ed. Elsevier Limited., USA. 146-149.

Stohs SJ, Bagchi D 1995. Oxidative mechanisms in the toxicity of metal ions. Free Radical Biology and Medicine 18(2): 321-336.

Strait JB, Lakatta EG 2012. Aging-associated cardiovascular changes and their relationship to heart failure. Heart Failure Clinics 8(1): 143-164.

Stroes E, Kastelein J, Cosentino F, Erkelens W, Wever R, Koomans H, Lüscher T, Rabelink T 1997. Tetrahydrobiopterin restores endothelial function in hypercholesterolemia. The Journal of Clinical Investigation 99(1): 41-46.

Su H, Li Z, Fiati Kenston SS, Shi H, Wang Y, Song X, Gu Y, Barber T, Aldinger J, Zou B, Ding M 2017. Joint toxicity of different heavy metal mixtures after a short-term oral repeated-administration in rats. International Journal of Environmental Research and Public Health 14(10): 1164-1181.

Sudarikova YV, Bakeeva LE, Tsiplenkova VG 1997. Ultrastructure of mitochondrial reticulum of human cardiomyocytes in alcohol cardiomyopathy. Biochemistry-New York-English Translation of Biokhimiya 62(9): 989-1002.

Sugo T, Nakamikawa C, Yoshida N, Niwa K, Sameshima M, Mimuro J, Weisel JW, Nagita A, Matsuda M 2000. End-linked homodimers in fibrinogen Osaka VI with a Bβ-chain extension lead to fragile clot structure. Blood 96(12): 3779-3785.

Sui L, Zhang RH, Zhang P, Yun KL, Zhang HC, Liu L, Hu MX 2015. Lead toxicity induces autophagy to protect against cell death through mTORC1 pathway in cardiofibroblasts. Bioscience Reports 35(2): 1-9.

Suwalsky M, Ungerer B, Villena F, Cuevas F, Sotomayor CP 2000. $HgCl_2$ disrupts the structure of the human erythrocyte membrane and model phospholipid bilayers. Journal of Inorganic Biochemistry 81(4): 267-73.

Suwalsky M, Villena F, Norris B, Cuevas F, Sotomayor CP 2004. Cadmium-induced changes in the membrane of human erythrocytes and molecular models. Journal of Inorganic Biochemistry 98(6):1061-1066.

Suzuki N, Yamamoto M, Watanabe K, Kambegawa A, Hattori A 2004. Both mercury and cadmium directly influence calcium homeostasis resulting from the suppression of scale bone cells: the scale is a good model for the evaluation of heavy metals in bone metabolism. Journal of Bone and Mineral Metabolism 22(5): 439-446.

Swanepoel AC, Emmerson O, Pretorius E 2017. The effect of endogenous and synthetic estrogens on whole blood clot formation and erythrocyte structure. Microscopy and Microanalysis 23(3): 599-606.

Swanepoel AC, Lindeque BG, Swart PJ, Abdool Z, Pretorius E 2014. Estrogen causes ultrastructural changes of fibrin networks during the menstrual cycle: a qualitative investigation. Microscopy Research and Technique 77(8): 594-601

Swanepoel AC, Nielsen VG, Pretorius E 2015. Viscoelasticity and ultrastructure in coagulation and inflammation: two diverse techniques, one conclusion. Inflammation 38:1707-1726.

Swanepoel AC, Pretorius E 2012. Scanning electron microscopy analysis of erythrocytes in thromboembolic ischemic stroke. International Journal of Laboratory Hematology 34(2): 185-191.

Swanepoel AC, Visagie A, Pretorius E 2016. Synthetic hormones and clot formation. Microscopy and Microanalysis 22: 878-886.

Swaney JS, Roth DM, Olson ER, Naugle JE, Meszaros JG, Insel PA 2005. Inhibition of cardiac myofibroblast formation and collagen synthesis by activation and overexpression of adenylyl cyclase. Proceedings of the National Academy of Sciences 102(2): 437-442.

Sweet LI and Zelikoff JT 2001. Toxicology and immunotoxicology of mercury: a comparative review in fish and humans. Journal of Toxicology and Environmental Health Part B: Critical Reviews 4(2):161-205.

Szuster-Ciesielska A, Łokaj I, Kandefer-Szerszeń M 2000. The influence of cadmium and zinc ions on the interferon and tumor necrosis factor production in bovine aorta endothelial cells. Toxicology 145(2-3): 135-145.

Tagliafierro L, Officioso A, Sorbo S, Basile A, Manna C 2015. The protective role of olive oil hydroxytyrosol against oxidative alterations induced by mercury in human erythrocytes. Food and Chemical Toxicology 82: 59-63.

Takabatake T, Ohta H, Ishida YI, Hara H, Ushiogi Y, Hattori N 1988. Low serum creatinine levels in severe hepatic disease. Archives of Internal Medicine 148(6):1313-1315.

Takamura A, Komatsu M, Hara T, Sakamoto A, Kishi C, Waguri S, Eishi Y, Hino O, Tanaka K, Mizushima N 2011. Autophagy-deficient mice develop multiple liver tumours. Genes Development 25: 795-800.

Tal MC, Sasai M, Lee HK, Yordy B, Shadel GS, Iwasaki A 2009. Absence of autophagy results in reactive oxygen species dependent amplification of RLR signaling. Proceedings of the National Academy of Science U S A 106: 2770-2775.

Tan YT, Wenzelburger F, Lee E, Heatlie G, Leyva F, Patel K, Frenneaux M, Sanderson JE 2009. The pathophysiology of heart failure with normal ejection fraction: exercise echocardiography reveals complex abnormalities of both systolic and diastolic ventricular function involving torsion, untwist, and longitudinal motion. Journal of the American College of Cardiology 54(1): 36-46.

Tandon SK, Singh S, Prasad S, Mathur N 2001. Hepatic and renal metallothionein induction by an oral equimolar dose of zinc, cadmium or mercury in mice. Food and Chemical Toxicology 39(6): 571-517.

Tannous P, Zhu H, Johnstone JL, Shelton JM, Rajasekaran NS, Benjamin IJ, Nguyen L, Gerard RD, Levine B, Rothermel BA, Hill JA 2008. Autophagy is an adaptive response in desmin-related cardiomyopathy. Proceedings of the National Academy of Sciences 105(28): 9745-9750.

Tansel B 2017. From electronic consumer products to e-wastes: Global outlook, waste quantities, recycling challenges. Environment International 98: 35-45.

Tchounwou PB, Ayensu WK, NinashviliN, Sutton D 2003. Environmental exposure to mercury and its toxicopathologic implications for public health. Environmental Toxicology 18: 149-175.

Tellez-Plaza M, Guallar E, Howard BV, Umans JG, Francesconi KA, Goessler W, Silbergeld EK, Devereux RB, Navas-Acien A 2013. Cadmium exposure and incident cardiovascular disease. Epidemiology 24: 421-429.

Tellez-Plaza M, Navas-Acien A, Crainiceanu CM, Guallar E 2008. Cadmium exposure and hypertension in the 1999-2004 National Health and Nutrition Examination Survey (NHANES). Environmental Health Perspectives 116(1): 51-56.

Teschke R, Brand A, Strohmeyer G 1977. Induction of hepatic microsomal gamma-glutamyltransferase activity following chronic alcohol consumption. Biochemical and Biophysical Research Communications 75(3): 718-724.

The World Health Organisation. Guidelines for drinking water quality. Geneva: WHO. 2011. www.who.int/water_sanitation_health/.../2011/9789241548151_annex.pdf. Accessed 22 Nov 2016.

The World Health Organisation. Ten chemicals of major public health concern. Geneva: WHO. 2015. www.who.int/ipcs/assessment/public_health/chemicals_phc/en/. Accessed 22 Nov 2016.

Thijssen S, Maringwa J, Faes C, Lambrichts I, Van Kerkhove E 2007. Chronic exposure of mice to environmentally relevant, low doses of cadmium leads to early renal damage, not predicted by blood or urine cadmium levels. Toxicology 229(1-2): 145-156.

Thomassin L, Werneck CC, Broekelmann TJ, Gleyzal C, Hornstra IK, Mecham RP, Sommer P 2005. The pro-regions of lysyl oxidase and lysyl oxidase-like-1 are required for deposition onto elastic fibers. Journal of Biological Chemistry 280(52): 42848-48855.

Thompson W, Smith E 1989. Atherosclerosis and the coagulation system. Journal of Pathology 159: 97-106.

Thophon S, Pokethitiyook P, Chalermwat K, Upatham ES, Sahaphong S 2004. Ultrastructural alterations in the liver and kidney of white sea bass, Lates calcarifer, in acute and subchronic cadmium exposure. Environmental Toxicology: An International Journal 19(1): 11-19.

Thurston SW, Bovet P, Myers GJ, Davidson PW, Georger LA, Shamlaye C, Clarkson TW 2007. Does prenatal methylmercury exposure from fish consumption affect blood pressure in childhood?. Neurotoxicology 28(5): 924-930.

Thyberg J, Blomgren K, Hedin U, Dryjski M 1995. Phenotypic modulation of smooth muscle cells during the formation of neointimal thickenings in the rat carotid artery after balloon injury: an electron-microscopic and stereological study. Cell and Tissue Research 281(3): 421-433.

Tinkov AA, Ajsuvakova OP, Skalnaya MG, Popova EV, Sinitskii AI, Nemereshina ON, Gatiatulina ER, Nikonorov AA, Skalny AV 2015. Mercury and metabolic syndrome: a review of experimental and clinical observations. Biometals 28(2): 231-54.

Tishkoff SA, Williams SM 2002. Genetic analysis of African populations: human evolution and complex disease. Nature Reviews Genetics 3(8): 611-621.

Tomera JF, Lilford K, Kukulka SP, Friend KD, Harakal C 1994. Divalent cations in hypertension with implications to heart disease: calcium, cadmium interactions. Methods and Findings in Experimental and Clinical Pharmacology 16(2): 97-107.

Tort L, Madsen LH 1991. The effects of the heavy metals cadmium and zinc on the contraction of ventricular fibres in fish. Comparative Biochemistry and Physiology Part C: Comparative Pharmacology 99(3): 353-356.

Tortora GJ, Derrickson B 2006. Principles of Anatomy and Physiology. 11th ed. John Whiley & Sons.Inc., USA.

Tran LT, Yuen VG, McNeill JH 2009. The fructose-fed rat: a review on the mechanisms of fructose-induced insulin resistance and hypertension. Molecular and Cellular Biochemistry 332(1-2): 145-149.

Traub O and Berk BC 1998. Laminar shear stress: mechanisms by which endothelial cells transduce an atheroprotective force. Arteriosclerosis, Thrombosis, and Vascular Biology 18(5): 677-685.

Tsutsui H, Ide T, Kinugawa S 2006. Mitochondrial oxidative stress, DNA damage, and heart failure. Antioxidants and Redox Signalling 8(9-10): 1737-1744.

Tsutsui H, Kinugawa S, Matsushima S 2009. Mitochondrial oxidative stress and dysfunction in myocardial remodelling. Cardiovascular Research 81(3): 449-456.

Tsutsui H, Kinugawa S, Matsushima S 2011. Oxidative stress and heart failure. American Journal of Physiology-Heart and Circulatory Physiology 301(6): H2181-H2190.

Türkcan A, Scharinger B, Grabmann G, Keppler BK, Laufer G, Bernhard D, Messner B 2015. Combination of cadmium and high cholesterol levels as a risk factor for heart fibrosis. Toxicological Sciences 145(2): 360-371.

Tuttolomondo A, Di Raimondo D, Di Sciacca R, Pecoraro R, Arnao V, Buttà C, Licata G, Pinto A 2012. Arterial stiffness and ischemic stroke in subjects with and without metabolic syndrome. Atherosclerosis 225(1): 216-219.

Undas A and Ariens RA 2011. Fibrin clot structure and function: a role in the pathophysiology of arterial and venous thromboembolic diseases. Arterial Thrombosis and Vascular Biology 31(12): e88-e99.

Undas A, Slowik A, Wolkow P, Szczudlik A, Tracz W 2010. Fibrin clot properties in acute ischemic stroke: relation to neurologic deficit. Thrombosis Research 125(4): 357-361.

Undas A, Szułdrzynski K, Stepien E, Zalewski J, Godlewski J, Tracz W, Pasowicz M, Zmudka K 2008. Reduced clot permeability and susceptibility to lysis in patients with acute coronary syndrome: Effects of inflammation and oxidative stress. Atherosclerosis 196: 551-557.

Undas A, Zawilska K Mariola Ciesla-Dul M, Lehmann-Kopydłowska A, Skubiszak A, Ciepłuch K, Tracz W 2009. Altered fibrin clot structure/function in patients with idiopathic venous thromboembolism and in their relatives. Blood 114(19): 4272-4278.

Undas A, Zeglin M 2006. Fibrin clot properties and cardiovascular disease. Vascular Disease Prevention 3(2): 99-106.

Uys CP 2016. An *in vitro* study investigating the effect of environmental metal pollutants on erythrocytes. MSc. University of Pretoria, Pretoria, South Africa.

Uzunhisarcikli M, Aslanturk A, Kalender S, Apaydin FG, Bas H 2016. Mercuric chloride induced hepatotoxic and hematologic changes in rats: The protective effects of sodium selenite and vitamin E. Toxicology and Industrial Health 32(9): 1651-1662.

Vacek TP, Vacek JC, Tyagi SC 2012. Mitochondrial mitophagic mechanisms of myocardial matrix metabolism and remodelling. Archives of Physiology and Biochemistry 118: 31-42.

Vadseth C, Souza JM, Thomson L, Seagraves A, Nagaswami C, Scheiner T, Torbet J, Vilaire G, Bennett JS, Murciano JC, Muzykantov V 2004. Pro-thrombotic state induced by post-translational modification of fibrinogen by reactive nitrogen species. Journal of Biological Chemistry 279(10): 8820-8826.

Valera B, Dewailly E, Poirier P 2008. Cardiac autonomic activity and blood pressure among Nunavik Inuit adults exposed to environmental mercury: a cross-sectional study. Environmental Health 7(1): 29-38.

Valera B, Dewailly É, Poirier P 2009. Environmental mercury exposure and blood pressure among Nunavik Inuit adults. Hypertension 54(5): 981-986.

Valera B, Dewailly E, Poirier P 2011. Impact of mercury exposure on blood pressure and cardiac autonomic activity among Cree adults (James Bay, Quebec, Canada). Environmental Research 111(8): 1265-1270.

Valera B, Dewailly É, Poirier P 2013. Association between methylmercury and cardiovascular risk factors in a native population of Quebec (Canada): a retrospective evaluation. Environmental Research 120: 102-108.

Valera B, Muckle G, Poirier P, Jacobson SW, Jacobson JL, Dewailly E 2012. Cardiac autonomic activity and blood pressure among Inuit children exposed to mercury. Neurotoxicology 33(5): 1067-1074.

Valko M, Rhodes C, Moncol J, Izakovic MM, Mazur M 2006. Free radicals, metals and antioxidants in oxidative stress-induced cancer. Chemico-Biological Interactions 160(1): 1-40.

Valles J, Lago A, Moscardo A, Parkhutic V and Santos MT 2013. TAX synthesis and COX1-independent platelet reactivity in aspirin-treated patients soon after acute cerebral stroke or transient ischemic attack. Thrombosis Research 132: 211-216.

Vallon V, Blantz RC, Thomson S 2003. Glomerular hyperfiltration and the salt paradox in early type 1 diabetes mellitus: a tubulo-centric view. Journal of the American Society of Nephrology 14(2): 530-537.

Van Rooy M and Pretorius E 2015. Metabolic syndrome, platelet activation and the development of transient ischemic attack or thromboembolic stroke. Thrombosis Research 135: 434-442.

Van Rooy MJ, Duim W, Ehlers R, Buys AV and Pretorius E 2015. Platelet hyperactivity and fibrin clot structure in transient ischemic attack individuals in the presence of metabolic syndrome: a microscopy and thromboelastography® study. Cardiovascular Diabetology 14: 86-98.

Van Rooy MJ. 2015. Blood coagulation in metabolic syndrome-induced transient ischemic attack. PhD, University of Pretoria, Pretoria, South Africa.

Van Walbeek C 2006. Industry responses to the tobacco excise tax increases in South Africa. South African Journal of Economics 74(1): 110-122.

Varoni MV, Palomba D, Gianorso S, Anania V 2003. Cadmium as an environmental factor of hypertension in animals: new perspectives on mechanisms. Veterinary Research Communications 27(1): 807-810.

Vaziri ND, Ding Y, Ni Z 2001. Compensatory up-regulation of nitricoxide synthase isoforms in leadinduced hypertension; reversal by a superoxide dismutase-mimetic drug. Journal of Pharmacology and Experimental Therapeutics 298(2): 679-685.

Velindala S, Gaikwad P, Ella KKR, Bhorgonde KD, Hunsingi P, Anop K 2014. Histochemical analysis of polarizing colours of collagen using Picro Sirius red staining in oral submucous fibrosis. Journal of Oral Health 6(1): 33-38.

Vendrov AE, Vendrov KC, Smith A, Yuan J, Sumida A, Robidoux J, Runge MS, Madamanchi NR 2015. NOX4 NADPH oxidase-dependent mitochondrial oxidative stress in aging-associated cardiovascular disease. Antioxidants and Redox Signalling 23(18): 1389-409.

Venter C, Oberholzer HM, Bester J, Van Rooy MJ, Bester MJ 2017. Ultrastructural, confocal and viscoelastic characteristics of whole blood and plasma after exposure to cadmium and chromium alone and in combination: An *ex vivo* study. Cellular Physiology and Biochemistry 43(3): 1288-1300.

Venter C, Oberholzer HM, Taute H, Cummings FR and Bester MJ 2015. An *in ovo* investigation into the hepatotoxicity of cadmium and chromium evaluated with light- and transmission electron microscopy and electron energy-loss spectroscopy. Journal of Environmental Science and Health A 50: 830-838.

Verma S, Kumar R, Khadwal A, Singhi S 2010. Accidental inorganic mercury chloride poisoning in a 2-year old child. The Indian Journal of Pediatrics 77(10): 1153-1155.

Versteeg HH, Heemskerk JW, Levi M, Reitsma PH 2013. New fundamentals in hemostasis. Physiology Reviews 93: 327-358.

Vijaykumar JBM and Lokesh BR 2004. Biological properties of curcumin-cellular and molecular mechanisms of action. Critical Reviews of Food Science and Nutrition 44: 97-111.

Vincent PC, Blackburn CR 1958. The effects of heavy metal ions on the human erythrocyte: i. Comparisons of the action of several heavy metals. Australian Journal of Experimental Biology and Medical Science 36(5): 471-478.

Vretou-Jockers E and Vassilopoulos D 1989. Skeletal muscle CK-B activity in neurogenic muscular atrophies. Journal of Neurology 236(5): 284-287.

Wada K, Fujii Y, Watanabe H, Satoh M, Furuichi Y 1991. Cadmium directly acts on endothelin receptor and inhibits endothelin binding activity. FEBS Letters 285(1): 71-74.

Wadley AJ, van Zanten JJV, Aldred S 2013. The interactions of oxidative stress and inflammation with vascular dysfunction in ageing: the vascular health triad. Age 35(3): 705-718.

Waisberg M, Joseph P, Hale B, Beyersmann D 2003. Molecular and cellular mechanisms of cadmium carcinogenesis. Toxicology 192: 95-117

Wakabayashi T 2002. Megamitochondria formation-physiology and pathology. Journal of Cellular and Molecular Medicine 6(4): 497-538.

Walczak-Drzewiecka A, Slusarczyk A, Wyczolkowska J, Dastych J 1999. Mercuric chloride synergistically increases ionophore-induced secretion of IL-4 from murine mast cells. Inflammation Research 48(13): 35-36.

Wan Q, Liu Z, Yang Y 2018. Puerarin inhibits vascular smooth muscle cells proliferation induced by fine particulate matter via suppressing of the p38 MAPK signaling pathway. BMC Complementary And Alternative Medicine 18(1): 146-154.

Wang G and Fowler BA 2008. Roles of biomarkers in evaluating interactions among mixtures of lead, cadmium and arsenic. Toxicology and Applied Pharmacology 233(1): 92-99.

Wang J, Li A, Wang Q, Zhou Y, Fu L, Li Y 2010. Assessment of the manganese content of the drinking water source in Yancheng, China. Journal of Hazardous Materials 182(1-3): 259-265.

Wang L, Li J, Li J, Liu Z 2010. Effects of lead and/or cadmium on the oxidative damage of rat kidney cortex mitochondria. Biological Trace Element Research 137(1): 69-78.

Wang W, Huang XR, Canlas E, Oka K, Truong LD, Deng C, Bhowmick NA, Ju W, Bottinger EP, Lan HY 2006. Essential role of Smad3 in angiotensin II–induced vascular fibrosis. Circulation Research 98(8): 1032-1039.

Wang Y, Bollard ME, Nicholson JK, Holmes E 2006. Exploration of the direct metabolic effects of mercury II chloride on the kidney of Sprague–Dawley rats using high-resolution magic angle spinning 1H NMR

spectroscopy of intact tissue and pattern recognition. Journal of Pharmaceutical and Biomedical Analysis 40(2):375-381.

Wani FA, Ibrahim MA, Moneim MM, Almaeen AR 2017. Cytoprotectant and anti-oxidant effects of olive oil on cadmium induced nephrotoxicity in mice. Open Journal of Pathology 8(1): 31-46.

Watkins BA, Hannon K, Ferruzzi M, Li Y 2007. Dietary PUFA and flavonoids as deterrents for environmental pollutants. The Journal of Nutritional Biochemistry 18(3): 196-205.

Weber KT 1999. Angiotensin II and connective tissue: homeostasis and reciprocal regulation. Regulatory Peptides 82(1-3): 1-7.

Weber KT 2000. Targeting pathological remodeling: concepts of cardioprotection and reparation. Circulation 102: 1342-1345.

Weber KT, Pick R, Jalil JE, Janicki JS, Carroll EP 1989. Patterns of myocardial fibrosis. Journal of Molecular and Cellular Cardiology 21: 121-131.

Weber KT, Sun Y, Bhattacharya SK, Ahokas RA, Gerling IC 2013. Myofibroblast-mediated mechanisms of pathological remodelling of the heart. Nature Reviews Cardiology 10(1):15-26.

Weber KT, Swamynathan SK, Guntaka RV, Sun Y 1999. Angiotensin II and extracellular matrix homeostasis. The International Journal of Biochemistry and Cell Biology 31(3-4): 395-403.

Wei S, Chow LT, Shum IO, Qin L, Sanderson JE 1999. Left and right ventricular collagen type I/III ratios and remodeling post-myocardial infarction. Journal of Cardiac Failure 5(2): 117-126.

Weigand KL, Reno JL, Rowley BM 2015. Low-level Mercury Causes Inappropriate Activation in T and B Lymphocytes in the Absence of Antigen Stimulation. Journal of the Arkansas Academy of Science 69(1): 116-123.

Weisel JW, Litinov RI 2013. Mechanisms of fibrin polymerization and clinical implications. Blood 121(10): 1712-1719.

Wheeler JB, Mukherjee R, Stroud RE, Jones JA, Ikonomidis JS 2015. Relation of murine thoracic aortic structural and cellular changes with aging to passive and active mechanical properties. Journal of the American Heart Association 4(3): 1-9.

Whelan RS, Kaplinskiy V, Kitsis RN 2010. Cell death in the pathogenesis of heart disease: mechanisms and significance. Annual Review of Physiology 72: 19-44.

Whitfield JB, Dy V, McQuilty R 2010. Genetic effects on toxic and essential elements in humans: arsenic, cadmium, copper, lead, mercury, selenium, and zinc in erythrocytes. Environmental Health Perspectives 118: 776-782.

Wierzbicki R, Prażanowski M, Michalska M, Krajewska U, Mielicki WP 2002. Disorders in blood coagulation in humans occupationally exposed to mercuric vapors. The Journal of Trace Elements in Experimental Medicine 15(1): 21-29.

Wilkinson IB, Cockcroft JR, McEniery CM 2015. Aortic stiffness as a cardiovascular risk predictor. British Medical Journal 351: 1-2.

Wirth JJ and Mijal RS 2010. Adverse effects of low-level heavy metal exposure on male reproductive function. Systems Biology in Reproductive Medicine 56(2): 147-167.

Witeska M, Kondera E, Szczygielska K 2011. The effects of cadmium on common carp erythrocyte morphology. Polish Journal of Environmental Studies 20: 783-788.

Wittsiepe J, Feldt T, Till H, Burchard G, Wilhelm M, Fobil JN 2017. Pilot study on the internal exposure to heavy metals of informal-level electronic waste workers in Agbogbloshie, Accra, Ghana. Environmental Science and Pollution Research 24(3): 3097-3107.

Wolberg AS, Aleman MM, Leiderman K, Machlus KR 2012. Procoagulant activity in hemostasis and thrombosis: Virchow's triad revisited. Anesthesia And Analgesia 114(2): 275-285.

Wolberg AS, Allen GA, Monroe DM, Hedner U, Roberts HR, Hoffman M 2005. High dose factor VIIa improves clot structure and stability in a model of haemophilia B. British Journal of Haematology 131(5): 645-55.

Wolberg AS. 2007. Thrombin generation and fibrin clot structure. Blood Reviews 21: 131-142.

World Health Organization (WHO) 2011. Cadmium. Guidelines for Drinking-Water Quality. pp. 327–328 Available from: http://www.who.int/water_sanitation_health/ publications/2011/9789241548151_ch12.pdf (Accessed 04 August 2017).

Wu AH, Wang XM, Gornet TG, Ordonez-Llanos J 1992. Creatine kinase MB isoforms in patients with skeletal muscle injury: ramifications for early detection of acute myocardial infarction. Clinical Chemistry 38(12): 2396-2400.

Wu H, Liao Q, Chillrud SN, Yang Q, Huang L, Bi J, Yan B 2016. Environmental exposure to cadmium: health risk assessment and its associations with hypertension and impaired kidney function. Scientific Reports 6: 1-9

Xia N, Daiber A, Habermeier A, Closs EI, Thum T, Spanier G, Li H 2010. Resveratrol reverses endothelial nitric-oxide synthase uncoupling in apolipoprotein E knockout mice. Journal of Pharmacology and Experimental Therapeutics 335(1): 149-154.

Xiao J, Ho CT, Liong EC, Nanji AA, Leung TM, Lau TYH, and Tipoe GL 2014. Epigallocatechin gallate attenuates fibrosis, oxidative stress, and inflammation in non-alcoholic fatty liver disease rat model through TGF/SMAD, PI3 K/Akt/FoxO1, and NF-kappa B pathways. European Journal of Nutrition 53(1): 187-199.

Xie M, Morales CR, Lavandero S, Hill JA 2011. Tuning flux: autophagy as a target of heart disease therapy. Current Opinion in Cardiology 26(3): 216-222.

Yadav N, Khandelwal S 2008. Effect of Picroliv on cadmium induced testicular damage in rat. Food and Chemical Toxicology 46(2):494-501.

Yamamoto C, Kaji T, Sakamoto M, Kozuka H 1993. Cadmium stimulation of plasminogen activator inhibitor-1 release from human vascular endothelial cells in culture. Toxicology 83 (1-3): 215-223.

Yanagisawa H, Davis EC, Starcher BC, Ouchi T, Yanagisawa M, Richardson JA, Olson EN 2002. Fibulin-5 is an elastin-binding protein essential for elastic fibre development *in vivo*. Nature 415(6868): 168-171.

Yang JM, Arnush M, Chen QY, Wu XD, Pang B, Jiang XZ 2003. Cadmium-induced damage to primary cultures of rat Leydig cells. Reproductive Toxicology 17: 553-560

Yang UJ, Yoon SR, Chung JH, Kim YJ, Park KH, Park TS, Shim SM 2012. Water spinach (*Ipomoea aquatic Forsk*) reduced the absorption of heavy metals in an in vitro bio-mimicking model system. Food and Chemical Toxicology 50(10): 3862-3866.

Yang Z and Klionsky DJ 2010. Mammalian autophagy: core molecular machinery and signalling regulation. Current Opinions in Cell Biology 22: 124-131.

Yasuda M, Miwa A, Kitagawa M 1995. Morphometric studies of renal lesions in Itai-Itai disease: chronic cadmium nephropathy. Nephron 69(1): 14-19.

Yau JW, Teoh H, Verma S 2015. Endothelial cell control of thrombosis. BMC Cardiovascular Disorders 15(1): 130-140.

Yazıhan N, Koçak MK, Akçıl E, Erdem O, Sayal A, Güven C, Akyürek N 2011. Involvement of galectin-3 in cadmium-induced cardiac toxicity. Anatolian Journal of Cardiology 11(6): 479-484.

Yiin SJ, Chern CL, Sheu JY, Lin TH 2000. Cadmium-induced liver, heart, and spleen lipid peroxidation in rats and protection by selenium. Biological Trace Element Research 78(1-3): 219-230.

Yoopan N, Watcharasit P, Wongsawatkul O, Piyachaturawat P, Satayavivad J 2008. Attenuation of eNOS expression in cadmium-induced hypertensive rats. Toxicology Letters 176(2): 157-161.

Yoshida T, Maulik N, Engelman RM, Ho YS, Magnenat JL, Rousou JA, Deaton D, Das DK 1997. Glutathione peroxidase knockout mice are susceptible to myocardial ischemia reperfusion injury. Circulation 96(9-Suppl II): 216-220.

Yoshizawa K, Rimm EB, Morris JS, Spate VL, Hsieh C, Spiegelman D, Stampfer MJ, Willett WC 2002. Mercury and the risk of coronary heart disease in men. New England Journal of Medicine 347(22): 1755-1760.

Young B, Heath JW 2006. Wheater's Functional Histology, a text and colour atlas. 5th ed. Elsevier Limited., USA.

Young D, Borland R, Hammond D, Cummings KM, Devlin E, Yong HH, O'Connnor RJ 2006. Prevalence and attributes of roll-your-own smokers in the International Tobacco Control (ITC) Four Country Survey. Tobacco Control 15(3): iii76-iii82.

Young SL 2010. Pica in pregnancy: new ideas about an old condition. Annual Review of Nutrition 30: 403-422.

Yuan G, Dai S, Yin Z, Lu H, Jia R, Xu J,Song X, Li L, Shu Y, Zhao X 2014. Toxicological assessment of combined lead and cadmium: acute and sub-chronic toxicity study in rats. Food and Chemical Toxicology 65: 260-268.

Zalba G, José GS, Moreno MU, Fortuño MA, Fortuño A, Beaumont FJ, Díez J 2001. Oxidative stress in arterial hypertension: role of NAD(P)H oxidase. Hypertension 38(6):1395-1399.

Zeneli L, Sekovanić A, Ajvazi M, Kurti L, Daci N 2016. Alterations in antioxidant defense system of workers chronically exposed to arsenic, cadmium and mercury from coal flying ash. Environmental Geochemistry and Health 38(1): 65-72.

Zeng X, Xu X, Boezen HM, Huo X 2016. Children with health impairments by heavy metals in an e-waste recycling area. Chemosphere 148: 408-415.

Zhai Q, Narbad A, Chen W 2015. Dietary strategies for the treatment of cadmium and lead toxicity. Nutrients 7(1): 552-571.

Zhang T, Zhang Y, Cui M, Jin L, Wang Y, Lv F, Liu Y, Zheng W, Shang H, Zhang J, Zhang M 2016. CaMKII is a RIP3 substrate mediating ischemia-and oxidative stress-induced myocardial necroptosis. Nature Medicine 22(2): 175-182.

Zhang W, Houb ST and Stanimirovic D 2015. Blood brain barrier protection in stroke: Taming tPA. In: The Blood-Brain Barrier in Health and Disease, Volume Two: Pathophysiology and Pathology. Dorovini-Zisp K, editor. CRC Press, USA, pp226.

Zhang X, Kumari N, Low S, Ang K, Yeo D, Yeoh LY, Liu A, Kwan PY, Tang WE, Tavintharan S, Sum CF 2018. The association of serum creatinine and estimated glomerular filtration rate variability with diabetic retinopathy in Asians with type 2 diabetes: A nested case-control study. Diabetes and Vascular Disease Research 15(6): 548-558

Zhang Y, Griendling KK, Dikalova A, Owens GK, Taylor W R 2005. Vascular hypertrophy in angiotensin II–induced hypertension is mediated by vascular smooth muscle cell–derived H_2O_2. Hypertension 46(4): 732-737.

Zhe-Wei S, Li-Sha G, Yue-Chun L 2018. The role of necroptosis in cardiovascular disease. Frontiers in Pharmacology 9:1-9.

Zhou G, Kandala JC, Tyagi SC, Katwa LC, Weber KT 1996. Effects of angiotensin II and aldosterone on collagen gene expression and protein turnover in cardiac fibroblasts. Molecular and Cellular Biochemistry 154(2): 171-178.

Zhou TL, Henry RM, Stehouwer CD, van Sloten TT, Reesink KD, Kroon AA 2018. Blood pressure variability, arterial stiffness, and arterial remodeling: The Maastricht study. Hypertension 72(4): 1002-1010.

Zhu H, Jia Y, Cao H, Meng F, Liu X 2014. Biochemical and histopathological effects of subchronic oral exposure of rats to a mixture of five toxic elements. Food and Chemical Toxicology 71: 166-175.

Zoccali C 2009. Overweight, obesity and metabolic alterations in chronic kidney disease. Prilozi 30(2): 17-31.

Zygner W, Gójska-Zygner O, Bąska P, Długosz E 2014. Increased concentration of serum TNF alpha and its correlations with arterial blood pressure and indices of renal damage in dogs infected with *Babesia canis*. Parasitology Research 113(4): 1499-1503.

APPENDIX A

Ethical clearance

UNIVERSITEIT VAN PRETORIA
UNIVERSITY OF PRETORIA
YUNIBESITHI YA PRETORIA

Faculty of Health Sciences

1 February 2019

Approval Certificate
Annual Renewal

Ethics Reference No.: 489/2015
Title: An in vivo and ex vivo investigation of effects of the heavy metals mercury and cadmium alone and in combination on the cardiovascular system

Dear Prof MJ Bester

The **Annual Renewal** as supported by documents received between 2019-01-07 and 2019-01-30 for your research, was approved by the Faculty of Health Sciences Research Ethics Committee on its quorate meeting of 2019-01-30.

Please note the following about your ethics approval:
- Renewal of ethics approval is valid for 1 year, subsequent annual renewal will become due on 2020-02-01.
- Please remember to use your protocol number (489/2015) on any documents or correspondence with the Research Ethics Committee regarding your research.
- Please note that the Research Ethics Committee may ask further questions, seek additional information, require further modification, monitor the conduct of your research, or suspend or withdraw ethics approval.

Ethics approval is subject to the following:
- The ethics approval is conditional on the research being conducted as stipulated by the details of all documents submitted to the Committee. In the event that a further need arises to change who the investigators are, the methods or any other aspect, such changes must be submitted as an Amendment for approval by the Committee.

We wish you the best with your research.

Yours sincerely

Dr R Sommers
MBChB MMed (Int) MPharmMed PhD
Deputy Chairperson of the Faculty of Health Sciences Research Ethics Committee, University of Pretoria

The Faculty of Health Sciences Research Ethics Committee complies with the SA National Act 61 of 2003 as it pertains to health research and the United States Code of Federal Regulations Title 45 and 46. This committee abides by the ethical norms and principles for research, established by the Declaration of Helsinki, the South African Medical Research Council Guidelines as well as the Guidelines for Ethical Research: Principles Structures and Processes, Second Edition 2015 (Department of Health)

Research Ethics Committee
Room 4-60, Level 4, Tswelopele Building
University of Pretoria, Private Bag X323
Arcadia 0007, South Africa
Tel +27 (0)12 356 3084
Email deepeka.behari@up.ac.za
www.up.ac.za

Fakulteit Gesondheidswetenskappe
Lefapha la Disaense tša Maphelo

UNIVERSITEIT VAN PRETORIA
UNIVERSITY OF PRETORIA
YUNIBESITHI YA PRETORIA

Animal Ethics Committee

PROJECT TITLE	An in vitro and in vivo investigation of effects of the heavy metals mercury and cadmium alone and in combination on the cardiovascular system
PROJECT NUMBER	H007-15
RESEARCHER/PRINCIPAL INVESTIGATOR	SS Arbi

STUDENT NUMBER (where applicable)	29351996
DISSERTATION/THESIS SUBMITTED FOR	PhD

ANIMAL SPECIES	Rats	
NUMBER OF ANIMALS	48	
Approval period to use animals for research/testing purposes		1 July 2015 – 30 June 2016
SUPERVISOR	Dr. HM Oberholzer	

<u>KINDLY NOTE:</u>

Should there be a change in the species or number of animal/s required, or the experimental procedure/s - please submit an amendment form to the UP Animal Ethics Committee for approval before commencing with the experiment

APPROVED	Date	29 June 2015
CHAIRMAN: UP Animal Ethics Committee	Signature	

S*4285-15*